University of Glasgow

Cholinergic modulation of *Candida albicans* virulence factors and the pathogenesis of candidiasis

Abeer Muhammad Alghamdi (BSc, MSc)

Submitted in fulfilment of the requirements for

the Degree of Doctor of Philosophy

School of Medicine
College of Medical, Veterinary and Life Sciences

University of Glasgow

February 2022

Abstract

Candida albicans is the most prevalent fungal pathogen causing both superficial and invasive fungal infections leading to various challenges on healthcare systems. Normally, *C. albicans* is a harmless commensal of the human body, but under certain conditions of stress, it can express virulence traits leading to disease. It causes a wide range of infections starting from superficial infections such as oropharyngeal candidiasis to systemic infections such as Candidemia. Biofilm formation is an important feature of *C. albicans* pathogenesis. There are several factors in *C. albicans* which contribute to this trait, such as morphological transition, expression of virulence factors, metabolic flexibility, and stress response machinery. Understanding the complexity of the pathways behind the virulence traits of *C. albicans* is essential for developing effective therapeutic strategies to combat superficial and life threatening systemic infections.

In this research, we present a novel antifungal activity of pilocarpine hydrochloride against *C. albicans* biofilms. We hypothesize that *C. albicans* may possess muscarinic like receptor(s) that mediate the ability of pilocarpine hydrochloride to inhibit biofilm formation. Pilocarpine hydrochloride reduced filamentation and biofilm formation significantly in a dose dependent manner in both the wild type strain and clinical isolates. The M5 allosteric modulator, similarly, inhibited the biofilm formation significantly in a dose dependent manner. Moreover, pilocarpine hydrochloride reduced the damage and inhibited the innate immune response stimulated by *C. albicans* infection in both TR146 cells and a three-dimensional human oral tissue model. The transcriptomic profile of *C. albicans* upon treatment with pilocarpine hydrochloride and acetylcholine revealed differential expression among crucial genes that play a vital role in *C. albicans* pathogenesis such as downregulation of hyphal specific genes; *HWP1*, *ECE1*, and *IHD1*. RNAseq data also revealed a considerable number of unannotated genes that may play a role in the cholinergic modulation of *C. albicans* biofilm formation by acetylcholine and pilocarpine hydrochloride.

The data generated herein suggest that *C. albicans* may possess a cholinergic receptor or receptors mediating *C. albicans* virulence factors. This research

provides a foundation to explore further cholinergic pathways in fungal pathogens and their involvement in pathogenicity. It also reveals potential novel effective antifungal therapeutic targets in *C. albicans*. Furthermore, it emphasizes the feasibility and effectiveness of repurposing known licensed drugs, used for treatment of other conditions, to treat *C. albicans* infections singularly or as an adjunctive therapy. In the light of the global increased resistance to antifungal and antimicrobial therapies, this work may contribute to the development of more effective therapeutic strategies.

Table of Contents

List of Tables

List of Figures

List of Accompanying Material

Appendices

I. Growth curve profile of clinical *Candida albicans* isolates cultured in the presence and absence of 50 mM pilocarpine hydrocholoride.

II. Growth curve profile of clinical *Candida albicans* isolates treated with caspofungin in the presence and absence of pilocarpine hydrocholoride.

III. Growth curve profile of clinical *Candida albicans* isolates treated with amphoetricin B in the presence and absence of pilocarpine hydrochloride.

IV. *Candida albicans* gene regulation in the presence and absence of pilocarpine hydrochloride.

V. *Candida albicans* gene regulation in the presence and absence of acetylcholine.

Acknowledgement

All praises and thanks be to Allah Almighty for blessing me with patience, strength, and people who supported me through my PhD journey. I would like to begin my sincere thanks to my supervisors; Dr. Christopher Nile and Professor Gordon Ramage for their invaluable guidance and support throughout my studies. Without your support, I would not have been able to achieve my goals.

I would also like to thank those who helped me during my studies and lab work, Dr. Jason Brown, Dr. Christopher Delaney, and Mr. Steven Milligan. Many thanks to my colleagues who made this journey a pleasure, including Bryn Short, Mark Butcher, Tracy Young, Om Alkhir Alshanta, William Johnston, Emily McKloud, Saeed Alqahtani and Sumaya Abusrewil. Khawlah Albashaireh, thank you for all the laughs and arguments that happened in the lab and at our dining tables. You made the heavy work in the immunology lab bearable.

My extreme gratitude to Al-Baha University and the Saudi Arabian Cultural Bureau for the financial support during my PhD years.

I am profoundly grateful to my husband Sahman for his encouragement and understanding during difficult times. There are no words can describe my heartfelt thanks. A big thank to my children, Mohammed and Abdullah for tolerating me despite my absence. This work is dedicated for you.

I would also like to thank my parents, brothers, and sisters for their unconditional love and support. I would also like to extend my deepest thanks to my friends, Haneen, Mariyam, Sarah, Jawhara, Ghada, Ebtihal, Rawaa, Sumaya, and Afnan. They made my days joyful and cheerful, and made sure I never forget that there is a life to be lived outside the lab.

Author's Declaration

I declare that I have carried out the work described in this thesis unless otherwise acknowledged or cited, under the supervision of Dr Christopher Nile and Professor Gordon Ramage. I further declare that this thesis has not been submitted for any other degree at the University of Glasgow or any other institution.

Abeer M Alghamdi

February 2022

Abbreviations

ABC: ATP-binding cassette

ACB1: Acyl- coenzyme – A – binding (ACB1)

ACh: Acetylcholine

ALS: Agglutinin-like sequences

AMB: Amphotericin B

APE: Arecaidine propargyl ester tosylate

ART: Antiretroviral therapy

ATP: Adenosine 5′-triphosphate

BEC: Buccal epithelial cells

BPE: Bovine pituitary extract

BSA: Bovine serum albumin

BSI: Bloodstream infection

C-HCL: Cevimeline hydrochloride

C. albicans: Candida albicans

cAMP-PKA: Cyclic Adenosine Monophosphate-Protein Kinase A

CAMP/ LL-37: Cathelicidin antimicrobial peptides

CC: Cellular component

CCL: Chemokine C-C motif ligand

cDNA: complementary DNA

CFU: Colony forming units

CFW: Calcofluor white

CGD: *Candida* genome database

ChAT: Choline acetyltransferase

CHX: Chlorhexidine

CLEC7A: C-type lectin domain family 7 member A

CLRs: C-type lectin receptors

COPD: Chronic obstructive pulmonary disease

CR: Complementary receptors

CrAT: Carnitine acetyltransferase

CREB: cAMP response element-binding protein

CRISPR: Clustered regularly interspaced short palindromic repeats

CSP: Caspofungin

CV: Crystal violet

CXCL8: Chemokine IL-8

DAG: Diacylglycerol

DC: Dendritic cell

DE: Differential expression

DMEM: Dulbecco's modified eagle's medium

DMSO: Dimethyl sulfoxide

DPBS: Dulbeco's phosphate buffered saline

DRF: Damage response framework

DS: Denture stomatitis

DSC: Deep seated candidiasis

ECM: Extra cellular matrix

eDNA: Extracellular DNA

EGF: Epithelial growth factor

EIP: Electrical impedance profile

ELISA: Enzyme linked immunosorbent assay

FA: Fulvic Acid

FBS: Fetal bovine serum

FM: Fluorescent microscopy

G-CSF/CSF3: Granulocyte-colony stimulating factor

G-proteins: Guanine nucleotide binding proteins

G. mellonella: Galleria mellonella

GAPDH: Glyceraldehyde 3-phosphate dehydrogenase

GCN: General amino acid control system

gDNA: Genomic DNA

GDP: Guanosine diphosphate

GM-CSF/CSF2: Granulocyte macrophage colony stimulating factor

GO: Gene ontology

GPA2: Guanine nucleotide-binding protein alpha-2

GPCR: G-protein coupled receptors

GPI: Glycosylphosphatiylinositol

GPR1: G protein-coupled receptor 1

GTP: Guanosine triphosphate

H & E: Haematoxylin and eosin stain

HBF: High biofilm former

HDC: Hematogenously disseminated candidiasis

Hgc1: Hyphal G1 cyclin

HIV: Human immunodeficiency virus

HK: Heat killed

HMDS: Hexamethyldisilazane

HOE: Human oral epithelium

IAC: Intraabdominal candidiasis

ICL1: Isocitrate lyase

IFN-y: Interferon gamma

IgG: Immunglobulin G

IL- ß: Interleukin-ß

IL-1α: Interlukin-1α

IL-1ß: Interleukin-1ß

IL-2: Interleukin-2

IL-6: Interlukin-6

IL-8: Interlukin-8

iNOS: Inducible nitric oxide synthase

IP_3: Inositol triphosphate

JF: J 104129 fumarate

KSFM: Keratinocyte serum-free medium

LBF: Low biofilm former

LCMV: Lymphocytic choriomeningitis virus

LDH: Lactate dehydrogenase

LIP: Secreted lipase

mAChR: Muscarinic acetylcholine receptor

MAPK: Mitogen-activated protein kinase

MCP-1: Monocyte chemoattractant protein 1

MF: Molecular function

MOI: Multiplicity of infection

mRNA: Messenger RNA

nAChR: Nicotinic acetylcholine receptor

NO: Nitric oxide

nTARs: Novel transcriptionally active regions

OPC: Oropharyngeal candidiasis

OVA: Ovalbumin

PAMP: Pathogen-associated molecular pattern

PAS: Periodic acid schiff

PBS: Phosphate Buffer saline

PCA: Principal component analysis

PCR: Polymerase chain reaction

PD: PD 102807

PHCl: Pilocarpine hydrochloride

PHO: Phosphate responsive signaling pathway

PI: Propidium iodide

PKC: Protein kinase C

PLB: Phospholipase B

PLC: Phospholipase C

PMA: Phorbol 12-myristate 13-acetate

PMBCs: Peripheral blood mononuclear cells

PMN: Polymorphonuclear neutrophil

PRRs: Pattern recognition receptors

PTX: Pertussis toxin

QS: Quorum sensing

RHE: Reconstituted human epithelium

RNA-Seq: RNA sequencing

ROS: Reactive oxygen species

RPMI1640 media: Roswell Park Memorial Institute-1640 media

RT: Room temperature

S. cerevisiae: Saccharomyces cerevisiae

SAP: Secreted aspartic protease

SCF: Skp1-cullin-F-box

SCP: Scopolamine

SDA: Sabouraud dextrose agar

SEM: Scanning electron microscopy

SIB: SIB 1508Y Maleate

SOD: Superoxide dismutase

SSA_1: Stress-Seventy subfamily A_1

TLR: Toll-like receptor

TMB: 3,3',5,5'-tetramethylbenzidine

TNF-α: Tumor necrosis factor alpha

TPRC1: Target of rapamycin complex 1

UBI4: Polyubiquitin

VSV: Vesicular stomatitis virus

Vu: Vu 0238429

VVC: Vulvovaginal candidiasis

XTT: 2,3-bis (2-Methoxy-4-nitro-5-sulfo-phenyl)-2 *H*-tetrazolium-5-carboxanilide

YM: YM 254890

YPD: Yeast extract peptone dextrose

1 General introduction

1.1 *Candida albicans*

Candida albicans (*C. albicans*) is a member of the normal microbiome in human body. It belongs to the Kingdom Fungi, Subkingdom Dikarya, Phylum *Ascomycota*, Subphylum *Saccharomycotina*, Class *Saccharomycetes*, Subclass *Saccharomycetidae*, Order *Saccharomycetales*, family *Metschnikowiaceae*, genus *Candida*, and species *albicans* (Gow and Yadav, 2017, Ali et al., 2018, Mayer et al., 2013). The genus *Candida* is made up of approximately 154 species, with *C. albicans* considered as the most abundant and significant species. It is a pleiomorphic opportunistic fungal pathogen that grows in variable morphological forms; either as a unicellular budding yeast cell, an elongated bud daughter cell (pseudohyphae) or as true hyphae (Figure1.1) (Sudbery et al., 2004, Sardi et al., 2013).

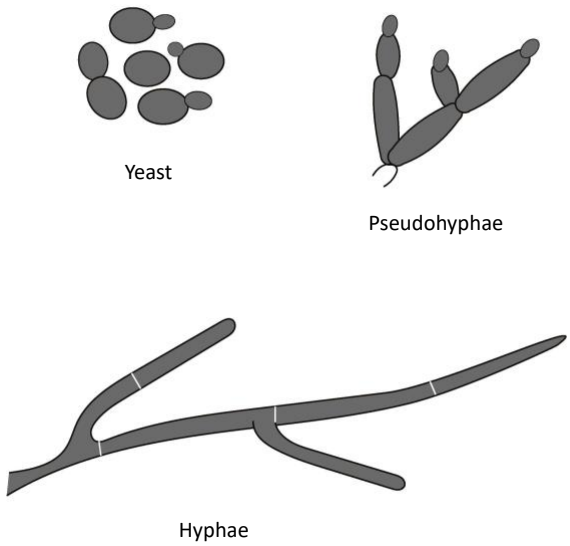

Figure 1.1 *C. albicans* morphology. Schematic of each morphology. Adapted from (Thompson et al., 2011).

C. albicans is adapted for commensalism at different mucosal surfaces of the human body such as the urinary tract, the gastrointestinal tract, the oesophagus, the vagina, the oral cavity, and the skin (Sardi et al., 2013, da Silva Dantas et al., 2016). However, *C. albicans* capable of causing serious infections such disseminated disease which is a clear indication of it's property as a pathogen

(Dadar et al., 2018). *C. albicans* is considered to be the most common pathogen among the 15 infectious agents of the *Candida* species and a major cause of invasive candidiasis (Prasad, 2017, Sardi et al., 2013, Yapar, 2014). *C. albicans* possesses several virulence factors that manifest in immunocompromised individuals such as intensive care unit patients and human immunodeficiency virus (HIV) patients (Kurzai, 2013).

Understanding the clinical risk factors for invasive candidiasis may aid in the prevention of mortality associated with those infections. Several risk factors can increase the risk of *Candida* species associated candidiasis which can be divided into two groups: health care associated factors such as wide spectrum antibiotics utilization, organ transplantation, and internal prosthetic devices and catheters. The other group is host related factors including age, chemotherapy, malignancies, and immunosuppressive diseases (Yapar, 2014). For example, research conducted by Cheng et al. (2005) investigated the risk factors of candidemia cases at Veterans General Hospital-Taipei, they found that age, intensive care surgeries, and an acute sepsis were the most important risk factors (Table 1.1). Another study by Shigemura et al. (2014) showed that postoperative status and cardiovascular diseases were the significant risk factors in *C. albicans* associated candidemia cases compared to other risk factors such as chemotherapy and cancer (Table 1.2). Overgrowth of *C. albicans* causes a broad spectrum of diseases, ranging from superficial mild infections such as oropharyngeal candidiasis (OPC) and vulvovaginal candidiasis (VVC), to severe invasive infections such as bloodstream infections (BSIs) (Yapar, 2014, Prasad, 2017).

Table 1.1 Characteristics of *C. albicans* associated bloodstream infection cases. Adapted from (Cheng et al., 2005).

Patient characteristics	Numbers (68)	%	P- Value
Central venus catheter	57	83.8	0.025
Age ≥ 65 years old	56	82.4	0.004
Sepsis/leukocytosis	Total= 67		0.0004
White blood cells count:			
≤ 3000/mm^3	4	6	
3000/mm^3 to 5000/mm^3	35	52.2	
> 15000/mm^3	28	41.8	
Bacterial urinary tract infection	23	33.8	0.026
Parenteral nutrition	50	73.5	0.029

Table 1.2 Risk factors of *C. albicans* associated bloodstream infection cases. Adapted from (Shigemura et al., 2014).

Patient characteristics		Numbers (61)	%	P- Value
Postoperative status	(-)	27	44.3	0.012
	(+)	34	55.7	
Cardiovascular diseases	(-)	43	70.5	0.018
	(+)	18	29.5	
Chemotherapy	(-)	58	95.1	0.032
	(+)	3	4.9	
Cancer	(-)	44	72.1	0.047
	(+)	17	27.9	
Age	≤ 70	23	37.7	0.048
	> 70	38	62.3	

1.2 Epidemiology

C. albicans is the causal agent of candidiasis which can be classified depending on the main site of infection such as vaginal candidiasis, oropharyngeal candidiasis, and the invasive candidiasis (Antinori et al., 2016, [CDC], 2021).

Vulvovaginal candidiasis (VVC) is one of the most common types of genitourinary candidiasis that affects healthy women, and the second most common genital infection (Prasad, 2017). Vaginal candidiasis is responsible for at least 1.4 million outpatient visits annually in the USA ([CDC], 2021). Normally, *C. albicans* inhabits the vaginal lumen asymptomatically. Yet, fungal overgrowth and epithelial invasion can result in symptomatic infection with the following symptoms: vaginal burning, redness, pain, and itching, which is often accompanied with vaginal discharge (Willems et al., 2020). The severity of VVC ranges from sporadic mild infections to recurrent severe infections where the latter may cause anxiety, low self-esteem and depression, affecting the sufferer's psychosocial life considerably (Brocklebank and Maraj, 2013). Although it is difficult to conclude the prevalence of VVC due to women's tendency to self-medicate, in the primary care setting about 40% of genital complaints are diagnosed as VVC infections. Furthermore, about 75% of all women have had VVC at least once during their reproductive age of 20 – 40 years, and 5 – 8% may suffer from recurrent infections (Brocklebank and Maraj, 2013, Prasad, 2017). Under normal conditions, *C. albicans* represents part of the normal flora in 20% of women. However, 90% of VVC infections are caused by *C. albicans*, and susceptibility to VVC is influenced by several risk factors such as use of drugs (contraceptives and antibiotics), diabetes and pregnancy (Brocklebank and Maraj, 2013, Sobel et al., 1998).

Oropharyngeal candidiasis (OPC) is another common type of mucocutaneous candidiasis infection that is primarily caused by *C. albicans* invading the oral epithelium (Laudenbach and Epstein, 2009, Swidergall and Filler, 2017). A lack of specific epidemiological surveillance studies of candida infections of the mouth and throat make it difficult to determine the exact number of people affected in the United States ([CDC], 2021). Nonetheless, the risk of these infections is heightened in patients with pre-existing medical conditions. For

instance, candidal infection of the mouth and throat is common in individuals with advanced HIV/AIDS, with evidence reporting that 99 of 122 AIDS patients using antiretroviral therapy (ART) in Texas (81.1%) were identified with oral yeast colonization and (33.3%) of these patients had symptomatic infection (Thompson et al., 2010). Similarly, different incidents of oral candidiasis were reported in AIDS patients such as; 43/55 (83%) in Brazil, 227/286 (79.4%) in Cote d'Ivoire, 27/141 (19.1%) in India, and 38/50 (76%) in Lebanon (Patil et al., 2018). Although OPC is considered to be a superficial fungal infection, infected patients suffer from significant morbidity which is presented as erythema, oral thrush and oedema (Laudenbach and Epstein, 2009, Kurzai, 2013). In immunosuppressed individuals, untreated OPC may lead to systemic candidiasis that causes a high mortality rate. Furthermore, it may initiate the dissemination of the infection from the oropharynx to the oesophagus, which may affect food consumption causing weight loss (Laudenbach and Epstein, 2009, de Repentigny et al., 2004).

C. albicans on mucosal surfaces can shift from being commensal to pathogenic when an individual is predisposed to several risk factors, which include local factors (hypofunction of the salivary gland and smoking cigarettes), systemic factors (immunosuppressed patients and diabetics), and medical management factors (use of wide spectrum antibiotics and cancer chemotherapy) (Laudenbach and Epstein, 2009, Samaranayake et al., 2009). Invasive candidiasis is a life-threatening infection in which *C. albicans* disseminates from the original infection site to colonise different parts of the human body, such as the eye, brain, cardiac tissue, kidneys, and bone among other parts of the body ([CDC], 2021, Kullberg and Arendrup, 2015, Nobile and Johnson, 2015, Kaufman et al., 2019). *C. albicans* is found to be the leading cause of invasive candidiasis in hospitalised individuals, the fifth highest hospital-acquired pathogen, and the fourth most frequent pathogen causing BSIs (Zaoutis et al., 2005, Yapar, 2014). In the United States, a study was conducted in 2000 to assess mortality outcomes of candidemia among pediatric and adult patients, and it revealed a mortality rate of 10.1% and 14.5% in children and adults, respectively (Zaoutis et al., 2005). Moreover, the estimated life-threatening *C. albicans* invasive infections per year worldwide was > 400,000 with mortality rates of 46% – 75% (Brown et al., 2012).

Similarly, a case-control study investigated mortality excess, length of hospitalization and treatment costs in the candidemia population found an overall high mortality rate of 19% – 24%, a crude mortality rate of 39% – 42%, total hospital charges of $ 6,000 to $ 29,000, hospitalization costs of $ 3,000 to $ 22,000 and hospitalization length of 3 – 13 days (Morgan et al., 2005). Invasive candidiasis has been reported to have 20 – 30 times higher prevalence in South Asian countries as compared to the western world. The highest incidence of candidemia (8.91/1000 admissions) was found in North India, and the lowest (3.61/1000 admissions) in South India. This was due to the low quality of hospital care practice in public hospitals where there are high numbers of patients, inadequate potentials to provide disposables, and high rates of yeast carriage (46 – 82%) by health care providers (Prasad, 2017). Globally, invasive candidiasis affects at least 250,000 people around the globe annually and leads to a minimum of 50,000 deaths (Ksiezopolska and Gabaldón, 2018, Kullberg and Arendrup, 2015). In addition, it is the infection that is commonly reported among the critically ill patients admitted to intensive care units with up to 50% morbidity and mortality rates (Rajendran et al., 2016a, Cortés and Corrales, 2018, Zhang et al., 2020). In the USA, the ([CDC], 2021) reported that at least 9 in every 100,000 people were diagnosed with invasive candidiasis between 2013 and 2017, and that there are approximately 25,000 cases of candidemia every year.

The most common form of invasive candidiasis is candidemia, in which the organism invades the bloodstream. The key patient groups at risk of invasive candidiasis include those who undergo stem cell and organ transplant, patients with granulocytopenia, patients on aggressive chemotherapy, patients who require central venous catheterization and patients who require lengthy stays in the intensive care units (ICU) and advanced life support ([CDC], 2021, Cortés and Corrales, 2018, Tsui et al., 2016). *C. albicans* is the main cause of the invasive fungal infections and acknowledged as a significant public health problem linked with cumulative economic and medical implications because of it's high cost of care and high mortality rates. It is known to be responsible for 50% of invasive candidiasis infections and results in high mortality rates (40 – 60%) (Quindós et al., 2018, Pfaller and Diekema, 2007, Prasad, 2017). In North American centres, an evaluation of the epidemiology of candidemia revealed that 45.6% of

candidemia incidents were due to *C. albicans* infections, with an overall 35.2% crude mortality rate (Horn et al., 2009).

1.3 Pathogenicity

Pathogenicity of *C. albicans* is attributed to several fitness characteristics and virulence factors that enable *C. albicans* to resist antifungal treatments, adapt to environmental stress, and circumvent the host immune system (Kurzai, 2013, da Silva Dantas et al., 2016). Fitness traits include metabolic flexibility, rapid adaptation to fluctuations in environmental pH, and powerful nutrient acquisition systems. Virulence factors include the morphological transition between yeast and hyphal forms (phenotypic switching), filamentation, biofilm formation and the expression of adhesins and invasins (Kurzai, 2013, Ene et al., 2012).

1.3.1 Fitness traits

1.3.1.1 Metabolic flexibility

C. albicans is metabolically flexible as indicated by it's adaptation to limitations in nutrient availability during the infection process and it's capacity for exploiting the host's sources of nutrition to survive. For instance, when *C. albicans* is engulfed by a phagosome it is exposed to an environment with inadequate nutrients, and the fungus therefore transitions from glycolysis to gluconeogenesis, activating the glyoxylate cycle, which plays a vital role in *C. albicans* pathogenicity (Kurzai, 2013, Ene et al., 2012). The ideal source of carbon for *C. albicans* is glucose, however, in niches that are glucose starved the fungus still can survive due it's ability to utilize other available host elements as non-glucose carbon sources through the secretion of extracellular enzymes. Secreted enzymes, for example, lipases and phospholipase B (PLBs), can degrade host lipids and phospholipids to obtain carbon. In addition, secreted aspartic proteases (SAPs) hydrolyse host proteins to provide sources of carbon and nitrogen by releasing peptides and amino acids (Kurzai, 2013).

The flexibility of *C. albicans* in growing on alternative sources of carbon instead of glucose, for example, oleic acid, galactose or pyruvate, influences it's

virulence by increasing it's resistance to antifungal treatments and environmental stress (osmotic and cell wall stress). This effect is due to alterations in the cell wall construction resulting in a smaller cell volume and a more rigorous cell wall, thus leading to osmotic stress endurance. However, it does depend on the infection site, for instance growth on oleic acid as a carbon source increases it's virulence in vaginal infections but reduces virulence in systemic infections. Furthermore, growth on lactate and subsequent cell wall remodelling increases it's resistance to antifungal drugs (Kurzai, 2013, Ene et al., 2012).

1.3.1.2 Key stress responses in *C. albicans*

C. albicans has adapted several mechanisms through which stress responses to key stressors were tuned to host surrounding environment. Heat shock response is regulated by the heat shock transcription factor Hsf1, which is important for viability. *C. albicans* responds to acute heat shock by Hsf1 phosphorylation and heat shock protein (*HSP*) genes expression, which leads to targeting proteins for refolding or degradation. In response to heat shock stress, other genes involved are polyubiquitin (*UBI4*) expression, which is required for resistance to thermal stress. In addition, the expression of *HSP90* gene in an Hsf1-dependent fashion, which modulates interacts with Hsf1 and downregulate the heat shock response after adaptation (Brown et al., 2014a).

Another pathway regulates stress responses such as osmotic and cationic stresses in *C. albicans* is Hog1. *C. albicans* exposure to osmotic and cationic stress may lead to cell size reduction due to water loss. This stress triggers the phosphorylation and accumulation of the stress-activated protein kinase (SAPK) Hog1. Hog1 pathway is a component of the mitogen-activated protein (MAP) kinase pathways. In *C. albicans*, activation of the (MAPK) is mediated by the MAP kinase kinase (MAPKK) Pbs2, which is activated by MAP kinase kinase kinase (MAPKKK), Ssk2. The Hog1 pathway is involved in cell wall functionality, adaptation to other stresses, and modulating cellular morphogenesis (Brown et al., 2014a).

C. albicans cell wall is an important component as being the first to encounter different stresses in the host niches, for instance, chemicals such as Calcofluor White, and antifungals such as caspofungin. *C. albicans* is equipped with different pathways that contribute to cell wall stress resistance and adaptation. The Hog1 pathway contributes to cell wall stress and regulates chitin biosynthetic functions. In addition, the cell integrity pathway (MAPK Mkc1 pathway), and the morphogenetic pathway (MAPK Cek1 pathway). The activation of Mkc1 is mediated via protein kinase C (Pkc1) signalling, and it's disruption results in cell wall stresses sensitivity. The activation of Cek1 pathway is mediated in response to cell wall damage via the cell surface sensor Msb2. The inactivation of Cek1 pathway components can inhibit filamentation and results in cell wall stresses sensitivity (Brown et al., 2014a).

C. albicans resistance to reactive oxygen species (ROS), is dependent on transcription factor Cap1, which targets detoxification of oxidative stress genes such as catalase and superoxide dismutase: *CAT1* and *SOD1*, glutathione synthesis genes such as gamma-glutamylcysteine synthetase: *GCS1*, redox homeostasis and oxidative damage repair genes such as glutathione reductase and thioredoxin: *GLR1* and *TRX1*. Those genes involved in detoxifying ROS and mediating stress response. The Hog1 MAPK pathway was also found to be involved in oxidative stress resistance since inactivation of Hog1 and the upstream key regulators rendered *C. albicans* sensitive to oxidative stress. Furthermore, inactivation of ROS detoxification genes attenuated the *C. albicans* virulence, and *cap1Δ* and *hog1Δ* mutants led to killing the fungus more effectively by phagocytes. Furthermore, *C. albicans* exposure to reactive nitrogen species (RNS) may lead to molecular damage, and the fungus responses to this stress by activating oxidative stress functions genes such as catalase (*CAT1*), glutathione-conjugating and -modifying enzymes, NADPH oxidoreductases and dehydrogenases, and *YHB1* expression *YHB1* gene encodes major nitric oxide dioxygenase which is responsible for nitric oxide detoxification (Brown et al., 2014a).

1.3.2 Virulence factors

1.3.2.1 Biofilm formation

Biofilm formation is an important process during the pathogenesis of *C. albicans* and a key virulent trait of the microorganism. The majority of the diseases resulting from *C. albicans* infections are associated with it's ability to form biofilms, and it is the most prolific of all species to form biofilms.

A biofilm can be defined as an organized three-dimensional complex microbial community embedded in an extracellular matrix (ECM) and attached to a biotic or abiotic surface (Andes et al., 2004). *C. albicans* biofilms consists of a basal layer for attachment, spheroid yeast cells, pseudohyphae (which are wide filaments with constrictions at the septal junction, mother bud neck, and no parallel sides) and true hyphae (long branching filaments of tubular cells with parallel walls and no constrictions at the septal junction). Another component of the biofilm matrix is extracellular DNA (eDNA), which plays a significant role in biofilm integrity and antifungal resistance by supporting the heterogeneity of the biofilm (Rajendran et al., 2014, Prasad, 2017, Martín and Di Pietro, 2012, Ghannoum et al., 2015).

Biofilm formation in *C. albicans* often takes place in a sequential manner over a period of 24 - 48 hours (Wall et al., 2019, Tsui et al., 2016). There are several stages in biofilm formation, summarized in (Figure 1.2), each stage making a contribution to virulence and disease establishment. First is the adherence step, in which single yeast cells adhere to abiotic or biotic surfaces forming the basal layer of yeast cells. Second is the initiation step, in which successful yeast cell adhesion would then induce cell proliferation and filamentation; whereby the attached cells develop into elongated projections. This process results in the formation of filamentous hyphal forms that penetrate the host epithelial tissues through two processes: endocytosis and active penetration. Endocytosis is a host-driven process, where the hyphal invasion triggers the host's immune system causing hyphae endocytosis into the host cells; this process does not require viable hyphae as even killed hyphae can be endocytosed. In contrast, active penetration is a fungal-driven process that requires viable fungal hyphae. The third step is the maturation stage: this stage involves the biofilm's

maturation and the production of an extracellular polysaccharide matrix. Finally, in the dispersal step, non-adherent yeast cells would disperse from the biofilm into the surrounding environment and colonize new surfaces (Tsui et al., 2016, Kurzai, 2013, Martín and Di Pietro, 2012, Gow et al., 2017). Therefore, the yeast form of the species allows for it's successful initial attachment and dissemination whereas the filamentous hyphal state allows *C. albicans* to successfully invade host tissues.

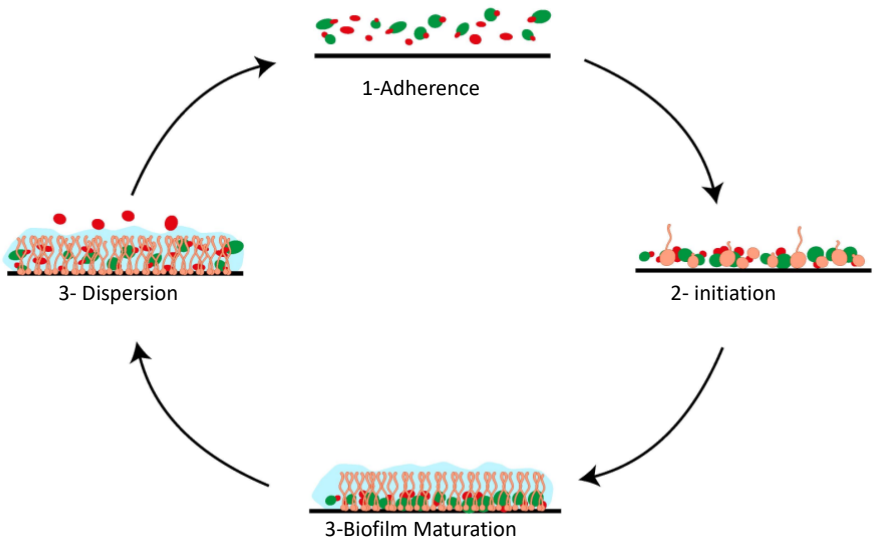

Figure 1.2 Biofilm formation stages. 1-Yeast cells adherence to the surface. 2- Cell proliferation and filamentation initiation. 3- Filamentation, biofilm formation maturation and extracellular matrix production. 4- Yeast cells release and dispersal from the biofilm to seed new surfaces. Adapted from (Nobile and Johnson, 2015).

The extracellular matrix in *C. albicans* biofilm is often complex with a large percentage of it's polysaccharide constituents being ß-1,6 glucan, α-mannan and the ß-1,3 glucan (Tsui et al., 2016, Zarnowski et al., 2014, Mathé and Van Dijck, 2013). Previous studies have associated the ß-1,3 glucan with the increased cases of antimicrobial resistance in *C. albicans* (Mathé and Van Dijck, 2013, Nett et al., 2007, Lima et al., 2019). Another important phenomenon that plays a central role in biofilm formation is cell-to-cell communication or quorum sensing, which also contributes to antifungal resistance. The phenomenon is associated with the postulation that the microbial responses or behaviours within the biofilm are overseen by the cell density, which is primarily mediated through the secretion of signaling molecules such as farnesol. Farnesol is an

extracellularly produced molecule, accumulates in maturing biofilms, and inhibits filamentation (Ramage et al., 2002, Yu et al., 2012, Kovács and Majoros, 2020).

Contributory factors, such as pH levels, serum, accessibility of amino acids, temperature and the presence of carbon dioxide, have been determined to help in triggering the occurrence of hyphal morphogenesis and biofilm formation, which is a key process that protects the *C. albicans* from being destroyed by the host phagocytic cells (Mba and Nweze, 2020).

1.3.2.2 Expressions of adhesins and invasins

During the process of colonization and biofilm formation, several virulence factors are employed by the fungus to facilitate infection. These enzymes are crucial elements in the invasion stage as they are involved in the damage and degradation of host tissue and nutrient acquisition (Schaller et al., 2005, Pandey et al., 2018).

Notably, Candidalysin, a cytolytic 31 amino acid peptide toxin that is derived from the gene *ECE1*, is a hyphal-specific protein and is the first toxin found in this human fungal pathogen. It is crucial for mucosal infection, fungal invasion, host cell damage, systemic infection, and epithelial immune cell response (Talapko et al., 2021, Chen et al., 2021, Naglik et al., 2019). At the interface with the epithelial cell membrane, the interaction with the candidalysin results in inflammation, membrane damage, and eventual destruction of the host tissue. Candidalysin can invade the epithelial membrane through creating pores and leading to the release of lactate dehydrogenase (LDH) and calcium influx. Thus, inducing the host immune response and activating chemokine and cytokine secretion (Swidergall et al., 2019, Chen et al., 2021). This toxin also facilitates the ability for the fungus to evade killing by macrophage phagocytosis. It plays a role in the activation of the NLRP3 inflammasome, and mediating interleukin-ß (IL-1ß) maturation and secretion in a caspase-1–dependent manner. This characteristic confers candidalysin as a characteristic of immunomodulatory molecule (Kasper et al., 2018).

Another virulence factor are adhesins and the increased expression and activation of transcription factors which control the expression of genes involved in filamentation, such as the hyphal G1 cyclin (*HGC1*). The capacity of *C. albicans* to produce a family of cell-wall adhesins called agglutinin-like sequences (ALS) allows for it's attachment to host tissues. For instance, *ALS3*, the hyphae-associated adhesion, is responsible for *C. albicans'* adherence to host surfaces or bacterial cells in mixed species microbial communities. Hyphal wall protein 1 (Hwp1) is another important adhesin that is expressed during the filamentation process and facilitates the attachment of *C. albicans* in the initial stages of biofilm formation. Other transcription factors are: Efg1, Tec1, Bcr1, Ndt80, Rob1 and Brg; which are involved in adhesion, biofilm formation regulation, ECM production and biofilm antimicrobial resistance. These roles are mediated by a circuit of transcription factors controlling the expression of each other and activating or suppressing pertinent target genes (Figure 1.3) (Prasad, 2017, da Silva Dantas et al., 2016, Tsui et al., 2016, Kurzai, 2013, Martín and Di Pietro, 2012).

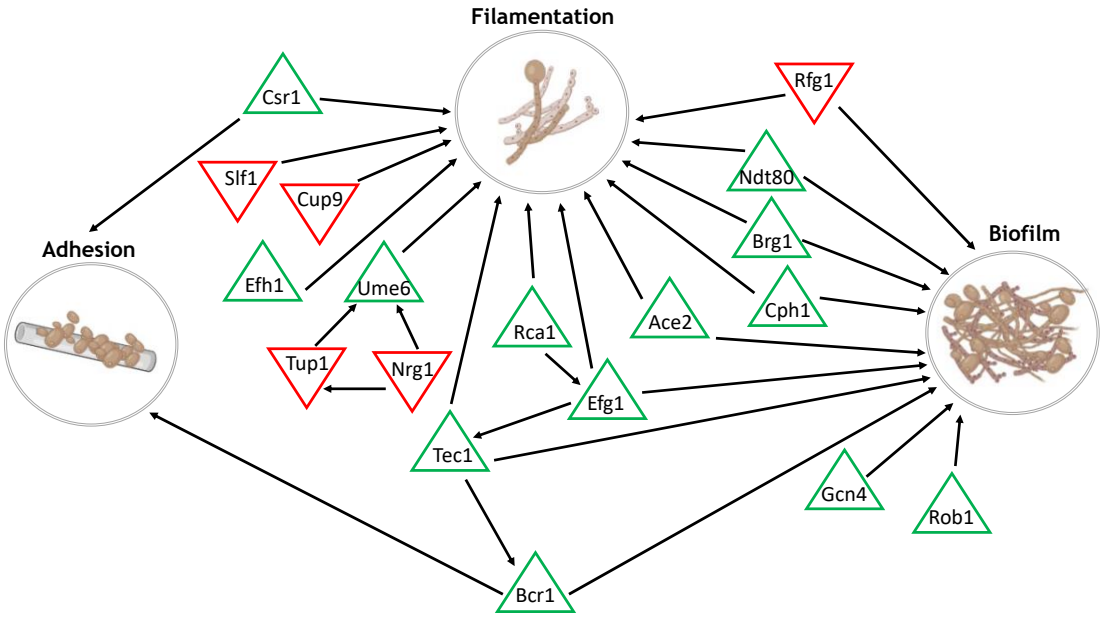

Figure 1.3 Circuit of transcription factors controlling virulence traits. The figure highlights the transcriptional factors involved in adhesion, filamentation, and biofilm formation. Green triangles indicate activators and red triangles indicate repressors. Arrows indicate the correspondence and participation of the transcription factor to the virulence trait. Adapted from (Cavalheiro and Teixeira, 2018).

1.3.3 Morphological transition

1.3.3.1 Cell wall plasticity

Morphogenesis in *C. albicans* includes the transition from white to opaque cells and the transition from yeast cells to pseudo-hyphae or true hyphae (Martín and Di Pietro, 2012). Yeast-hyphae switching in *C. albicans* is a key virulence factor that contributes to the fungal fitness and pathogenicity, and promotes biofilm formation. In order to facilitate phenotypic switching *C. albicans* demonstrates cell wall plasticity.

The *C. albicans* cell wall constitutes 30 - 50% of the cell dry weight and is an essential structure of the cell for several reasons: (1) it provides contact with the surrounding environment, (2) it provides protection, shape, integrity, and stability to the cell, and (3) it plays a critical role in commensalism and pathogenicity of the fungus since it contains the adhesins and molecules that are required for both lifestyles and for immune recognition by the host. *C. albicans* cell wall components are unique and not present in human cells, which confers

the cell wall additional importance as a putative therapeutic target for novel drug development (Kurzai, 2013, Gow et al., 2017)

C. albicans does not have a static structured cell wall, but a dynamic one that allows it to undergo compositional remodelling in order to adapt to the surrounding environment (Ikezaki et al., 2019, Reyna-Beltrán et al., 2019). The elasticity of the *C. albicans* is mainly influenced by the presence of fibrous and gel-like carbohydrate polymers which form a tensile and robust core framework onto which proteins and superficial components are added to make it stronger and flexible (Lima et al., 2019).

Biosynthesis of cell wall components in *C. albicans* vary depending on growth form, stage, and condition with most variability in the outermost layer (Calderone and Braun, 1991, Gow et al., 2017). Generally, the *C. albicans* cell wall comprises of 10% protein and 90% polysaccharide, which includes O-linked and N-linked mannosylated glycoproteins (mannoproteins), ß- 1,3 and 1,6 glucans, and chitin. These key components have been primary targets for discovering and developing new drugs in recent years (Ikezaki et al., 2019, Reyna-Beltrán et al., 2019). Overall, two different layers of the *C. albicans* cell wall can be distinguished by electron microscopy. The outer layer of the *C. albicans* cell wall was determined to be around 150 nm in width. The internal layer is of a similar size and primarily composed of chitin and polysaccharide matrix and is highly electron translucent compared to the outer layer, which is mainly enriched with mannoproteins. This layer is composed of additional thin electron-dense layer which is placed next to the cell membrane (Gow et al., 2017, Reyna-Beltrán et al., 2019, Chaffin, 2008). In terms of the structure, the outer layer of the cell wall always has vertically aligned fibrils of different lengths with surface hydrophobicity. The organization of the cell wall into different layers is important for it’s integrity and promotes it’s ability to protect the internal components (Chaffin, 2008, Reyna-Beltrán et al., 2019) (Figure 1.4).

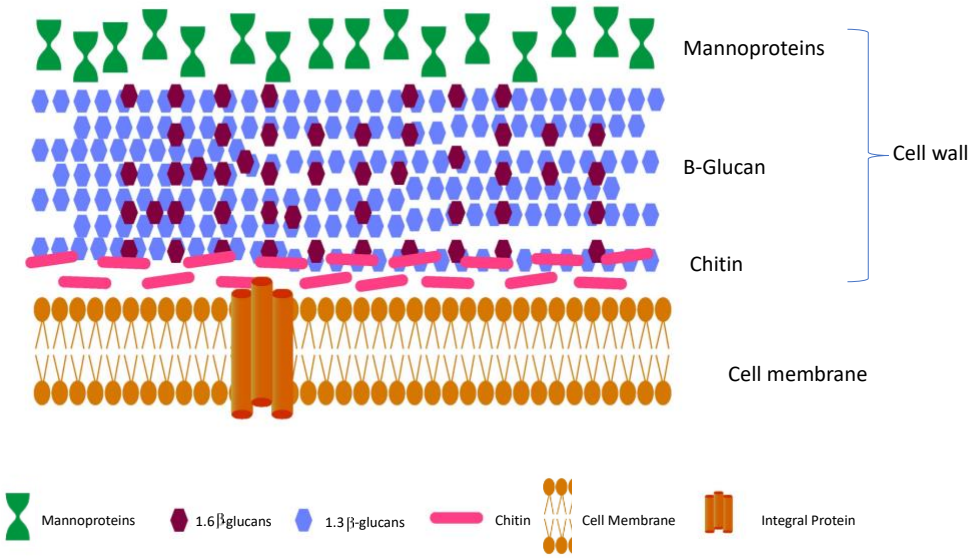

Figure 1.4 Cell wall structure. The outer layer enriched with mannoproteins, and the inner layer composes of polysaccharides and chitin. Adapted from (Anwar et al., 2017).

The inner layer of the *C. albicans* cell wall is made up of the structural skeleton while the outer layer is considerably heterogeneous and structured to meet the physiological needs of the microorganism. The inner layer of *C. albicans* cell wall is comprised of expediently attached ß-1,3 glucan with between 3 - 4% interchain and chitin. In this layer, ß-1,3-glucans are the most abundant molecule in *C. albicans*, which is linked to ß-1,6-glucans connecting the inner and outer cell wall. The outer wall mainly repleted with mannoproteins, which correspond to about 40% of the *C. albicans* cell wall contents and consider to be important in immune evasion as it is the first defense line interacting with host immune system (Reyna-Beltrán et al., 2019, Garcia-Rubio et al., 2020). Embedded within the *C. albicans* cell wall is a host of different virulence factors that enhance adherence, cell damage and invasion, and which it also uses for sensing and evading the host immune system (Reyna-Beltrán et al., 2019, Gow and Hube, 2012).

Key cell wall proteins include Glycosylphosphatidylinositol (GPI) anchored cell wall proteins, transglycosidases, yapsins, adhesins and the hydrophobins. Adhesins facilitate the attachment of *C. albicans* to host tissues. Yapsins facilitate remodelling of the cell wall and maintenance of shape. Hydrophobins have the ability to self-assemble to form rodlets and generate a hydrophobic

interface between *C. albicans* and it's environment. The cell wall also contains proteins that cross-link other cell wall proteins to each other. The main cross linkers of cell wall components are Phr family members. Namely, *C. albicans* has five genes encoding members of this family: *PHR1*, *PHR2*, *PHR3*, *PGA4*, and *PGA5* genes. In addition, the protein ß-1,3 glucanases acts as linker molecules, cross linking ß-1,3- glucan and ß-1,6-glucan (Reyna-Beltrán et al., 2019, Gow et al., 2017).

1.3.3.2 Environmental triggers of morphogenesis

All of the organisms, including higher eukaryotes, bacteria and yeast, have different strategies that they use to respond to the changes within their environments (Biswas et al., 2007). Host environmental niches expose *C. albicans* to a variety of different stressors. *C. albicans* has, therefore, developed robust mechanisms for coping with environmental stress. One crucial characteristic of *C. albicans* pathogenesis is it's evolution of environmental stress adaptation, this characteristic enabled the fungus to compensate for different limitations and survive host niches. Thus, *C. albicans* has developed stress response machinery to overcome environmental stresses, and in response to that the fungus undergo morphogenesis. A large range of environmental cues can affect *C. albicans* morphogenesis and promote hyphae formation or maintain the yeast form, such as nutrient availability, amino acids depletion, CO_2, temperature, oxidative stress, pH levels, and metals availability (e.g. iron) (Mayer et al., 2013, Brown et al., 2014b).

Amino acids act as an alternative source of carbon, a key source of nitrogen, and as a ligand for the membrane receptors regulating the virulence and cellular morphology in *C. albicans* (Biswas et al., 2007, Garbe and Vylkova, 2019, Brown et al., 2014a). *C. albicans* growth on amino acids as a carbon source confers the fungus more resistance to environmental stresses and increases it's virulence (Kurzai, 2013). The fungus has several sources of amino acids within the host, and *C. albicans* is equipped with hydrolase enzymes (secreted aspartyl proteinase gene family) to convert and break proteins into peptides and amino acids, which can be taken up by peptide transporters and amino acid permeases (Kraidlova et al., 2016). Extracellular amino acids can be sensed by *C. albicans*

through different systems, such as Csy1 sensor, a homolog of the yeast protein Ssy1; the general amino acid permease Gap1, which has dual roles as sensor and transporter; the GPCR Gpr1, which plays a role in sensing methionine; and Mep2 which acts as protein transceptor and ammonium sensor and transporter (Biswas et al., 2007).

In amino acid depleted niches, *C. albicans* will be stressed by deficiency in nitrogen uptake, which is important in growth and morphogenesis. A study by Han et al. (2019), revealed that in single gene knock out mutants of *gdh2Δ* and *gdh3Δ*, glutamate dehydrogenases involved in nitrogen metabolic pathways resulted in yeast morphology in proline medium as the sole carbon and nitrogen source. In addition, the *gdh2/gdh2Δ* mutant revealed to be unable to grow on arginine or proline as the sole carbon and nitrogen source. In cases of amino acids starvation, *C. albicans* stimulates morphogenesis and general amino acid control system like response (GCN) such as in *Saccharomyces cerevisiae*. These responses are regulated by, Gcn4, a general amino acid control involved in amino acid metabolism and filamentation regulation (Biswas et al., 2007). On the other hand, cyclin *PCL5* in *C. albicans*, which is *PHO85* cyclin homolog in *Saccharomyces cerevisiae*, plays a role in modulating *C. albicans* filamentation in amino acid rich media (Gildor et al., 2005). This study showed that *PCL5* plays a role in Gcn4 degradation and a *pcl5Δ* mutant exhibited strongly reduced filamentation with shorter and less efficient hyphae.

In *C. albicans*, it is believed that the loss of Csy1, an amino acid sensor, may negatively impact the amino acid-mediated activation and inadequate induction of the transcription of particular amino acid permease genes; hence limiting the success of morphogenesis. In addition to being an essential functional homolog for the budding yeast genes, *C. albicans* Gap1 transporter, an amino acid permease, may also initiate the signaling of the transduction pathways which would eventually lead to the morphogenesis and virulence of *C. albicans*. Ammonium permeases Mep1 and Mep2, mediate the ammonium transportation in *C. albicans*. In addition, Mep2 functions as a receptor mediating hyphal growth under nitrogen starvation condition (Biswas et al., 2007). Therefore, the changes that take place in the *C. albicans* genome as a result of either presence or

absence of amino acids can be used to formulate antifungals targeting such regions.

A key example of such environmental factors is carbon dioxide. Within the human body, *C. albicans,* is often found in areas with higher concentrations of carbon dioxide which enhances filamentous growth. Therefore, the *C. albicans* cells that grow on the skin are likely to be deprived of adequate carbon dioxide compared to those that grow in the blood and intestine. The presence of at least 5% carbon dioxide would influence the development of pseudo-hyphae as well as the invasion, which is an important response that can successfully take place in the presence of a catalytic domain of the adenylate cyclase (Kadosh and Lopez-Ribot, 2013, Pentland et al., 2020, Ciurea et al., 2020, Klengel et al., 2005, Hall et al., 2010).

Another fitness attribute of *C. albicans* is it's ability to sense and adapt to the ambient pH in the environment. This can range from alkaline to acidic levels depending on the host niches. Alterations in pH levels can affect *C. albicans* morphology. For example, *C. albicans* maintain growth in yeast form at low pH levels (< 6), while higher levels of pH (> 7) induce hyphal growth. The latter level of pH causes a stress on *C. albicans* because it impairs pH sensitive proteins and nutrient acquisition. Furthermore, *C. albicans* growth in an acidic environment resulted in cell wall remodelling and unmasking chitin and ß-glucan (Sherrington et al., 2017, Mayer et al., 2013). Therefore, *C. albicans* developed a mechanism by which it can sense and adapt to a fluctuation in pH levels via the Rim101 signal transduction pathway. Activating this pathway induces a signaling cascade which in turn leads to Rim101 transcriptional factor activation and thus mediating a pH dependent response. There are different proteins involved in pH change induced adaptation among them are cell wall ß-glycosidases Phr1, expressed in alkaline and neutral pH conditions, and Phr2, expressed in acidic pH conditions. In addition, *C. albicans* can modulate the extracellular pH. For example, in instances of nutrient starvation, such as glucose absence or an acidic environment, *C. albicans* can uptake and breakdown amino acids to produce ammonia and alkalize the surrounding environment. This mechanism promotes *C. albicans* filamentation (Mayer et al., 2013, Du and Huang, 2016). Additionally, *C. albicans* growth on the sugar *N*-

acetylglucosamine (GlcNAc) neutralizes the acidic media and induces hyphal formation. A recent study by Danhof et al. (2016), revealed a novel phenomenon through which *C. albicans* can alkalinize an acidic environment by utilizing carboxylic acids without generating ammonia or inducing hyphal formation.

Cell-to-cell signaling and communication in *C. albicans* occurs through quorum sensing (QS) mechanisms. Quorum sensing is a phenomenon that contributes to *C. albicans* morphogenesis regulation and it is known to play a role in hyphal growth regulation and biofilm formation (Kruppa, 2009). An example of a QS molecule is farnesol which has been shown to inhibit the yeast to hyphae transition and is produced during planktonic growth. Another QS molecule is tyrosol, which is produced in both forms of growth planktonic and biofilm, and controls physiological activities in *C. albicans*. Both molecules play vital roles in regulating biofilm formation. While farnesol inhibits filamentation at later stages of biofilm formation to allow yeast cells dispersal, tyrosol promotes filamentation at early stages. Moreover, farnesol prevents germ tube formation when the cell density is high, and tyrosol promotes growth and germ tube formation when the cell density is low. The accumulation of these molecules can result in a resistant biofilm phenotype. The QS mechanisms indicate that a *C. albicans* biofilm is an organized community of cells (Figure 1.5) (Chauhan and Mohan Karuppayil, 2021, Ramage et al., 2002, Sandai et al., 2016).

1.3.4Signalling pathways

Morphogenesis in *C. albicans* is controlled by transcription factors, such as Efg1, Tup1, Tec1, Ume6, Rbf1 among others, which are either activated by various signaling pathways. Those pathways along with fitness aspects of *C. albicans* contribute crucially to filamentation and biofilm formation (Villa et al., 2020, Kornitzer, 2019). Various environmental cues can activate *C. albicans* filamentation through Mitogen-activated protein kinase pathways and Cyclic adenosine monophosphate-protein kinase A pathway.

1.3.4.1 Mitogen-activated protein kinase pathways.

There are three major Mitogen-activated protein kinase (MAPK) pathways that are activated in *C. albicans:* Hog1, Cek1, and Mkc1, and each pathway is a series

of phosphorylation and transcription factor activation events (Hall et al., 2009). The Mkc1 pathway is responsible for cell wall salvage, biogenesis, and cell wall integrity. The Cek1 pathway facilitates filamentation and mating. The Hog1 pathway plays a role in cell wall formation, thermal stress responses and morphogenesis, which are crucial factors in influencing virulence. These pathways are considered to be key signaling pathways that are involved in thermo-tolerance, cell wall remodeling and subsequently regulation of the morphological changes in *C. albicans* and biofilm formation positively or negatively (Kurzai, 2013, Leach et al., 2012).

The Cek1-mediated MAPK pathway plays an important role in filamentation through activating the downstream transcription factor Cph1, which in turn positively regulates filamentation. Cek1 signaling pathway can be activated by several factors such as cell wall damage, low N_2, osmotic stress, and embedding matrix. In low N_2 Ras1regulates *C. albicans* morphogenesis through MAPK signaling pathways via the sensor Mep2. Ras1 interacts with Cdc24, leading to Cdc42 activation. Upon Cdc42 activation, series of activation and phosphorylation of the Ste11 (MAPKKK), Hst7 (MAPKK), and Cek1 (MAPK) are triggered resulting in Cph1 activator stimulating hyphal growth. Under cell wall damage or osmotic stress conditions, the Cek1-mediated MAPK pathway can be activated through the upstream transmembrane proteins, Sho1, Opy2, and Msb2. These proteins form a complex that interacts with Cdc42 and Cst20, which triggers Cek1 phosphorylation. Embedded matrix condition can also activate Cph1 via Cek1 through the Cek1-mediated MAPK pathway (Figure 1.5) (Chow et al., 2021).

Under osmotic and nutritional stress, the protein kinase C (PKC) MAPK pathway is activated. commonly known as the cell wall integrity pathway. Pkc1 activation instigates a series of MAPK activation of Bck1 (MAPKKK), Mkk1 (MAPKK), and Mkc1 (MAPK). The PKC MAPK pathway co-regulate cAMP signaling pathway leading to *C. albicans* filamentation stimulation. Rho1 is a master regulator involved in this pathway, activated by Rom2 and inactivated by Lrg1. Rho1 regulates filamentation through Pkc1, which is involved in adenylyl cyclase Cyr1 regulation (Figure 1.5) (Chow et al., 2021).

1.3.4.2 Cyclic Adenosine Monophosphate-Protein Kinase A pathway.

The Cyclic Adenosine Monophosphate-Protein Kinase A (cAMP-PKA) pathway is a significant element in the filamentous growth of *C. albicans* and other microorganisms such as *S. cerevisiae*. For example, the starvation of nitrogen in *S. cerevisiae* would influence the development of the elongated buds known as pseudo-hyphae, a process that is fully achieved following the instigation of the cAMP-PKA pathway. Correspondingly, high levels of cAMP influence the occurrence of yeast-to-hypha transition, which the induction of this transition can be achieved by inhibiting the cAMP phosphodiesterase (Biswas et al., 2007). It was established that the addition of serum would result in rapid responses, similar to the results observed with glucose. Therefore, it is important to note that glucose is a key factor in serum that may impact the morphogenesis process in *C. albicans* (Lin and Chen, 2018, Antonini and Sudbery, 2004, Huang et al., 2019, Brown et al., 2014b).

The cAMP-PKA pathway can either directly triggered through the adenylyl cyclase Cyr1 or via Ras1, depending on the surrounding environmental cue activating filamentation. Cyr1 drives the conversion of ATP to cAMP, which binds the homodimer regulatory subunit Bcy1. Upon binding, PKA holoenzyme is activated which then release the two catalytic subunits, Tpk1 and Tpk2. The latter subunits lead to downstream activation of target proteins or genes and thus leading to activators such as Efg1, Ume6, and Tec1 to regulate hypha-associated genes and induce hyphal growth. Tpk1 and Tpk2 are required for hyphal formation on solid media, and in liquid media and invasive growth into solid media, respectively. Levels of cAMP are negatively regulated by Pde1 and Pde2 through cAMP degradation. This pathway can be activated by several cues such as Co_2 concentrations. In addition, can be activated by amino acids and low glucose via the activation of the heterotrimeric G-protein α subunit Gpa2 by the G-protein-coupled receptor Gpr1 and binding to Cyr1.Indirect activation of cAMP-PKA pathway via Ras1 can be due to encountering various environmental cues such as serum and low N_2. Upon Ras1 Activation, Ras1 directly interacts with Cyr1, transduces extracellular signals to Cyr1, and stimulates cAMP production. Serum can stimulate morphogenesis through cAMP-PKA activation via

Ras1. Glucose also induces cAMP synthesis through Cds25-Ras1 interaction. On the other hand, temperature elevation and Quorum sensing molecules such as farnesol can block the hyphal growth by inhibiting the activity of Cyr1 (Figure 1.5).

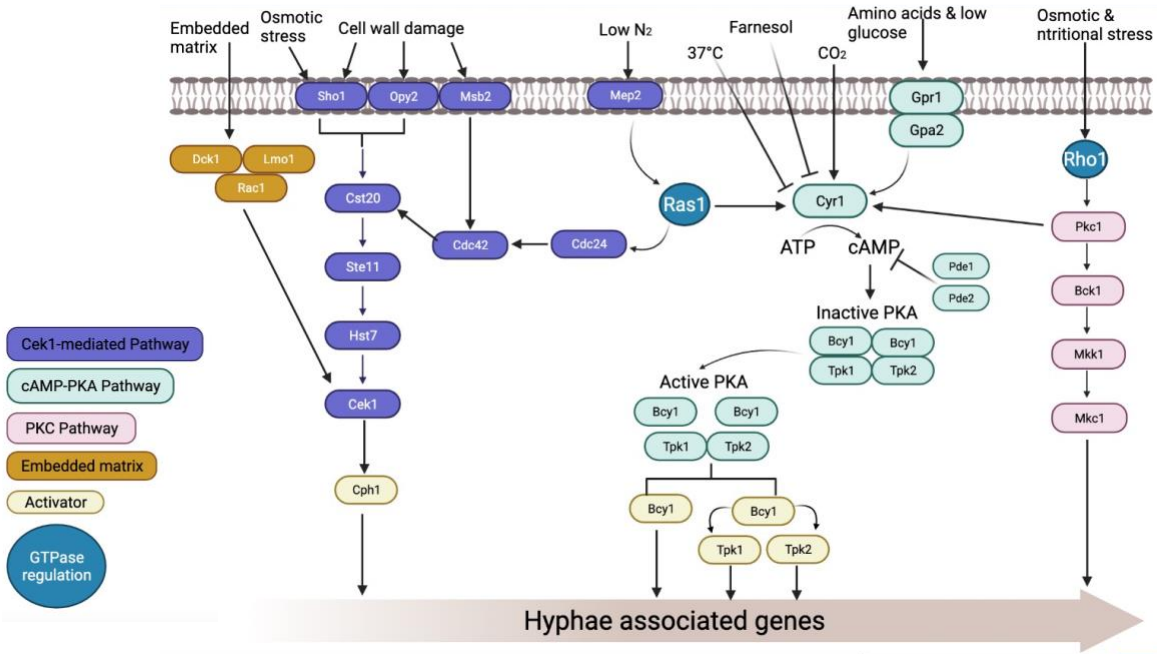

Figure 1.5 Signaling pathways regulating morphogenesis in *C. albicans*. Various environmental cues and signal transduction pathways activate filamentation; the cAMP-PKA pathway, the Cek1-mediated pathway, and the PKC pathway. Adapted from (Chow et al., 2021).

1.4 Host response to *Candida albicans* infections

The first line of protection against any type of invasive pathogen, including *C. albicans*, is the innate immune system. The morphological shift of *C. albicans* from the yeast form to the hyphal form enables it to invade host mucosal barriers and access the underlying host tissues (Qin et al., 2016, Weindl et al., 2010). After successful adhesion of the *C. albicans* onto the host tissues, the interaction is initially realized through the detection of the fungal cell wall components such as the proteins and carbohydrate polymers (Tronchin et al., 1991, Wächtler et al., 2012, Chaffin et al., 1998). Due to the presence of mannoproteins in the outer layer, both ß-1,3- and ß-1,6-glucans in the inner layer and chitin in the innermost layer, the host immune system specifically relies on the pattern recognition receptors (PRRs) in order to recognize these pathogen-associated molecular patterns (PAMPs) (Agustinho et al., 2017). This

recognition is important in triggering the signaling pathways and activating the innate immune response and facilitating the development of adaptive immunity.

The PRRs that play a central role in fungal identification are Toll-like receptors (TLRs) and the C-type lectin receptors (CLRs). TLR2 and TLR4 are primarily involved in the recognition of phospholipomannan, O-bound mannan, and α-linked mannose structures, respectively. Successful recognition by TLRs leads to the activation of various intracellular signaling pathways, influencing the expression of chemokines and cytokines. The CLRs that help in *C. albicans* recognition include dectin-1, -2 and -3, mannose receptors, MINCLE and DC-SIGN (Dendritic cell specific). Like TLRs, CLR activation leads to intracellular signaling and expression of chemokines and cytokines. It has been observed that the ability of these receptors to recognize *C. albicans* cells is compromised in immunocompromised individuals (Qin et al., 2016, Yadav et al., 2020, Zheng et al., 2015, Tang et al., 2018, Goyal et al., 2018).

Dectin-1 recognises ß glucans, whilst dectin-2 and -3 are responsible for recognizing the α-mannan and high-mannose structures in hyphae. MINCLE may also recognize *C. albicans* α-mannose residues, and it's primary function is thought to improve host defense against the yeast form of *C. albicans*. Even though the intracellular signaling motifs have not been identified in the mannose receptors at the cytoplasmic tail, they are essential for pro-inflammatory and anti-inflammatory cytokine production. Their key roles include performing endocytosis, mediating internalization of the ligands, and influencing the antigen presentation. The epithelium plays a central role in limiting the dissemination of *C. albicans* by initiating activation of pathways inducing the production of cytokines and chemokines which are responsible for recruiting and activating host immune cells. However, these fungal cells often attack the host cells in large numbers, hence overwhelming the host and reducing the chances of the epithelial cells preventing their invasion (Verma et al., 2017, Naglik, 2014, Carpino et al., 2017, Gazi and Martinez-Pomares, 2009, Martinez-Pomares, 2012, Qin et al., 2016, Zheng et al., 2015)

Generally, fungal infections caused by *C. albicans* are categorized based on their site of infection. The mucosal epithelial cells have been identified to be the first

line of defense after the *C. albicans* invasion of the host cells. There are two approaches that *C. albicans* may use to invade the epithelium; active penetration and induced endocytosis, and the type of mechanism often depends on the type of epithelium. For example, *C. albicans* uses active penetration to invade the oral, stomach and intestine epithelium. The interaction between PRRs and PAMPs is necessary for recognizing the fungal infections and both the TLRs and CLRs play an important role in detecting *C. albicans*. TLR2, TLR4, TLR6, and TLR9 are expressed in the oral epithelium whilst TLR4 is actively involved in promoting an immune response against *C. albicans* by vaginal epithelial cells (Dreschers et al., 2016, Qin et al., 2016, Yang et al., 2014, Zheng et al., 2015).

C. albicans can spread and migrate from tissues into the circulation and influence the occurrence of widespread organ damage and systematic candidiasis among immunocompromised individuals (Quindós et al., 2018, Zhang et al., 2020). The blood-borne *C. albicans* which have not been destroyed through phagocytosis must first adhere and infiltrate into the endothelial cells prior to dissemination into deep tissue organs (Tsui et al., 2016). However, the endothelium often acts as a barrier to inhibit dissemination of *C. albicans*. The PRRs mediate adhesion of the *C. albicans* onto the endothelial cells, a process that leads to the activation of both TLR2 and TLR4. Additionally, the N-cadherin which is expressed on the endothelium binds to the agglutinin-like protein 3 (Als3) and Stress-Seventy subfamily A_1 (Ssa_1) of the *C. albicans*, a process that activates the endothelial cell microfilaments leading to the production of pseudopods that engulf the pathogen (Dreschers et al., 2016, Phan et al., 2007, Sun et al., 2010).

Despite the different immune response mechanisms that endothelial cells employ, *C. albicans* still have developed strategies to evade destruction. After being phagocytosed, *C. albicans* physically burst out of macrophages or initiate pyroptotic cell death by hyphae to escape phagocytosis. In addition, *C. albicans* encodes superoxide dismutases (SODs), which helps the pathogen to purify reactive oxygen species (ROS). Another mechanism enables *C. albicans* to evade host immunity is inducible nitric oxide synthase (iNOS) secretion which is a mediator that actively block nitric oxide (NO) production by macrophages (Qin et

al., 2016, Liu and Filler, 2011, Grubb et al., 2008, Tsui et al., 2016). The *C. albicans* cell wall also can act as an evasion mechanism by shielding ß-glucan in the outer mannoprotein layers which is the recognition sites by the host immune system. Moreover, when *C. albicans* is phagocytosed, it can face different challenges such as ROS or nutrient limitation. However, the fungus adapts to this stress by shifting to gluconeogenesis by using amino acids. Thus, leading to alkalinization of the environment and help escaping the phagocytosis by damaging the macrophage phagosome (Ciurea et al., 2020).

Within the innate cellular immune system in the host defense, the polymorphonuclear leukocytes (PMNs), such as neutrophils, are the principal phagocytes providing the first line of protection through engulfing *C. albicans*. Different types of pro-inflammatory cytokines influence the relocation of PMNs to the sites of *C. albicans* infections, such as interleukin 6, 8 and 17 as well as tumor necrosis factor alpha (TNF-α). PMNs play a key role in the phagocytosis of *C. albicans* as well as acting as modulators during inflammation. Indeed, in addition to promoting proinflammatory responses to *C. albicans* infection they can also weaken the response following effective *C. albicans* clearance by producing proteases that promote degradation and inactivation of cytokines, such as interleukin-1ß (IL-1ß) and TNF-α (Gresnigt et al., 2012, Qin et al., 2016).

1.5 Antifungals, their mechanism of action and antifungal resistance

The development of new and effective antifungals is an important goal that the global pharmaceutical industry is striving to achieve (Roemer and Krysan, 2014, Pianalto and Alspaugh, 2016, Mroczyńska and Brillowska-Dąbrowska, 2020). Caspofungin, which acts by inhibiting fungal ß-1,3 glucan synthesis, was approved by the United States Food and Drug Administration, and it belongs to the echinocandins antifungal class (Akins and Sobel, 2009). Clinical trials have shown that the drug has the ability to treat both mucosal and invasive candidiasis (Saravolatz et al., 2003, Ben-Ami, 2018). Nonetheless, Vatanshenassan et al. (2018) reported that *C. albicans* acquires mutations which enable it to develop resistance to caspofungin. Specifically, *FKS1* gene mutations, which is located on the chromosome 1, and encodes the catalytic

subunit of the drug target 1,3-ß-glucan synthase (Akins and Sobel, 2009). Therefore, *C. albicans* can develop resistance, not only to caspofungin, but also other echinocandins.

Fluconazole is another key antifungal agent for managing *C. albicans* and other non-*albicans* fungal infections (Morio et al., 2017). Fluconazole belongs to the azole antifungal class and acts by interrupting the conversion of lanosterol to ergosterol through binding to cytochrome P450. The process leads to the eventual disruption of the fungal cell wall and cell membrane integrity (Gintjee et al., 2020, Moosa et al., 2004). With reference to the fact that fluconazole is fungistatic, it's treatment influences the development of acquired resistance, especially by *C. albicans* (Akins and Sobel, 2009, Morio et al., 2017). The mechanism that enables *C. albicans* to become resistant to fluconazole is by the occurrence of genome rearrangements which lead to the concurrent loss of the heterozygosity for the mutated allele and the mating type locus. The mechanism allows the drug-resistant *C. albicans* cells to switch to the mating-competent opaque morphology and mate with each other, hence leading to the combination of the individually acquired resistance traits (Hampe et al., 2017, Morio et al., 2017, Popp et al., 2019, Shapiro et al., 2011).

Voriconazole is often used in treating serious fungal infections, such as invasive candidiasis, emerging fungal infections, and invasive aspergillosis, that mainly affect patients who are immunocompromised (Greer, 2003). Being a member of the azole antifungal class, voriconazole acts by hindering the fungal cytochrome P450 dependent enzyme, leading to the reduced production of ergosterol; hence interfering with cell membrane formation (Ghannoum and Rice, 1999, Morio et al., 2017). Therefore, *C. albicans* may also use the same mechanism to develop resistance against the activities by both voriconazole and fluconazole.

Amphotericin B is a broad-spectrum antifungal agent that is used for managing serious fungal infections such as candidiasis, cryptococcosis and coccidioidomycosis (Chandrasekar, 2008, Chang et al., 2017, Sugar, 1995). Amphotericin B's mechanism of action involves binding with the ergosterol and causing pore formation on the cell membrane resulting in the leakage of monovalent ions such as K^+, Na^+, H^+ and Cl^- that eventually cause cell death

(Carolus et al., 2020, Bhattacharya et al., 2020). Different studies have provided substantial evidence to demonstrate antifungal resistance to amphotericin B (Ellis, 2002, Spampinato and Leonardi, 2013, Sterling and Merz, 1998). The increased cases of invasive infections due to antifungal resistance to amphotericin B are associated with the rising number of non-*albicans Candida* species. For example, a study by Kalantar et al. (2014), showed that non-*albicans Candida* species were the predominant isolate species in blood samples from cancer patients with candidemia, and among all these isolates, high resistance to amphotericin B was observed. Some of those species showed intrinsic resistance such as *Candida lusitaniae*, and some showed acquired resistance such as *C. albicans*. The mechanism behind amphotericin B resistance was found to be an alteration or a reduction in the sterol composition in the cell membrane (Carolus et al., 2020, Eliopoulos et al., 2002, Kalantar et al., 2014).

1.6 Current treatments and conventional antifungal limitations

In comparison with the antibacterial agents, the obtainability of antifungal agents to facilitate the management of fungal infections, such as those caused by the *C. albicans*, is significantly lower. The main factor for such a low arsenal of antifungal agents is the fact that fungi are eukaryotes. This makes identification of drug targets, that have the ability of selectively killing the fungal pathogens without causing toxicity effects on the host, challenging (LeBlanc et al., 2020, Rauseo et al., 2020). The classification of the antifungals is often based on their cellular targets and the mode of action (Ghannoum and Rice, 1999, Polak, 2004). Despite the increasing cases of fungal infections, there are only five classes of drugs which are available for the treatment of fungal infections, and they include azoles, echinocandins, polyenes, allylamines and the antimetabolites (Gintjee et al., 2020). The limited number of antifungals may also be one factor that has contributed to the increasing incidences of *C. albicans* infections, as there are higher chances that the fungus has developed resistance against almost all the available drugs.

Each class of antifungal drug has specific advantages and limitations associated with it’s mode of action and the spectrum of activity. *C. albicans* biofilms are

characteristically tolerant to therapy and there is still low susceptibility of the *C. albicans* biofilms to the existing therapeutic agents, with the exclusion of the echinocandins (Gulati and Nobile, 2016, Pereira et al., 2020). The polyenes, which act by directly biding to ergosterol located within the cell membrane of the fungi, are not widely used because they can cause partial nephrotoxicity. This is a result of the resemblance between the fungal cell ergosterol and cholesterol, which is the equivalent sterol in the mammalian cell membrane (Bodge and Cumpston, 2019, Ghannoum and Rice, 1999). On the other hand, the incorporation of liposomal formulations for amphotericin B delivery has helped in reducing the possibility of such toxicity. Yet, the prohibitive cost of this method of formulation for amphotericin B and other echinocandins has limited it's application in the treatment of fungal infections (Adler-Moore and Proffitt, 2002, Stone et al., 2016). Therefore, each of the available antifungal medications have both strengths and limitations which must be comprehensively assessed before making a decision about the one to use.

The azole antifungals were mainly developed in order to help in addressing the issues previously experienced during the production and usage of echinocandins and polyenes (Neville et al., 2015). The azoles exhibit improved bioavailability, wide range of action against different types of fungal pathogens as well as reduced cost of production. Moreover, the azoles are fungistatic. However, overuse of azole-based antifungals, such as fluconazole, may influence the establishment of resistant strains, especially among people with HIV/AIDS because of high cases of oral candidiasis among individuals in this population (Campoy and Adrio, 2017, Gintjee et al., 2020, Owotade et al., 2016, Singh et al., 2014). In recent years, there are different types of echinocandin-based antifungals, such as micafungin and anidulafungin, which have been developed to act as alternatives to the polyenes and azoles. Therefore, the echinocandin-based antifungals primarily act by inhibiting the activities of ß-1,3-glucan synthase enzyme which is required for the biosynthesis of glucan components within the fungal cell walls; hence leading to the disruption of their integrity (Antinori et al., 2016, Vardanyan and Hruby, 2016).

1.7 Challenges in treating biofilm infections

A biofilm always shows different characteristics compared to planktonic cells, which are important survival strategies for any microorganism capable of biofilm formation. General characteristics includes the three-dimensional structure, ability to adhere to each other and onto different types of surfaces and ability to decrease the antimicrobial susceptibility and host defense system (Cavalheiro and Teixeira, 2018). Based on the fact that the formation of *C. albicans* biofilms is a multifaceted process, the end product is a complex structure whose primary function is to help the microorganism survive under different environmental conditions (Kabir et al., 2012, Rapala-Kozik et al., 2018). For example, the attached *C. albicans* often produce the extracellular polymeric substances that influence the maturation of a three-dimensional biofilm structure; hence making it's treatment with antimicrobial agents challenging. *C. albicans* biofilm formation *in vivo* was found to be quicker compared to *in vitro* with several yeast cell layers and hyphae observed after just 8 hours. Thus, the transformation of *C. albicans* from the yeast form to the hyphal state within the shortest time possible limits the ability of the already developed antifungals to eliminate them from infected tissues (Cavalheiro and Teixeira, 2018, Jadhav and Karuppayil, 2017).

Similarly, in a study conducted by Cavalheiro and Teixeira (2018), it was observed that the *C. albicans* biofilm maturation within a rat central venous catheter took place after 24 hours compared to between 36 hours and 72 hours in an *in vitro* setting. Therefore, the short period for the *C. albicans* cells to transform from the ordinary yeast cells to the hyphae state pose an important challenge to *C. albicans* infection treatment as it results in rapid transformation into thick layered biofilms. Furthermore, most of the adhesins found in *C. albicans* biofilms belong to the agglutinin-like sequence family, which are known to have the ability to bind to several proteins through their C-terminal regions and are associated with severe biofilm defects compared to the wild-type parental strains (Cota and Hoyer, 2015, McCall et al., 2019). Unfortunately, locating, treating and deleting these adhesins from *C. albicans* biofilms might be very challenging because of their thick-layered cell walls.

Successful adhesion of the *C. albicans* cells onto a surface influences the continuation of biofilm formation through morphologic modifications, such as increase in the number of cells and the production of extracellular polymeric substances. *C. albicans* biofilms do often present highly diverse morphological forms compared to the other *Candida* spp. For example, the oval budding, the continuous separate hyphae and pseudo-hyphae. Moreover, mature biofilms depend on the extracellular polymeric substances production for it's structural orientation. The extracellular polymeric substances give the *C. albicans* biofilms the gel-like hydrated three-dimensional structure within which the cells are partially immobilized (Cavalheiro and Teixeira, 2018, Sandai et al., 2016, Tsui et al., 2016, Jadhav and Karuppayil, 2017). Correspondingly, other key roles of the extracellular matrix in the *C. albicans* biofilm identified by Dewasthale et al. (2018), which include offering protection against phagocytosis, providing scaffold necessary for ensuring biofilm integrity as well as prevention of drug diffusion into the internal structures of the biofilms. The previous information clarifies the difficulty to eliminate *C. albicans* from the host after biofilm formation and highlights the need to develop new strategies which specifically target biofilms for successful management of the associated infections.

The characteristic of biofilm formation impacts clinical outcomes negatively. For instance, biofilm formation on medical devices provides a reservoir for constant frequent infections, increases the resistance to conventional antifungals and protects from the host immune system. Additionally, patients with biofilm forming isolates are more vulnerable to longer hospital stay and mortality, and economically cost more to treat (Martín and Di Pietro, 2012, Rajendran et al., 2016a, Ramage et al., 2002, Tsui et al., 2016). The fact that *C. albicans* is classified as a eukaryote poses a challenge in terms of finding an optimal antifungal that targets the fungus for eradication or disables it's pathogenicity while not causing toxicity or collateral damage to host cells; and this exacerbates the problem of treatment resistance (Ghannoum et al., 2015, Tsui et al., 2016). Recent studies have explained some of the mechanisms that contribute to the antifungal resistance of *C. albicans* biofilms such as cell density, gene expression alteration, persister cells, efflux pump activity and the formation of an extracellular matrix (ECM) (Tsui et al., 2016).

A study investigating the role of cell density on biofilm resistance revealed that high cell density plays a role in the phenotypic resistance of *C. albicans* biofilms (Tsui et al., 2016, Perumal et al., 2007). Another study revealed a significant increase in ergosterol biosynthesis gene expression (*ERG1, ERG3, ERG11* and *ERG25*) following treatment of the biofilm with an azole, which elucidates the resistance of the biofilm to the drug since ergosterol is a component of the fungal cell membrane. Moreover, mutations in the genes *ERG3, ERG5* and *ERG11* result in an alteration in the targeted substrate that may hinder the drug's function. Persister cells are dormant cells embedded deep in the biofilm and resistant to drugs. These cells have the ability to transform from being dormant to being metabolically active and form biofilms after treatment. The efflux pump is another mechanism through which the drug is transported extracellularly instead of being dispersed intracellularly. The extracellular matrix provides the protection, stability and attachment for the biofilm (Tsui et al., 2016).

1.8 Molecular studies of *Candida albicans* to identify new therapeutic targets

Gene expression studies conducted using the hybridization-based microarrays provided valuable insight into gene expression of key regulators during morphogenesis and biofilm formation. However this technology has now been largely replaced by RNA-Seq technology due to issues such as the poor quantification of highly and lowly expressed genes, occurrence of cross-hybridization artifacts, and microarray analysis required prior knowledge of the sequence (Basso et al., 2018, Lowe et al., 2017). As a result of the high rate of genetic mutation in *C. albicans*, there has been a need to develop a technique that can track such changes. In contrast to microarray analysis, RNA-seq technology can accurately quantify expression levels, capture transcriptomic dynamics across different conditions and during development and normal physiological changes, and identify novel transcribed regions (Wang et al., 2009).

Whole transcriptome or RNA sequencing (RNA-Seq) is an important technology-based sequencing technique that utilizes next-generation sequencing in order to

determine the existence and quality of RNA within a genetic sample, by analyzing the continuously transforming cellular transcriptome (Wang et al., 2009). RNA-Seq is specifically used for assessing the alternative gene spliced transcripts, gene fusion, mutations or the transformation in gene expressions in diverse groups or treatments. RNA-Seq may also be used for evaluating the different populations of RNAs and mRNAs in order to include small RNA such as miRNA, ribosomal profiling and tRNA (Han et al., 2015).

RNA-Seq has been widely used for the purpose of investigating and characterizing the *C. albicans* transcriptomes under different types of growth conditions, for example hyphal induction, oxidative stress, pH stress, and inductive cell wall damage (Cottier et al., 2015, Hovhannisyan and Gabaldón, 2018, Romo et al., 2019, Wang et al., 2017, Yang et al., 2016). Such analyses have facilitated the generation of new knowledge necessary for updating the existing gene annotations as well as helping in the characterization of 602 novel transcriptionally active regions (nTARs) which may successfully present the non-coding or the regulatory RNAs. Furthermore, RNA-Seq has been successfully used, together with microarray analysis, to expand the identification of the nTARs as well as the characterization of the regulatory network that is needed for *C. albicans* biofilm formation (Giosa et al., 2017, Riccombeni and Butler, 2012). In the study by Nobile et al. (2012) six important transcription factors were identified to be involved in *C. albicans* biofilm formation, namely Bcr1, Tec1, Efg1, Ndt80, Rob1 and Brg1. Similarly, Chong et al. (2018) revealed that a combination between the chromatin immunoprecipitations and the transcriptional profiling factors and their targets belong to a single network which is involved in the moderation of the biofilm development. Therefore, the application of RNA-Seq has helped in the identification of specific regions within the *C. albicans* genome that can be targeted by antifungals in order to facilitate improved outcomes. Understanding the molecular mechanisms that confer *C. albicans* pathogenesis may aid in combating *C. albicans* infections and therapy development (Prasad, 2017, Tsui et al., 2016).

1.9 Acetylcholine and cholinergic signaling

A recent study aimed to investigate the effect of acetylcholine (ACh) on biofilm formation and the host immune response to *C. albicans* infection using the *Galleria mellonella* infection model. This study revealed that ACh inhibits *C. albicans* transition from the yeast to the hyphae form and biofilm formation. In addition, the authors demonstrated that ACh could modulate the host's innate immune system to promote an effective haemocyte response resulting in clearance of the pathogenic threat with limited bystander damage (Rajendran et al., 2015).

Acetylcholine is synthesised by both eukaryotic and prokaryotic cells. Signal transduction is mediated by cholinergic receptors within both the somatic and autonomic nervous system. In eukaryotes, neuronal ACh, released from the efferent vagus nerve terminals, and non-neuronal ACh, released from various cells outside of the neural network, play a crucial role in host-pathogen interactions, immune system regulation and determination of infection outcomes. ACh signaling is mediated through two types of cholinergic receptor: the ionotropic cationic nicotinic acetylcholine receptors (nAChRs) and the metabotropic muscarinic acetylcholine receptors (mAChRs). Both types of receptors are expressed in both neuronal and non-neuronal mammalian cells (Albuquerque et al., 2009, Carlson and Kraus, 2020, Pavlov and Tracey, 2005, Rajendran et al., 2015).

Muscarinic receptor expression has been detected in various cells of the body including muscle fibers, endothelial cells, epithelial cells, and immune cells (Liu et al., 2007). Different types of mAChRs found to be expressed in lymphocytes and leukocytes. In addition, muscarinic receptors have also been shown to modulate immune responses functions to pathogens (Darby et al., 2015, Fryer et al., 2012, Verbout and Jacoby, 2012). For example, activation of M1 and M2 muscarinic receptor by ACh, enhances the production of interleukin-2 (IL-2), (Reale and Costantini, 2021). Furthermore, a study by Razani-Boroujerdi et al. (2008) revealed that oxotremorine, a selective mAChRs agonist, stimulated T-cell proliferation which was inhibited by atropine, an mAChRs antagonist. Atropine also inhibited tissue injury and leukocyte chemotaxis. Muscarinic

signaling in epithelial cells also resulted in Wnt pathway downstream induction leading to C-type lectin and lysozyme genes expression and enhanced the host immune response to *Caenorhabditis elegans* (Labed et al., 2018).

Acetylcholine signaling has been identified in primitive organisms lacking a nervous system such as, primitive plants, algae, sponge, protozoa, bacteria, and fungi (Radu et al., 2017, Wessler and Kirkpatrick, 2008). These organisms release acetylcholine which binds to muscarinic receptors to regulate phenotypic cell functions. For example, *Urtica dioica* plant developed binding sites for acetylcholine and uses cholinergic signaling to regulate phenotypic functions. Morphological changes in their leaves were observed using 1 mM atropine, where leaves became dry. This effect was blocked by adding acetylcholine. Also blocking the binding sites resulted in water homeostasis failure and photosynthesis changes. Another example is the reduction in motility of two photosynthetic bacteria, *Rhodospirillum rubrum* and *Thiospirillium jenense*, by atropine and other cholinesterase inhibitors such as physostigmine (Wessler and Kirkpatrick, 2012). These examples indicate the role of non-neuronal cholinergic signaling in primitive organisms.

1.10 Acetylcholine and fungi

There is enormous evidence indicating the capability of fungi to produce and degrade ACh. Initially, ACh was discovered in the fungus *Claviceps purpurea* and has also been found to be synthesized by *S. cerevisiae*. Yet, ACh produced by *S. cerevisiae* was not inhibited by selective *CarAT* and ChAt inhibitors (Horiuchi et al., 2003). Hence, this suggests that ACh is synthesised by alternative routes. Furthermore, it was found that *Candida rugosa* and *Geotrichium candidum* fungi have a lipase that shows 25% similarity with human acetylcholinesterase, which indicates that fungi are also capable of ACh degradation (Grochulski et al., 1993). Additionally, a lipase with functional activity of cholinesterase was found to be possessed by *Candida anatartica* (Googheri et al., 2014, Grochulski et al., 1993, Sadeghi Googheri et al., 2015, Schwarz et al., 2014). Yet, the precise mechanisms and functions of cholinergic systems and their importance in fungal species are not adequately explored and explained.

Current evidence has revealed that fungi are responsive to ACh interactions, specifically, *C. albicans*. A recent study revealed that acetylcholine stimulates hyphal formation in *C. albicans* through a cAMP pathway. Intriguingly, dicyclomine, a human M1 receptor antagonist was found to inhibit morphogenesis induced by ACh. The molecular inhibitory mechanism carried out by dicyclomine via downregulating genes involved in cAMP signaling pathway such as *UME6*, *ECE1*, and *PDE2* and upregulating the gene responsible for negative regulation of filamentation *tUP1* (Ali et al., 2018). Analysis using *in silico* techniques also revealed that the *RRP9* gene in *C. albicans*, which is the potential target for interaction with dicyclomine, exhibited homology to the human M1 protein with 71% similarity and 54% identity (Ali et al., 2017). On the contrary, ACh inhibited filamentation and biofilm formation *in vitro* and *in vivo* using *Galleria mellonella* infection model (Greetham et al., 2017, Rajendran et al., 2015). Furthermore, a decrease in the fungal burden and expression of important genes involved in biofilm formation such as, *ALS3* and *HWP1* were observed in association with biofilm formation inhibition (Rajendran et al., 2015). This inhibitory effect of ACh is not due to cytotoxicity, yet further investigations need to be conducted to explore the inhibitory mechanism. Additionally, pilocarpine hydrochloride (PHCl), a general muscarinic receptor agonist, inhibited *C. albicans* biofilm formation *in vitro*, while SIB 1508Y maleate, the general nicotinic receptor agonist has no effect on morphogenesis and biofilm formation. Similarly, to the ACh inhibitory effect, the mechanism by which PHCl carry out the inhibitory effect remains still to be investigated. However, the authors proposed that the inhibitory effect is mediated via an unknown receptor since scopolamine, a general muscarinic receptor antagonist blocked the inhibitory effect of PHCl (Nile et al., 2019). Although findings from studies mentioned above are conflicting, they highlight the suggestion that *C. albicans* has an uncharacterized cholinergic receptor similar to human muscarinic receptors that is involved in filamentation and biofilm formation regulation.

Muscarinic receptors are G protein coupled receptors (GPCRs). The GPCRs are the largest family of transmembrane receptors that are involved in the transduction of the extracellular signals to promote the occurrence of intracellular signals, which principally involve the complex intracellular-signaling

networks (Brown et al., 2018, Rosenbaum et al., 2009). The GPCRs consist of seven segments of the transmembrane domain. The G proteins are heterotrimeric containing three subunits, the alpha, gamma and beta, and they are specialized to bind the nucleotides guanosine triphosphate (GTP) in active form, or guanosine diphosphate (GDP) in inactive form. In the absence of a ligand, e.g., an agonist, the GDP attaches the alpha subunit, and the G-protein-GDP complex binds the GPCR. However, in the presence of the ligand, GTP binds to the alpha subunit forming a complex of GTP-α that detaches from the ß and γ subunits, which form the ß-γ dimer and mediate the signal's transduction (Figure 1.6) (Li et al., 2002).

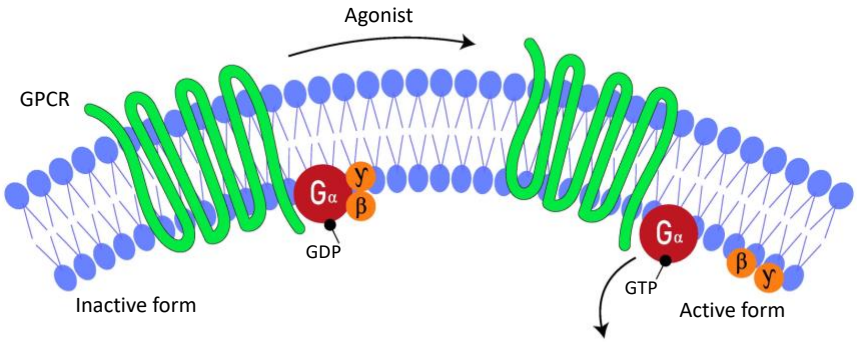

Figure 1.6 G-protein coupled receptor activation. In inactive form the GDP molecule binds the alpha subunit constituting a complex which in turn binds the GPCR. Upon receptor stimulation by a ligand or agonist, the GTP molecule attaches with alpha subunit forming a complex that detaches from ß and γ subunits dimer, thus mediating signaling transduction. Adapted from (Li et al., 2002).

In the human genome, there are 27 α, 5 ß, and 14 γ subunit isoforms, which means that the muscarinic receptors can activate different signaling pathways. Generally the main signaling mechanisms of the muscarinic receptors are in two classes: first, the subtypes of M_1, M_3, and M_5 are coupled to the G_q and G_{11} proteins, and the stimulation of these subtypes activates PLC, resulting in the production of inositol triphosphate (IP_3) and diacylglycerol (DAG), thus leading to an increment in intracellular [Ca^{2+}] and protein kinase C (PKC) activation. Second, in contrast, the muscarinic subtypes of M_2 and M_4 are coupled to G_i and

G_o proteins, and the stimulation of theses subtypes decreases the synthesis of cAMP through adenylyl cyclase inhibition and potassium conductivity activation (Figure 1.7) (Kawashima et al., 2012, Ockenga et al., 2013).

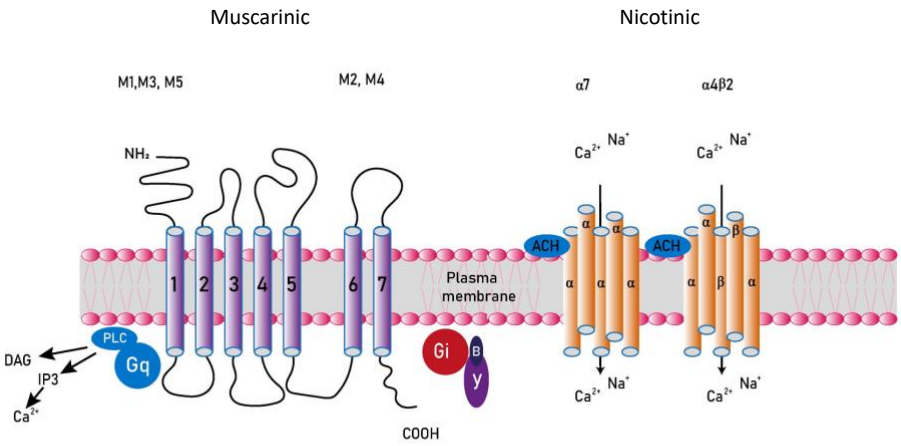

Figure 1.7 Muscarinic and Nicotinic receptor's structure. Muscarinic receptors are seven transmembrane proteins. The M1, M3, and M5 mAChRs selectively couple to the Gq/G11- proteins. The M2 and M4 mAChRs preferentially couple to Gi/Go- proteins. Nicotinic receptors are ligand-gated ion channels. Adapted from (Jones et al., 2012).

C. albicans contains significant number of GPCRs encoding genes within it's genome which play a significant number of roles in promoting morphogenesis, virulence and mating. Generally, fungi comprise two types of GPCRs; the pheromone receptors and the nutrient sensing receptors. Successful binding of the pheromones influences the occurrence of conformational changes in the pheromone receptors and the activation of the signaling cascades promoting to growth arrest and mating, specifically within the D receptors Ste2 and Ste3 of *C. albicans*. In addition, the primary function of nutrient sensing GPCRs is to detect the presence or absence of nutrients (Dijck, 2009, El-Defrawy and Hesham, 2020, Xue et al., 2008). Therefore, successfully targeting *C. albicans* GPCRs by antifungals may influence the induction of signaling pathways which help in controlling processes such as morphogenesis, virulence and metabolism.

The G protein-coupled receptor 1 (Gpr1) which encodes for putative GPCR and the guanine nucleotide-binding protein alpha-2 (Gpa2) which encodes for the G-

alpha subunit, are needed for the formation of hypha and morphogenesis in *C. albicans*. Hence, the mutants that lack either *gpr1Δ* or *gpa2Δ* are often defective during the formation of hypha as well as morphogenesis on the solid hypha-inducing media. Furthermore, deletion of *gpr1Δ* from the *C. albicans* genome interfered with the effectiveness of other components of cAMP-PKA pathway, such as Cdc35 and Ras1; therefore, severely impacting the virulence of the fungi (Brown et al., 2018, Van Ende et al., 2019, Villa et al., 2020). A study by Miwa et al. (2004) revealed that deletion of the *gpr1Δ* may slightly affect virulence of the fungi, but both *GPR1* and *GPA2* are not necessary during the morphogenesis process in *C. albicans*, especially when the microorganism is grown in a liquid fetal bovine serum (FBS) medium. There are other alternative pathways that would be induced to facilitate *C. albicans* morphogenesis through the detection of various external signals (Biswas et al., 2007, Maidan et al., 2005, Miwa et al., 2004). Yet, there is need for further research in this area in order to identify it's precise role, especially in *C. albicans* morphogenesis.

There is no concrete evidence that shows that the function of Gpr1 receptors in *C. albicans* is associated with the function of the homologous receptors in *S. cerevisiae*, whose deletion leads to limited or total absence of cAMP. In *C. albicans*, deletion of *gpr1Δ* influences normal signaling of cAMP following the addition of glucose. However, accumulation of downstream constituents of cAMP-PKA pathway and the accumulation of cAMP have the ability of limiting the morphogenesis phenotypes that are often observed following the elimination of *GPR1* from the *C. albicans* genome. *C. albicans GPA2* is actively involved in influencing the mating pathway; this is in addition to it's function in the cAMP pathway (Biswas et al., 2007, Brown et al., 2018, Dijck, 2009, Maidan et al., 2005, Miwa et al., 2004, Xue et al., 2008). The significant roles played by the *GPA2* and *GPR1* in the virulence and mating of *C. albicans*, highlights that there are higher chances that developing drugs that specifically target such regions may lead to management of *C. albicans* infections.

1.11 Summary

In this chapter, detailed information about *C. albicans* has been provided as a commensal in the human body and a pathogen. *C. albicans* is a leading cause of bloodstream infections, increasing the morbidity and mortality due to organ damage. *C. albicans* known to be a commensal which resides upon mucosal surfaces. However, it possesses a unique array of virulence factors that contribute to it's pathogenicity, such as the morphological transformation from yeast to hyphae and biofilm formation. Although there are different types of immune responses that are employed by the host following the invasion by *C. albicans*, biofilm formation provides a lot of challenges during infection and hinders treatment with antifungals. The evidence suggests an effective role of acetylcholine in suppressing *C. albicans* pathogenicity and promoting the host immune response. This suggests that ACh can modulate *C. albicans* virulence, by an uncharacterized mechanism. Acetylcholine plays a crucial role in host innate immune system regulation during infections through the cholinergic anti-inflammatory pathway. *C. albicans* genomic sequencing and initial pharmacological investigations suggests that *C. albicans* possesses a putative cholinergic receptor with homology to human nicotinic and/or muscarinic receptors. Therefore, understanding the molecular basis of *C. albicans* infection and biofilm formation by cholinergic systems may lead to the discovery of new therapeutic targets and novel therapeutic agents to treat *C. albicans* infections.

1.12 Hypothesis and Aims

Genome sequencing of *C. albicans* reveals the presence of putative genes encoding the enzymes carnitine acetyltransferase (*CrAT or CAT*) and choline acetyltransferase (*ChAT*), which are responsible for ACh synthesis. For example, carnitine acetyltransferases known to play different roles. *CAT2* (C4_02020W_A), induced in macrophages; Hog1-repressed; stationary phase enriched; farnesol-upregulated in biofilm; Spider biofilm induced. *CAT1* (C1_01740W_A), required for growth on nonfermentable carbon sources, not for hyphal growth or virulence in mice. *CAT3* (C3_04000C_A), induced by macrophage engulfment, hyphal growth, starvation, nonfermentable carbon sources; rat catheter, Spider biofilm induced. In addition, there is evidence that speculates the presence of cholinergic receptors in *C. albicans* (Borghi et al., 2015). Taken together, the genome sequencing data and the effect of ACh on *C. albicans* morphogenesis, it is hypothesized that *C. albicans* may possess a functional cholinergic receptor(s) with similarity to the muscarinic receptors in humans, which mediate the signaling pathways modulating biofilm formation in *C. albicans*.

The aims of this study were: (1) investigate the subtype of the potential receptor and the signaling pathway(s) by which the inhibitory effect of acetylcholine on *C. albicans* biofilm formation is mediated, and (2) investigate the effect of cholinergic compounds in modulating the host immune response and determining the outcome of *C. albicans* infections

2 Cholinergic interactions and biofilm formation in *Candida albicans* infections

2.1 Introduction

Recent research in the literature has investigated the effect of cholinergic compounds on *C. albicans* biofilm formation and host immune response to *C. albicans* infection. For example, Rajendran et al. (2015) revealed that acetylcholine (ACh) inhibits *C. albicans* yeast to hyphae transition, biofilm formation, and promotes effective immune response to clear the infection. Furthermore, a study conducted by Ali et al. (2018) has revealed that the human muscarinic acetylcholine receptor antagonist dicyclomine was capable of inhibiting *C. albicans* biofilm formation, adhesion, planktonic growth, and killed *C. albicans* in 15 minutes of exposure. Acetylcholine, as previously described, is a cholinergic compound that is produced by both eukaryotic and prokaryotic cells. Acetylcholine can exert it's effect through binding to two types of receptors: the nicotinic acetylcholine receptors (nAChRs) and the muscarinic acetylcholine receptors (mAChRs) (Rajendran et al., 2015, Pavlov and Tracey, 2005, Albuquerque et al., 2009).

The nAChRs form a ligand gated ion channel, induce fast activity (micro-second to sub micro-second), and are divided into two subtypes: neuronal and muscle nAChRs. The muscle type receptors are heteropentamers that consist of five subunits: ß1, α1, γ, ε, and δ. The neuronal receptors can be heteropentamers consisting of several arrangements of the subunits: α2– α6 with ß2– ß4 and α7 with ß2 subunits and α9 with α10 subunits, or homopentamers consisting of α7, α8 or α9 subunits. Signaling mechanisms of nAChRs in human cells include Ca^{2+} and Na^{+} influx, stimulation of Ca^{2+} dependent kinases, and activation of transcription factors, such as CREB, the cAMP response element binding. Despite their nomenclature the expression of neuronal nChRs is not limited to cells of the nervous system. Indeed, for example the α7 nAChR has been shown to be expressed by epithelial cells and immune cells. The α7 nAChR has been found to interact with ACh and down regulate the immune response by down-regulation of pro-inflammatory cytokine expression through the cholinergic anti-inflammatory pathway. The mAChRs are G-protein coupled receptors (GPCR), slower in activation: milliseconds to seconds, which activate the trimeric guanine nucleotide binding proteins (G-proteins). The muscarinic receptor family consists of 5 subtypes: M_1, M_2, M_3, M_4 and M_5, and their activation, depending on

the subtype, results in modifying the cellular homeostasis of phospholipase C (PLC), inositol trisphosphate (IP_3), cAMP and free calcium (Ca^{2+}) (Albuquerque et al., 2009, Carlson and Kraus, 2020, Ockenga et al., 2013, Rajendran et al., 2015, Kawashima et al., 2012).

Evidence from *C. albicans* genome sequencing suggests the presence of CrAT and ChAT genes which encode enzymes responsible for ACh synthesis (Borghi et al., 2015). Recent research mentioned above revealed the effect of cholinergic compounds such as ACh and dicyclomine in *C. albicans* morphogenesis and pathogenesis inhibition (Rajendran et al., 2015). Furthermore, *in silico* modelling studies revealed that ACh and bethanechol, a general muscarinic receptor agonist can bind to *C. albicans RRP9* gene which encodes a protein that has structural homology to the human muscarinic receptor type 1 (M1) (Ali et al., 2017, Ali et al., 2018). The muscarinic receptor type 1 (M1) signaling pathway activates the $G\alpha_{q/11}$ protein signal transducer which in turn activates the effector molecule, phospholipase C (PLC). Subsequently, this activation leads to production of second messenger molecules such as (IP_3, Ca^{2+}, DAG, and cAMP) and activation of protein kinase pathways (Falkenburger et al., 2010). Therefore, the evidence in combination infers the potential presence of putative cholinergic receptors in *C. albicans* homologous to human muscarinic receptors.

In this chapter, we aim to characterize the subtype of the potential receptor and the signaling pathway(s) involved in pilocarpine hydrochloride inhibitory effect on *C. albicans* biofilm formation.

Publications pertaining to this chapter:

Nile C., Falleni M., Cirasola D., **Alghamdi A.**, Anderson O., Delaney C., Ramage G., Ottaviano E., Tosi D., Bulfamante G., Morace G., Borghi E. (2019) Repurposing Pilocarpine Hydrochloride for the treatment of Candida albicans infections. mSphere, 4(1),e0068918.(doi:10.1128/mSphere.0068918) (PMID:30674648)(PMCID:PMC6344604)

2.2 Materials and Methods

2.2.1 Strains and reagents

Strains used in this study are the wild type *C. albicans* SC5314, low and high biofilm forming clinical isolates of *C. albicans* isolated from blood, vagina, and oral cavity, (Table 2.1 and table 2.2) (Rajendran et al., 2016b, Sherry et al., 2017, O'Donnell et al., 2017). The pharmacological agonists, antagonists, and inhibitor molecules used in this study are shown in (Table 2.3). In all instances, stocks were prepared based on solubility and solvents recommended by the manufactures. Either Roswell Park Memorial Institute-1640 media (RPMI1640 media) or Dimethyl sulfoxide (DMSO) was used as a diluent for all stock concentrations of compounds which were subsequently aliquoted into vials and stored at − 20°C.

Table 2.1 *C. albicans* low biofilm forming isolates.

C. albicans strain	Source	Reference
SC 17 A	Bloodstream	(Rajendran et al., 2016b)
SC 25	Bloodstream	(Rajendran et al., 2016b)
SC 71	Bloodstream	(Rajendran et al., 2016b)
SC 88 C	Bloodstream	(Rajendran et al., 2016b)
SC 89 B	Bloodstream	(Rajendran et al., 2016b)
SC 204	Bloodstream	(Rajendran et al., 2016b)
SVS 11	Vaginal swabs	(Sherry et al., 2017)
SVS 19	Vaginal swabs	(Sherry et al., 2017)
SVS 26	Vaginal swabs	(Sherry et al., 2017)
SVS 38	Vaginal swabs	(Sherry et al., 2017)
SVS 43	Vaginal swabs	(Sherry et al., 2017)
SVS 57	Vaginal swabs	(Sherry et al., 2017)
GSK 31	Denture wearers	(O'Donnell et al., 2017)
GSK 53	Denture wearers	(O'Donnell et al., 2017)
GSK 65	Denture wearers	(O'Donnell et al., 2017)
GSK 72	Denture wearers	(O'Donnell et al., 2017)
GSK 113	Denture wearers	(O'Donnell et al., 2017)
GSK 123	Denture wearers	(O'Donnell et al., 2017)

Table 2.2 *C. albicans* high biofilm forming isolates.

C. albicans strain	Source	Reference
SC 31	Bloodstream	(Rajendran et al., 2016b)
SC 39	Bloodstream	(Rajendran et al., 2016b)
SC 44 A	Bloodstream	(Rajendran et al., 2016b)
SC 63 A	Bloodstream	(Rajendran et al., 2016b)
SC 177 A	Bloodstream	(Rajendran et al., 2016b)
SC 198	Bloodstream	(Rajendran et al., 2016b)
SVS 1	Vaginal swabs	(Sherry et al., 2017)
SVS 14	Vaginal swabs	(Sherry et al., 2017)
SVS 117	Vaginal swabs	(Sherry et al., 2017)
SVS 128	Vaginal swabs	(Sherry et al., 2017)
SVS 137	Vaginal swabs	(Sherry et al., 2017)
SVS 219	Vaginal swabs	(Sherry et al., 2017)
GSK 04	Denture wearers	(O'Donnell et al., 2017)
GSK 10	Denture wearers	(O'Donnell et al., 2017)
GSK 25	Denture wearers	(O'Donnell et al., 2017)
GSK 61	Denture wearers	(O'Donnell et al., 2017)
GSK 90	Denture wearers	(O'Donnell et al., 2017)
GSK 93	Denture wearers	(O'Donnell et al., 2017)

Table 2.3 Different cholinergic compounds and signaling pathway inhibitors used in the study to investigate the subtype of AChRs.

Compound	Mode of action	Source	Reference
Pilocarpine Hydrochloride (PHCl)	General muscarinic receptor agonist	Sigma Aldrich (P6503)	(Marchi et al., 2009)
SIB 1508Y Maleate	General nicotinic receptor agonist	TOCRIS (4766)	(Cosford et al., 1996)
Cevimeline hydrochloride (C-HCL)	selective M1 receptor agonist	TOCRIS (3689)	(Fisher et al., 2003)
Arecaidine propagryl ester tosylate (APE)	M2 receptor agonist	TOCRIS (0383)	(Barlow and Weston-Smith, 1985)
J 104129 fumarate (JF)	M3 receptor antagonist	TOCRIS (2507)	(Sterin-Borda et al., 2011)
PD 102807 (PD)	M4 receptor antagonist	TOCRIS (1671)	(Kitaichi et al., 1999)
Vu 0238429 (Vu)	M5 allosteric modulator	TOCRIS (3634)	(Fryer et al., 2012)
YM 254890	G_q protein inhibitor	Wako (257-00631)	(Takasaki et al., 2004)
Pertussis Toxin (PTX)	G_i protein inhibitor	TOCRIS (3097)	(Schijns and O'Hagan, 2016)
U73122	Phospholipase C inhibitor (PLC)	Abcam (ab120998)	(Bosch et al., 1998)

2.2.2*Candida albicans* culture

C. albicans wild type and clinical isolates were sub-cultured on Sabouraud dextrose agar (SDA) media (Sigma-Aldrich, Dorset, UK). Plates were stored at 4°C after incubation for 48 hours at 30°C. Every 2 – 3 weeks *C. albicans* was transferred on to fresh SDA agar plates. Prior to conducting experiments, cells were propagated in yeast extract-peptone-dextrose medium (YPD) (Sigma-Aldrich, Dorset, UK) at 37°C overnight (16 – 18 hours) using an orbital shaking aerobic incubator. Cells from overnight broths were then washed by centrifugation at 3000 rpm for 5 minutes in phosphate buffered saline (PBS) (Sigma-Aldrich, Dorset, UK), and re-suspended to the required concentration, based on the individual experiment requirement, in RPMI-1640 media (Sigma-Aldrich, UK) (Rajendran et al., 2015)

2.2.3 *In vitro* biofilm formation in the presence and absence of cholinergic pharmacological agonists, antagonists, or signaling pathways inhibitors

C. albicans biofilms were grown in 96-flat bottom well plates (Fisher Scientific, Loughborough, UK) and cultured in RPMI-1640 medium (Sigma-Aldrich, UK); which promotes hyphal growth (Morioka et al., 2013, Van Dyck et al., 2020). Cell suspensions were standardized to 1×10^6 cells/mL in RPMI for biofilm formation ± various compounds. Based on the individual experiment, cells were treated with a range of different concentrations of each compound and incubated for 24 hours at 37°C. Positive and negative controls were included in each experiment. The positive controls were cells in RPMI alone, untreated with any of the compounds. The negative controls were blank wells containing only RPMI media without cells. Wherever DMSO was used as a diluent, a further DMSO only control was also included (Sherry et al., 2014). For each compound, the experiment was performed in triplicate on at least three independent occasions.

2.2.4 2,3-bis (2-Methoxy-4-nitro-5-sulfo-phenyl)-2 *H*-tetrazolium-5-carboxanilide reduction assays

To assess metabolic activity, 2,3-bis (2-Methoxy-4-nitro-5-sulfo-phenyl)-2 *H*-tetrazolium-5-carboxanilide (XTT) assays were performed after 24 hours of incubation. XTT solution (0.25 g/L) was prepared following the standard procedure described by the manufacturer, aliquoted into 10 mL aliquots, and stored at − 80°C. Before experiments, aliquots were thawed and 1 µL of menadione (10 mM) was added to 10 mL of XTT solution. After the incubation period, biofilms were washed using PBS then 100 µL of XTT/menadione mixture was added into each well of the plate. The plate was incubated at 37°C for 2 − 3 hours to allow the reaction to develop. After incubation, 75 µL was transferred from each well into a new 96-flat bottom well plate. The resultant change in colour correlated to the metabolic activity of the cells. The microtiter plate reader (FLuoStar Omega, BMG labtech, UK) was used to measure the absorbance of the colorimetric reaction at 492 nm. The experiments were repeated on at least three independent occasions in quadruplicate (Jose et al., 2010).

2.2.5 Crystal violet assay

Crystal violet (CV) assays were performed using 0.05% w/v crystal violet dye to quantify the total biofilm biomass after 24 hours of incubation. After assessing the viability of *C. albicans* cells, the biofilm was air dried at room temperature. The biofilm then was stained with 100 µL of crystal violet and incubated at room temperature for 15 – 20 minutes. After incubation, excess dye was removed by gently washing under tap water until the water ran clear. To destain the biofilm, 100 µL of ethanol (100%) was added to each well and 75 µL was then transferred directly to a new 96-flat bottom well plate. A microtiter plate reader (FLuoStar Omega, BMG labtech, UK) was used to measure the absorbance at 570 nm. The experiments were repeated on at least three independent occasions in quadruplicate (Rajendran et al., 2015).

2.2.6 Microscopic analysis

2.2.6.1 Light microscopy

Microscopic analysis was used to visualize *C. albicans* growth. For light microscopy, *C. albicans* SC5314 was grown on Thermanox™ plastic coverslips of 13-mm-diameter (Fisher-Scientific, Loughborough, UK) in 24-well plates and incubated for 24 hours at 37°C in the presence and absence of compounds, as described above. After incubation, media was removed, and coverslips were washed gently with PBS and stained with crystal violet (0.05%) for analysis on a fluorescence microscope run in light microscopy mode (EVOS, life technologies, USA). Images were representative of at least three independent experiments performed in quadruplicate.

2.2.6.2 Fluorescent microscopy

For fluorescent microscopy, *C. albicans* SC5314 was cultured on coverslips as described in 2.2.6.1 and stained with Calcofluor White (5 µM) (Invitrogen, Fisher Scientific, Loughborough, UK), which binds to cellulose and chitin in the cell wall, and propidium Iodide (20 µM) (Sigma-Aldrich, UK) that intercalates into the double stranded nucleic acid of dead cells or cells with a compromised cell wall. After 15 – 20 minutes of incubation, coverslips were washed gently with PBS to

remove any excess of dye and mounted on slides using 20 µL of mounting media. Slides were then analysed on a fluorescence microscope (EVOS, life technologies, USA). Images were representative of at least three independent experiments performed in quadruplicate.

2.2.6.3 Scanning electron microscopy

Scanning electron microscopy (SEM) analysis was performed as described previously (Millhouse et al., 2014). Briefly, biofilms were washed with PBS and fixed with a fixative solution containing; 2% paraformaldehyde, 2% glutaraldehyde, 0.15 M sodium cacodylate, and 0.15% alcian blue (pH 7.4). After 2 – 22 hours, the fixative solution was removed and 0.15 M sodium cacodylate buffer was added, and biofilms stored in the fridge until processed.

For processing, the biofilms were washed 3 times for 5 minutes each with fresh buffer to remove any gluteraldehyde remnants and incubated for 1 hour with 1% osmium tetroxide in a fume hood. After incubation, samples were washed with distilled water to remove osmium 3 times for 10 minutes each and incubated for 1 hour on the bench in the dark with 0.5% uranyl acetate. Uranyl was removed quickly, and biofilms were rinsed with distilled water. For ethanol dehydration, samples were dehydrated in different concentrations of alcohol increasingly as follows: 30% (2 X 5 minutes), 50% (2 X 5 minutes), 70% (2 X 5 minutes), 90% (2 X 5 minutes), absolute alcohol (4 X 5 minutes) and dried absolute alcohol (4 X 5 minutes). Hexamethyldisilazane (HMDS) was added to the samples which were then incubated for 5 minutes and then the HMDS removed. Samples were then transferred to a new plate and HMDS was added again for 5 minutes prior to being placed into a desiccator to evaporate and dry overnight. The samples were then mounted, and gold patter coated in an argon filled chamber before processing for viewing and imaging using a JEOL JSM-6400 scanning electron microscope (JEOL Ltd, Hertfordshire, UK). Coverslips were prepared in duplicate for different concentrations of PHCl. Experiments were repeated on at least two independent occasions. Different magnifications were used for visualizing and imaging.

2.2.7 Propidium iodide uptake assay

Propidium iodide (PI) uptake assays were conducted for further investigation of cell viability. A *C. albicans* SC5314 suspension was standardized to 5 x 10^7 cells mL, treated with 50 mM PHCl, and incubated at 37°C for 1 hour. Positive and negative controls were included. Positive controls were: 0.2% chlorhexidine (CHX) treated cells and heat killed cells (HK). The Negative control was *Candida* cells cultured in RPMI only. Following treatment, cells were washed by centrifugation in phosphate buffered saline (PBS) and re-suspended in propidium iodide (2 µM PI dye in PBS) for 15 minutes at 37°C. Cell suspensions were then transferred to a black 96-well plate, and fluorescence was measured using a microtiter plate reader (FLuoStar Omega, BMG labtech, UK) at excitation 485 and emission 620 for 1 hour (Sherry et al., 2012). The experiment was performed in triplicate on three independent occasions.

2.2.8 Adenosine 5′-triphosphate bioluminescent assay

The Adenosine 5′-triphosphate (ATP) Bioluminescent Assay Kit (Sigma-Aldrich) was used to quantify the ATP release into supernatants from cells exposed to different experimental conditions. Cells were standardized to 5 x 10^7 cells/mL, treated with 50 mM PHCl, and 2% Fulvic Acid (FA), separately, and incubated for 1 hour. A negative control of untreated *C. albicans* cells was included. Following treatment, supernatants were collected, filtered using 0.22 µM filters to remove cells and the filtrate adjusted to pH ~ 7.0 when required. The supernatants were then transferred to a white 96-well plate, and the ATP assay mix added. The assay was performed according to the manufacturer's instructions and standards were included in the assay. The ATP assay mix was dissolved in sterile water and adjusted to pH 7.8. This mix was diluted 25-fold using the ATP assay mix dilution buffer, which was dissolved previously in 50 mL sterile water. A microtiter plate reader (FLuoStar Omega, BMG labtech, UK) was used to measure the luminescence (Sherry et al., 2012). The experiment was performed in triplicate on three independent occasions.

2.2.9 The xCELLigence real time analysis of cellular impedance

C. albicans cells were cultured in 96-well electronic microtiter plates (E-plate) which are coated with gold microelectrode biosensors (ACEA, Biosciences Inc., San Diego, California, USA) at 1 X 10^6 cells/mL in the presence or absence of 25 mM PHCl ± different concentrations of antifungals (caspofungin and amphotericin B). Plates were incubated at 37°C aerobically and growth was monitored in a real time manner, continuously, over 24 hours by measuring the electrical impedance on the xCELLigence machine (ACEA, Biosciences Inc., San Diego, California, USA). To monitor growth the impedance was recorded every five minutes over 24 hours. The data is represented as normalized (blank background subtracted) cell index, which represents a quantitative measure of cell impedance when adhered to the electrodes and correlates with proliferation or differentiation (Junka et al., 2012, Alshanta et al., 2019). The experiment was performed on three independent occasions in quadruplicate.

2.2.10 Statistical analysis.

Statistical analysis was performed on raw data using PRISM. Each data set was tested for normality and homogeneity using Shapiro-Wilk, Kolmogorov-Smirnov or D' D'Agostino & Pearson tests. Then, for parametric data an ANOVA was performed and for non-parametric data a Kruskal-Wallis test was applied. Significance was determined if $P < 0.05$. A Dunnet test for multiple comparisons was performed on parametric data where required. Likewise, for non-parametric data, a Mann-Whitney test was performed.

2.3 Results

2.3.1 Pilocarpine hydrochloride specifically inhibits *Candida albicans* biofilm formation

A recent study by Rajendran et al. (2015) found that ACh inhibits *C. albicans* pathogenesis by inhibiting transition from yeast to hyphae and biofilm formation. This finding suggests that *C. albicans* may possess a cholinergic receptor that mediates the inhibitory effect of ACh. In order to characterise the subtype of the putative receptor: firstly, the effect of pilocarpine hydrochloride (PHCl), a general muscarinic receptor agonist of humans, and SIB 1508Y Maleate (SIB), a general nicotinic receptor agonist of humans, on total *C. albicans* biofilm biomass and metabolic activity when cultured in a biofilm forming media (RPMI) was investigated.

After 24 hours incubation, biofilm biomass assessment using CV assay revealed that PHCl reduced the total biofilm biomass significantly in a dose dependent manner at concentrations: 3.125, 6.25, 12.5, 25, and 50 mM (Figure 2.1 A). In contrast to PHCl, SIB had no significant inhibitory effect on biofilm biomass at any concentrations investigated (0 – 10mM) (Figure 2.1 B). Metabolic activity assays revealed that PHCl caused a slight significant reduction in *C. albicans* metabolic activity at concentrations of 6.25, 12.5, 25, and 50 mM (Figure 2.1 C). In contrast, SIB did not affect *C. albicans* metabolic activity at any of the tested concentrations (0 – 10 mM) (Figure 2.1 D).

To confirm that the inhibitory effect of PHCl was specifically mediated by a potential muscarinic-like receptor, biomass and metabolic activity of the biofilm were evaluated in the presence of PHCl, ± different concentrations of scopolamine (SCP), a nonspecific muscarinic receptor antagonist. SCP inhibits the PHCl induced reduction in biofilm formation in a dose-dependent manner at concentrations of 16, 32, 64, and 128 µM; as evidenced by the fact that with these concentrations of SCP there was no longer a significant reduction in the total biofilm biomass compared to cells treated with PHCl alone (Figure 2.2 A). In addition, there was no longer any effect on metabolic activity when cells were treated with PHCl in the presence of SCP (Figure 2.2 B) as previously observed (Figure 2.2).

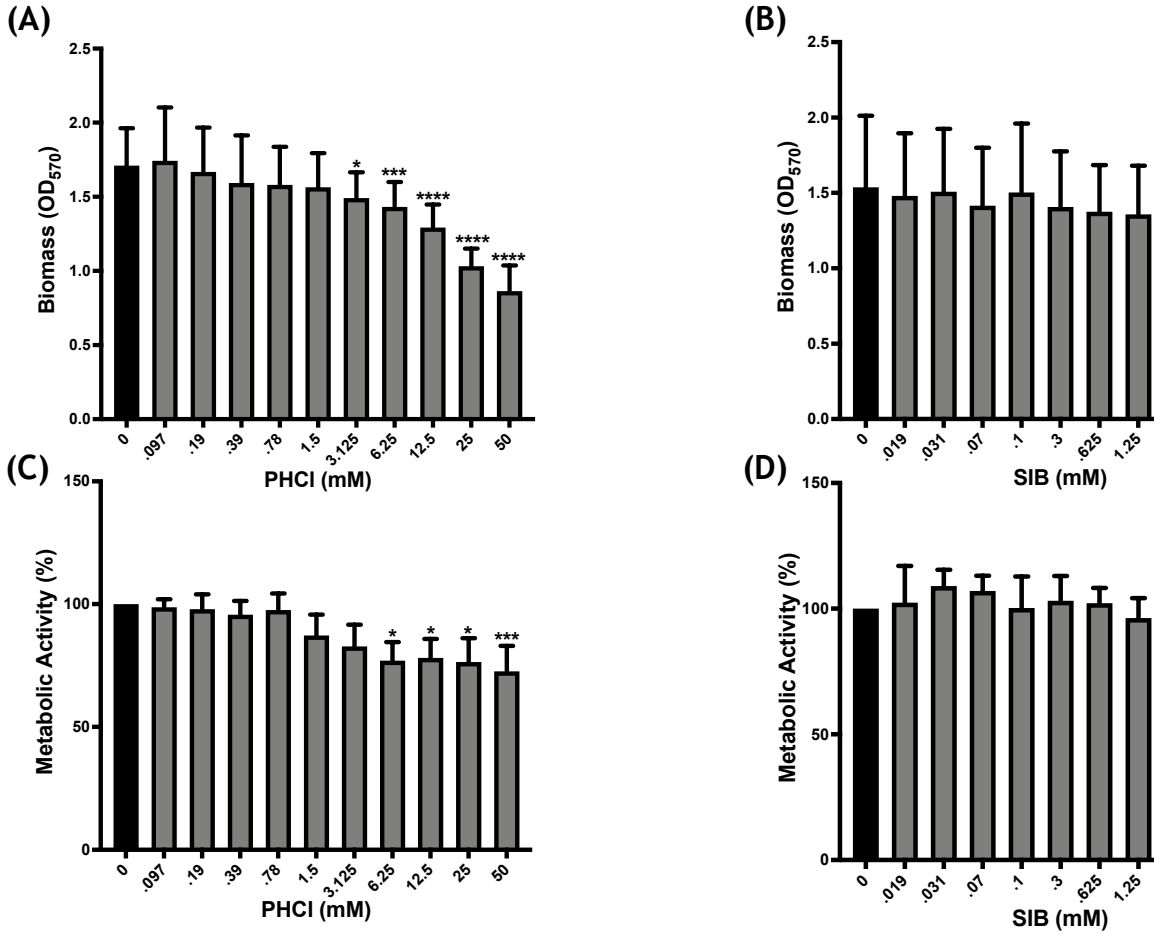

Figure 2.1 Pilocarpine hydrochloride inhibits *C. albicans* biofilm formation. Cells were incubated for 24 hours to allow biofilm formation in the presence and absence of (0-50 mM) PHCl and (0-10 mM) SIB 1508Y. Total biofilm biomass was assessed using crystal violet assay (A and B). Biofilm metabolic activity was assessed using XTT assay (C and D). Data represents at least six independent experiments. Statistical analysis; *, $P < 0.05$; **, $P < 0.01$; ***, $P < 0.001$; ****, $P < 0.0001$. * significant difference from control (cells cultured alone).

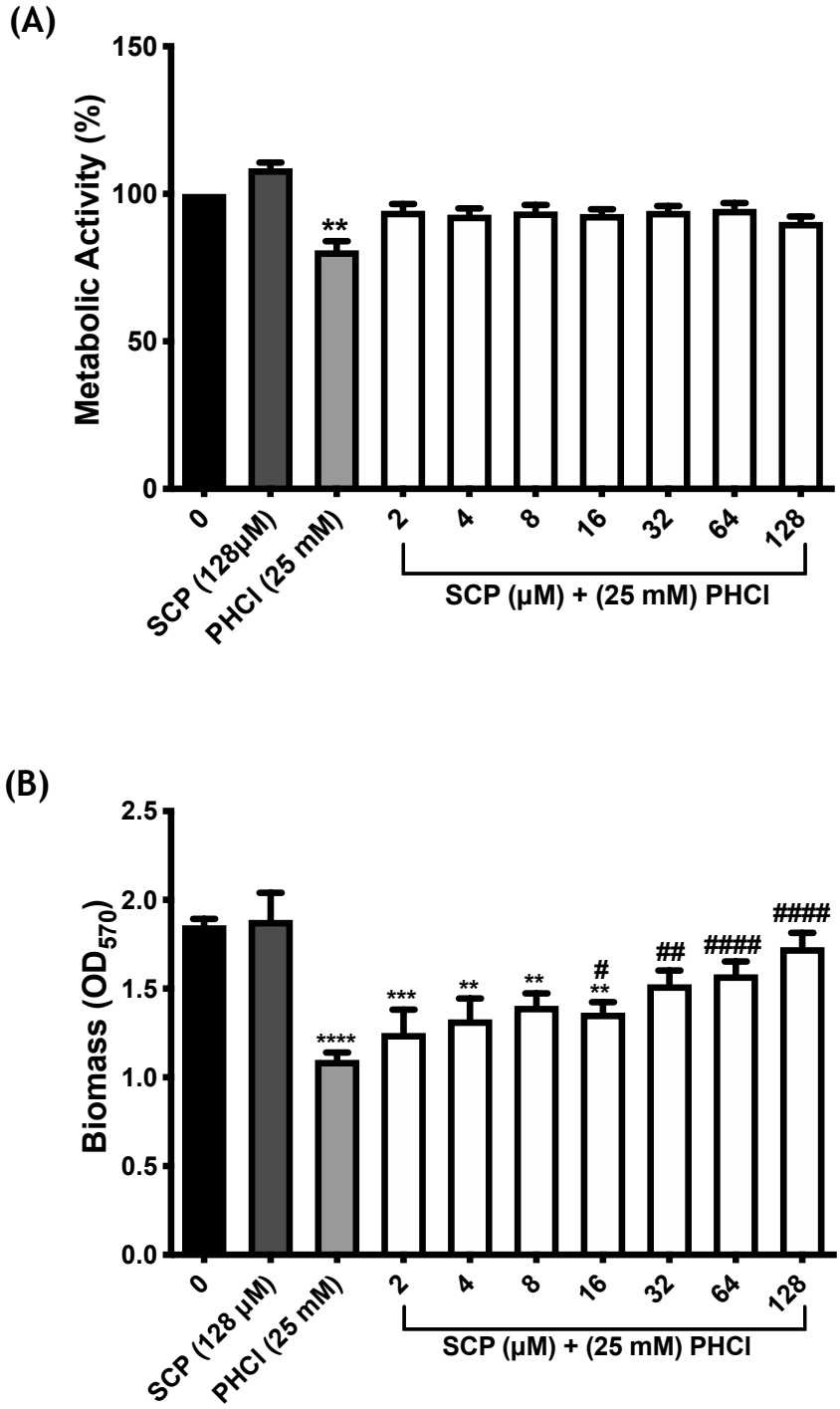

Figure 2.2 The inhibitory effect of pilocarpine hydrochloride was mediated specifically through muscarinic like receptors. Cells were incubated for 24 hours to allow biofilm formation in the presence and absence of PHCl (0-50 mM) and SCP (0-128 μM) SCP. Biofilm metabolic activity was assessed using XTT assay (A). Total biofilm biomass was assessed using crystal violet assay (B). Data represents at least six independent experiments. Statistical analysis; *, $P < 0.05$; **, $P < 0.01$; ***, $P < 0.001$; ****, $P < 0.0001$, or #, $P < 0.05$; ##, $P < 0.01$; ###, $P < 0.001$; ####, $P < 0.0001$. # significant difference from cells treated with PHCl alone; * significant difference from control (cells cultured alone).

2.3.2 Pilocarpine hydrochloride has no cytotoxic effects on *Candida albicans*

To investigate the viability of *C. albicans* SC5314 following PHCl treatment ATP release was quantified using an ATP assay kit. This assay revealed no significant difference in the concentrations of ATP released following 50 mM PHCl treatment (PHCl) compared to the control (untreated cells). However, a significant difference was observed in released ATP concentrations when treated with FA (2%) compared to PHCl (50 mM) treated cells or untreated cells (Figure 2.3 A). In addition, the uptake of PI dye by dead cells after PHCl treatment was quantified. This revealed considerably high PI uptake by heat killed cells and cells treated with 0.2% CHX. In contrast, cells cultured alone (control), or treated with 50 mM PHCl, revealed no PI uptake following treatment (Figure 2.3 B).

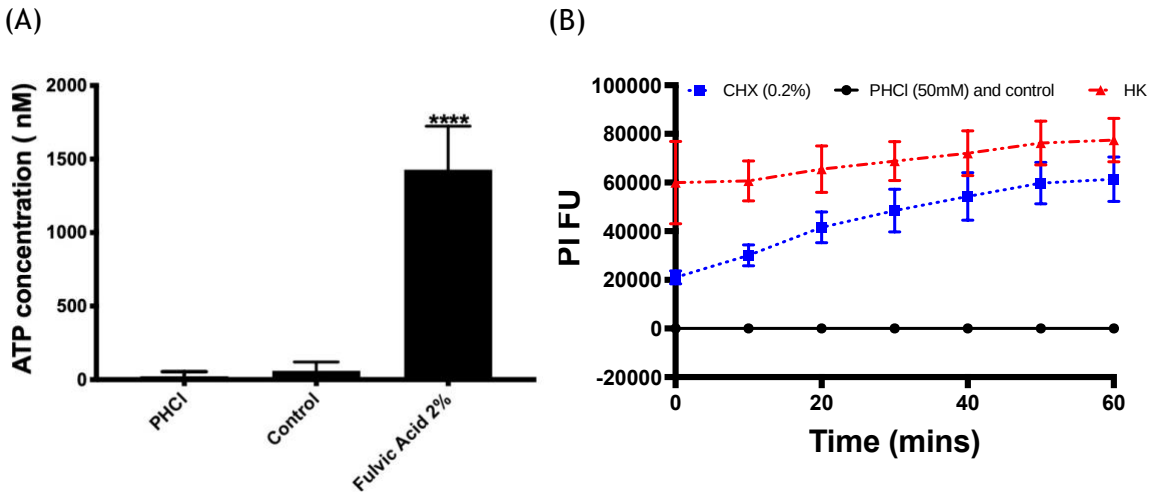

Figure 2.3 Pilocarpine Hydrochloride does not affect *C. albicans* SC5314 viability or cell wall integrity. (A) ATP assay, cells were treated with 50 mM of PHCl and incubated for 1 hour. Supernatant was collected and filtered prior to conducting the assay. Standards, negative and positive controls were included. The positive control was Fulvic Acid (FA) 2%. The negative control was cells cultured in media alone. The assay was performed according to manufactures' instructions. (B) PI uptake assay, cells were treated with PHCl, incubated for 1 hour, and re-suspended in 2 µM PI. The positive controls were heat killed cells (HK) and 0.2% chlorhexidine treated cells (CHX). The negative control was cells cultured in media alone. Data represents at least three independent experiments.

2.3.3 Effect of pilocarpine hydrochloride on *Candida albicans* morphogenesis and biofilm formation.

To investigate the effect of PHCl on *C. albicans* morphology and biofilm formation microscopy was employed. Light microscopic analysis revealed an alteration in biofilm formation and cell morphology. Considerable visual decreases in true hyphae, and an abundance of yeast cells with the presence of some pseudohyphae were observed in biofilms treated with PHCl (50 mM) compared to untreated biofilms (control); where true hyphae were significantly dominant and mature biofilms formed (Figure 2.4 A, B, and C). Visually, the number of yeast and pseudohyphae decreased at lower concentrations (25 mM and 12.5 mM), while true hyphae formation increased gradually in a dose dependent manner. These findings were supported by the SEM analysis which visually demonstrated a reduction in the hyphal form and biofilm formation as the concentrations of PHCl increased, compared to untreated biofilms (Figure 2.4 B). Fluorescent microscope analysis visually demonstrated no major differences in cell viability between all concentrations of PHCl and untreated cells when stained with CFW (blue) and PI (red) (Figure 2.4 C).

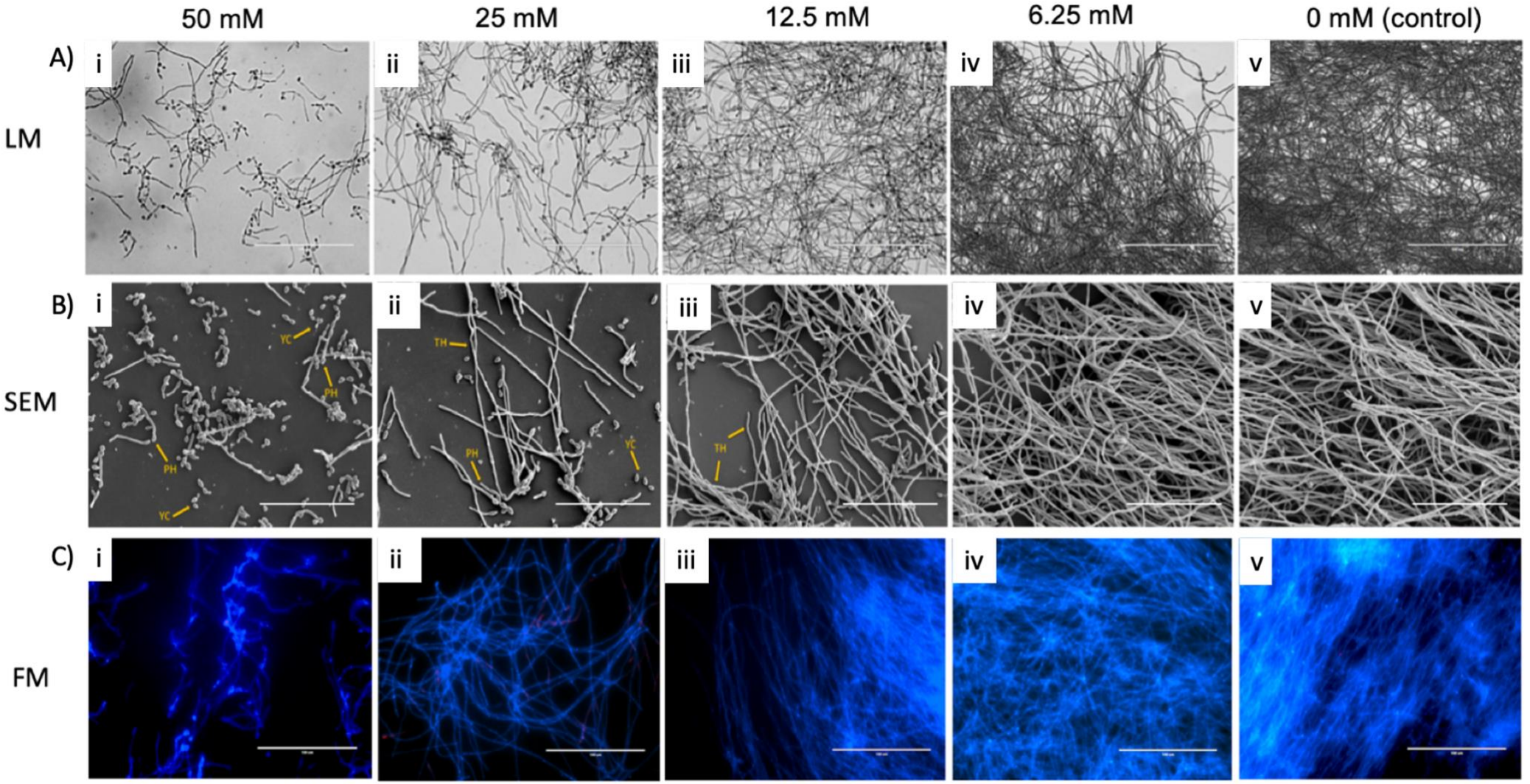

Figure 2.4 Morphological changes in *C. albicans* SC5314 induced by pilocarpine hydrochloride. To assess this effect microscopic analysis was employed. (A) light microscopy (LM) and (B) Scanning electron microscopy (SEM) was used to visualize the changes in biofilm biomass and cell morphology when cultured with different

concentrations of PHCl (0 to 50 mM) respectively represented by numbers (i to v). Images showed that PHCl inhibit *C. albicans* filamentation and biofilm formation in a dose dependent manner. (C) Fluorescence microscopy (FM) was also used to evaluate the viability of the cells upon PHCl treatment. Visually images confirmed the inhibition of the yeast-to-hypha transition in the presence of PHCl. Viability was assessed using calcofluor white (CFW, blue) and propidium iodide (PI, red) staining, which also revealed that PHCl was not toxic to *C. albicans and* did not affect cell viability under any of the PHCl concentrations used in the experiment. Scale bars are depicted on individual images. 100X magnification was used for fluorescent and light microscope images, and 700X was used for SEM. Images are representative of duplicate or triplicate coverslips from at least 2 independent experiments. Yellow arrows indicate yeast cells (YC), true hyphae (TC) and pseudo hyphae (PH).

2.3.4 Pharmacological characterisation of putative *Candida albicans* muscarinic receptor

To begin to elucidate the receptor-based mechanisms by which cholinergic compounds regulate *C. albicans* biofilm formation, a pharmacological approach was undertaken. *C. albicans* was treated with several muscarinic agonists and antagonists which target specific subtypes of human muscarinic receptors to delineate the potential subtype of receptor(s) possessed by *C. albicans* which may mediate cholinergic signaling. To determine if specific muscarinic like receptors with homology to human M1 – M5 receptors were expressed by *C. albicans* we investigated the effects of different specific agonist or antagonist compounds (Table 2.3) on *C. albicans* viability and biofilm biomass. For the M1 receptor, cevimeline hydrochloride (C-HCL) (M1AChR agonist) was used and for the M2 receptor, arecaidine propagryl ester tosylate (APE) (M2AChR agonist) agonist was used. For the M3, 4, and 5 receptors, there were no commercially specific agonists available at the time of experimentation. Therefore, for the M3 and M4 type receptors, J 104129 fumarate (JF) (M3AChR) and PD 102807 (PD) (M4AChR) antagonists, respectively were used in the presence of PHCl. For the M5 receptor, Vu 0238429 (Vu), an M5 allosteric modulator, was used.

C. albicans cells cultured in RPMI in the presence of 0 –100 μM C-HCL (M1AChR agonist) showed a negligible decrease but no dose dependent reduction in the total biofilm biomass and metabolic activity (Figure 2.5). Treatment with APE (M2AChR agonist) resulted in a slight, yet significant reduction in biofilm biomass at concentrations of 100 and 50 μM; with no significant inhibitory effect on metabolic activity (Figure 2.6). When *C. albicans* was cultured in the presence of (50 mM) PHCl and JF (M3AChR antagonist) (Figure 2.7), or PD (M4AChR antagonist) (Figure 2.8), no disruption of the PHCl induced inhibition of *C. albicans* biofilm formation and metabolic activity was observed at any of the concentrations used (0 – 100 μM). However, when *C. albicans* was cultured with VU 0238429 (M5 allosteric modulator) a significant dose dependent reduction in the total biofilm biomass was observed at concentrations (12.5, 25, 50, and 100 μM) which was accompanied by a significant reduction in metabolic activity at concentrations (25, 50, and 100 μM) (Figure 2.9).

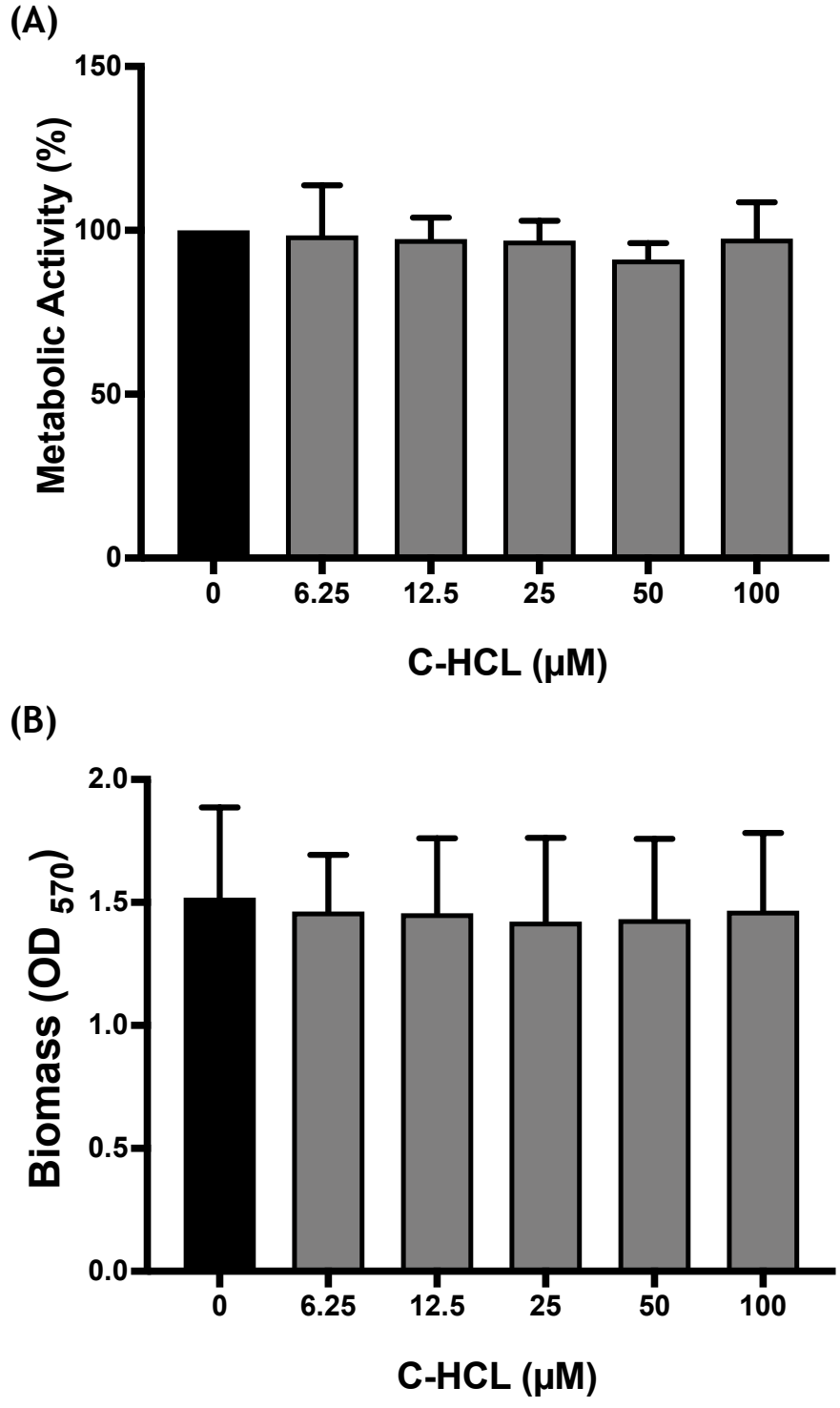

Figure 2.5 Effect of M1AChR agonist C-CHL on *C. albicans* biofilm formation and metabolic activity. Cells were incubated for 24 hours to allow for biofilm formation in the presence and absence of C-HCL. Biofilm metabolic activity was assessed using XTT assay (A). Total biofilm biomass was assessed using crystal violet assay (B). The experiment was repeated on at least three independent occasions. Statistical analysis; *, $P < 0.05$; **, $P < 0.01$; ***, $P < 0.001$; ****, $P < 0.0001$. * significant difference from control (cells cultured alone).

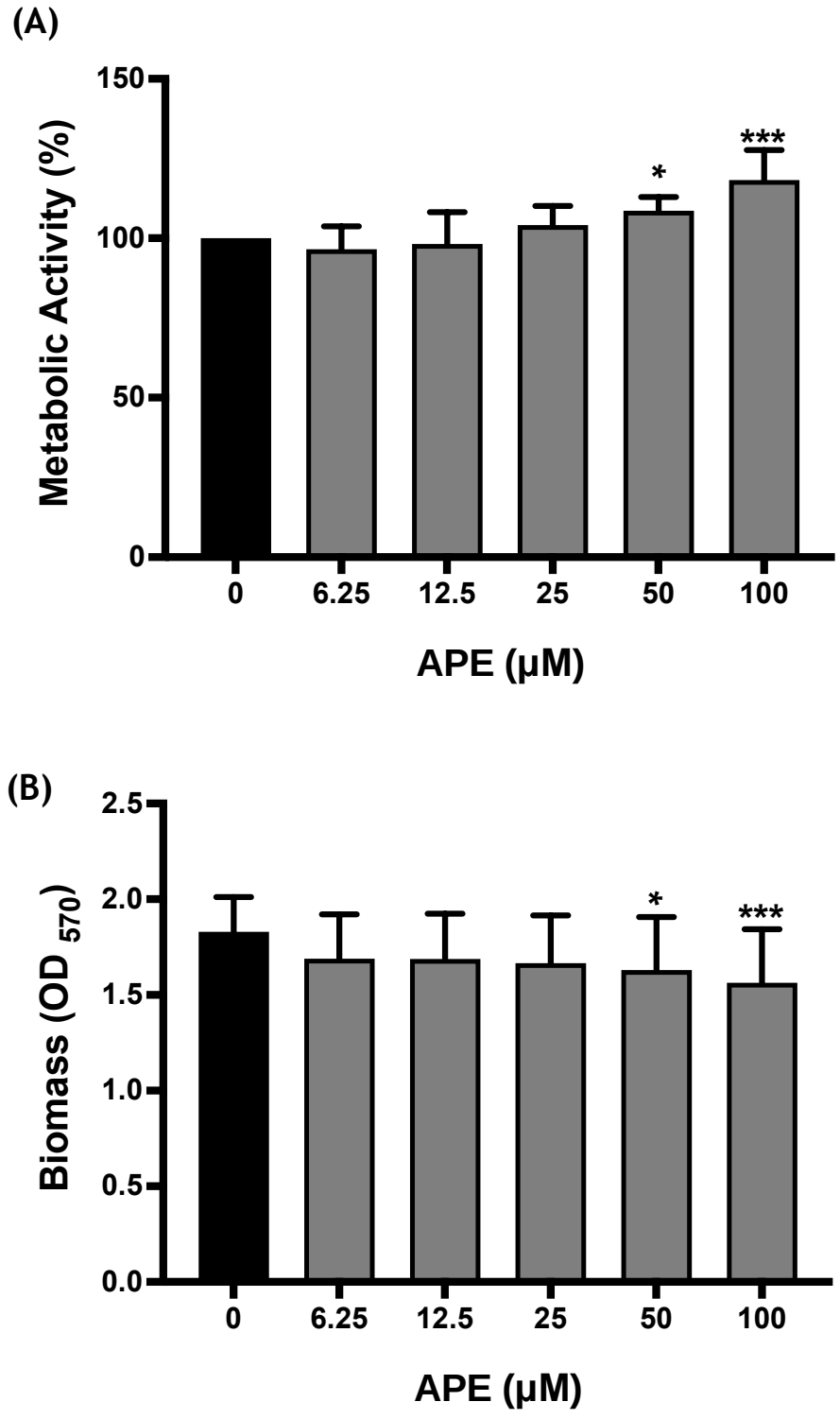

Figure 2.6 Effect of M2AChR agonist APE on *C. albicans* biofilm formation and metabolic activity. Cells were incubated for 24 hours to allow for biofilm formation in the presence and absence of APE. Biofilm metabolic activity was assessed using XTT assay (A). Total biofilm biomass was assessed using crystal violet assay (B). The experiment was repeated on at least three independent occasions. Statistical analysis; *, $P < 0.05$; **, $P < 0.01$; ***, $P < 0.001$; ****, $P < 0.0001$. * significant difference from control (cells cultured alone).

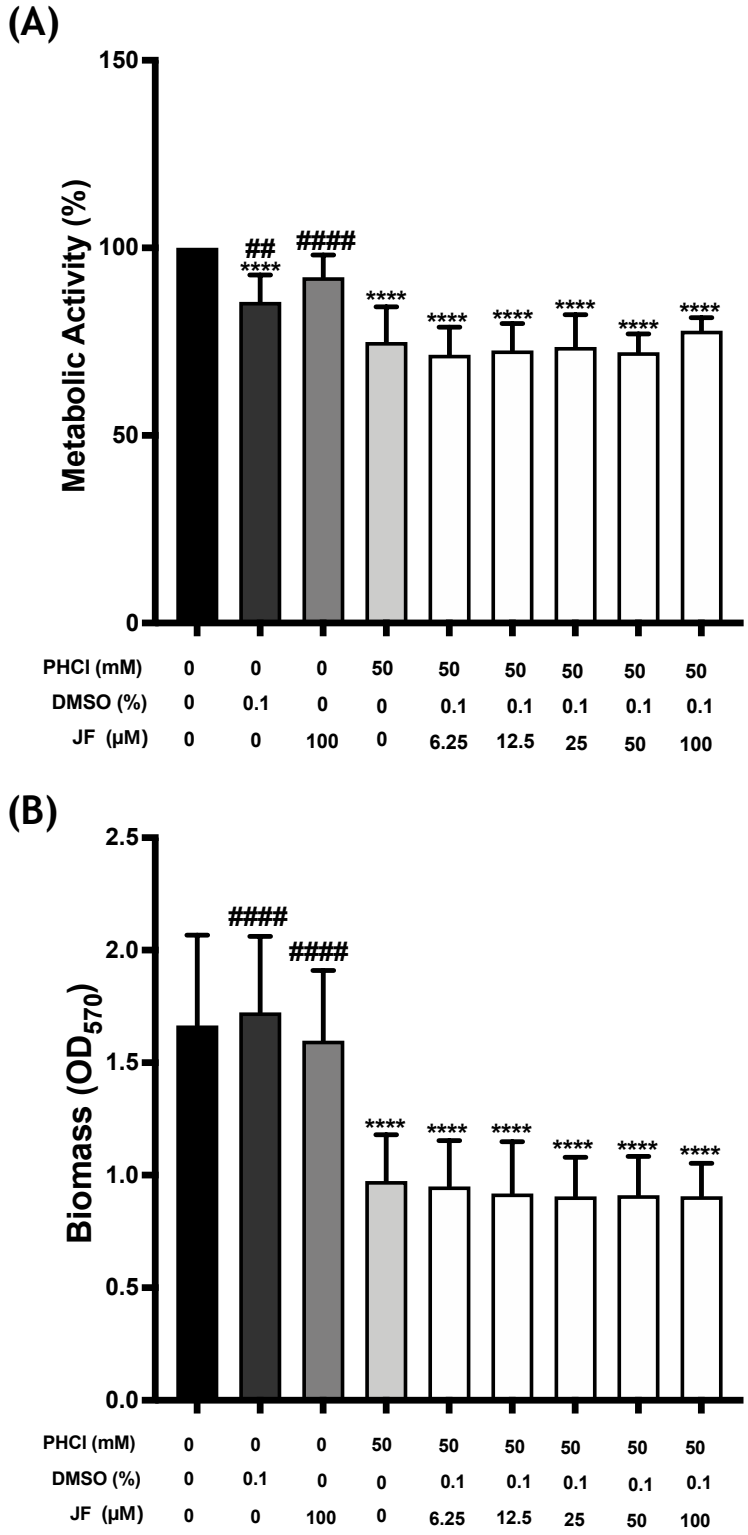

Figure 2.7 Effect of M3AChR antagonist JF on *C. albicans* biofilm formation and metabolic activity. Cells were incubated with for 24 hours to allow for biofilm formation in the presence and absence of PHCl (50 mM) and various concentrations of JF. Biofilm metabolic activity was assessed using XTT assay (A). Total biofilm biomass was assessed using crystal violet assay (B). The experiment was repeated on at least three independent occasions. Statistical analysis; *, $P < 0.05$; **, $P < 0.01$; ***, $P < 0.001$; ****, $P < 0.0001$, or #, $P < 0.05$; ##, $P < 0.01$; ###, $P < 0.001$; ####, $P < 0.0001$. # significant difference from cells treated with PHCl alone; * significant difference from control (cells cultured alone).

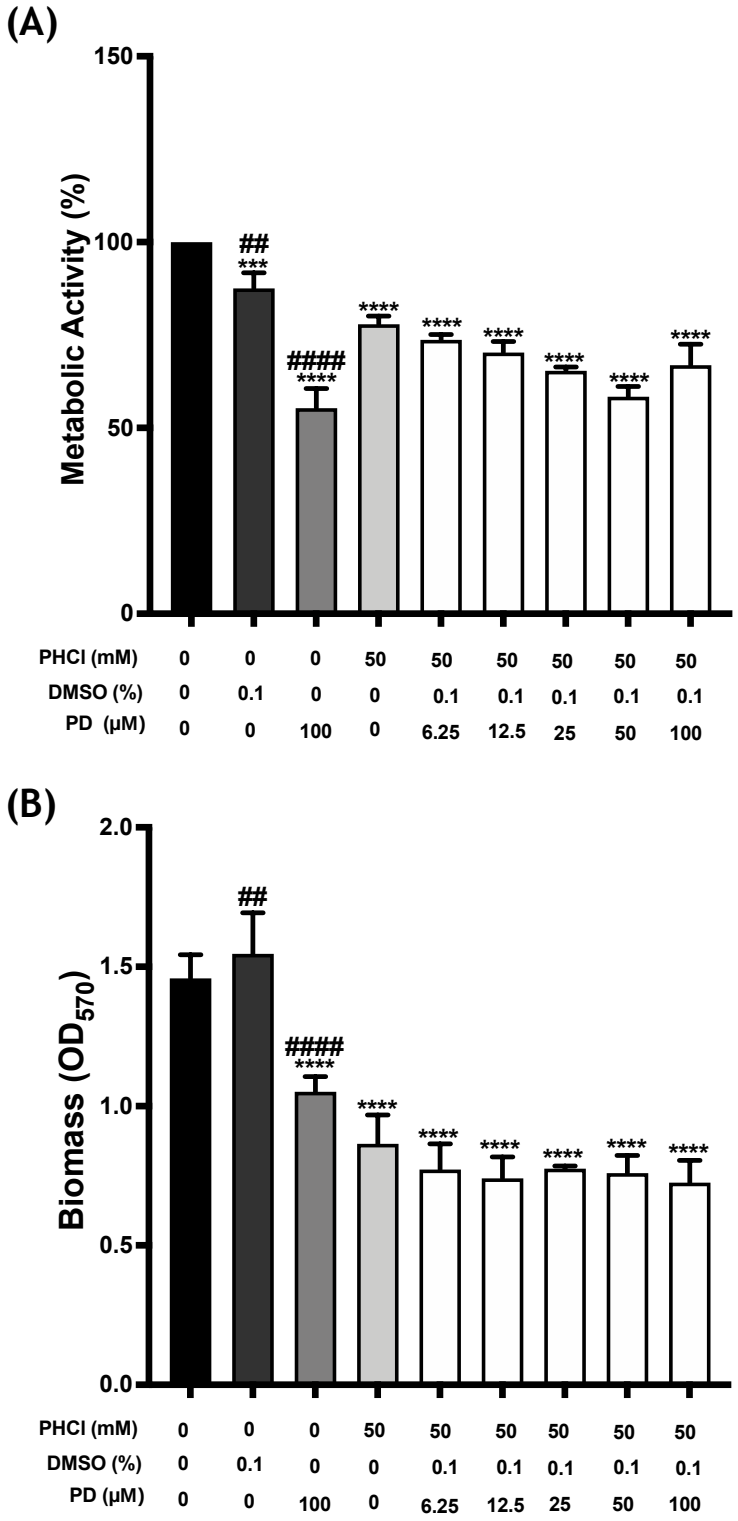

Figure 2.8 Effect of M4AChR antagonist PD on *C. albicans* biofilm formation and metabolic activity. Cells were incubated with for 24 hours to allow for biofilm formation in the presence and absence of PHCl (50 mM) and various concentrations of PD. Biofilm metabolic activity was assessed using XTT assay (A). Total biofilm biomass was assessed using crystal violet assay (B). The experiment was repeated on at least three independent occasions. Statistical analysis; *, $P < 0.05$; **, $P < 0.01$; ***, $P < 0.001$; ****, $P < 0.0001$, or #, $P < 0.05$; ##, $P < 0.01$; ###, $P < 0.001$; ####, $P < 0.0001$. # significant difference from cells treated with PHCl alone; * significant difference from control (cells cultured alone).

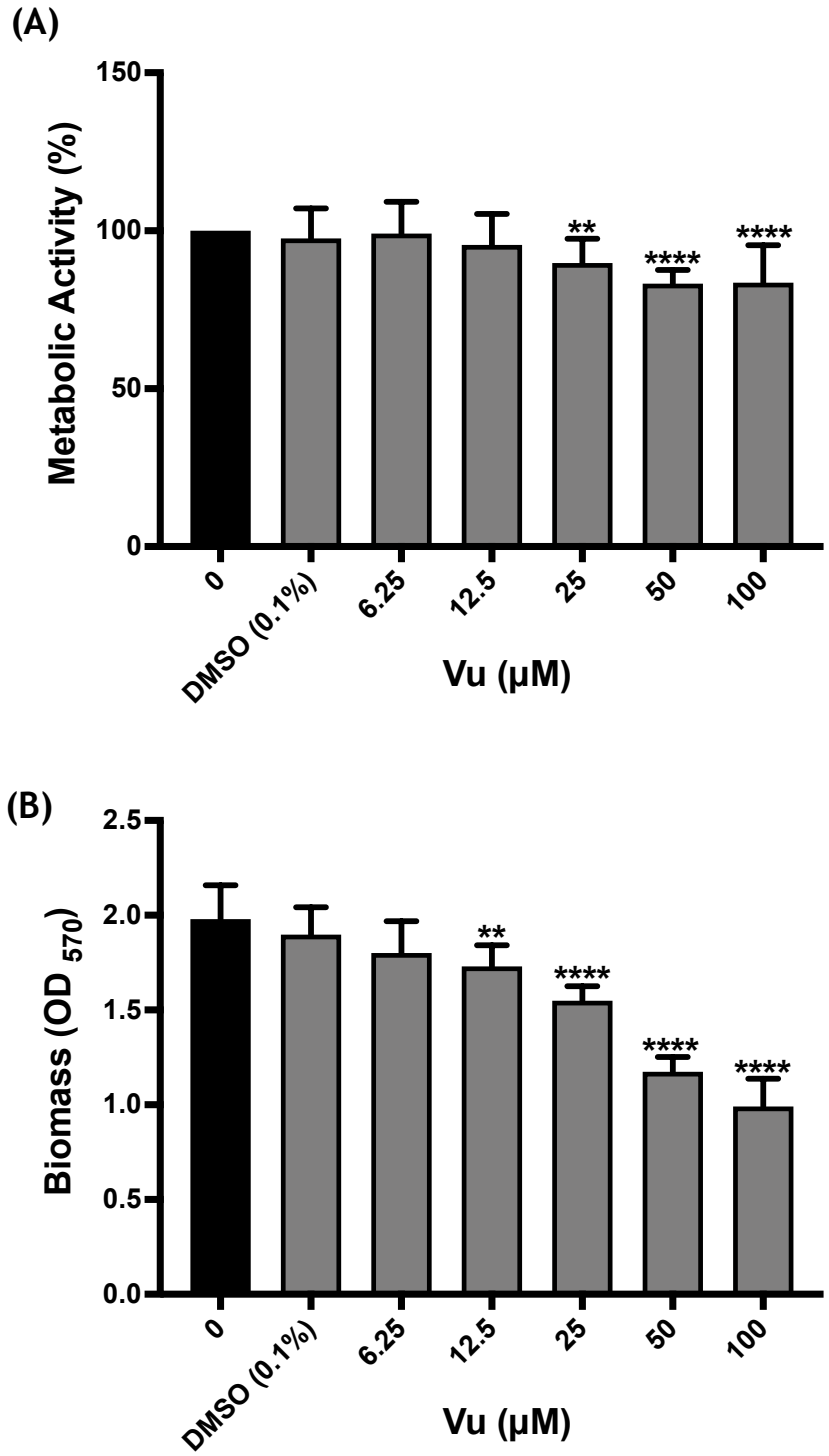

Figure 2.9 Effect of Vu 0238429, M5AChR allosteric modulator on *C. albicans* biofilm formation and metabolic activity. Cells were incubated for 24 hours to allow for biofilm formation in the presence and absence of Vu 0238429. Biofilm metabolic activity was assessed using XTT assay (A). Total biofilm biomass was assessed using crystal violet assay (B). The experiment was repeated on at least three independent occasions. Statistical analysis; *, $P < 0.05$; **, $P < 0.01$; ***, $P < 0.001$; ****, $P < 0.0001$. * significant difference from control (cells cultured alone).

2.3.5 Characterisation of a G protein subtype coupled to acetylcholine muscarinic receptor

Human muscarinic receptors are G protein coupled receptors. M1, M3, and M5 receptors are coupled to Gq proteins which when activated initiate a signaling cascade that results in phospholipase C (PLC) activation and intracellular Ca^{+} release. On the other hand, M2 and M4 are coupled to G_i and G_o proteins and their activation initiates the cAMP pathway and potassium conductivity (Fryer et al., 2012, Hesham et al., 2020).

Further investigations were conducted to identify whether a certain G protein homologue was involved in downstream receptor signaling to inhibit biofilm formation in *C. albicans*. To this aim, cells were treated with YM, a G_q protein inhibitor and PTX, a G_i protein inhibitor, in the presence and absence of PHCl. Both inhibitors (YM and PTX) did not significantly inhibit the PHCl induced reduction in biofilm biomass or metabolic activity (Figure 2.10) and (Figure 2.11). However, microscopic analysis revealed considerably more hyphal growth in presence of YM compared to when cells were treated with PHCl alone (Figure 2.12 A).

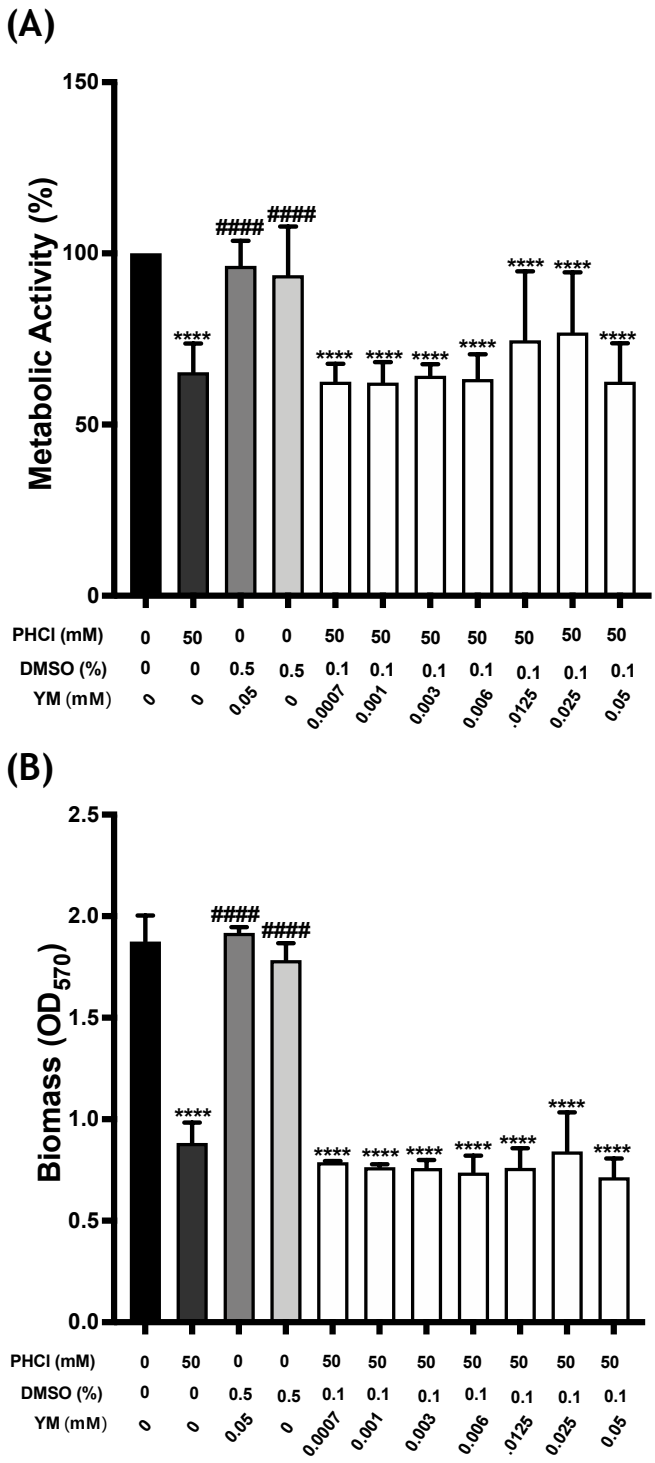

Figure 2.10 Effect of YM 254890 (G_q protein inhibitor) on *C. albicans* biofilm formation and metabolic activity. Cells were incubated for 24 hours to allow for biofilm formation in the presence and absence of small molecule inhibitor YM 254890, combined with PHCl (50 mM). Metabolic activity assessed using XTT assay (A). Total biofilm biomass evaluated using crystal violet assay (B). The experiment was repeated on at least three independent occasions. Statistical analysis; *, $P < 0.05$; **, $P < 0.01$; ***, $P < 0.001$; ****, $P < 0.0001$, or #, $P < 0.05$; ##, $P < 0.01$; ###, $P < 0.001$; ####, $P < 0.0001$. # significant difference from cells treated with PHCl alone; * significant difference from control (cells cultured alone).

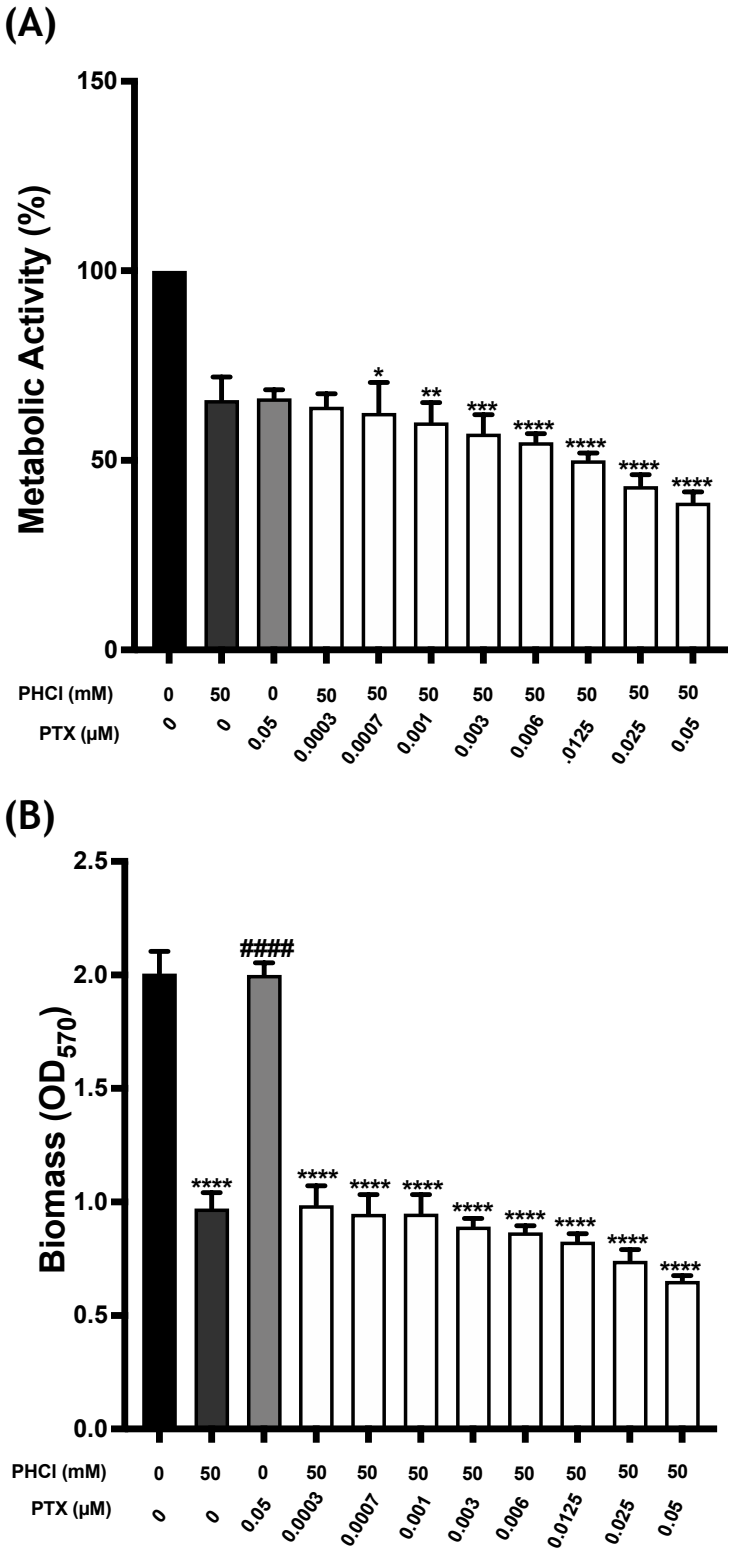

Figure 2.11 Effect of PTX (G_i protein inhibitor) on *C. albicans* biofilm formation and metabolic activity. Cells were incubated for 24 hours to allow for biofilm formation in the presence and absence of small molecule inhibitor PTX, combined with PHCl (50 mM). Metabolic activity assessed using XTT assay (A). Total biofilm biomass evaluated using crystal violet assay (B). The experiment was repeated on at least three independent occasions. Statistical analysis; *, $P < 0.05$; **, $P < 0.01$; ***, $P < 0.001$; ****, $P < 0.0001$, or #, $P < 0.05$; ##, $P < 0.01$; ###, $P < 0.001$; ####, $P < 0.0001$. # significant difference from cells treated with PHCl alone; * significant difference from control (cells cultured alone).

2.3.6 Effect of U73122, the phospholipase C inhibitor on PLC signaling

G_q proteins, when activated, initiate a signaling cascade that results in phospholipase C (PLC) activation and intracellular Ca^+ release. Therefore, cells were exposed to 25 mM PHCl in the presence and absence of U73122 (0.003 and 0.0007 mM), an inhibitor of PLC downstream of G_q in the M1, M3, and M5 signaling pathway. Treating cells with the PLC inhibitor resulted in a significant biofilm biomass reduction at both concentrations used compared to untreated cells. Yet, it showed considerable survival of biofilm biomass in presence of PHCl compared to when cells treated with PHCl alone (Figure 2.12 B).

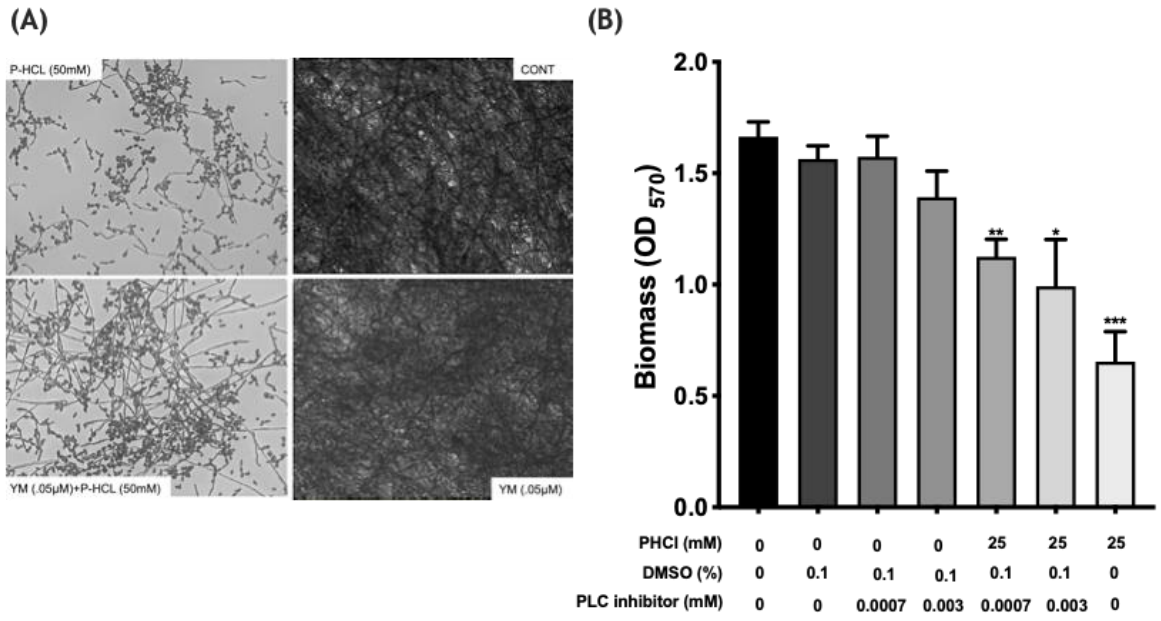

Figure 2.12 Small molecule inhibitors rescued biofilm formation in presence of PHCl. Cells were incubated for 24 hours for biofilm formation in the presence and absence of small molecule inhibitors (A) YM 254890 and (B) U73122 combined with PHCl (25 mM). (A) Light microscopy images show considerable hyphal growth was observed when cells were treated with PHCl in presence of YM compared to PHCl only treated cells. (B) Crystal violet assay shows rescued biofilm biomass when cells were treated with PHCl (25mM) in presence of U73122 (0.0007mM and 0.003mM), The experiment was repeated on at least three independent occasions. Statistical analysis; *, $P < 0.05$; **, $P < 0.01$; ***, $P < 0.001$; ****, $P < 0.0001$.* significant difference from control (cells cultured alone).

2.3.7 Effect of pilocarpine hydrochloride on the total biofilm biomass of *Candida albicans* clinical isolates

The effect of PHCl on the total biofilm biomass of clinical *C. albicans* isolates was evaluated. Isolates used in this study were from three different sites; blood, vagina, and the oral cavity. From each site, 6 low biofilm forming isolates and 6 high biofilm forming isolates were evaluated for total biomass. Crystal violet assessment for those isolates revealed a dose dependent decrease in *C. albicans* biofilm biomass when treated with 50 mM PHCl. Generally, isolates showed susceptibility to PHCl independently of biofilm forming ability (Figure 2.13 A). Post treatment with 50 mM PHCl, high biofilm forming bloodstream isolates revealed a significant reduction in total biomass; SC31, SC44A, SC39, and SC198. A similar finding was observed with all high biofilm forming vaginal isolates used in this study. The same was true for high biofilm forming oral isolates; GSK 4, 25, 61, 90, and 93 (Figure 2.13 B). Low biofilm forming blood isolates also showed significant reduction in biofilm biomass after treatment with 50 mM PHCl; SC25, SC71, SC88C, SC89B, and 204. A similar finding was observed in low biofilm forming vaginal isolates; SVS11, SVS43, and SVS57 and low biofilm forming oral isolates; GSK31, GSK53, GSK65 (Figure 2.13 C).

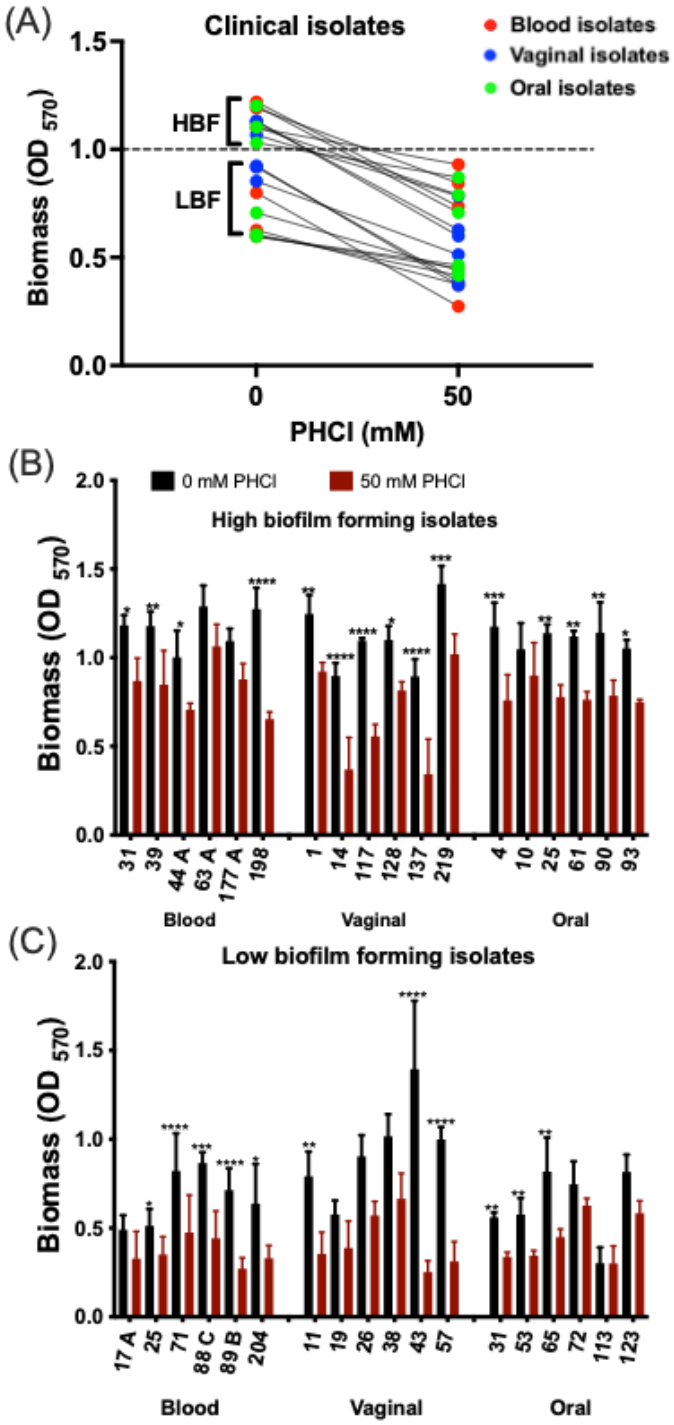

Figure 2.13 The effect of pilocarpine hydrochloride on the biofilm biomass of clinical *C. albicans* isolates. Clinical isolates from the bloodstream, vagina and oral cavity were evaluated for the total biofilm biomass following PHCl treatment at a concentration of 50mM (red bars). 0 mM (black bars) represent the absence of the treatment. Crystal violet assay shows (A) biofilm biomass reduction induced by PHCl. This effect was independent of biofilm forming ability. (B) high biofilm forming isolates, (C) low biofilm forming isolates. Each isolate was assessed in triplicate on at least three independent occasions. Statistical analysis; *, $P < 0.05$; **, $P < 0.01$; ***, $P < 0.001$; ****, $P < 0.0001$.

2.3.8 Effect of pilocarpine hydrochloride, caspofungin, and amphotericin B on cell proliferation, viability, and morphology of *Candida albicans*

C. albicans cell proliferation, viability and morphological changes were monitored in real time using the xCELLigence RTCA machine (ACEA biosciences, Inc) in the presence and absence of PHCl by quantifying electrical impedance. Figure 2.14A shows the electrical impedance profile (EIP) for *C. albicans* SC5314 (laboratory strain) cultured in the presence and absence of 50 mM PHCl for 24 hours. In the absence of PHCl, *C. albicans* demonstrates an irregular EIP. In contrast, in the presence of PHCl a smoother EIP is observed. Likewise, Figure 2.14B and Figure 2.14C show similar representative EIPs for a low (SC17 LBF) and high (SVS128 HBF) biofilm forming clinical isolates, respectively, demonstrating PHCl effect on cell proliferation and morphology. This effect of PHCl was also observed with other clinical isolates shown in appendix I (Figure 1 - 3). This was confirmed visually as shown in (Figure 2.14 B and C).

Combination of PHCl and antifungals were investigated to test the potential use of PHCl as adjunctive therapy to impair *C. albicans* virulence to be more vulnerable to conventional antifungals. The effect of caspofungin (CSP) and amphotericin B (AMB) on *C. albicans* in the presence and absence of PHCl was also investigated using the xCELLigence RTCA reader. Cells treated with a combination of PHCl (25 mM) and CSP (16 µg/mL) resulted in less viability (Figure 2.15 A, B, and C). However, as CSP concentration decreases the viability of the cells increases in the presence of PHCl overtime (data not shown). Post AMB treatment (0.25 µg/mL), the laboratory strain SC5314 showed recovery or an increase in viability after 24 hours incubation in 25 mM PHCl compared to cells treated with AMB alone at concentrations (0.25 µg/mL) (Figure 2.15 D, E, and F). The effect of antifungals on *C. albicans* isolates EIP was also investigated and shown in appendix I and II (Figure 4) and (Figure 5). Cells were killed at higher concentrations of AMB (0.5 – 32 µg/mL) regardless of PHCl presence or absence (data not shown).

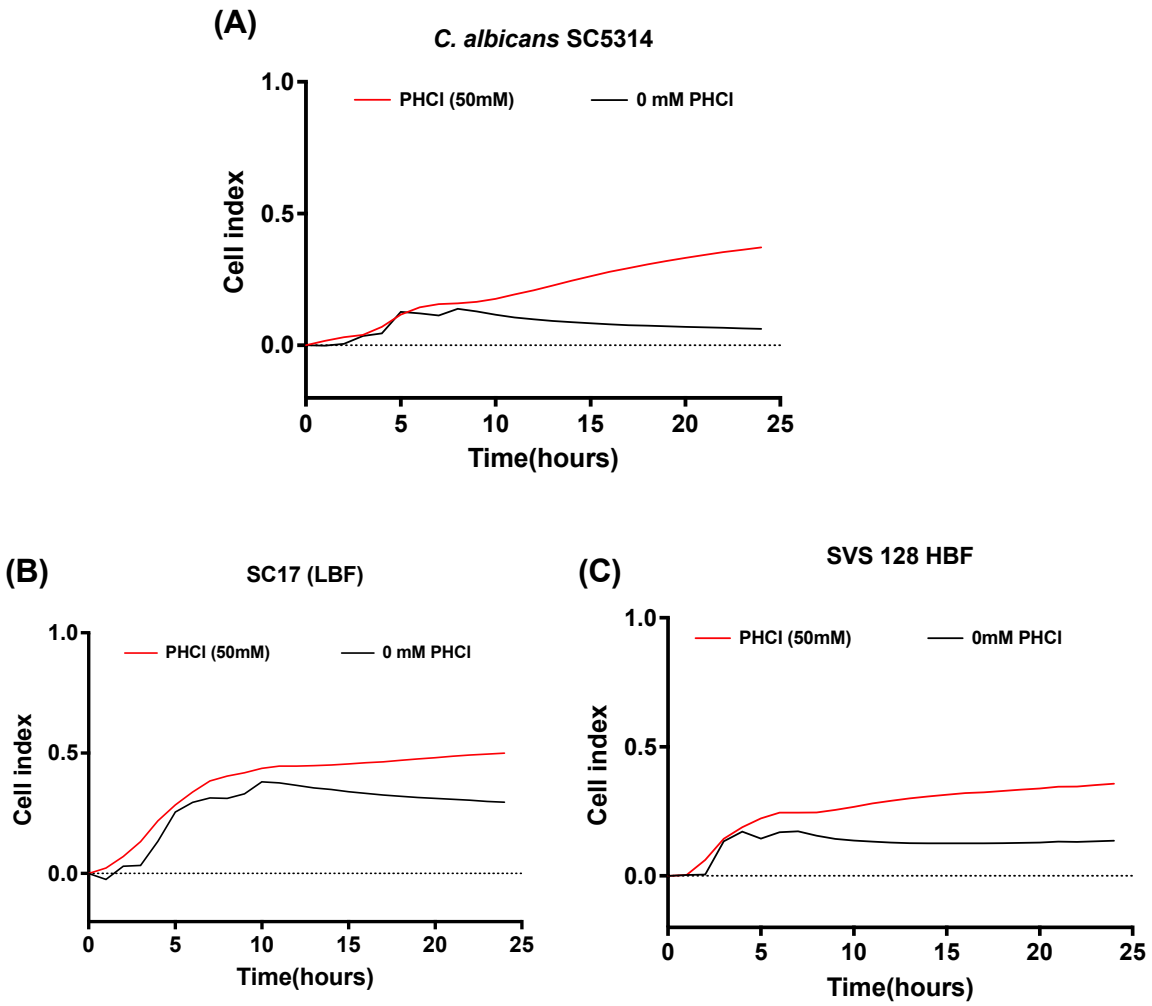

Figure 2.14 Electrical impedance profile of *C. albicans* cultured in the presence and absence of pilocarpine hydrochloride. Cells were cultured on E- plate in RPMI biofilm forming media in the presence and absence of 50 mM PHCl and growth was monitored over 24h in a real time manner by measuring the electrical impedance profile (EIP). (A) Laboratory strain SC5314, (b) a representative low biofilm forming isolate, and (c) a representative high biofilm forming isolate. The experiment was repeated once due to time limitation.

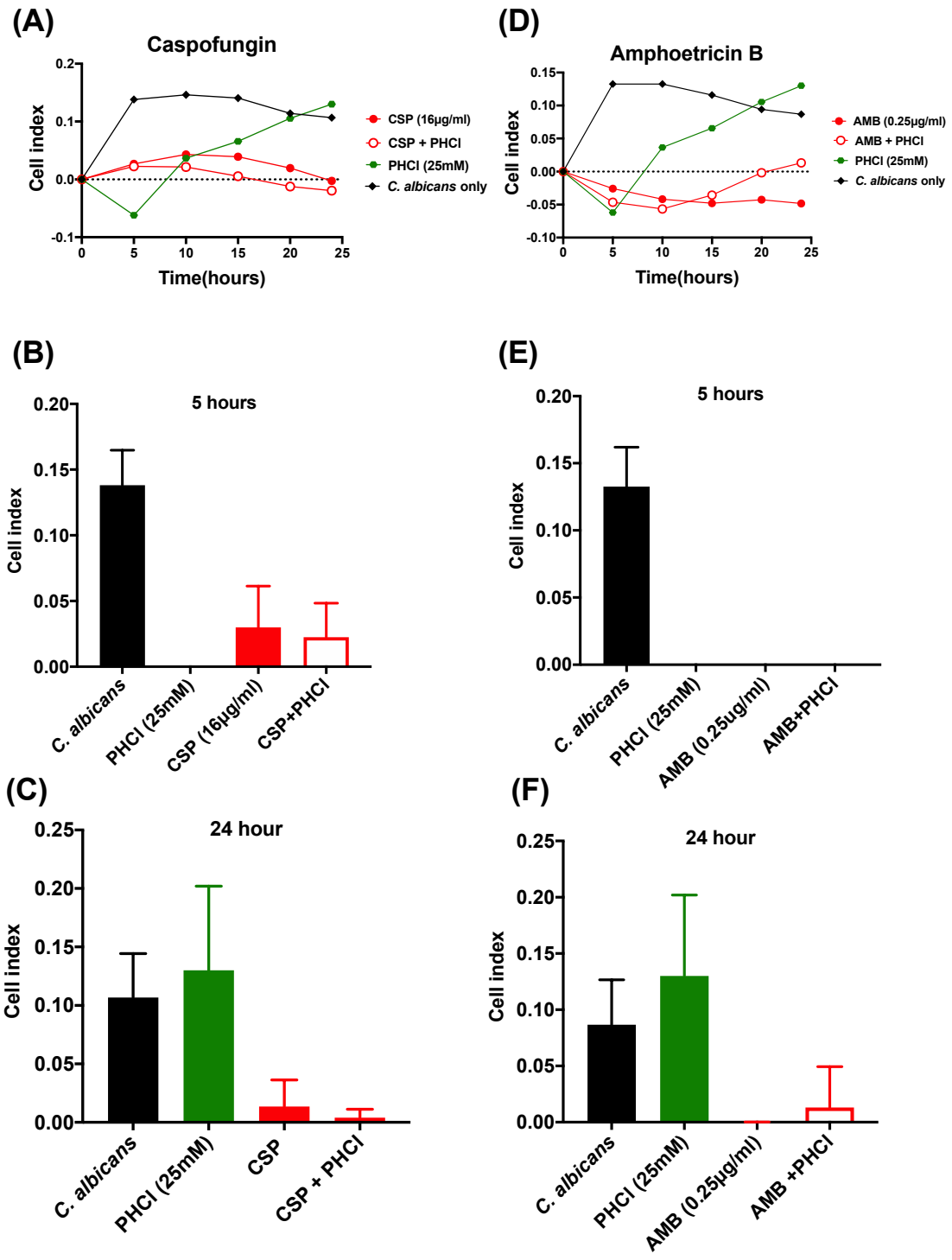

Figure 2.15 Electrical impedance profile of *C. albicans* cultured with antifungals in the presence and absence of pilocarpine Hydrochloride. Cells were cultured on E- plate in presence and absence of 50 mM PHCl. Growth curve was monitored on real time manner by measuring the electrical impedance profile (EIP). (A, B, and C) demonstrates effect of antifungal caspofungin on cells proliferation and morphology in presence and absence of PHCl. (D, E, and F) demonstrates effect of the antifungal amphotericin B on cells proliferation and morphology in presence and absence of PHCl. Statistical analysis; *, $P < 0.05$; **, $P < 0.01$; ***, $P < 0.001$.

2.4 Discussion

C. albicans is a dimorphic fungus considered to be the most predominant fungal pathogen in humans that causes a wide range of diseases from mild infections to severe systemic infections (Yapar, 2014, Sardi et al., 2013, Prasad, 2017). *C. albicans* pathogenicity is attributed to several virulence factors. However, morphogenesis and biofilm formation are key factors. The ability of *C. albicans* to switch from yeast to hyphae and form biofilms contribute to it's ability to resist conventional antifungals (da Silva Dantas et al., 2016, Kurzai, 2013).

Recently, PHCl was found to reduce biofilm formation by inhibiting the transformation from yeast to hyphae in *C. albicans* (Nile et al., 2019). This effect was proved to be clinically relevant by evaluating the effect of PHCl on biofilm formation in clinical isolates from the blood stream, vagina and the oral cavity (Figure 2.13). Despite the variability in biofilm formation amongst the clinical isolates, overall data obtained from high biofilm formers revealed that most showed a similar response to PHCl treatment i.e. a statistically significant reduction in the total biofilm biomass (Sherry et al., 2014). Similarly, low biofilm formers also showed a significant reduction in total biofilm biomass. PHCl is a non-selective muscarinic receptor (mAChRs) agonist, known to be clinically effective as a treatment for glaucoma and xerostomia (Burr et al., 2012, Evans et al., 2015, Gil-Montoya et al., 2016, Marchi et al., 2009, Sun and Dai, 2019). Therefore, the current findings support the hypothesis that *C. albicans* may possess a putative cholinergic receptor that can regulate filamentation and biofilm formation, similar to muscarinic receptors in human.

The mAChRs are G-protein coupled receptors (GPCRs), and consists of 5 subtypes: M_1, M_2, M_3, M_4 and M_5. The G- protein coupled receptors are heterotrimeric receptors that contain different subunits, alpha, gamma and beta and can activate a diverse array of signaling pathways. For instance, stimulation of the M_2 and M_4 subtypes, which are coupled to G_i and G_o proteins, decreases the synthesis of cAMP through adenylyl cyclase inhibition and activation of potassium conductivity. The M_1, M_3, and M_5 subtypes are coupled to $G_{q/11}$ proteins, and their stimulation activates phospholipase C (PLC), resulting in the production of inositol triphosphate (IP_3) and diacylglycerol (M Harandi and

Medaglini, 2010), thus leading to an increase in intracellular $[Ca^{2+}]_i$ and protein kinase C (PKC) activation. *C. albicans* and mammalian cells exhibit similarities as both are eukaryotic cells. Recent studies have illustrated the role of calcium signaling in *C. albicans* virulence. Activation of Ca^+ dependent transduction pathways contribute vitally to *C. albicans* survival under environmental stressors, pathogenicity and hyphal growth regulation, and antifungal resistance (Blankenship and Heitman, 2005, Rajendran et al., 2016b, Yu et al., 2015). It has been shown that unrestricted uptake of Ca^+ by *C. albicans* or leakage of intracellular Ca^+ to the medium result in filamentation inhibition, which highlights the regulatory role of Ca^+ in morphogenesis (Holmes et al., 1991, Sakaguchi et al., 1997).

Although PHCl is a general muscarinic agonist, it has selectivity for the M_1 and M_3 subtypes over the M_2 and M_4 subtypes (Ockenga et al., 2013, Kawashima et al., 2012, Figueroa et al., 2009). Therefore, in order to determine more accurately whether *C. albicans* possesses a receptor homologue of a specific human muscarinic receptor subtype a plethora of cholinergic compounds was employed. The investigation revealed that 1) C-HCL, a M1AChR agonist and APE, a M2AChR agonist, had no dose dependent inhibitory effect on biofilm formation (Figure 2.5 and 2.6). 2) JF, a M3AChR antagonist, and PD, a M4AChR antagonist, did not block the inhibitory effect of PHCl when used in combination (Figure 2.8 and 2.7). Due to the lack commercially available M_5 agonists and antagonists at the time of this investigation, Vu 0238429 (Vu), a M_5 allosteric modulator was used to investigate the presence of a functional M_5 receptor (Bridges et al., 2010, Fryer et al., 2012). Vu resulted in a significant reduction in biofilm biomass in a dose dependent manner similar to the decrease observed with PHCl (Figure 2.9).

The complexity and diversity of the signaling pathways that are activated by muscarinic receptors, emphasize the need to explore the potential pathways involved in the cholinergic inhibition of biofilm formation in *C. albicans* that are exerted by ACh and PHCl. Therefore, the preliminary data from the investigation into specific cholinergic compounds suggested that prioritizing G_q protein coupled receptor pathways warranted further investigation. Experiments were therefore conducted to investigate the ability of blocking the inhibitory effect of the PHCl using several G_q protein inhibitors, known to suppress either the G_q

protein directly or block specific secondary molecules downstream of the G_q signaling cascade, and thus inhibiting the signaling pathway. For this purpose, we tested the effect of YM-254890 (YM), a G_q protein inhibitor, and U73122, a phospholipase C (PLC) inhibitor. Quantitative assessment of biofilm biomass did not show significant biofilm biomass reduction when *C. albicans* was treated with YM in presence of PHCl. However, microscopic analysis suggested that YM-254890 may have slightly inhibited the ability of PHCl to block the yeast-hyphae transition by *C. albicans* (Figure 2.12). Furthermore, a PLC inhibitor (U73122) inhibited the effect of PHCl on *C. albicans* as evidenced by an increase in biofilm biomass when compared to treatment with PHCl alone.

Compounds and signalling pathways inhibitors used in this study were used in the literature for targeting human muscarinic signalling pathways. Whether those compounds validated to function in yeast are not investigated yet. Due to yeast cell wall structure and rigidity, it may prevent permeability of those compounds into the cells. Furthermore, PHCl effect might be mediated via direct uptake of the compound by the fungus, via fungal specific receptor possessed by *C. albicans* that bind to PHCl, or via activating different downstream signalling pathways of receptors similar to human muscarinic receptors. To answer these hypotheses further investigations are required.

Microscopic analysis has aided the study to visualize the morphological changes in *C. albicans* in presence PHCl treatment, yet appropriate imaging techniques can provide critical details regarding the morphological characteristics and more comprehensive conclusions. In general, microscopic analysis used in this study were useful to gather information about the size, shape, and morphology. For instance, although basic light microscopy is rapid and simple, it cannot provide detailed or accurate comprehensive information about biofilm structure and layers. This can be explored more in depth using quantitative applications of the biofilm structure and high resolution confocal microscopy which can provide better information about the 3 dimensional structure (Robson et al., 2018). For example, adapting the methodology by Bogachev et al. (2018) can be useful to evaluate biofilm embedded cells and produce statistical analysis using fluorescent microscopy, confocal laser scanning microscopy, and suggested software tool *BioFilmAnalyzer*.

GPCRs play a key role in transmitting extracellular signals into intracellular biological responses. In fungi, GPCR signaling pathways regulate different aspects of fungal development, virulence, and metabolism, by responding to signals from the environment e.g., hormones, nutrients, ions, and proteins (El-Defrawy and Hesham, 2020). Different GPCRs are known to play a role in *C. albicans* pathogenicity. For instance, *Ca*Gpr1 class III, promotes morphogenesis and invasive candidiasis, and *Ca*Ste2 and 3, promote cell conjugation, phenotypic switching, adhesion, filamentation, biofilm formation, and virulence (Brown et al., 2018). In accordance, the findings of this study propose that the cholinergic agonists, Vu 0238429 and PHCl, inhibited biofilm formation and yeast-to-hyphae transition in *C. albicans* through G- protein coupled receptors possibly similar to those in human. In light of this it is important to mention that PHCl was also found to significantly reduce cell surface hydrophobicity in *C. albicans* (Nile et al., 2019). This highlights the importance of conducting further investigations toward studying the effect of these agonists on biofilm formation by *C. albicans* relevant to other virulence factors such as adherence and invasion and their associated signaling pathways.

The interaction between Vu 0238429 /PHCl and muscarinic receptors might result in instigating an increase in Ca^{+} uptake or influx by *C. albicans* which might reduce morphogenesis. It could therefore be hypothesised that this interaction was blocked by YM-254890, a G_q protein inhibitor and U73122, a phospholipase C inhibitor (PLC). These experiments may present an initial assumption of the potential receptor in this study. Therefore, it is feasible to speculate that potential receptor(s) possessed by *C. albicans* regulating morphogenesis may share homology with human G_q protein coupled receptors (M_1, M_3, or M_5). However, signaling pathway analysis was not conducted in this study herein and further investigations will be required to validate this assumption. For instance, confocal microscopy can be exploited for this purpose to monitor Ca^{+} influx or efflux by *C. albicans* in the presence and absence of certain treatments. Moreover, intracellular Ca^{+} concentration can be measured using a fluorescent Ca^{2+} indicator (Fura-2 acetoxymethyl ester) both before and after PHCl or Vu treatment (Nishimura et al., 2006). Molecular biological tools; e.g. RNAseq and CRISPR, can also be employed to study the molecular basis of *C. albicans* virulence factors and signaling transduction pathways moving forwards.

Substantial knowledge of the molecular mechanisms and signaling pathways through which *C. albicans* biofilms resist antifungal treatments and evade the host's immune system may provide promising insights regarding new therapeutic targets (Prasad, 2017, Tsui et al., 2016). The current study may disclose novel therapeutic strategies for development of antifungal drugs by targeting key GPCRs relevant to specific virulence factors which may minimize the potential collateral damage to the host (Brown et al., 2018). In the present study, PHCl significantly reduced filamentation and biofilm formation in *C. albicans* and showed no toxic effect on the cells as evident by measuring the uptake of propidium iodide and the concentration of released ATP following the treatment.

The role played by *C. albicans* cell wall in pathogenicity is already established. Cell wall structure provides protection against host defense mechanisms and facilitates infection by promoting adherence to surfaces and disturbance of homeostatic equilibrium in the host (Ruiz-Herrera et al., 2006). The xCELLigence technology enabled the quantification of changes in cell viability, proliferation, and differentiation by measuring the electrical impedance from cells adhering to a surface. *C. albicans* hyphae adhere more efficiently than yeast cells due to hypha-associated adhesin expression (*ALS3* and *HWP1*) (Wilson et al., 2016). This might explain the irregularities observed in EIPs of untreated cells compared to PHCl treated cells, where more regular cell index curve correlates with non-hyphal adherent and irregular curve correlates with hyphal growth. This was also observed when cells were treated with antifungals (CSP and AMB). However, at some concentrations, when antifungals were combined with PHCl, the viability of the cells increases over time, and this might be due to the ability of PHCl to enhance the proliferation of the cells as previously elucidated by other studies where PHCl enhanced proliferation of acinar secretory cells (Burlage et al., 2009). Herein, CSP and AMB antifungals were used in combination with PHCl to investigate their effects on *C. albicans* virulence. CSP is an echinocandin antifungal that targets beta-(1,3)-D-glucan synthesis in the fungal cell wall for inhibition. AMB, on the other hand, binds to ergosterol in the cell membrane increasing the permeability and results in intracellular component leakage (Brajtburg et al., 1990, Stevens et al., 2004). For future work, the effect of these antifungals in combination with PHCl on *C. albicans* pathogenicity and the

possibility of using PHCl as an adjunctive therapy in combination with conventional antifungals will be explored more in depth.

In conclusion, the data obtained from this chapter suggests the presence of putative muscarinic cholinergic receptors in *C. albicans* that are responsible for modulating the transition between yeast and hyphae forms and biofilm formation. Yet, further investigations are required to fully characterize the specific type of receptor and to identify the relevant signaling pathways. Consequently, this research may give insight into a promising potential therapeutic target to treat lethal fungal infections.

Key summary points:

- PHCl, a general muscarinic receptor agonist, inhibited *C. albicans* biofilm formation and hyphal growth in a dose dependent manner in a wild type strain and LBF and HBF clinical isolates.

- Scopolamine, a general muscarinic receptor antagonist, blocked the inhibitory effect of PHCl in a dose dependent manner.

- Small molecule inhibitors, U73122 and YM 254890 which target the G_q signaling pathway utilised in humans by the M1, M3 and M5 receptor rescued *C. albicans* hyphal growth in presence of PHCl.

- Vu 0238429, an M5 allosteric modulator had a similar effect as PHCl on *C. albicans* as it inhibited the biofilm formation significantly in a dose dependent manner.

- There is tentative evidence to suggest that *C. albicans* may possess a receptor with homology to the human M5 receptor which can modulate the yeast-hyphae transition and biofilm formation.

3 *Candida albicans* infection and host innate immune response

3.1 Introduction

Numerous opportunistic pathogens reside on or within the human body. These opportunistic pathogens respond to changes in their surrounding environment or environmental stresses and in adapting to these can become pathogenic. Among this group of opportunistic pathogens is *Candida albicans*. Although *C. albicans* is an indigenous fungus that is part of the normal human flora, it is the most isolated fungus from superficial infections and systemic candidiasis patients, particularly if they are immunocompromised (Pellon et al., 2020, Kiyoura and Tamai, 2015). *C. albicans* is perfectly adapted to respond and adapt to changes in it's environment. Therefore, maintaining commensalism requires a delicate balance between fungal proliferation, commensal microbial communities, and localised host immune factors. Due to the limited effectiveness of the current arsenal of antifungals, a greater understanding of the interactions between the host and *C. albicans* may prove to be vital for finding novel effective treatments or therapeutic interventions for life threatening fungal infections (Qin et al., 2016).

Epithelial cells provide a physical barrier preventing the invasion of pathogens. However, their involvement in discriminating between commensal and pathogenic microbes, developing and initiating immune responses and attracting immune cells to the infection site is still not fully understood (Pellon et al., 2020). The innate immune response is the first-line, non-specific, defense against pathogens, such as viruses, bacteria, and fungi. *C. albicans* first physically contacts and adheres to epithelial cells and through this initial proximal contact promote epithelial cells to initiate an innate immune response via the production of immunoregulatory and antifungal proteins; such cytokines, chemokines and antimicrobial peptides (Kiyoura and Tamai, 2015).

Epithelial cells recognise pathogen-associated molecular patterns (PAMP), such as ß-glucans and mannan, on *C. albicans* through various pattern recognition receptors (PRR), including the C-type lectin receptors and toll-like receptors (TLRs). Recognition by these receptors initiates an intracellular signaling cascade that induces the expression and release of proinflammatory chemokines and cytokines. This immune response varies according to the site of infection and

morphology of *C. albicans*. For example, in systemic infections, yeast cells are the most immunogenic form, whereas in mucosal infections hyphae contribute more to the immune response (Pellon et al., 2020, Kiyoura and Tamai, 2015, Weindl et al., 2010). Following adhesion, live *C. albicans* can form hyphae and invade host tissues. This invasive process can be via active penetration or through induced endocytosis, depending on the infection site, stage, and cell morphology. For example, invasion of intestinal tissues is mediated via active penetration and via endocytosis during the early stages of infection. The latter process of endocytosis or phagocytosis can contribute to host immune cells damage and evasion via *C. albicans* cytolytic peptide toxin, candidalysin (*ECE1*), which provides an escape route for the fungi by damaging the immune cells (Pellon et al., 2020, Yang et al., 2014, König et al., 2020).

The damage response framework (DRF), a concept first introduced by Casadevall and Pirofski (1999), defines microbial virulence as an outcome of the interaction between host and pathogen. This concept can be used to explain the pathogenesis of *C. albicans* and it's adaptation to the host (Jabra-Rizk et al., 2016). The DRF relies on the notion that there are no exclusive commensals, opportunists, or pathogens. However, pathogenesis requires a host and a microbe interaction where the outcome is damage to the host. The DRF suggests that the outcome is a result of host and/or microbial factors where the response of the host contributes to the amount of damage. This concept classifies outcomes into six classifications based on microbe and strength of immune response at a specific site of infection. Interestingly, *C. albicans* infections fit into all these classifications based on infection site and host immune response (Figure 3.1). In this framework the level of host damage is dependent on whether the immune response to the microbe was strong or weak. Based on the DRF, pathogens cause damage to the host that is perpetuated by both strong and weak immune responses. Where the immune response is weak, infections are promoted causing pathogen-mediated damage and when the immune response is strong, excessive inflammation driven tissue damage occurs (Jabra-Rizk et al., 2016).

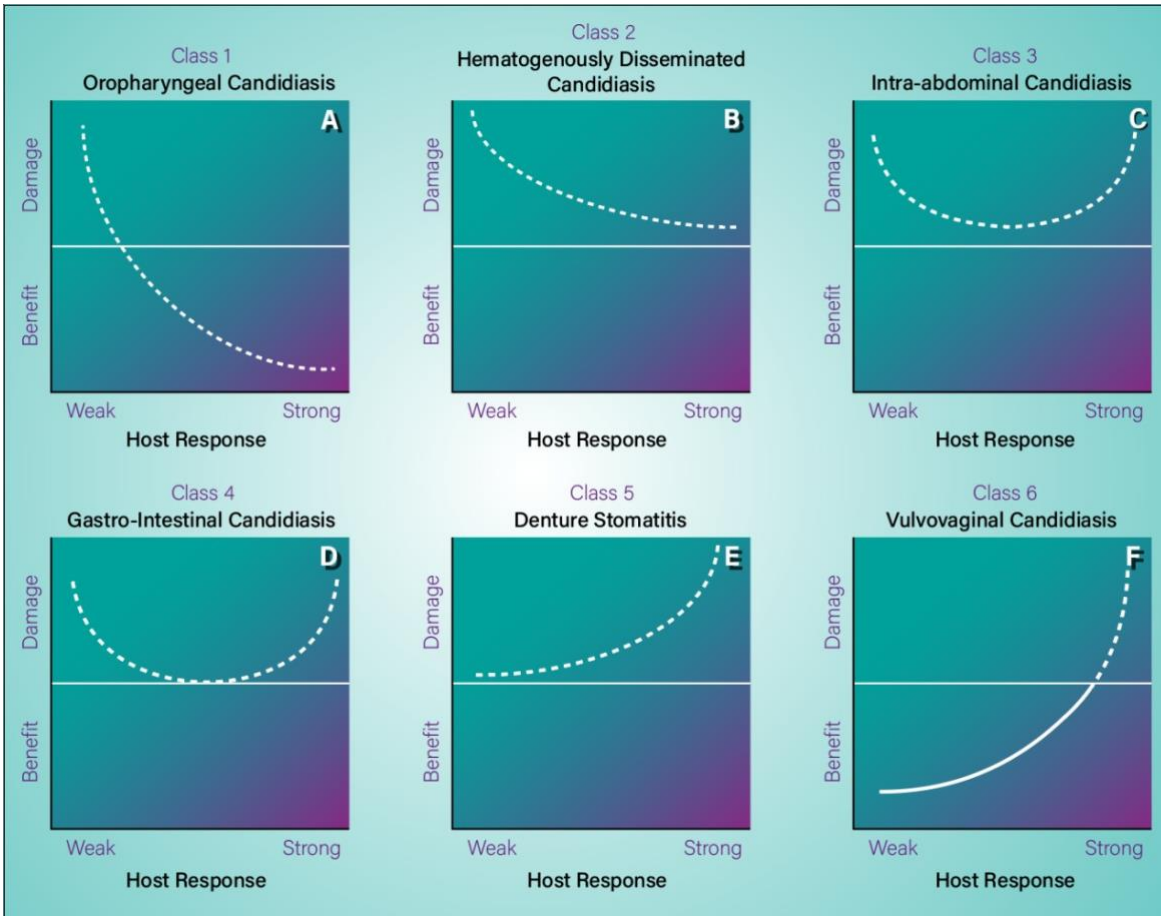

Figure 3.1 *C. albicans* damage response framework with an associated anatomical site of infection and host immune response. (A) Class 1, damage only in weak host immune response. (B) Class 2, damage caused in normal or weak immune host response. (C) Class 3, damage caused in continuous weak, strong, appropriate host immune response. (D) Class 4, damage caused in extremes, weak and strong host immune responses. (E) Class 5, damage caused across the immune response scale, and exacerbated in a strong immune response. (F) Class 6, damage caused only in strong host immune responses. Adapted from (Jabra-Rizk et al., 2016).

Candida albicans can adapt to the dynamic environment of the host, like changes in the microbiota and immune status, and in adapting to specific host environments they can cause a wide range of systemic or superficial infections in both immunocompromised and immunocompetent people. For instance, when the immune response is weak due to individuals being immunocompromised, *C. albicans* can cause oropharyngeal candidiasis (OPC), which rarely occurs in immunocompetent patients, where *C. albicans* has a symbiotic relationship with the host. In addition, when the immune response is weak such as in neutropenic patients or at a normal level such as in non-neutropenic patients, invasive candidiasis can cause hematogenously disseminated candidiasis (HDC), which leads to deep seated candidiasis (DSC) where *C. albicans* infects internal organs.

Intraabdominal candidiasis (IAC) can cause damage to the host during the continuum of immune responses but *C. albicans* exacerbates damage under either extremes. Even during an optimal or sufficient immune response, IAC can lead to inflammatory diseases, such as peritonitis. Different environmental condition such as diet or antibiotic usage can lead to *C. albicans* overgrowth in the gastrointestinal tract causing gastrointestinal candidiasis which results in damage at both ends of immune response spectrum. Therefore, transplant and impaired host immune patients are at risk of gastrointestinal candidiasis, and *C. albicans* colonization in the gastrointestinal tract can be a contributory cause for host inflammatory diseases. Another damage scenario of *C. albicans* infections is when the damage occurs across the scale of immune responses but worsens during a strong host immune response for example, in denture stomatitis (DS). DS is common in healthy individuals causing inflammation to the denture bearing mucosa which worsens when damage occurs to the protective mucosal barrier leading to *C. albicans* infiltration into the tissue and resulting in a strong chronic immune response exacerbating the damage to the host. In vulvovaginal candidiasis (VVC), *C. albicans* exists asymptomatically as a resident of the normal vaginal microbiota. However, symptomatic VVC is found to be associated with aggressive local inflammatory responses causing mucosal damage (Jabra-Rizk et al., 2016, Casadevall and Pirofski, 1999).

The cholinergic system as a therapeutic target for treating inflammatory diseases has garnered much attention in recent years (Fujii et al., 2017, Lu and Wu, 2021). Cholinergic systems operate in both central and peripheral immune cells. The cholinergic anti-inflammatory pathway is a neural mechanism that inhibits inflammatory cytokine release via the alpha 7 nicotinic receptor (α7nAChR) on cells. The pathway is mediated by the vagus nerve and plays a vital role in immunological homeostasis. The α7nAChR is expressed on immunocompetent cells such as macrophages. Activation of the α7nAChR on immune cells has been found to modulate inflammatory responses by inhibiting proinflammatory mediator expression and down regulating potentially strong immune responses and thus protecting against local or systemic tissue damage (Czura et al., 2007).

In addition to the α7nAChR, muscarinic ACh receptors have also been found to play a role in modulation of immune responses. Muscarinic receptors are expressed by a variety of immune cells such as macrophages, dendritic cells (DCs), and lymphocytes. According to Darby et al. (2015), muscarinic receptors are important for optimal adaptive immunity against bacterial infections. For instance, cholinergic signaling through the M3 receptor coordinates Th1- and Th2-type responses which are pivotal in the immune reaction. Furthermore, literature showed that muscarinic receptors play an important role in regulating immune function and inflammatory responses. For example, comparing immune responses of wild type mice and M1 and M5 mAChR gene-knockout (M1/M5-KO) mice which were immunized with ovalbumin (OVA) revealed significant decrease in TNF-α, IFN-γ, and IL-6 and anti OVA specific IgG1 concentration in the blood of M1/M5-KO mice. Another example of muscarinic receptor mediated immune response regulation is the inhibition of leukocyte migration to sites of inflammation and reduced tissue injury by atropine in a turpentine-induced sterile abscess model (Fujii et al., 2017, Razani-Boroujerdi et al., 2008).

In addition, muscarinic receptors are known to be expressed by epithelial cells and fibroblasts and have also been shown to modulate the expression of tissue remodelling and inflammatory mediators by these cells. For example, it has been shown that the presence of muscarinic receptors in human and mouse scleral fibroblasts play a functional role in remodelling human and mouse sclera in myopia cases by mediating scleral fibroblast cell proliferation using muscarinic agents. In addition, inflammation of airways such as in asthma and chronic obstructive pulmonary disease (COPD) is known to be regulated by muscarinic receptors. While carbachol, a cholinergic agonist was found to increase the expression of the mucin gene MUC5AC, the muscarinic antagonist, aclidinium, had an inhibitory effect (Barathi et al., 2009, Karakiulakis and Roth, 2012, Koarai et al., 2012)

Muscarinic receptor agonists have been demonstrated to inhibit the yeast to hyphae transition by fungal pathogens including *C. albicans* (Wakharde and Karuppayil, 2018, Nile et al., 2019). Muscarinic agonists, specifically pilocarpine hydrochloride (PHCl), can inhibit filamentation, which is a key factor in the

pathogenicity of *C. albicans*. Thus, PHCl prevents the invasive growth of fungi that is likely to cause disease (Nile et al., 2019). Research has shown that muscarinic receptors have been found in several types of epithelia. Namely, the skin epithelium, biliary epithelium, and the scleral epithelium, with a specifically high abundance being reported to be expressed in the oral epithelium. Muscarinic receptors have several and diverse functions in these cell types, for example, wound healing in the cornea and tear production in the eye (Elsing et al., Arredondo et al., 2003, Barathi et al., 2009). Therefore, signaling through these receptors may be important for coordination of immune responses against fungal infections. Indeed, preliminary evidence using a Galleria *mellonella* infection model has shown that PHCl can not only protect against candidiasis by inhibiting *C. albicans* yeast to hyphae transition but also by coordinating an effective immune response by the host to clear the pathogenic threat (Nile et al., 2019). However, the exact mechanisms by which muscarinic receptor agonists can modulate the immune response to *C. albicans* infection are to be determined.

The overall aim of this chapter was to use *in vitro* model systems to determine the effect of PHCl on the innate immune response of the oral epithelium to *C. albicans* infection.

To achieve this aim the following were evaluated:

1. The effect of live and heat-killed *C. albicans* infection on the innate immune response of host oral epithelial cell monolayers and the ability of PHCl to modulate the *C. albicans* induced expression of proinflammatory mediators.

2. The ability of PHCl to modulate the *C. albicans* induced innate immune responses in a three-dimensional tissue model of the human oral epithelium.

3.2 Materials and Methods

3.2.1 TR146 cell line growth and maintenance

The TR146 cell line (Cancer Research Technology, London, UK) was used to initially investigate the innate immune response of epithelial cells to *C. albicans* infections. TR146 cell line was used in this study to optimize and validate host pathogen interaction investigations because it grows fast and cheap. In addition, it is well characterized and studied in the literature as oral epithelium model of *C. albicans* infections.

Frozen glycerol stocks of TR146 cells at a concentration of 1×10^6 cells/mL were thawed quickly at 37°C, then transferred into a universal container containing 9 mL of keratinocyte serum-free medium (KSFM) (GibcoTM, Fisher-Scientific, Loughborough, UK) supplemented with penicillin (100 U/mL), streptomycin (100 µg/mL) (Sigma-Aldrich, Irvine, UK), bovine pituitary extract (BPE) (25 µg/mL), epithelial growth factor (EGF) (0.2 ng/mL), and $CaCl_2$ (0.4 mM) (Sigma-Aldrich, Irvine, UK). The universal container was centrifuged at 1000 rpm for 5 minutes and the medium was discarded. The pelleted cells were resuspended in 10 mL of KSFM medium and seeded at a density of 1×10^5 cells/mL in a T75 cell culture flask (Corning Life Sciences, High Wycombe, UK) for continuous culture at 37°C and 5% CO_2.

After 2 – 3 days, the old medium was replaced with 15 mL of fresh medium, which consisted of 50% supplemented KSFM (as above) and 50% Dulbecco's modified Eagle's medium (DMEM) supplemented with penicillin (100 U/mL), streptomycin (100 µg/mL), 10% foetal bovine serum (FBS), and L-glutamine. Cells were monitored daily and whenever 70 – 90% confluency was reached, the cells were passaged.

For passage, the medium was removed and cells were washed three times using Dulbecco's phosphate-buffered saline (DPBS). Trypsin EDTA (0.05%) (Sigma-Aldrich, Irvine, UK) was then added and the cells were allowed to detach from the flask surface. The activity of trypsin was then neutralised using 15 mL of DMEM-supplemented medium. The detached cells in DMEM were collected in a

universal and centrifuged at 1000 rpm for 10 minutes to pellet the cells. The DMEM was removed and the pelleted cells were resuspended in 10 mL KSFM. Cells were counted using a haemocytometer and a light microscope (Olympus, Southend, UK). For counting, to aid visualisation cells were stained with 0.04% trypan blue in phosphate buffered saline (PBS) (Fisher Scientific, Loughborough, UK) by adding 10 µl of trypan blue to 10 µl of cell suspension. To maintain growth, cells were standardised to 1×10^5 cells/mL and re-seeded into T75 flasks containing KSFM and DMEM whenever needed.

3.2.2 Human oral epithelium tissue maintenance

To more authentically replicate infection of the oral epithelium *in vivo*, a 3D model of the normal human oral epithelium was used in *in vitro* infection studies.

Human oral epithelium (HOE) was purchased from Episkin™ (Skinethic™ laboratories, Lyon, France). The SkinEthic™ HOE model consists of four cell layers of well-stratified and non-keratinised TR146 cells (derived from a squamous cell carcinoma of the buccal mucosa), cultivated on a 0.5 cm^2 inert polycarbonate filter at the air—liquid interface in a chemically-defined medium. This model forms an epithelial tissue devoid of stratum corneum, histologically resembling the mucosa of the oral cavity. The tissue was shipped at a temperature of 37°C at 5% CO_2 with saturated humidity. Once received, the colour—temperature indicator was checked to ensure the shipment was maintained at the recommended temperature. The tissue inserts were delivered in a 24-well plate containing nutrient agar and these were immediately transferred to a 12-well plate containing 1 mL of SkinEthic chemically-defined maintenance medium (Episkin™, Skinethic™) at room temperature (RT). Plates were incubated overnight at 37°C at 5% CO_2 before further experiments were conducted.

3.2.3 *Candida albicans* preparation for stimulation experiments

C. albicans strain SC5314 was sub-cultured on Sabouraud dextrose agar (SDA) (Sigma-Aldrich, Dorset, UK). Cells were propagated in yeast extract peptone

dextrose medium (YPD) (Sigma-Aldrich, Dorset, UK) in universal containers at 37°C overnight (16 – 18 hours) using an orbital shaking aerobic incubator. After overnight incubation, cells were washed by centrifugation at 3000 rpm for 5 minutes in PBS (Sigma-Aldrich, Dorset, UK) and standardised to the required cell density based on each individual experiment requirements. For heat-killed stimulation experiments, cells were standardised to a stock density of 1×10^8 cells/mL and pelleted by centrifugation. Next, cells were resuspended in KSFM medium, immersed in a ≥ 60°C water bath to heat kill, and serially diluted to different densities according to the required multiplicity of infection (M.O.I). For live *C. albicans* stimulation of HOE tissue and the TR146 cell line, following the washing steps, the *C. albicans* cells were standardised to the desired density in defined media.

3.2.4 TR146 cell line stimulation experiments

When the TR146 cells achieved 70 – 90% confluency, the cells were seeded into 24-well plates at a density of 2×10^5 cells/mL. The plates were then incubated at 37°C in 5% CO_2 overnight to promote adherence. The next day, cells were stimulated with live or heat-killed *C. albicans* at different M.O.Is and incubated for 4 and 24 hours. Phorbol 12-myristate 13-acetate (PMA) at a concentration of 100 ng/mL (Sigma-Aldrich, Irvine, Scotland) was used as a positive control for stimulation. The medium alone (no *C. albicans*) was used as the negative control. After stimulation, the supernatants were collected in Eppendorf™ tubes (Fisher Scientific, Loughborough, UK) and stored at – 20°C for ELISA and LDH assays. Adherent cells were then harvested by scraping off the cells from the surface in to 350 µl RLT (Qiagen Ltd, Crawley, UK) buffer and ß-mercaptoethanol (source ME; 1% v/v) (Sigma-Aldrich, UK) and stored at – 80°C for gene expression analysis.

To investigate how PHCl can modulate the inflammatory response to *C. albicans* in TR146 cells, the experiments were repeated as above in the presence and absence of concentrations of PHCl varying from 0.005 – 50 mM. Once again, after incubation for 24 hours under the same conditions as above, supernatants and cells were harvested as described above.

3.2.5 Human oral epithelium tissue stimulation experiments

Prior to the stimulation experiments, the human oral epithelium HOE tissue inserts were incubated overnight in chemically-defined maintenance medium. Inserts containing tissues were transferred to new 12-well plates prefilled with 1 mL of fresh SkinEthic chemically-defined maintenance medium. The HOE tissue was exposed to live *C. albicans* at a density of 2×10^5 cells/mL in the presence and absence of 0.05 — 50 mM PHCl. As a positive control, 100 ng/mL PMA was included and the tissue alone with no infection or treatment was used as a negative control. Each condition was performed in triplicate. Plates were incubated for 24 hours as described above. After incubation, the supernatants were collected to investigate cytokine responses and tissue viability. Next, using a 19G needle (Fisher Scientific, Loughborough, UK), the tissue was cut out of the inserts carefully. For gene expression analysis, two of the tissues were transferred in to 350 µl RLT buffer with ME and stored at — 80°C. For histological analysis, one tissue for each condition was transferred to tubes containing 500 µl of 10% neutral-buffered formalin and the tissue was fixed overnight at RT prior to processing for histological analysis.

3.2.6 Human oral epithelium histological analysis

After the HOE tissue was fixed in formalin overnight at RT, samples were kindly processed by Ms. Lynn Stevenson (Veterinary Pathology, University of Glasgow). Briefly, samples were dehydrated using an increasing concentration of ethanol (70 — 100%) and then the ethanol was gradually replaced with xylene. Next, the samples were embedded in a paraffin wax. Once the wax had set, the HOE tissue was cut into 2-µm sections using a Shandon Finnesse ME+ microtome (Fisher Scientific, Loughborough, UK) and the sections placed onto Superfrost™ Ultra Plus Microscope Slides (Gerhard Menzel, Germany). Sections were stained with either periodic acid–Schiff (PAS) stain or haematoxylin & eosin (H&E) stain. Stained sections were viewed using a Leitz Dialux 20 microscope (LabMakelaar Benelux BV, The Netherlands) and images were taken using the ColorView II soft imaging system.

3.2.7 Enzyme-linked immunosorbent assay.

Cytokine and chemokine concentrations in cell culture supernatants were measured by enzyme-linked immunosorbent assay (ELISA) according to the kit manufacturer's instructions (Invitrogen, Fisher Scientific, Loughborough,or Peprotech, UK).

For the Invitrogen kits, the reagents were provided in stock concentrations and diluted whenever required. For the Peprotech kits, reagents were prepared as follows: the blocking buffer was made of bovine serum albumin (BSA) in PBS at a concentration of 1%. This was diluted after filtration to 0.1%, and 0.05% Tween® 20 (Sigma-Aldrich, UK) was added to make the diluent. Although various kits from various sources were used in this study, the general assay principal was the same with some subtle differences which are detailed in Table 3.1.

Briefly, 96-well Nunc™ Maxisorp® flat-bottomed high affinity protein binding microtiter plates (Fisher Scientific, Loughborough, UK) were coated with 100 µl/well of the capture antibody diluted to the required concentration. The plates were then sealed and incubated overnight either at 4°C or at RT (as per the manufacturer's instructions). After incubation, plates were washed 3 – 5 times with washing buffer (PBS + 0.05% Tween® 20). The plates were then blocked with 300 µl/well of blocking buffer for 1 hour at RT, after that, plates were washed again 3 – 5 times and blotted to remove the excess washing buffer. Samples and standards of known concentration diluted in diluent were then added to the wells and the plates were sealed and incubated for 2 hours at RT or overnight at 4°C. After washing the plate 3 – 5 times, the detection antibody was added, and plates were incubated for 1 hour at RT. Plates were washed again 3 – 5 times and Streptavidin-HRP added and the plates were incubated for 30 minutes at RT. Finally, the plates were washed and a 3,3',5,5'-tetramethylbenzidine (TMB) solution was added to each well and the plates incubated for 15 minutes in the dark for colour development. After incubation, 1 M HCl was added to each well to stop the reaction. The absorbance was read at wavelengths indicated by the manufacturer using a FLUOstar Omega microplate reader (BMG Labtech, Buckinghamshire, UK).

ELISA	Supplier	Coating antibody	Blocking	Detection antibody	Peroxidase	Substrate	Detection wavelength	Samples and standards
IL-8	Invitrogen, UK	Diluted in coating buffer, incubated overnight at 4°C	Use ELISA/ELISPOT diluent for 1 hour at RT	Dilute using supplied ELISA/ELISPOT diluent and incubated at RT for 1 hour.	Avidin HRP 30 minutes incubation at RT.	TMB	450 – 570 nm	Incubated overnight at 4°C
IL-6					Streptavidin HRP 30 minutes incubation at RT.			
IL-8	PeproTech, USA	Diluted in PBS, incubated overnight at RT	Use blocking buffer for 1 hour at RT	Diluted in diluent and incubated at RT for 2 hours with samples.	Streptavidin HRP 30 minutes incubation at RT.	TMB	450 – 620 nm	Incubated 2 hours at RT
IL-1α								

Table 3.1 Variations in the ELISA procedures according to the different manufacturers.

3.2.8 Lactate dehydrogenase activity assay

The Pierce™ lactate dehydrogenase (LDH) cytotoxicity colorimetric assay kit was utilised to determine the cytotoxic effects of *C. albicans* and PHCl on TR146 cells or the HOE tissue. The assay was performed as per the manufacturer's instructions (Fisher Scientific, Loughborough, UK). Briefly, 20 µL of the TR146-cell or HOE-tissue supernatant was transferred to a flat 96-well plate (Corning Life Sciences, High Wycombe, UK). Then, 20 µL of reaction mixture substrate was added and the plates were incubated in the dark at RT for 30 minutes. An LDH positive control provided by the supplier with the kit was included on the plates. After incubation, 20 µL of a stop solution (provided by the manufacturer) was added to the samples to stop the reaction and absorbance was measured at wavelengths of 490 nm and 680 nm using the FLUOstar Omega plate reader. Data are shown as optical density readings. The percentage cytotoxicity was calculated in relation to the positive control.

3.2.9 RNA extraction and quantification

RNA was extracted from the TR146 cells using an RNeasy Mini kit [Qiagen Ltd, Crawley, UK] according to the manufacturer's instructions. Briefly, after cells were lysed with RLT buffer, the lysates were transferred to a 1.5 mL RNase-free Eppendorf™ tube and 350 µL of a 70% ethanol were added and mixed by pipetting to precipitate the RNA molecules. Next, the 700 µL samples were transferred into an RNeasy mini spin column placed within a 2 mL collection tube. Samples were centrifuged for 15 seconds at ≥ 8000 x g (13 000 rpm), and the flow-through was discarded. Next, samples were washed with 350 µL RW1 buffer and centrifuged for 15 seconds at ≥ 8000 x g (13 000 rpm), discarding the flow-through. Samples were then subjected to DNase digestion using a DNase digestion kit (Qiagen Ltd, Crawley, UK) as per the manufacturer's instructions. A DNase I stock solution was prepared in aliquots by injecting 500 µL RNase-free water into the DNase vial by syringe and mixing gently. The aliquots were stored at − 20°C until required. For DNase digestion, 10 µL of DNase I stock and 70 µL buffer RDD were added onto the RNeasy column membrane and incubated at RT for 15 − 20 minutes. After incubation, 350 µL of RW1 buffer was added to the column and centrifuged as previously; the flow-through was discarded. Next, 500 µL of buffer RPE was used to perform two washing steps, followed by

centrifugation as above, except the wash centrifugation was for 2 minutes. The spin column was then transferred to another 2 mL fresh collection tube and centrifuged again at full speed for 1 minutes to dry the membrane. To elute the RNA, columns were placed in a new 1.5 mL RNase-free microfuge tube, 30 µL of RNase-free water was added directly to the membrane, and columns were centrifuged at ≥ 8000 x g for 1 minute. Finally, the elution step was repeated by placing the eluent back on the membrane and centrifuging again to concentrate the RNA and ensure total release from the membrane.

The RNA was extracted from the HOE tissue as per the methodology above with the following modifications. Prior to the precipitation step, the HOE sample lysates were transferred to 2 mL screwcap Eppendorf™ tubes containing 100 µL of 0.5 mm glass beads (Thistle Scientific, Glasgow, UK). Samples were homogenised for 30 second in three cycles using the Bead Mill 24 Multi Sample Homogeniser (Fisher-Scientific, Loughborough, UK) and stored on ice.

Extracted RNA was assessed for quality and quantity using a NanoDrop 1000 spectrophotometer (Fisher Scientific, Loughborough, UK). The purity of the RNA was determined using the 260 nm and 280 nm ratio. RNA with a 260/280 ratio between 1.8 – 2.2 was considered acceptable for gene expression analysis. The RNA was stored at – 80°C until further use.

3.2.10 Reverse transcription

The RNA concentrations were standardised and complementary DNA (cDNA) was synthesised using a high-capacity cDNA reverse transcription kit (Fisher Scientific, Loughborough, UK). To generate cDNA from RNA samples, 2 × RT master mix were prepared for each sample according to the manufacturer's instructions detailed in Table 3.2. A negative control (−RT) to detect genomic DNA (gDNA) contamination was also prepared. For each reverse transcription reaction, a mixture of 10 µL RT master mix and 10 µL RNA sample were mixed, sealed, and centrifuged to eliminate air bubbles. Finally, samples were loaded into a MWG-Biotech Primus 96 plus thermal cycler to generate cDNA under the following thermal cycling conditions: 25°C for 10 minutes, 37°C for 120 minutes, and, finally, 85°C for 5 minutes. Samples were stored at − 20°C long term or processed for PCR analysis immediately.

Table 3.2 Volumes used from each component to prepare the master mix for the cDNA synthesis.

Component	Volume/ Reaction (µl)	
	−RT	+RT
10× RT Buffer	2	2
20× dNTP Mix (100mM)	0.8	0.8
10× RT random primers	2	2
MultiScribeTM reverse transcriptase	—	1
Nuclease-free H2O	5.2	4.2
Total master mix/reaction (µL)	10	10

3.2.11 Gene Expression Analysis

Single-plex analysis of inflammatory mediator expression was performed by quantitative PCR. Genes assessed in this study and primer sequences are listed in Table 3.3. For TR146 cells, validated primers and SsoAdvanced Universal SYBR Green Supermix were purchased from Bio-Rad, UK. For each reaction, 19 µL of master mix was made up from 10 µl Universal SYBR Green Supermix,1 µL primers, and 8 µL nuclease-free water. Next, 19 µL of master mix and 1 µL of cDNA sample were added into a MicroAmp fast-optical 96-well 0.1 mL reaction

plate (Applied Biosystems, California, USA) and loaded into the StepOnePlus™ real-time PCR system (Applied Biosystems, California, USA). The thermal cycling protocol was 3 seconds at 95°C for polymerase activation, followed by 40 amplification cycles at 95°C for 5 seconds and 60°C for 30 seconds. All samples were run in duplicate and two negative controls were included: a no-template control (NT), which contained only RNase free H_2O, and a no reverse-transcriptase control (−RT). Gene expression results were normalised to the housekeeping gene *GAPDH* and presented as log-fold change.

For the HOE tissue, a multiplex custom designed RT^2 Profiler PCR Array (Qiagen Ltd, Crawley, UK) was used to assess a panel of 12 genes listed in Table 3.4. For each reaction, the master mix included 12.5 µL SYBR® GreenER™, 11.5 µL RNase-free H_2O, and 1 µl cDNA sample to make a total of 25 µL. The RT^2 profiler plates already contained the forward and reverse primers, so the 25 µL of the master mix was added to each well of the RT^2 profiler plate and loaded in the MxProP quantitative PCR machine. The following thermal cycling conditions were used: 95°C for 10 minutes followed by 40 cycles of 15 seconds at 95°C and 60 seconds at 60°C. Data was assembled using MxProP 3000 software (Stratagene, Netherlands), normalised to the housekeeping gene *GAPDH*, and presented as a Log_2-fold change.

Table 3.3 Primer sequences for the genes analysed using single-plex PCR gene expression analysis.

Genes	Symbol	Sequence	NCBI reference	Bio-Rad unique assay ID
			NC_000012.11	qHsaCED0038674
Glyceraldehyde 3-phosphate dehydrogenase	*GAPDH*	GTATGACAACGAATTTGGCTACAGCAACAGGGTGGTG GACCTCATGGCCCACATGGCCTCCAAGGAGTAAGACCC CTGGACCACCAGCCCCAGCAAGAGCACAAGAGGAAGA GAGAGACCCTCACTGCTGGGGAGTCCCTGCCACAC		
Interleukin-8	*IL8*	GAGCACTCCATAAGGCACAAACTTTCAGAGACAGCAGA GCACACAAGCTTCTAG GACAAGAGCCAGGAAGAAACCACCGGAAGGAACCATC TCACTGTGTG	NC_000004.11	qHsaCED0046633
Interleukin-6	*IL6*	TGAAAAAGATGGATGCTTCCAATCTGGATTCAATGAGG AGACTTGCCTGGTGAAAATCATCACTGGTCTTTTGGAG	NC_000007.13	qHsaCID0020314

		TTTGAGGTATACCTAGAGTACCTCCAGAACAGATTTGA GAGTAGTGAGGAACAAGCCAGAGCTGTGCAGATGAGT A		
Interleukin-1α	*IL1*α	TGAAATAGTTCTTAGTGCCGTGAGTTTCCCAGAAGAAG AGGAGGTTGGTCTCACT ACCTGTGATGGTTTTGGGTATCTCAGGCATCTCCTTCA GCAGCACTGGTTGGTCT TCATCTTGGGCAGTCACATACAATTGAGTTTTTGAGAT TCTTAGAA	NC_000002.11	qHsaCID0016254

Table 3.4 List of genes assessed for expression in HOE tissue samples using a custom designed multiplex RT^2 profiler PCR Array.

No.	Genes	Abbr.	Assay ID
1	Glyceraldehyde 3-phosphate dehydrogenase	*GAPDH*	PPH00150F
2	Interleukin-8	*CXCL8*	PPH00568A
3	Interleukin-6	*IL6*	PPH00560C
4	Interleukin-1α	*IL1a*	PPH00690A
5	Granulocyte macrophage colony stimulating factor	*GM-CSF/CSF2*	PPH00576C
6	Tumour necrosis factor alpha	*TNF-* α	PPH00341F
7	Chemokine C-C motif ligand 2	*CCL2*	PPH00192F
8	Toll-like receptor 2	*TLR2*	PPH01808A
9	Toll-like receptor 4	*TLR4*	PPH01795F
10	C-type lectin domain family 7 member A	*CLEC7A*	PPH05563F
11	cathelicidin antimicrobial peptides	*CAMP*	PPH09430A
12	Granulocyte-colony stimulating factor	*G-CSF/CSF3*	PPH00723B

3.2.12 Statistical Analysis.

Statistical analysis was performed using PRISM. Each data set was tested for normality and homogeneity using both a Shapiro—Wilks and a Kolmogorov—Smirnov test. If the data was found to be normally distributed,

differences between conditions were determined using a one-way ANOVA using a Dunnett's post-test. For non-parametric data, differences were determined using a Kruskal—Wallis test followed by a Dunn's post-test. Data were considered significant if $p < 0.05$.

3.3 Results

3.3.1 Optimisation of an *in vitro Candida albicans* stimulation methodology using TR146 cell monolayers

Preliminary investigations were undertaken to optimise the stimulation conditions and to ensure that *C. albicans* SC5314 had no cytotoxic effects on the TR146 cells. TR146 cells were stimulated with varying multiplicity of infection (M.O.I) of both live and heat-killed *C. albicans* ranging from 0.01 — 100 for 4 and 24 hours. Cytotoxicity was determined by measuring lactate dehydrogenase (LDH) release into the culture supernatants. Live and heat-killed *C. albicans* at all M.O.I tested showed no statistically significant difference in the LDH released into the bathing supernatants relative to unstimulated cells (Figure 3.2 A—D).

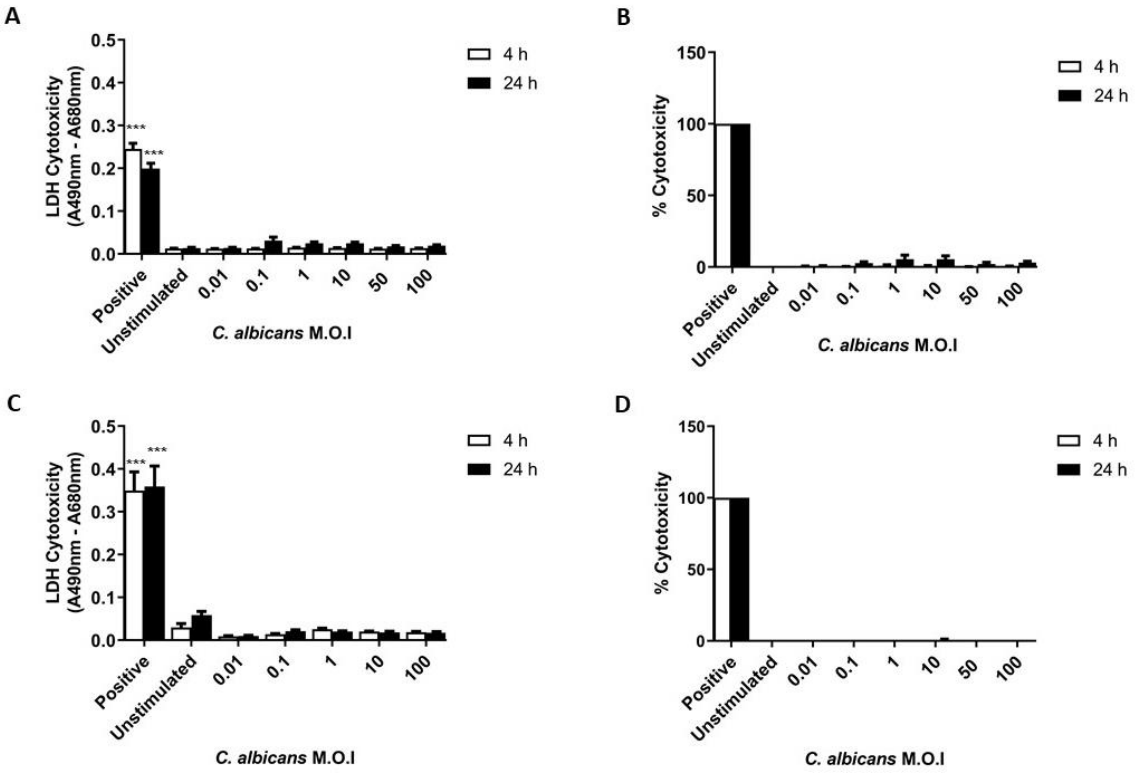

Figure 3.2 Lactate dehydrogenase release by TR146 cells after stimulation with live and heat-killed *C. albicans* over 4 hours and 24 hours. Release of LDH into culture supernatants was quantified using an LDH cytotoxicity assay kit. (A) Stimulation with live *C. albicans* at various M.O.I and data presented as raw OD values for statistical analysis; (B) stimulation with live *C. albicans* at various M.O.I and data are presented as percent cytotoxicity in relation to positive control; (C) stimulation with heat-killed *C. albicans* at various M.O.I and data are presented as raw OD values for statistical analysis; and (D) stimulation with heat-killed *C. albicans* at various M.O.I and data are presented as percent cytotoxicity in relation to the positive control. All experiments were performed in duplicate on at least four independent occasions. ***$p < 0.001$ in comparison to the unstimulated cells.

As previously demonstrated (Figure 3.2), *C. albicans* SC5314 had negligible cytotoxic effects on TR146 cells cultured *in vitro*. Therefore, the ability of *C. albicans* SC5314 to induce expression of the chemokine *IL-8* (*CXCL8*) was investigated. In the subsequent analysis, chosen M.O.I's were 0.1-50.

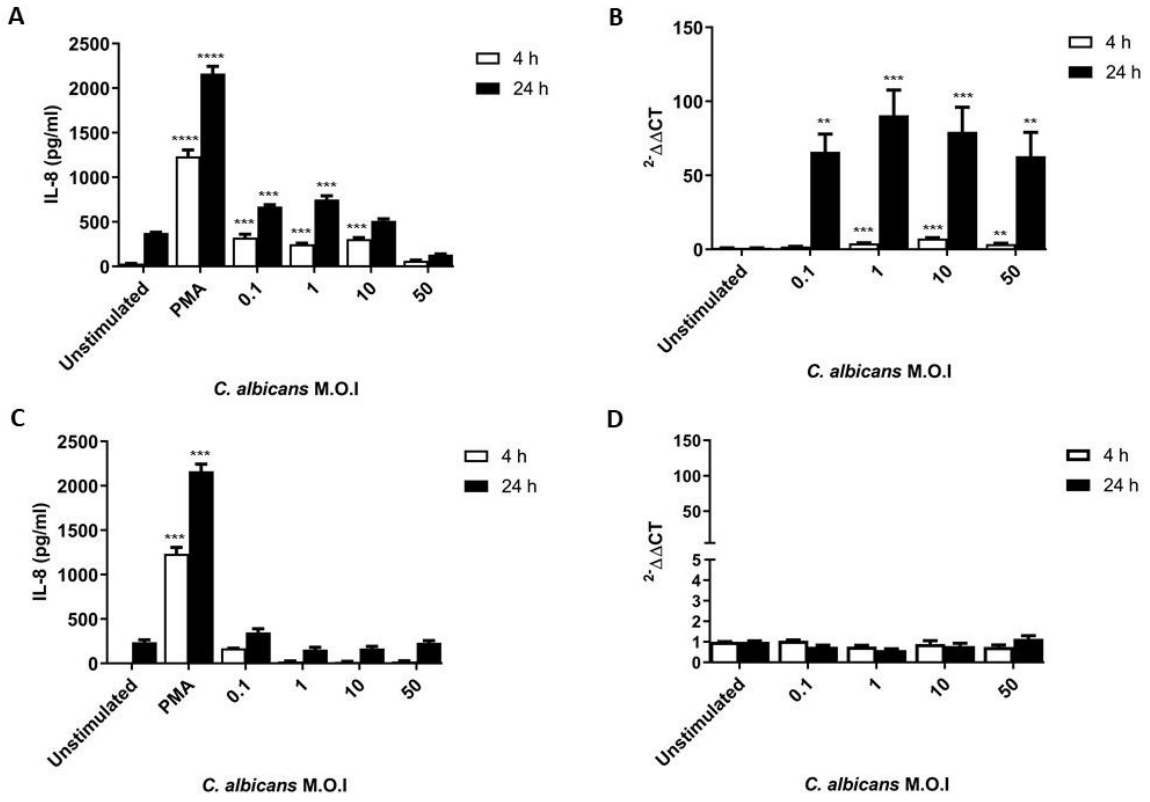

Figure 3.3 Expression and release of IL-8 by TR146 cells in response to stimulation with live and heat-killed *C. albicans*. TR146 cells seeded into 24-well plates were stimulated with various M.O.I of live or heat-killed *C. albicans* SC5314 over 4 hours and 24 hours. Release of IL-8 into culture supernatants was determined by ELISA and changes in *IL-8* expression by real-time PCR. PMA was used as a positive control (100 ng/mL). (A) IL-8 release by TR146 cells upon stimulation with live *C. albicans* SC5314; (B) *IL-8* expression by TR146 cells upon stimulation with live *C. albicans* SC5314; (C) IL-8 release by TR146 cells upon stimulation with heat-killed *C. albicans* SC5314; and (D) *IL-8* expression by TR146 cells upon stimulation with heat-killed *C. albicans* SC5314. The data are derived from duplicate wells of at least three independent experiments. **p* < 0.05, ***p* < 0.01, ****p* < 0.001, *****p* < 0.0001

In the initial experiments, PMA was used as a positive control (100 ng/mL) for stimulation and induced a significant IL-8 release from TR146 cells at both 4 hours and 24 hours (Figure 3.3A and Figure 3.3C). This confirmed the cells were viable and functionally responsive to inflammatory stimuli.

In response to stimulation with live *C. albicans*, significant release of IL-8 at both 4 hours and 24 hours was observed at M.O.Is of 0.1, 1, and 10 (all $p < 0.001$) (Figure 3.3A). Consistent with the ELISA data, expression levels of *IL-8* were

significantly upregulated when TR146 cells were stimulated with live *C. albicans* for 4 hours and 24 hours with all M.O.Is investigated (0.1 – 50; all $p < 0.01$) (Figure 3.3B). In contrast, stimulation with heat-killed *C. albicans* for 4 hours and 24 hours had no significant effect on IL-8 release or *IL-8* expression by TR146 cells at any of the M.O.Is investigated (Figure 3.3C and Figure 3.3D). These data suggested that *in vitro* TR146 cells were immunologically responsive to only live *C. albicans* SC5314.

The innate immune response of TR146 cells to live *C. albicans* was further investigated by analysing the expression and release of the cytokines IL-6 and IL-1α. Figure 3.4 A shows that live *C. albicans* induced significant release of IL-6 from TR146 cells *in vitro* after stimulation for both 4 hours and 24 hours with M.O.Is of 0.1, 1, and 10 (all $p < 0.05$). In addition, expression of *IL-6* was significantly upregulated after 4 hours stimulation with M.O.Is of 1, 10, and 50 (all $p < 0.05$) and after 24 hours stimulation with M.O.Is of 0.1, 1, 10, and 50 (all $p < 0.05$) (Figure 3.4 B). Similarly, Figure 3.4 C shows that live *C. albicans* induced significant release of IL-1α from TR146 cells *in vitro* after stimulation for 4 hours with a M.O.I of 10 ($p < 0.001$) and 24 hours with M.O.Is of 1, 10, and 50 (all $p < 0.01$). Consistent with the ELISA data, live *C. albicans* induced significantly increased expression of *IL-1*α after 4 hours stimulation with M.O.Is of 10 and 50 (all $p < 0.001$) and after 24 hours stimulation with M.O.Is of 0.1, 1, 10, and 50 (all $p < 0.05$) (Figure 3.4 D). At higher M.O.I of 50, reduction in IL-8, IL-6, and IL-1α release was observed due to the high density of *C. albicans* cells which did not allow for hyphal formation.

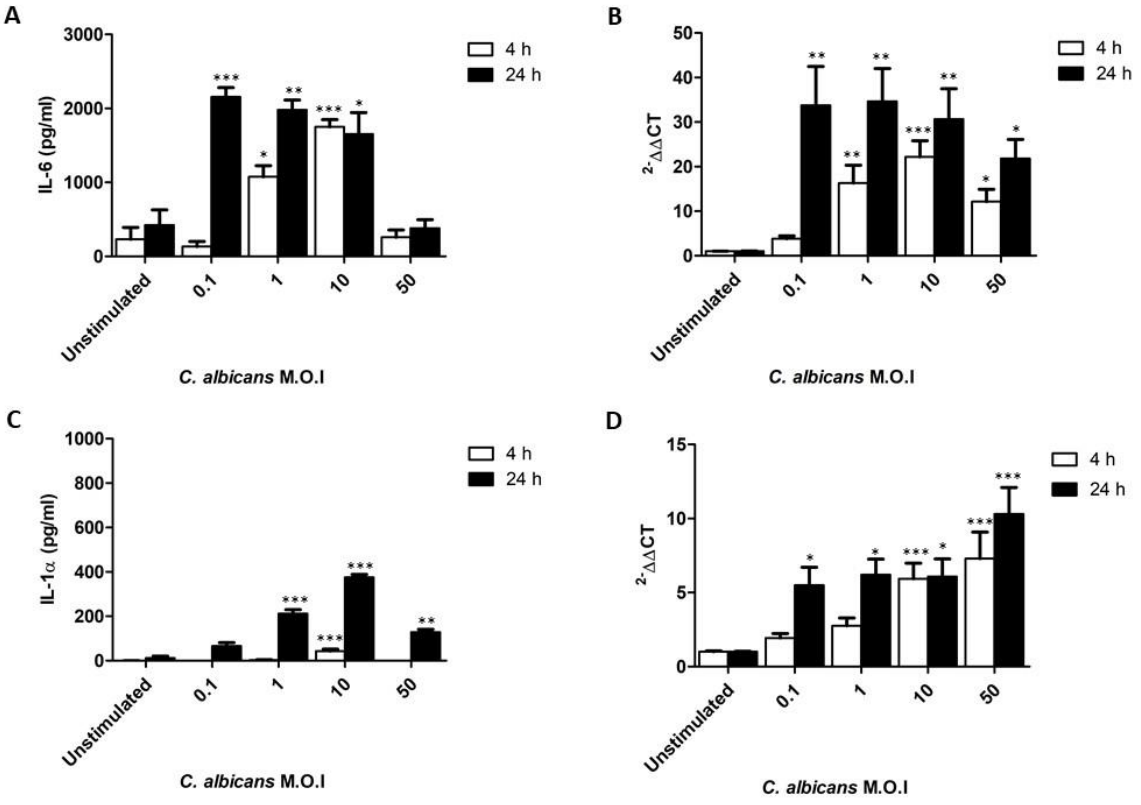

Figure 3.4 Expression and release of IL-6 and IL-1α by TR146 cells in response to stimulation with live *C. albicans*. TR146 cells seeded into 24-well plates were stimulated with various M.O.I of live *C. albicans* SC5314 over 4 hours and 24 hours. Release of IL-6 and IL-1α into culture supernatants was determined by ELISA and changes in *IL-6* and *IL-1α* expression by real-time PCR. (A) IL-6 release by TR146 cells upon stimulation with *C. albicans* SC5314; (B) *IL-6* expression by TR146 cells upon stimulation with *C. albicans* SC5314; (C) IL-1α release by TR146 cells upon stimulation with *C. albicans* SC5314; and (D) *IL-1α* expression by TR146 cells upon stimulation with *C. albicans* SC5314. The data are derived from duplicate wells of at least three independent experiments. *$p < 0.05$, **$p < 0.01$, ***$p < 0.001$, **** $p < 0.0001$

Taken together (Figure 3.2—Figure 3.4), these data show that TR146 cells initiate an innate immune response to live *C. albicans* but not heat-killed cells at 24 hours with an optimal M.O.I of 1. The optimization experiments have shown that M.O.I 1 consistently stimulated significant release of IL-8, IL-1α and IL-6 in relation to their gene expression analysis. In addition, hyphal growth observed under microscope at M.O.I 1 revealed proper level of biofilm formation compared to lower or higher M.O.Is where more yeast form can be observed covering the epithelial cells. Therefore, these conditions were utilised for all subsequent experiments.

3.3.2 The effect of PHCl on *Candida albicans* induced expression of chemokines and cytokines by TR146 cell monolayers

Before determining the effect of the general muscarinic receptor agonist PHCl on the innate immune responses of TR146 cells to *C. albicans*, any possible cytotoxic effects of the compound were first investigated. Figure 3.5 shows that PHCl alone or in combination with *C. albicans* at concentrations ranging from 0.005 — 50 mM had no significant cytotoxic effect on TR146 cells as determined by the LDH release assay.

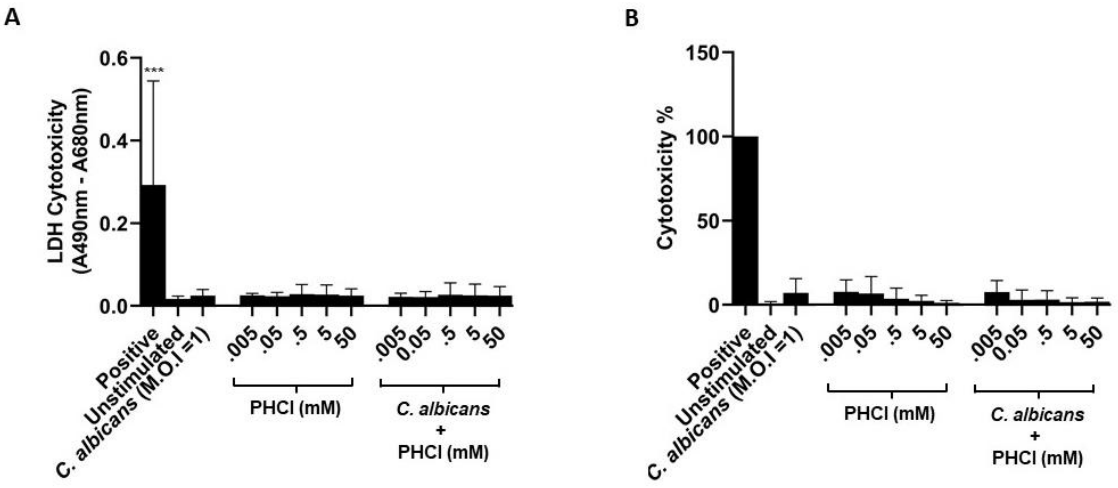

Figure 3.5 LDH release by TR146 cells after stimulation with live *C. albicans* in the presence and absence of PHCl over 24 hours. Release of LDH into culture supernatants was quantified using an LDH cytotoxicity assay kit. (A) Stimulation with live *C. albicans* at M.O.I = 1 in the presence and absence of 0.005—50 mM PHCl. Data presented as raw OD values for statistical analysis; (B) stimulation with live *C. albicans* at M.O.I = 1 in the presence and absence of 0.005–50 mM PHCl. The data are presented as percent cytotoxicity in relation to positive control. All experiments were performed in duplicate on at least three independent occasions. ***$p < 0.001$ in comparison to unstimulated cells.

As none of the concentrations of PHCl investigated exhibited any cytotoxicity against TR146 cells either alone or in combination with *C. albicans* (Figure 3.5), investigations were undertaken to determine the effect of the compound on the innate immune responses of the TR146 cells *in vitro*.

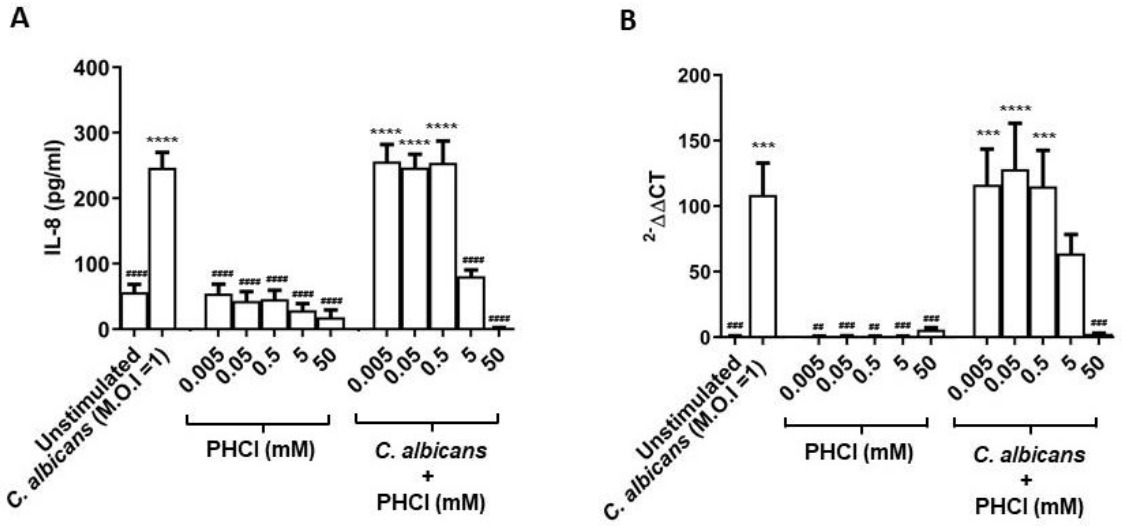

Figure 3.6 Modulation of *C. albicans* induced TR146 cell expression and release of IL-8 by PHCl. TR146 cells seeded into 24-well plates were stimulated with various concentrations of PHCl alone (0.005—50 mM) or *C. albicans* SC5314 (M.O.I =1) with various concentrations of PHCl (0.005—50 mM) for 24 hours. Release of IL-8 into culture supernatants was determined by ELISA and changes in *IL-8* expression by real-time PCR. (A) IL-8 release by TR146 cells upon exposure to PHCl alone (0.005—50 mM) and stimulation with live *C. albicans* SC5314 in the presence of PHCl (0.005—50 mM); (B) *IL-8* expression by TR146 cells upon exposure to PHCl alone (0.005—50 mM) and stimulation with live *C. albicans* SC5314 in the presence of PHCl (0.005—50 mM). Unstimulated cells and cells stimulated with *C. albicans* SC5314 (M.O.I =1) alone were used as controls. The data are derived from duplicate wells of at least three independent experiments. *$p < 0.05$, **$P < 0.01$, ***$p < 0.001$, and ****$p < 0.0001$ versus unstimulated cells. $^{\#}p < 0.05$, $^{\#\#}p < 0.01$, $^{\#\#\#}p < 0.001$, and $^{\#\#\#\#}p < 0.0001$ versus *C. albicans*-stimulated cells

Figure 3.6 shows that PHCl alone, at all concentrations investigated (0.005—50 mM), had no significant effects on IL-8 release from TR146 cells compared to unstimulated cells (Figure 3.6A). As expected, stimulation of TR146 cells with *C. albicans* (M.O.I = 1) for 24 hours induced significant release of IL-8 in comparison to control unstimulated cells ($p < 0.0001$). In comparison to the *C. albicans* stimulated cells, PHCl inhibited the *C. albicans*-induced release of IL-8 at concentrations of 5 mM ($p < 0.0001$) and 50 mM ($p < 0.0001$) (Figure 3.6A). This inhibitory effect on IL-8 production was mediated at the transcriptional level (Figure 3.6B). In comparison to unstimulated cells, *IL-8* mRNA expression significantly increased in TR146 cells stimulated with *C. albicans* alone ($p < 0.001$). In contrast, PHCl alone at any of the concentrations investigated had no significant effects on *IL-8* expression in TR146 cells when compared to the unstimulated control. However, in comparison to the *C. albicans*-stimulated cells, 50 mM PHCl inhibited the *C. albicans*-induced expression of *IL-8* ($p < 0.001$) (Figure 3.6B).

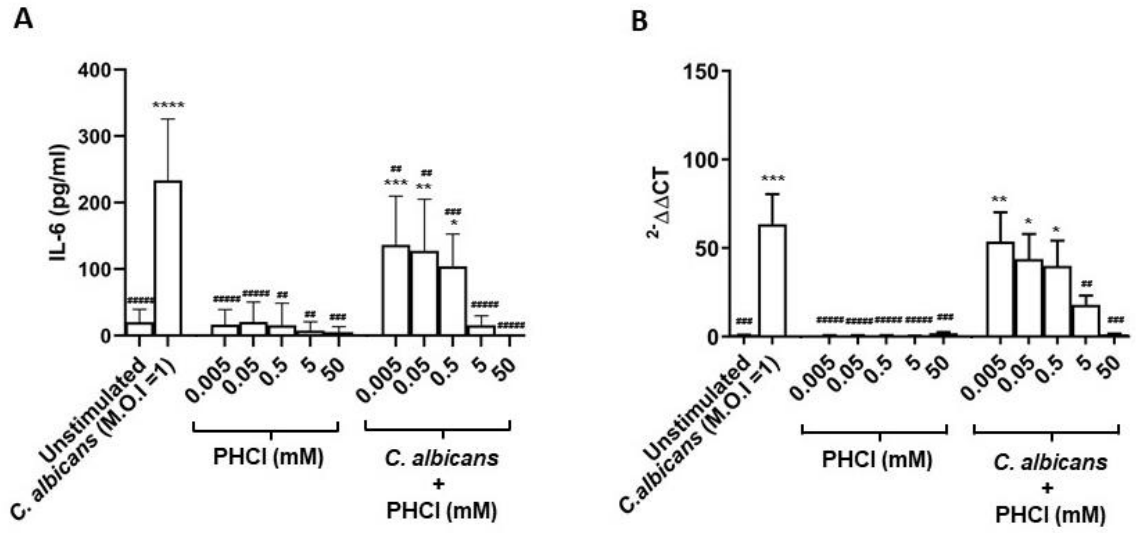

Figure 3.7 Modulation of *C. albicans*-induced TR146 cell expression and release of IL-6 by PHCl. TR146 cells seeded into 24-well plates were stimulated with various concentrations of PHCl alone (0.005—50 mM) or *C. albicans* SC5314 (M.O.I =1) with various concentrations of PHCl (0.005—50 mM) for 24 hours. Release of IL-6 into culture supernatants was determined by ELISA and changes in *IL-6* expression by real-time PCR. (A) IL-6 release by TR146 cells upon exposure to PHCl alone (0.005—50 mM) and stimulation with live *C. albicans* SC5314 in the presence of PHCl (0.005—50 mM); (B) *IL-6* expression by TR146 cells upon exposure to PHCl alone (0.005—50 mM) and stimulation with live *C. albicans* SC5314 in the presence of PHCl (0.005—50 mM). Unstimulated cells and cells stimulated with *C. albicans* SC5314 (M.O.I = 1) alone were used as controls. Data is derived from duplicate wells of at least three independent experiments. *$p < 0.05$, **$P < 0.01$, ***$p < 0.001$, and ****$p < 0.0001$ versus unstimulated cells. $^{\#}p < 0.05$, $^{\#\#}p < 0.01$, $^{\#\#\#}p < 0.001$, and $^{\#\#\#\#}p < 0.0001$ versus *C. albicans*-stimulated cells

Figure 3.7 shows that PHCl alone, at all concentrations investigated (0.005—50 mM), had no significant effects on IL-6 release from TR146 cells compared to unstimulated cells (Figure 3.7A). As expected, stimulation of TR146 cells with *C. albicans* (M.O.I = 1) for 24 hours induced significant release of IL-6 in comparison to control unstimulated cells ($p < 0.0001$). In comparison to the *C. albicans*-stimulated cells, PHCl inhibited the *C. albicans*-induced release of IL-6 at concentrations of 0.005 mM ($p < 0.01$), 0.05 mM ($p < 0.01$), 0.5 mM ($p < 0.001$), 5 mM ($p < 0.0001$) and 50 mM ($p < 0.0001$) (Figure 3.7A). This inhibitory effect on IL-6 production was mediated at the transcriptional level (Figure 3.7B). In comparison to unstimulated cells, *IL-6* mRNA expression was significantly increased in the TR146 cells stimulated with *C. albicans* alone ($p < 0.001$). In contrast, PHCl alone at any of the concentrations investigated had no significant effects on *IL-6* expression in TR146 cells when compared to the unstimulated control. However, in comparison to the *C. albicans*-stimulated cells, 5 mM ($p < 0.01$) and 50 mM ($p < 0.01$) PHCl inhibited the *C. albicans*-induced expression of *IL-6* (Figure 3.7B).

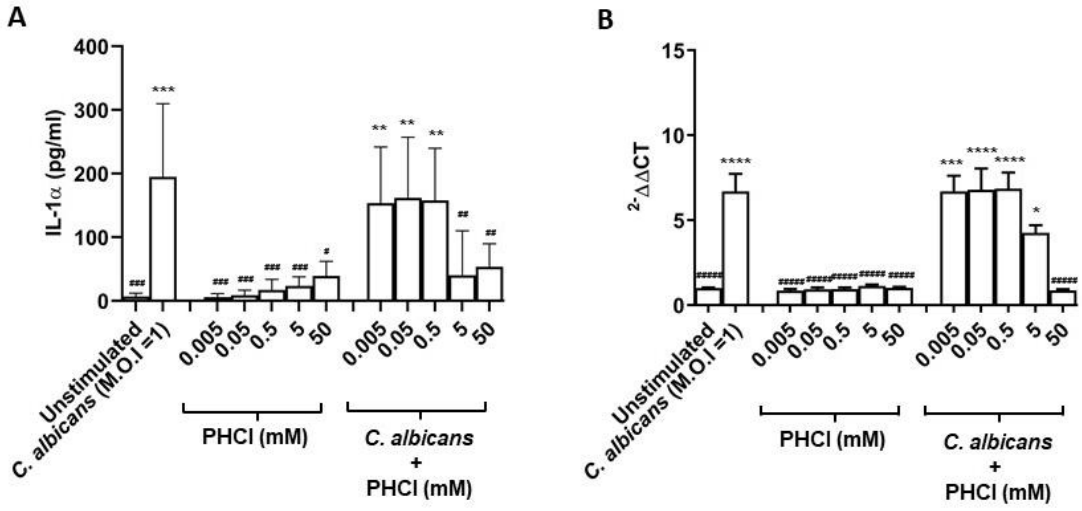

Figure 3.8 Modulation of *C. albicans* induced TR146 cell expression and release of IL-1α by PHCl. TR146 cells seeded into 24-well plates were stimulated with various concentrations of PHCl alone (0.005—50 mM) or *C. albicans* SC5314 (M.O.I = 1) with various concentrations of PHCl (0.005—50 mM) for 24 hours. Release of IL-1α into culture supernatants was determined by ELISA and changes in *IL-1α* expression by real-time PCR. (A) IL-1α release by TR146 cells upon exposure to PHCl alone (0.005—50 mM) and stimulation with live *C. albicans* SC5314 in the presence of PHCl (0.005—50 mM); (B) *IL-1α* expression by TR146 cells upon exposure to PHCl alone (0.005—50 mM) and stimulation with live *C. albicans* SC5314 in the presence of PHCl (0.005—50 mM). Unstimulated cells and cells stimulated with *C. albicans* SC5314 (M.O.I = 1) alone were used as controls. The data are derived from duplicate wells of at least three independent experiments. *p < 0.05, **P < 0.01, ***p < 0.001, and ****p <0.0001 versus unstimulated cells. $^{\#}p$ < 0.05, $^{\#\#}p$ < 0.01, $^{\#\#\#}p$ < 0.001, and $^{\#\#\#\#}p$ < 0.0001 versus *C. albicans*-stimulated cells.

Figure 3.8 shows that PHCl alone, at all concentrations investigated (0.005 — 50 mM), had no significant effects on IL-1α release from the TR146 cells compared to unstimulated cells (Figure 3.8A). As expected, stimulation of TR146 cells with *C. albicans* (M.O.I = 1) for 24 hours induced significant release of IL-1α in comparison to control unstimulated cells ($p < 0.001$). In comparison to the *C. albicans* stimulated cells, PHCl inhibited the *C. albicans*-induced release of IL-1α at concentrations of 5 mM ($p < 0.01$) and 50 mM ($p < 0.01$) (Figure 3.8A). This inhibitory effect on IL-1α production was mediated at the transcriptional level (Figure 3.8B). In comparison to unstimulated cells, *IL-1a* mRNA expression significantly increased in TR146 cells stimulated with *C. albicans* alone ($p < 0.0001$). In contrast, PHCl alone at any of the concentrations investigated had no significant effects on *IL-1a* expression in TR146 cells when compared to the unstimulated control. However, in comparison to the *C. albicans*-stimulated cells, 50 mM PHCl inhibited the *C. albicans* induced expression of *IL-1a* ($p < 0.0001$) (Figure 3.8B).

3.3.3 The effect of PHCl on *Candida albicans* infection of a 3D human oral epithelium tissue model

Previous data demonstrate that TR146 cells can initiate an innate immune response to *C. albicans* infection and, in addition, this response is modulated by the general muscarinic receptor agonist PHCl. To further investigate this host inflammatory immune response in a model that better mimics the *in vivo* buccal mucosa, a 3D human oral epithelium (HOE) tissue model was employed.

The viability of the HOE tissue under all experimental conditions was first evaluated using the LDH release assay. Figure 3.9 shows that stimulation with live *C. albicans* alone or in combination with PHCl had no significant effect on tissue viability as determined by LDH release. PMA at a concentration of 100 ng/mL was also included as a positive control for tissue stimulation and demonstrated no significant effect on tissue viability.

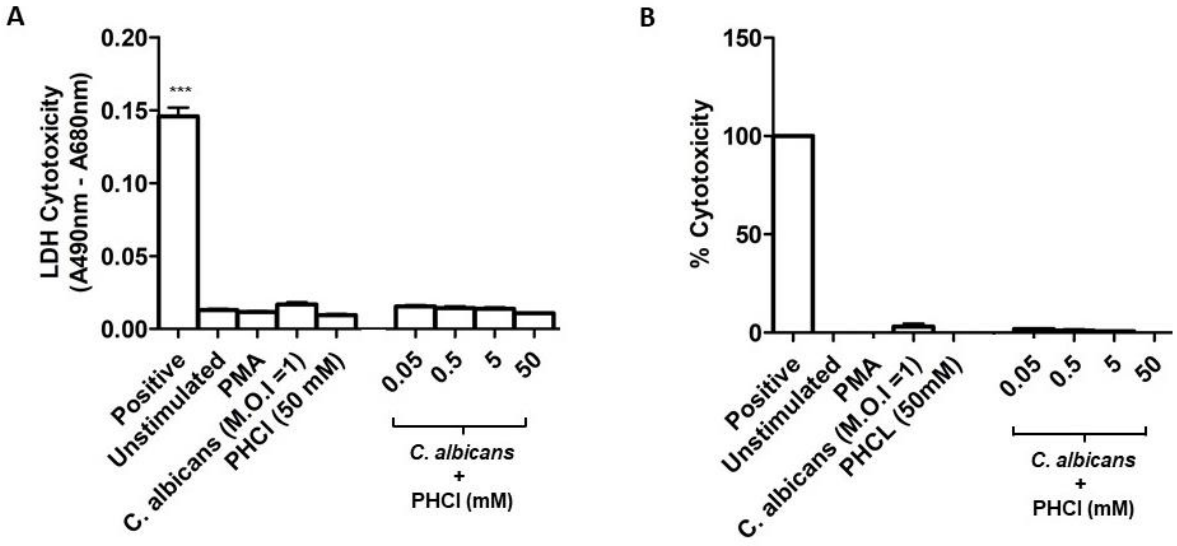

Figure 3.9 LDH release by human oral epithelial tissue after stimulation with live *C. albicans* in the presence and absence of PHCl over 24 hours. The release of LDH into culture supernatants was quantified using an LDH cytotoxicity assay kit. (A) Stimulation with live *C. albicans* at M.O.I = 1 in the presence and absence of 0.05—50 mM PHCl—data are presented as raw OD values for statistical analysis; (B) stimulation with live *C. albicans* at M.O.I = 1 in the presence and absence of 0.05—50 mM PHCl. Data are presented as percent cytotoxicity in relation to the positive control. All experiments were performed in triplicate on at least two independent occasions. ***p <0.001 in comparison to unstimulated cells.

As PHCl, PMA, and *C. albicans* at the concentrations or M.O.I used in this study exhibited no cytotoxicity against the HOE 3D tissue model (Figure 3.9), investigations were undertaken to determine their effects, either in isolation or combination, on the HOE innate immune response *in vitro*. A custom RT^2 profiler

array, which investigated the expression of 11 genes (*IL1a, IL6, TNFa, GM-CSF/CSF2, G-CSF/CSF3, IL8, CCL2, TLR2, TLR4, CLEC7A,* and *CAMP*) known to play a role in the innate immune responses to *C. albicans* infection was used to assess the HOE innate immune responses to *C. albicans* (M.O.I = 1) alone or in combination with a range of PHCl concentrations (0.05−50 mM).

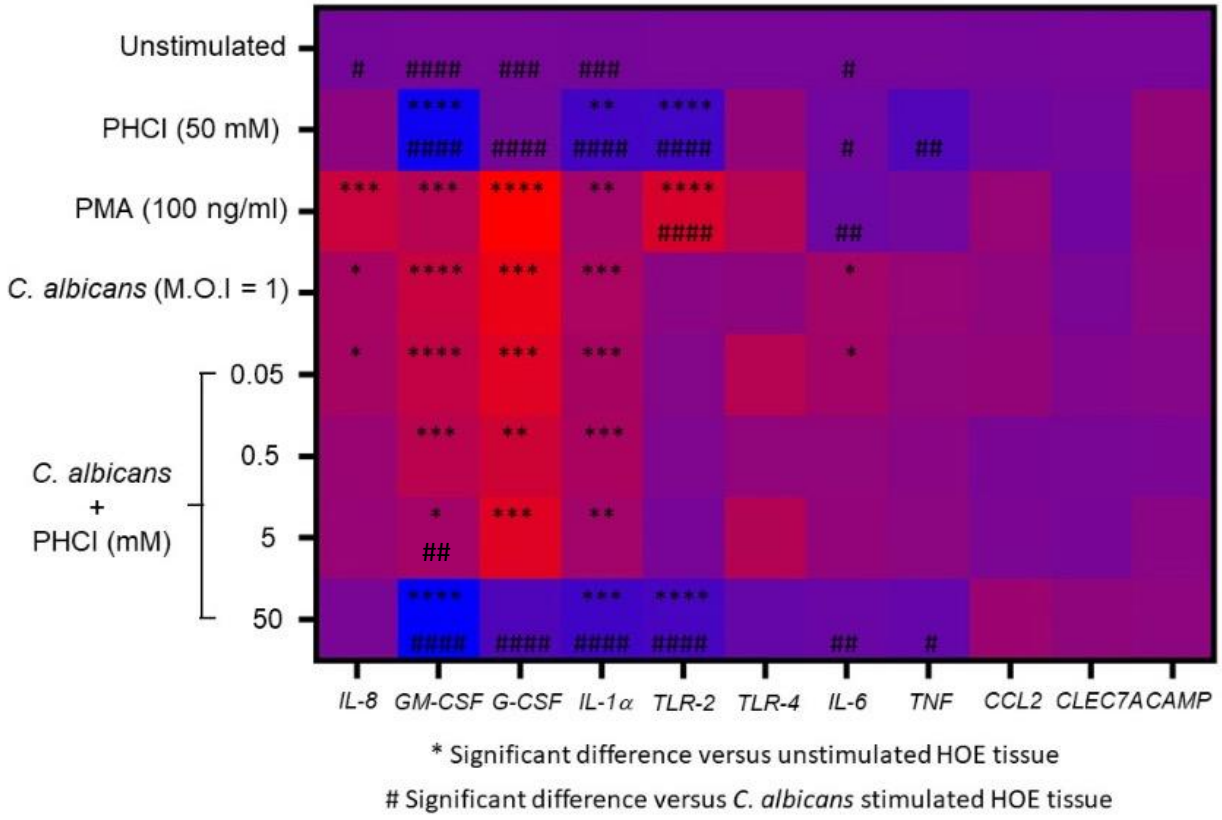

Figure 3.10 A heat map showing the differential expression of genes involved in the innate immune response to *C. albicans* infection by human oral epithelial tissue after stimulation with *C. albicans* in the presence and absence of PHCl. HOE tissue was stimulated with live *C. albicans* for 24 hours in the presence or absence of PHCl at different concentrations (0.05−50 mM). Unstimulated cells exposed to the highest concentration of PHCl (50 mM) were used as negative controls. PMA was used as a positive control for stimulation. Data for expression of each gene was normalised to the housekeeping *GAPDH* and fold induction calculated using the $^{2\text{-}}\Delta\Delta$CT method. Data is presented as $\log_2$-fold change relative to the unstimulated HOE tissue. The experiment was repeated in duplicate on two independent occasions. For statistical analysis, the differences in $\log_2$ fold change between either unstimulated cells or *C. albicans*-stimulated cells were determined using a one-way ANOVA with a Dunnett's post-test. $^{*}p < 0.05$, $^{**}p < 0.01$, $^{***}p < 0.001$, and $^{****}p < 0.0001$ versus unstimulated HOE tissue. $^{\#}p < 0.05$, $^{\#\#}p < 0.01$, $^{\#\#\#}P < 0.001$, and $^{\#\#\#}p < 0.0001$ versus *C. albicans*-stimulated tissue.

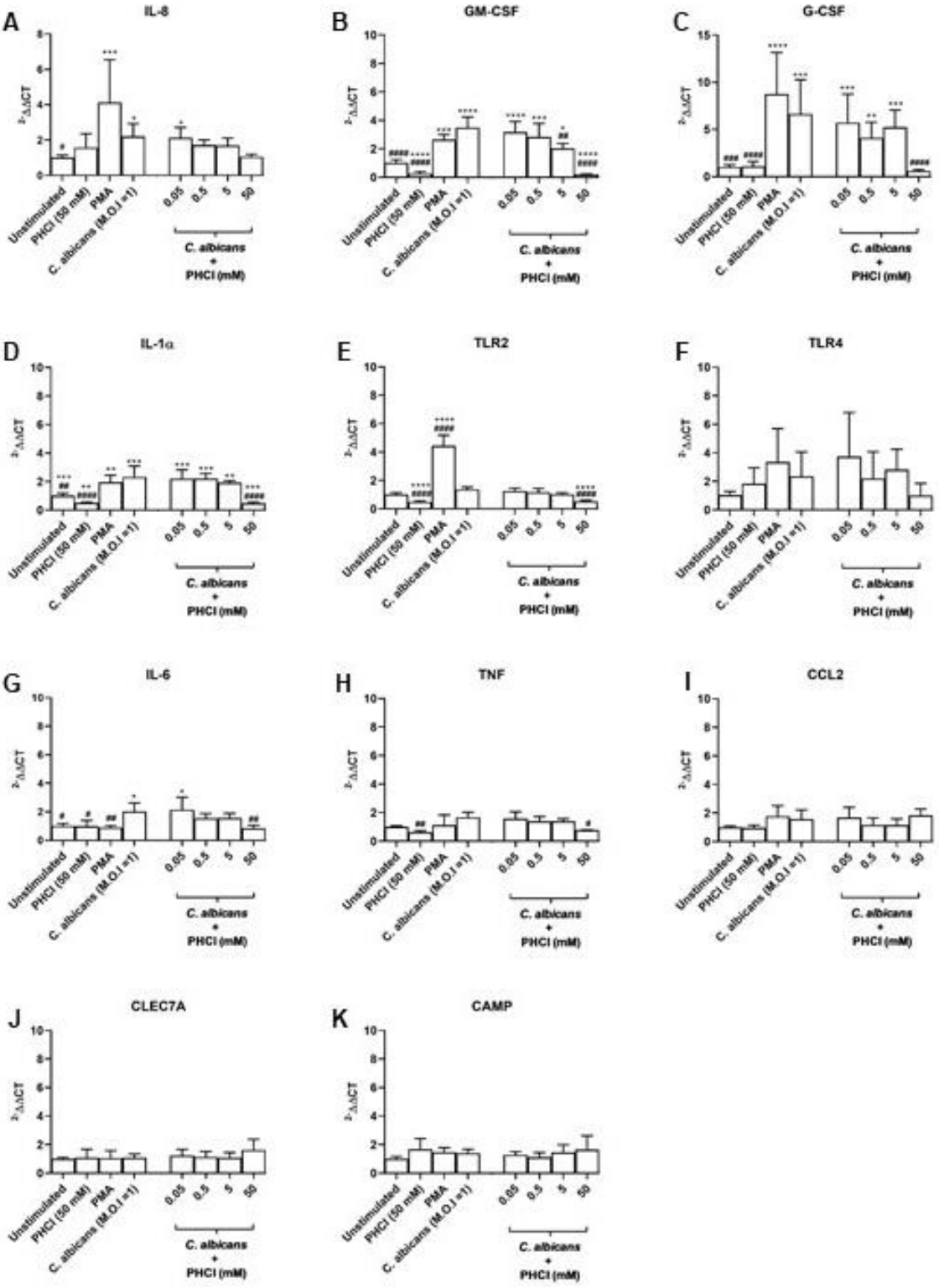

Figure 3.11 Fold induction changes in the expression of genes involved in the innate immune response to *C. albicans* infection by the HOE tissue after stimulation with *C. albicans* in the presence and absence of PHCl. HOE tissue was stimulated with live *C. albicans* for 24 hours in the presence or absence of PHCl at different concentrations (0.05—50 mM). Unstimulated cells exposed to the highest concentration of PHCl (50 mM) were used as negative controls. PMA was used as a positive control for stimulation. Data for expression of each gene was normalised to the housekeeping *GAPDH* and fold induction was calculated using the $^{2\text{-}}\Delta\Delta$CT method. (A) *IL-8* (CXCL8); (B) *GM-CSF/CSF2*; (C) *G-CSF/CSF3*; (D) *IL1-*α; (E) *TLR2*; (F) *TLR4IL6*; (G) *IL-6*, (H) *TNF*; (I) *CCL2*; (J)

CLEC7A; and (K) *CAMP*. *p < 0.05, **P < 0.01, ***p < 0.001, and ****p <0.0001 versus unstimulated cells. $^{\#}p$ < 0.05, $^{\#\#}p$ < 0.01, $^{\#\#\#}p$ < 0.001, and $^{\#\#\#\#}p$ < 0.0001 versus *C. albicans*-stimulated cells.

Figure 3.10 and 3.11 show that 5 of the 11 genes were significantly upregulated upon stimulation of the HOE tissue with PMA over 24 hours: *IL-8* (p < 0.001), *GM-CSF/CSF2* (p < 0.001), *G-CSF/CSF3* (p < 0.0001), *IL1-*α, (p < 0.01), and *TLR2* (p < 0.0001). Likewise, stimulation of the HOE tissue with *C. albicans* (M.O.I = 1) significantly upregulated expression of *IL-8* (p < 0.05), *GM-CSF/CSF2* (p < 0.0001), *G-CSF/CSF3* (p < 0.001), *IL1-*α (p < 0.001), and *IL-6* (p < 0.05). Interestingly, exposure of HOE tissue to PHCl (50 mM) alone caused significant downregulated expression of *GM-CSF/CSF2* (p < 0.0001), *IL1-*α (p < 0.01), and *TLR2* (p < 0.0001). Furthermore, compared to HOE tissue stimulated with *C. albicans* alone, PHCl was observed to cause a dose-dependent reduction in *C. albicans*-induced expression of *IL-8*, *GM-CSF/CSF2*, *G-CSF/CSF3*, *IL1-*α, *IL-6*, and TNF with a significant difference in expression being obtained in the presence of 50 mM PHCl (*GM-CSF/CSF2* = p < 0.0001, *G-CSF/CSF3* = p < 0.0001, *IL1-*α = p < 0.0001, and *IL-6* = p <0.01). No effects on the expression of *CCL2*, *CLEC7A*, and *CAMP* were observed under any of the experimental conditions.

Figures 3.10 and 3.11 demonstrate that PHCl could modulate the *C. albicans*-induced expression of several inflammatory genes by a HOE 3D tissue model. Therefore, investigations were undertaken to determine whether this effect on transcript expression resulted in an effect on the release of the functional protein.

Figure 3.12A shows that stimulation of the HOE tissue with PMA and *C. albicans* (M.O.I = 1) for 24 hours induced a significant release of IL-8 in comparison to unstimulated tissue (p < 0.001 and p < 0.05, respectively). In comparison to the *C. albicans*-stimulated tissue, 50 mM PHCl inhibited the *C. albicans*-induced release of IL-8 from the HOE tissue (p < 0.05). Figure 3.12B shows that stimulation of the HOE tissue with PMA and *C. albicans* (M.O.I = 1) for 24 hours induced a significant release of IL-6 in comparison to the unstimulated tissue (both p < 0.001). In comparison to the *C. albicans*-stimulated tissue, 50 mM PHCl inhibited the *C. albicans*-induced release of IL-6 from the HOE.

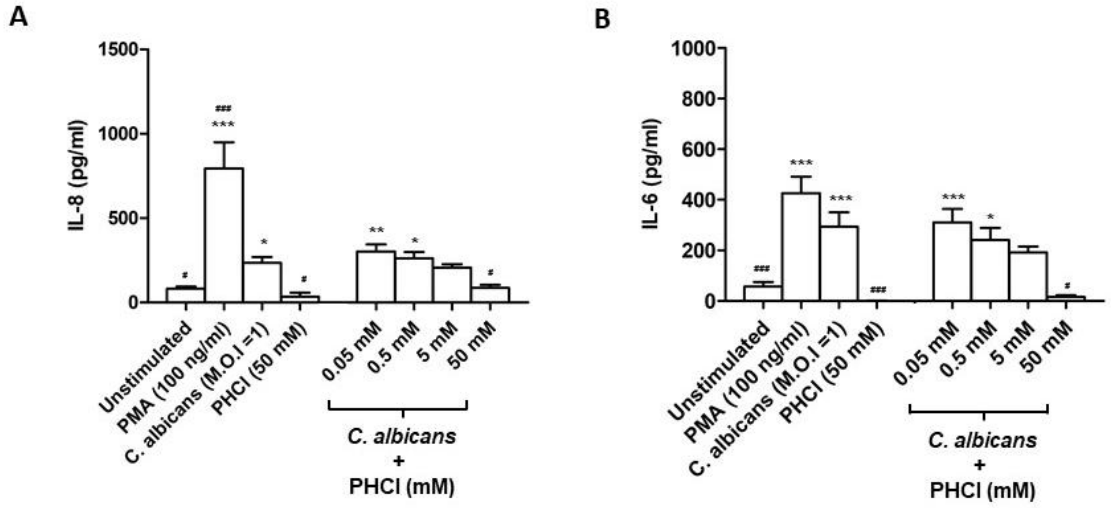

Figure 3.12 Modulation of *C. albicans*-induced HOE release of IL-8 and IL-6 by PHCl. The HOE tissue was stimulated with *C. albicans* SC5314 (M.O.I = 1) and various concentrations of PHCl (0.05—50 mM) over 24 hours. Release of IL-8 and IL-6 into culture supernatants was determined by ELISA. PMA (100 ng/mL) was included as a positive stimulation control. PHCl alone (highest concentration = 50 mM) was used as an additional negative control to unstimulated tissue alone. (A) IL-8 release by HOE tissue upon exposure to *C. albicans* SC5314 (M.O.I = 1) alone or in combination with PHCl (0.05—50 mM); (B) IL-6 release by HOE tissue upon exposure to *C. albicans* SC5314 (M.O.I = 1) alone or in combination with PHCl (0.05—50 mM). The data are derived from triplicate wells of two independent experiments. *$p < 0.05$, **$p < 0.01$, and ***$p < 0.001$ versus unstimulated cells. $^{\#}p < 0.05$, $^{\#\#}p < 0.01$, and $^{\#\#\#}p < 0.001$ versus *C. albicans*-stimulated cells.

Previous studies have demonstrated that the transition of *C. albicans* from the yeast form to the hyphal form is a key driver of the mucosal innate immune response to this organism (Nikou et al., 2019, Pellon et al., 2020). In chapter two, it was demonstrated that PHCl could inhibit this transition and, therefore, histological analysis was undertaken to investigate whether this may be a mechanism for the PHCl-induced downregulation of inflammatory genes observed in (Figures 3.10 and 3.11). The HOE tissue from each experimental condition was processed and stained with H&E (Figure 3.13) and PAS (Figure 3.14).

Microscopy revealed that uninfected control tissue had an organised structure with attached and coherent cell layers (Figure 3.13A and 3.14A). In addition, exposure to PHCl alone (Figure 3.13B and 3.14B) and stimulation with PMA (Figure 3.13C and 3.14C) did not cause any observable detrimental damage to the morphology of the tissue or detachment of the cells. However, the PMA-stimulated cell layers (Figure 3.13C and 3.14C) were less coherent with observable spaces between cells. In contrast, infection with *C. albicans* resulted in profound damage that reached the basal layer of the tissue and caused

detachment of the cell layers and modifications to the tissue architecture. Furthermore, *C. albicans* yeast cells and more noticeable hyphal growth was observed in the areas of tissue damage (Figure 3.13D and 3.14D). Interestingly, however, when tissues were stimulated with *C. albicans* in the presence of various concentrations of PHCl a dose-dependent effect on the extent of the tissue damage was observed. PHCl at 50 mM caused a noticeable reduction in the accumulation of *C. albicans* cells on the outer layers of the tissue with significantly reduced hyphae formation and observable tissue damage (Figure 3.13E and 3.14E). As the concentrations of PHCl decreased (5, 0.5, and 0.05 mM), the *C. albicans* hyphae and yeast cells become more prominent and the extent of the tissue damage increased to levels comparable to the untreated *C. albicans*-infected tissue (Figure 3.13F, G, H and 3.14F, G, H).

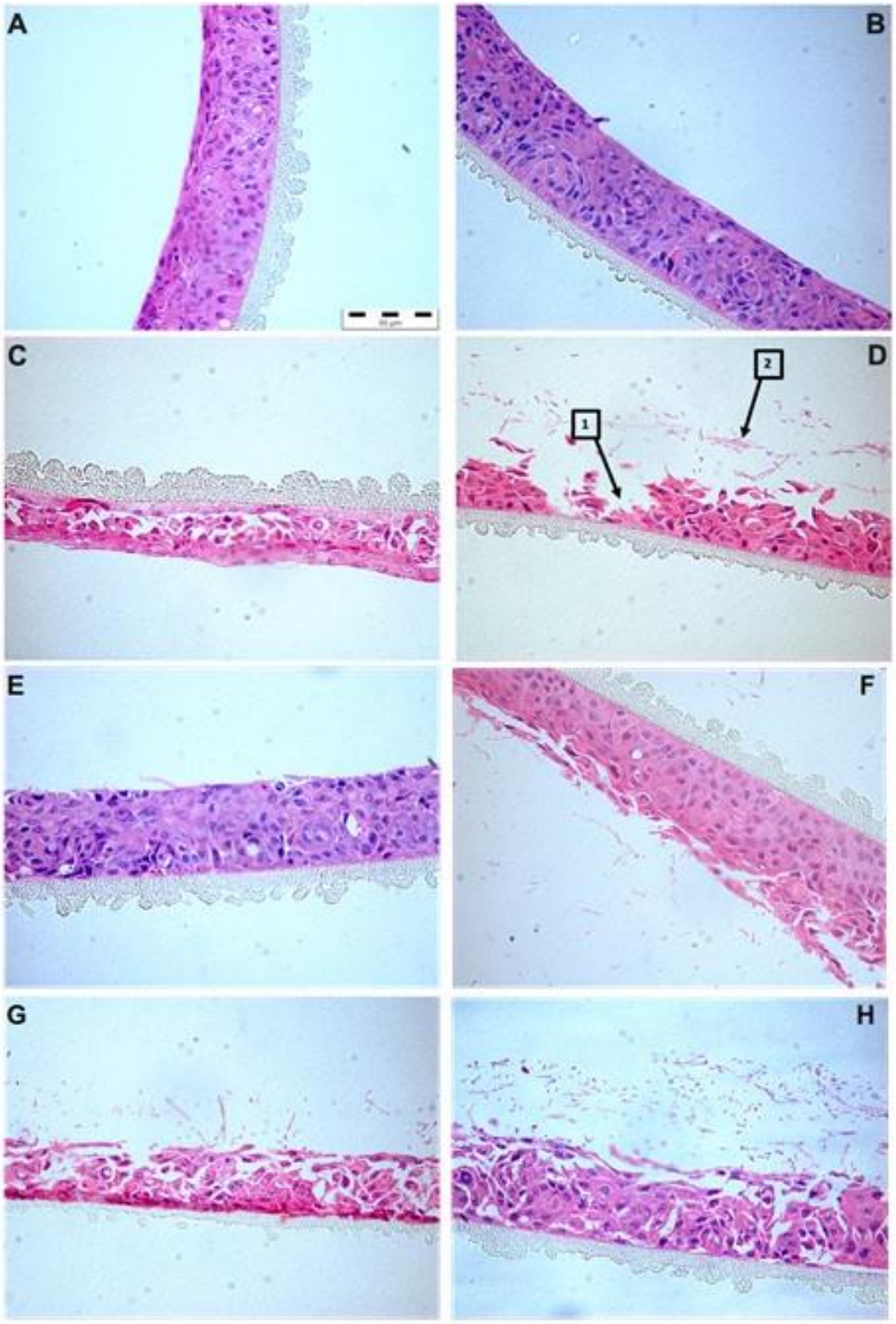

Figure 3.13 H&E staining of *C. albicans*-infected HOE treated with PHCl. (A) uninfected HOE tissue; (B) uninfected tissue treated with 50 mM PHC only; (C) uninfected tissue stimulated with PMA; (D) *C. albicans* (M.O.I =1)-infected tissue; (E) *C. albicans* (M.O.I = 1)-infected tissue + 50 mM PHCl; (F) *C. albicans* (M.O.I = 1)-infected tissue + 5 mM PHCl; (G) *C. albicans* (M.O.I = 1)-infected tissue + 0.5 mM PHCl; and (H) *C. albicans* (M.O.I = 1)-infected tissue + 0.05 mM PHCl. Arrow 1 = detachment of cell layers and Arrow 2 = *C. albicans* hyphae. The scale bar for all images is shown in (A). Images are representative of two technical replicates of two independent experiments.

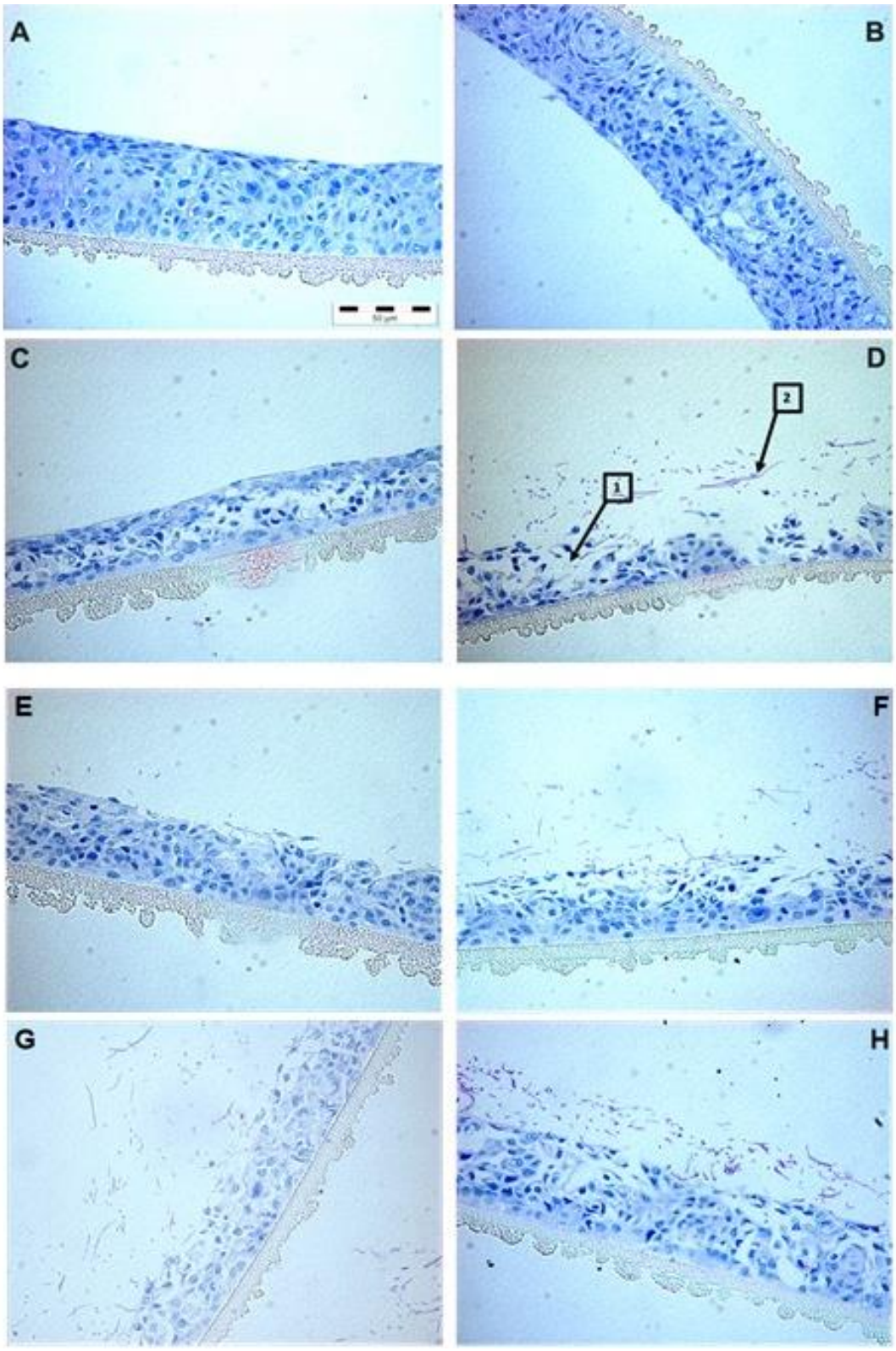

Figure 3.14 PAS staining of *C. albicans*-infected HOE treated with PHCl. (A) uninfected HOE tissue; (B) uninfected tissue treated with 50 mM PHC only; (C) uninfected tissue stimulated with PMA; (D) *C. albicans* (M.O.I = 1)-infected tissue; (E) *C. albicans* (M.O.I = 1)-infected tissue + 50 mM PHCl; (F) *C. albicans* (M.O.I = 1)-infected tissue + 5 mM PHCl; (G) *C. albicans* (M.O.I = 1)-infected tissue + 0.5 mM PHCl; and (H) *C. albicans* (M.O.I =1)-infected tissue + 0.05 mM PHCl. Arrow 1 = detachment of the cell layers and Arrow 2 = *C. albicans* hyphae. The scale bar for all images shown is in (A). Images are representative of two technical replicates of two independent experiments.

3.4 Discussion

This chapter investigated the innate immune response of oral epithelial cells and tissues to *C. albicans* infection and the immunomodulatory effect of PHCl. *C. albicans* infects different sites of the human body, including epithelia, and triggers an innate immune response (Moyes et al., 2015). An effective immune response is required to protect against pathogen invasion. However, an excessive inflammatory response can, in some circumstances, lead to serious damage of host tissues (Carpino et al., 2017, Whibley and Gaffen, 2014, Shoham and Levitz). Pilocarpine hydrochloride (PHCl) is a cholinergic compound and it's inhibitory effect on *C. albicans* pathogenicity has been demonstrated previously (Nile et al., 2019). It is known that cholinergic receptors, including muscarinic receptors, are expressed by non-neuronal cells including those found in the oral mucosa and targeting cholinergic receptors as a therapeutic avenue is a well-established principle (Pohanka, 2012, D'Souza and Waldvogel, 2016). Therefore, it was reasoned that PHCl can modulate the oral innate immune response to *C. albicans* infection, and this was investigated using the TR146 cell line and a 3D model of the human oral epithelium.

In the first part of this chapter, the aim was to optimise the stimulatory conditions for investigating the immunomodulatory effects of PHCl using the TR146 cell line. TR146 cells are an undifferentiated, non-keratinised cell line, derived from a human squamous cell carcinoma of the buccal mucosa (Rupniak et al., 1985, Jacobsen et al., 1995, Mørck Nielsen and Rømer Rassing, 2000). TR146 cells are simple to maintain and affordable; but do not mimic the architecture of host tissue and after isolation they have been suggested to undergo morphological changes resulting in disruptions to structure, organisation, cell signaling mechanisms and response to external stimuli (Kapałczyńska et al., 2018). Initial investigations compared the innate immune response of the TR146 cell line against heat-killed and live *C. albicans* using *IL-8* (CXCL8) expression as a marker of an inducible innate immune response. The findings in this chapter demonstrated that only live *C. albicans*, and not heat killed, could stimulate TR146 cells to release IL-8. Unlike the findings in this work, it has previously been shown that heat-killed *C. albicans*, in the yeast form but not the hyphal form, significantly increased the expression of *TNF-a*

and other cytokines by human peripheral blood mononuclear cells (PMBCs) (Mukaremera et al., 2017). This was hypothesised to be due to the effect of heat treatment on the outer layer of the cell wall and exposure of the ß-glucan to the host pattern-recognition receptors (PRRs) (Cheng et al., 2012). However, the immune response to *C. albicans* can vary between cells and tissues and may reflect their PRR expression profile. Indeed, previous studies have also demonstrated that heat killed *C. albicans* fails to elicit an immune response in oral epithelial cells (Schaller et al., 2002) as observed in this study. Moreover, the stimulation of both professional and non-professional immune cells with different morphological forms of *C. albicans* has demonstrated that they have differing immunoregulatory properties (Moyes et al., 2015).

The ability of the immune system to discriminate *C. albicans* morphology and respond accordingly is a crucial determinant of commensalism or pathogenicity. Along with a dramatic inflammatory response by the host, the yeast to hyphae transition exacerbates damage to host tissue and organs (Matuschak and Lechner, 1997). It has been noted that *C. albicans* at higher cell densities, however, do not form hyphae due to inhibition by farnesol, a quorum sensing molecule (Ciurea et al., 2020). The data reported in this chapter revealed that live *C. albicans* at an M.O.I of 1 stimulated optimal upregulated expression and release of IL-8, IL-6 and IL-1α from TR146 cells. Furthermore, stimulation with higher M.O.Is showed sub-optimal expression and release of these proinflammatory mediators and this was associated with a greater number of yeast cells visible on the cell monolayer surface (data not shown). These data therefore confirm the important role of the morphogenesis process in stimulating the TR146 cell innate immune response. Therefore, for optimal stimulation in the further experiments reported in this chapter, live *C. albicans* at an M.O.I of 1 was used.

During *C. albicans* infection, the host immune system initiates an immune response via recognition of conserved pathogen associated molecular patterns (PAMPs) through recognition receptors (PRRs) such as the Toll-like receptors (TLRs) and C-type lectin receptors (CLRs). Polysaccharide components of the *C. albicans* cell wall such as mannan, chitin, ß-1,3-glucan and ß-1,6-glucan are PAMPs recognized by host PRRs. Recognition of fungal PAMPs, consequently,

instigates a series of signaling pathways that activate inflammatory cytokine and chemokine expression such as *IL-6, IL-8*, and *IL-1*α, which in turn result in recruitment and activation of innate phagocytic cells such as neutrophils and monocytes (Chin et al., 2014, Netea et al., 2015, Romani, 2011).

Interleukin-6 (IL-6) is released as part of the innate immune responses. Some of the cell wall components of *C. albicans* stimulate the production of IL-6 (Chin et al., 2014). Secretion of IL-6 helps in eliminating invasive *C. albicans*. A study by Van Enckevort et al. (1999) showed that mice deficient in IL-6 were more susceptible to systemic candidiasis. The role of IL-6 in neutrophil activation is important in *C. albicans* infections and it has been shown that mice lacking IL-6 could not generate an effective neutrophil response. The lack of IL-6 production by deficient mice also led to increased fungal load and decreased survival rates. Indeed, despite the production of other pro-inflammatory cytokines such as IL-1α and TNF, the lack of IL-6 still leads to fungal outgrowth in various organs during *C. albicans* infection further emphasising the importance of this cytokine in an effective immune response to *C. albicans* (Chin et al., 2014).

Interleukin-8 (IL-8) plays a crucial role in innate immunity against *C. albicans*. It is a key host immune response chemokine with a vital role in protecting against oral fungal infections. IL-8 is a potent chemoattractant, drives monocyte antifungal effects and can enhance keratinocyte proliferation during *C. albicans* infection, preventing invasive or chronic illnesses. IL-8 production drives the recruitment of phagocytes such as neutrophils to sites of infection and is an important initiator of an inflammatory response. However, activation of IL-8 can also exacerbate oral epithelial cell lysis in the presence of *C. albicans* through an IL-1α driven mechanism. Indeed, IL-1α is an important potent stimulator of IL-8 secretion by oral epithelial cells during a *C. albicans* infection. Coculturing *C. albicans* with oral epithelial cells in the presence and absence of a neutralizing anti IL-1α antibody or IL-1 Receptor antagonist (IL-1Ra) resulted in approximately 50% inhibition of IL-8 secretion. Furthermore, production of IL-8 was *Candida* strain-specific and required the germination of the yeast into hyphae. Strain SC5314 was found to be the most potent inducer of IL-8 expression when compared to ATCC28366 and ATCC32077 *Candida* strains (Dongari-Bagtzoglou and Kashleva, 2003). This finding implies that only viable *C.*

albicans can effectively trigger an IL-8 response which is in agreement with data reported in this study.

Another important interleukin in combating *C. albicans* infection is IL-1α. Interleukin-1 cytokines were the first interleukins to be identified and are crucial for the host innate response to infection and are linked with both acute and chronic inflammation. Interleukin-1 cytokines (except IL-1Ra) are expressed in a precursor form, which itself can be biologically active, or requires subsequent cleavage and posttranslational modification. Both IL-1α and IL-1ß are proinflammatory cytokines and in general share similarities in terms of their biological functions, yet they do differ in some respects. Interleukin-1α is expressed by mesenchymal and epithelial cells during an inflammatory response. IL- 1α further promotes inflammation via binding to receptor ILR1 and functions also as an active membrane bound precursor. On the other hand, IL-1ß is produced mainly by mononuclear phagocytes as an inactive precursor (Griffiths et al., 2021). Smeekens et al. (2015) reported that *C. albicans* stimulates the mannose receptors on macrophages, leading to the cleavage of immature IL-1ß by monocytes and release of active IL-1ß which subsequently plays a role in the induction of immune responses against *C. albicans* infections. Mice deficient in IL-1 receptors succumbed to candida infections. Furthermore, IL-1ß induced Th17 responses lead to protection of the skin and mucosa against *C. albicans*. An important consideration is the presence of IL-1Ra, which is a natural antagonist of IL-1ß whose role is to counterbalance the inflammatory response initiated by IL-1 cytokines and prevent severe tissue damaging inflammation in response to *C. albicans*. However, *C. albicans* has developed a host immune response evasion strategy whereby it can induce overexpression of IL-1Ra, through it's ß -glucans, which nullify the host IL-Iß response and promotes it's pathogenicity (Smeekens et al., 2015, Griffiths et al., 2021). Vonk et al. (2006) showed that IL-1ß and IL-1α mounted protective host responses against disseminated candidiasis. IL-1ß recruits polymorphonuclear leukocytes (PMNs) to the infected sites. However, IL-1α was required for the PMNs to kill the pseudohyphae of *C. albicans* and promote an effective Th1 response. Indeed, Interleukin 1 is believed to protect the host against *C. albicans* infection by increasing the influx of PMNs and enhancing granulopoiesis (Vonk et al., 2006).

Muscarinic receptors are expressed on different cells that play roles in host immune responses such as fibroblasts, leukocytes, and epithelial cells. The role of muscarinic receptors in modulating the immune response during infection is relatively understudied. However, Darby et al. (2015) revealed the important role of the M3 receptor in modulating the immune response against *Salmonella typhimurium* and *Nippostrongylus brasiliensis*. Mice that were deficient in M3 receptors had reduced CD4 T-cell cytokine production in primary and secondary infections. Another study by Razani-Boroujerdi et al. (2008), revealed that chronic treatment with oxotremorine, a muscarinic receptor agonist, in a rat model stimulated the T-cell-proliferative responses. Okuma and Nomura et al. (2001), reported that treating human peripheral blood lymphocytes with oxotremorine, enhanced phytohemagglutinin induced IL-2 production. Another study by Vezys et al. (2007) demonstrated that muscarinic receptor type 1 (M1) knockout mice infected with lymphocytic choriomeningitis virus (LCMV) or vesicular stomatitis virus (VSV) were deficient in the development of a cytotoxic T cell response. The first evidence for a role of muscarinic receptors in modulation of the immune response against fungal infections was reported by Nile et al. (2019), using a *Galleria mellonella infection* model. This study demonstrated that PHCl can modulate the host immune response by inducing effective clearance of *C. albicans* and limiting host tissue damage.

The data presented in this chapter show that treating TR146 cells with different concentrations (0.05—50 mM) of PHCl during *C. albicans* infection at a M.O.I of 1 resulted in reduced *IL-8, IL-1a*, and *IL-6* expression and release. These findings were not due to cytotoxic effects of PHCl (Figure 3.5). Modulation of the TR146 cell immune response by PHCl suggests the involvement of muscarinic receptor controlled signaling pathways which remain to be elucidated. Furthermore, as PHCl is a general muscarinic receptor, further investigations using specific muscarinic receptor agonists/antagonists are needed to characterise the specific subtypes of muscarinic receptor involved in mediating this response.

As discussed previously, the use of the TR146 cell line in host-*Candida* interaction studies has it's limitations. Therefore, even though it is more expensive and time consuming, using 3D HOE tissue compensates for cell line disadvantages and better imitates *in vivo* tissue. Furthermore, a more holistic

approach to determining the effects of PHCl on innate immune response regulation was taken in this study by employing RT-profiler analysis, which allowed simultaneous investigation of the expression of 11 genes previously reported to be involved in the innate immune response to *C. albicans* infection. Furthermore, immunohistological analysis facilitated investigations into the interaction between the host tissue and *C. albicans* during early infection events. The data in this chapter shows that, as observed with the TR146 cell line, live *C. albicans* stimulates upregulated expression of *IL-6, IL-1*α and *IL-8* (*CXCL8*), from HOE tissue and this is inhibited by treatment with PHCl. Furthermore, the LDH cytotoxicity results suggest that the effect of PHCl on *C. albicans* induced chemokine and cytokine expression in HOE tissue is due to a specific mechanism rather than any cytotoxic effect of PHCl administration. The RT^2 profiler analysis also revealed that *C. albicans*, in addition to *IL-6, IL-8* and *IL-1*α*,* also induced upregulated expression of the *GM-CSF* and *G-CSF* genes in HOE tissue which were once again inhibited by administration of PHCl.

Granulocyte- colony stimulating factor (G-CSF) and granulocyte macrophage-colony stimulating factor (GM-CSF) are members of the colony stimulating factor (CSF) family of cytokines. They are homodimeric cytokines essential to overall immune competence. Granulocyte- colony stimulating factor (G-CSF) promotes the growth, differentiation, survival and function of neutrophils. G-CSF promotes neutrophil recruitment and protects against infections in non myeloid malignancy patients (Flaherty, 2012, Trapnell and Abe, 2006). Literature has demonstrated that deficient mice lacking G-CSF or both G-CSF and IL-6 have chronic neutropenia and decreased neutrophil mobilization and increased susceptibility to *C. albicans* infection. (Lieschke et al., 1994, Wan et al., 2015, Basu et al., 2008). Furthermore a study by Gaviria et al. (1999) reported that administration of G-CSF to healthy human volunteers enhanced neutrophil-mediated activity against *C. albicans* pseudohyphae.

Granulocyte macrophage- colony stimulating factors (GM-CSF) stimulates growth of myeloid progenitors as well as the survival and function of neutrophils and macrophages (Flaherty, 2012, Trapnell and Abe, 2006). Interestingly, both G-CSF and GM-CSF immunomodulatory therapies have been considered for treatment of invasive fungal disease. Although they did not directly result in improvements in

invasive fungal disease occurrence and mortality, they were found to enhance some patients' recovery process (Sam et al., 2018).However, Wan et al. (2015), reported that using GM-CSF as prophylactic therapy in patients with neutropenia decreased invasive fungal disease by promoting neutrophil migration to the site of infection. In addition, GM-CSF can enhance neutrophils expression of CD64, ICAM-1, and complementary receptors CR-1 and CR-3 and thus promote phagocytosis (Bober et al., 1995). Another study by Mehta et al. (2015) reported that GM-CSF also increased neutrophils cytotoxicity capabilities to eradicate *C. albicans*.

The data reported in this chapter showed that *C. albicans* mainly stimulated a number of pro-inflammatory and regulatory chemokines and cytokines which enhance antifungal activity by recruiting and activating immune cells, such as polymorphonuclear leukocytes (PMNs) and macrophages (Kurzai, 2013, Feller et al., 2014). However, the RT^2 profiler analysis showed no significant changes in expression of cathelicidin antimicrobial peptide (*CAMP*) or C-type lectin domain family 7 member A (*CLEC7A*). *CAMP* plays a role in direct pathogen killing through phagocytosis and regulates pro and anti-inflammatory immune responses (Lowry et al., 2014, Raker et al., 2016). In contrast to data reported here, *CAMP* was found to be expressed and upregulated by different immune cells when stimulated with *C. albicans* (Chromek et al., 2006, López-García et al., 2005, Lowry et al., 2014, Rivas-Santiago et al., 2008). Expression of *CLEC7A* (Dectin 1), a C-type lectin domain that acts as a recognition receptor for fungal ß-glucan, was shown to be down regulated during *C. albicans* infection of the oral epithelium (Moyes et al., 2014). This finding highlights the suggestion proposed that the *C. albicans*-induced immune response was instigated by factors other than ß-glucan exposure, such as candidalysin (Naglik et al., 2019). Interestingly, expression of *TLR2* that detects fungal mannan, was demonstrated to be upregulated by PMA treatment compared to *C. albicans* stimulated and unstimulated HOE tissue. In addition, it was downregulated by PHCl at a concentration of 50 mM. On the other hand, *TLR4* expression was not modulated under any of the conditions investigated. The data reported here therefore suggests that *C. albicans* may have developed a strategy to circumvent recognition by host PRRs which has been reported before in several studies. For example, cell wall remodelling upon exposure to environmental stress, *C.*

albicans filamentation can eventually lead to macrophages piercing. Another example is changing or shielding PAMP structure such as shielding β-glucan by the outer cell wall which prevents recognition by host immune cells (Bourgeois and Kuchler, 2012, Cheng et al., 2012).

In agreements to a study reported by Lu et al. (2006), the immunostaining data presented in this chapter clearly showed that damage occurred in HOE tissue when infected with *C. albicans* and was associated with fungal growth and hyphae formation. The observed damage presented as detachment of cell layers. On the other hand, no visible damage was observed in infected, as well as uninfected, HOE tissue when treated with PHCl. Treatment with different concentrations of PHCl afforded protection against *C. albicans* induced damage in a concentration dependent manner. Yet, the mechanism by which PHCl modulates the immune response, reduces tissue damage and inhibits hyphae formation is still to be investigated and elucidated in detail. Whether PHCl effect is via downregulating virulence known genes such as *ECE1*, which is known to contribute to immune cells damage, or via cholinergic pathways mediated by immune cell receptors require further investigations.

In conclusion, the findings presented in this chapter highlight the crucial role of *C. albicans* morphogenesis in inducing a pro-inflammatory immune response. Furthermore, PHCl afforded protection against *C. albicans* infection to oral cells and tissues by inhibiting the yeast-hyphae transition and down regulation of innate immune responses. This study suggests, therefore, that muscarinic receptors on oral epithelial cells may modulate the host response to infection. Yet, the data herein do not dictate if the downregulation effect of the inflammatory immune response is due to the inhibition of yeast to hyphae transition in the presence of PHCl or due to direct effect of PHCl on the muscarinic receptors of tissues and mucosal cells. This requires further investigations to understand the specific receptors and signaling mechanisms by which PHCl can regulate the inflammatory response of mucosal cells and tissues.

Key summary points:

- Heat-killed *C. albicans* failed to induce a significant immune response against *C. albicans* infection.

- Live *C. albicans* significantly induced an innate immune response by the TR146 cell line and HOE tissue.

- The yeast-to-hyphae transition is a crucial process for initiation of an innate immune response by host mucosal tissues. PHCl could inhibit the *C. albicans* stimulated innate immune response and prevented extensive tissue damage.

4 Molecular regulation of *Candida albicans* virulence factors

4.1 Introduction

Even though the normal relationship of *C. albicans* within the human is thought to be commensalism, the ability of the microorganism to cause potent disseminated disease is a clear indication that it's property as a pathogen often outshines it's commensal properties (Dadar et al., 2018, Mayer et al., 2013). *C. albicans* is polymorphic in nature, occurring in a unicellular yeast form, as hyphae, pseudo-hyphae, or as a chlamydospore (Mayer et al., 2013, Neville et al., 2015). Phenotypic switching is a process undertaken by *C. albicans* in order to respond to various stressors and is important for the establishment of commensalism or pathogenesis (Neville et al., 2015). Morphological switching has been identified as the key factor that dictates the primary phases of host invasion, growth and propagation. Subsequently, the morphology, metabolism and transcriptome of *C. albicans* may also be transformed, despite the fact that the colonizing cells often present as a yeast (Dadar et al., 2018, Mba and Nweze, 2020).

The production of hyphae by *C. albicans* is an important indicator of biofilm formation and is considered a major virulence factor (Romo et al., 2019, Wall et al., 2019). Different sets of genes are expressed through the various stages of the biofilm formation process. For instance, during hyphal formation, *ALS3* and *HWP1* are predominantly expressed to facilitate cell adhesion. The proteases (*SAPs* 1−10) and phospholipase genes are also predominantly expressed to promote hyphal invasion of host tissues (Chong et al., 2018). At this stage, treating the infection with antifungals is problematic due to the resistance characteristics of biofilms. Antifungal tolerance by *Candida* biofilms is considered as multifactorial and it varies based on the biofilm phase. For instance, during early stages, the efflux pump activity contributes to tolerance, while during the maturation stages, this is more associated with persister cells and formation of an extracellular matrix consisting of ß-1,3 glucan and extracellular DNA (Taff et al., 2013). The steady growth in the number of antifungal drugs to help in the management of these infections has also influenced the occurrence of selection pressures with consequent resistance of the *Candida* spp. For example, use of azoles such as fluconazole for prophylaxis contributed to the increase of non- *albicans* candidemia patients. In addition,

the continued use of 3rd generation cephalosporins was associated with neonatal candidemia caused by *C. parapsilosis* in infants (Fu et al., 2017).

Unraveling the genetic processes that influence commensalism and pathogenicity in *C. albicans* could possibly facilitate the development of novel drug-based strategies to help in reducing or eliminating the risks associated with the *C. albicans* infections among immunocompromised individuals (Chen and Huang, 2018, Neville et al., 2015). In previous studies, ACh and PHCl (a general muscarinic receptor agonist) have shown to have an inhibitory effect on *C. albicans* biofilm formation and virulence (Nile et al., 2019, Rajendran et al., 2015). Yet, the molecular mechanism by which these compounds function as inhibitors of biofilm formation remain unknown. Therefore, high-throughput transcriptome sequencing (RNA-Seq) was employed to investigate changes in the transcriptional profile of *C. albicans* in the presence and absence of these compounds.

The *Candida* genome database (CGD) contains information about approximately 6400 genes and allows for the evaluation and assessment of genomic sequence data, as well as providing manually curated evidence as to the functionality of genes and proteins expressed by *C. albicans*. The CGD can, therefore, be used to comprehensively understand the molecular behavior of *C. albicans* and to develop molecular-based strategies for managing it's health impacts. So far, numerous genes have been catalogued which are vital for *C. albicans* survival in the host; such as secreted aspartyl proteinase (*SAP*) genes, secreted lipase (*LIP*) genes, agglutinin (*ALS*) genes and genes involved in iron assimilation. However, more than 1000 *C. albicans* genes are of unknown function with no obvious ortholog in the yeast *Schizosaccharomyces* or the fungus *S. cerevisiae*. These genes may also play important roles in host pathogen interactions and infection (Arnaud et al., 2005, Odds et al., 2004, database, 2004-2021). Of interest to this research is the morphological transformation inhibition in *C. albicans* by PHCl and ACh, which implies the presence of functional cholinergic receptor(s). Additionally, the *C. albicans* genome sequencing data indicate that *C. albicans* possesses genes responsible for ACh synthesis; the carnitine acetyltransferase gene (*CrAT*) and the choline acetyltransferase gene (*ChAT*) (Borghi et al., 2015, Rajendran et al., 2015). This therefore infers that *C. albicans* possesses more

complex cholinergic machinery and has the ability to synthesis and respond to cholinergic signals which have yet to be investigated.

Hypothesis and aims:

Significant inhibition of filamentation and biofilm formation was observed when *C. albicans* was treated with PHCl and ACh. Hence, it is hypothesized that PHCl and ACh treatment influence pathogenesis through downregulating hyphal growth and biofilm formation and this effect is mediated through an as yet uncharacterized receptor. To address the hypothetical question in this study accurately, we used RNA sequencing (RNA-seq) to investigate the impact of PHCl and ACh on the whole transcriptome of *C. albicans* and understands better how these compounds inhibit biofilm formation.

The aims of this chapter is:

- Explore the differential regulation of virulence genes during PHCl and ACh treatment.

- Understand the molecular regulation of *C. albicans* virulence factors under the investigated conditions.

- Explore unannotated genes that could potentially aid in characterizing potential receptors that modulate biofilm formation in response to PHCl and ACh.

- Attempt to unravel the signaling pathways mediating the inhibitory effects of PHCl and ACh.

4.2 Materials and Methods

4.2.1 Biofilm growth and experiment set up

The wild type laboratory strain SC5314 was used in this study. *C. albicans* was sub-cultured on Sabouraud dextrose agar (SDA) (Sigma-Aldrich, Dorset, UK) media and plates were stored at 4°C after incubation for 48 hours at 30°C. Every 2 – 3 weeks, *C. albicans* was transferred on to fresh SDA agar plates. Prior to conducting experiments, one colony of *C. albicans* was suspended in yeast extract - peptone - dextrose medium (YPD) (Sigma-Aldrich, Dorset, UK) and incubated overnight (16 – 18 hours) at 37°C using an orbital shaking aerobic incubator set at 200 rpm and 30°C. Cells from overnight broths were then washed by centrifugation at 3000 rpm for 5 minutes in phosphate buffered saline (PBS) (Sigma-Aldrich, Gillingham, UK) and cells were counted on a haemocytometer and re-suspended to a final concentration of 1 x 10^6 CFU/mL in RPMI-1640 media (Sigma-Aldrich, Dorset, UK) (Rajendran et al., 2015). Following standardisation, *C. albicans* was cultured for 4 and 24 hours in T75 cell culture flasks in the presence and absence of PHCl and ACh at concentrations of 5 and 25 mM. Untreated cells were used as control. The experiment was performed on at least 3 independent occasions.

At each time point, media was removed and cells were washed with PBS prior to addition of 1 mL RNA*later* (Thermo Fisher®, USA). Cells were then scraped into suspension, which was subsequently transferred to a sterile microcentrifuge tube and stored at – 80°C.

4.2.2 RNA extraction

RNA extraction was performed using the RiboPure™ Yeast RNA Extraction Kit (ThermoFisher, CA, USA) according to the manufacturer's instructions. The experimental pipeline is summarized in Figure 4.1. Briefly, bead beating tubes were prepared with 750 µl beads in advance, then RNA samples were centrifuged at full speed for 10 minutes. Supernatant was discarded without disturbing the pellet. Samples were then resuspended in lysis reagent which includes 480 µl lysis buffer, 48 µl of 10% SDS, and 480 µl phenol:chloroform:IAA and vortexed for 10 – 15 seconds. Next, the mixture of cells and lysis reagents was transferred to

the prepared bead beating tubes. Cells were vortexed in the bead beater using a BeadBug™ 3 Position Bead Homogenizer (Benchmark scientific, USA) vigorously at 350 rpm for 3 cycles × 60 seconds to lyse the yeast cells. In between beating cycles, samples were stored on ice. Samples were next centrifuged at 16,100 x g at room temperature for 5 minutes to separate the aqueous phase containing the RNA from the organic phase. The aqueous phase was then transferred to fresh falcon conical 15 mL tubes. Then, for final RNA purification, 1.9 mL binding buffer was added to each sample of aqueous phase collected previously and mixed thoroughly. Then, 1.25 mL of 100% ethanol was added to the mixture and mixed thoroughly. In a collection tube, 700 µl of the mixture was applied to a Filter Cartridge. This step required to be repeated several times for application of the whole sample volume. Samples were centrifuged for 1 minute until the mixture passed through the filter into the collection tube and the flow through discarded. Filters were then washed with 700 µl wash solution 1 by centrifugation for 1-minute and the flow- through discarded. Another 2 washing steps were conducted using 500 µl wash solution 2/3 and the flow through was discarded. Samples were next centrifuged for 1 minute to remove any excess wash solution. Filters were then transferred to a new 2 mL collection tube. Preheated elution solution was applied to the centre of the filters at a volume of 45 µl in two steps to elute RNA. Samples were centrifuged for 1 minute to collect eluted RNA into collection tubes. Quality and quantity of extracted RNA were assessed using a Bioanalyser (Aligent, USA) with a minimum quantity of 2.5 µg and minimum integrity number (RIN) = 7.0 for each sample.

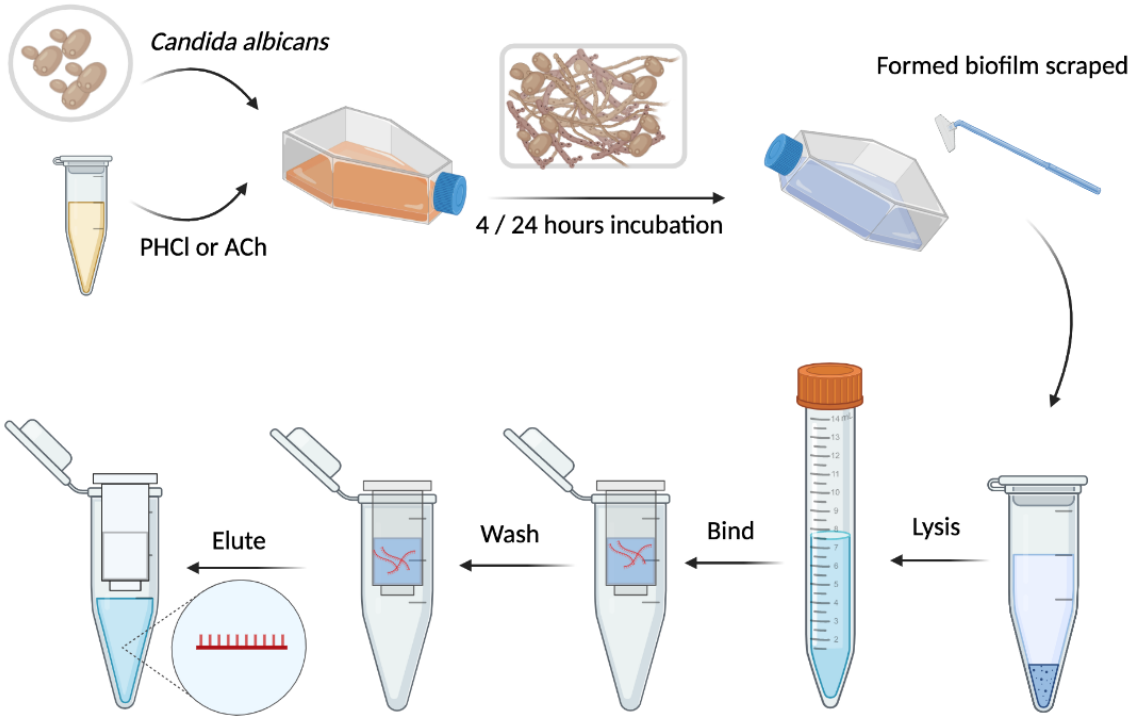

Figure 4.1 Experimental pipeline. *C. albicans* incubated with 25 and 5 mM PHCl or ACh in RPMI and cultured for 4 or 24h in a T75 cell culture flask. Biofilm biomass was scraped into RNA later suspension for extraction. Extractions were preformed following manufacturers' instructions. First, biofilm cells were lysed using zirconia beads, then RNA was purified and bound to spin columns and contaminants were washed using manufacturers buffers. Finally, RNA was eluted using 100µL nuclease free water. Image was created using BioRender.

4.2.3 RNA sequencing

Extracted RNA sequencing was performed by Edinburgh Genomics (genomics.ed.ac.uk) using a NovaSeq 6000 platform and produced 100 bp paired end reads. FastQC was used to assess sequence data quality and produce quality control scores for the produced reads (Wingett and Andrews, 2018). This process was followed by trimming and filtering poor quality reads, adapters, and primers using TrimGalore(Javorka et al., 2019). Then, HISAT2 was used to align and map the reads to a reference *C. albicans* genome (candidagenomedatabase.org) (Kim et al., 2019). FeatureCounts was used to count the number of reads that were aligned to a specific gene (Liao et al., 2014). A FeatureCounts table was gathered and subsequently read into RStudio (version 3.6.3). Differentially expressed genes for pairwise comparisons were analysed using DESeq2 package (Costa-Silva et al., 2017). The Bioinformatics pipeline is summarised in (Figure 4.2). Quality control, sequence trimming, read alignment and enumeration were performed with the assistance of Dr. Christopher Delaney (University of Glasgow).

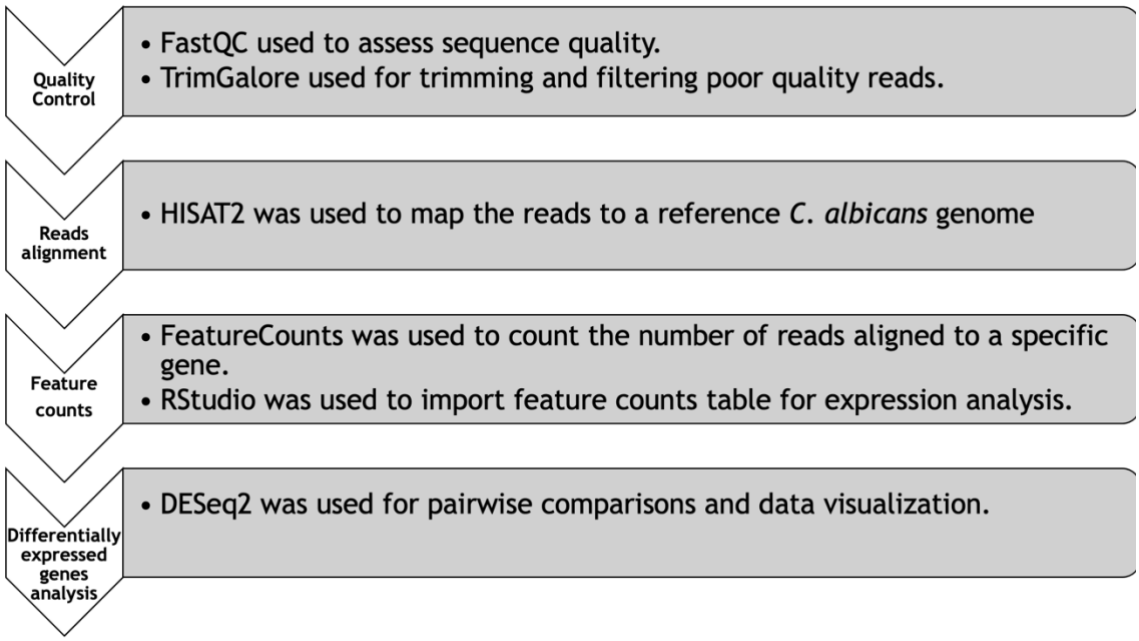

Figure 4.2 Bioinformatic analysis pipeline. The schematic shows the bioinformatics pipeline used for the RNA-seq data analysis. First, sequences were assessed and trimmed to achieve high quality reads. Reads were aligned to a reference *C. albicans* genome, and the number of aligned genes were counted. Then, differentially expressed genes were analysed using DSeq2.

4.2.4Statistical analysis

Figures in this chapter were produced using different packages in Rstudio to visualize differential gene expression analysis (Figure 4.2). Pairwise comparisons were performed between samples considering the variables of incubation time and concentration of treatments using the DESeq2 package. Genes were considered significantly differentially expressed between both conditions when the cut off of $\log_2$ fold change ($\log_2$FC) ≥1.5 and p-value of ≤0.01 were met. Following that, ClueGo application in Cytoscape (v3.7.2) (cytoscape.com) was used to display gene interaction networks. ClueGO (v2.5.7) plugin was used to annotate and group the genes functionally using gene ontology (GO) into categories represented by the most significant term using the hypergeometric test. Functional categories were considered enriched when the adjusted p-value was ≤0.05. ClueGO genes interaction networks were grouped by function, taking into account their three gene ontology (GO) terms; molecular functions (MF), cellular components (CC) and biological processes (BP) (Bindea et al., 2009, Shannon et al., 2003).

4.3 Results

4.3.1 Principal component analysis

Whole transcriptomic sequencing was performed to investigate the differences in gene expression when *C. albicans* was treated with 5 and 25 mM PHCl and ACh for 4 and 24 hours. Conditions chosen for transcriptomic analysis were based on the findings from previous work investigating the effect of ACh and PHCl on *C. albicans* viability and biofilm formation at different concentrations. Preliminary data from xCELLigenece real time analysis showed that growth curve exhibits irregularities after 4-5 hours of incubation. The concentration 25 mM had an effective inhibitory effect and 5 mM also was used to investigate the minimum effect by the treatment. In addition, significant downregulation of genes such as *ALS3* and *HWP1* in *C. albicans* was also observed at 4 and 24 hours by ACh. The two compounds (ACh and PHCl) were used to gain better understanding of the differences and similarities of the molecular basis behind their inhibitory effect which may aid in characterizing the potential receptor(s). Acquired sequenced data were processed for differential expression (DE) analysis to identify gene expression changes between different conditions. Multivariate analysis using principal component analysis (PCA) showed that the first most important variance between samples was by 67% based on time of incubation (4 hours and 24 hours), where the second most important variance between samples was by 9% due to different treatment (ACh and PHCl). One Sample treated with 5 mM PHCl for 4 hours was excluded from the analysis due to failure to pass quality control criteria (Figure 4.3).

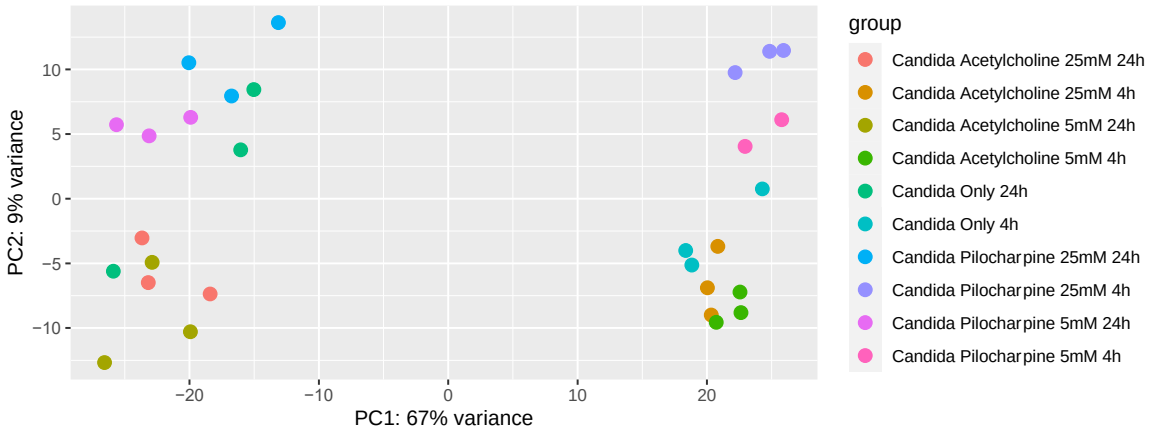

Figure 4.3 Principal component analysis. PCA plot shows first largest variance along PC1 (67%) by time of incubation and second largest variance along PC2 (9%) by different treatment.

4.3.2 Differential expression in response to PHCl treatment

Volcano plots revealed variations in *C. albicans* transcriptomic profile in the presence and absence of PHCl. Large numbers of differentially expressed genes have passed the Log_2 cut-offs of +1.5 and −1.5 after PHCl treatment. However, some failed to reach statistical significance. A number of differentially expressed genes increased at a concentration of 25 mM and time point 4 hours (Figure 4.4). Heatmaps show the top 50 differentially expressed genes with their relative expression in the presence and absence of the treatment. Many differentially expressed genes are uncharacterized and referred to by their gene ID (Figure 4.5).

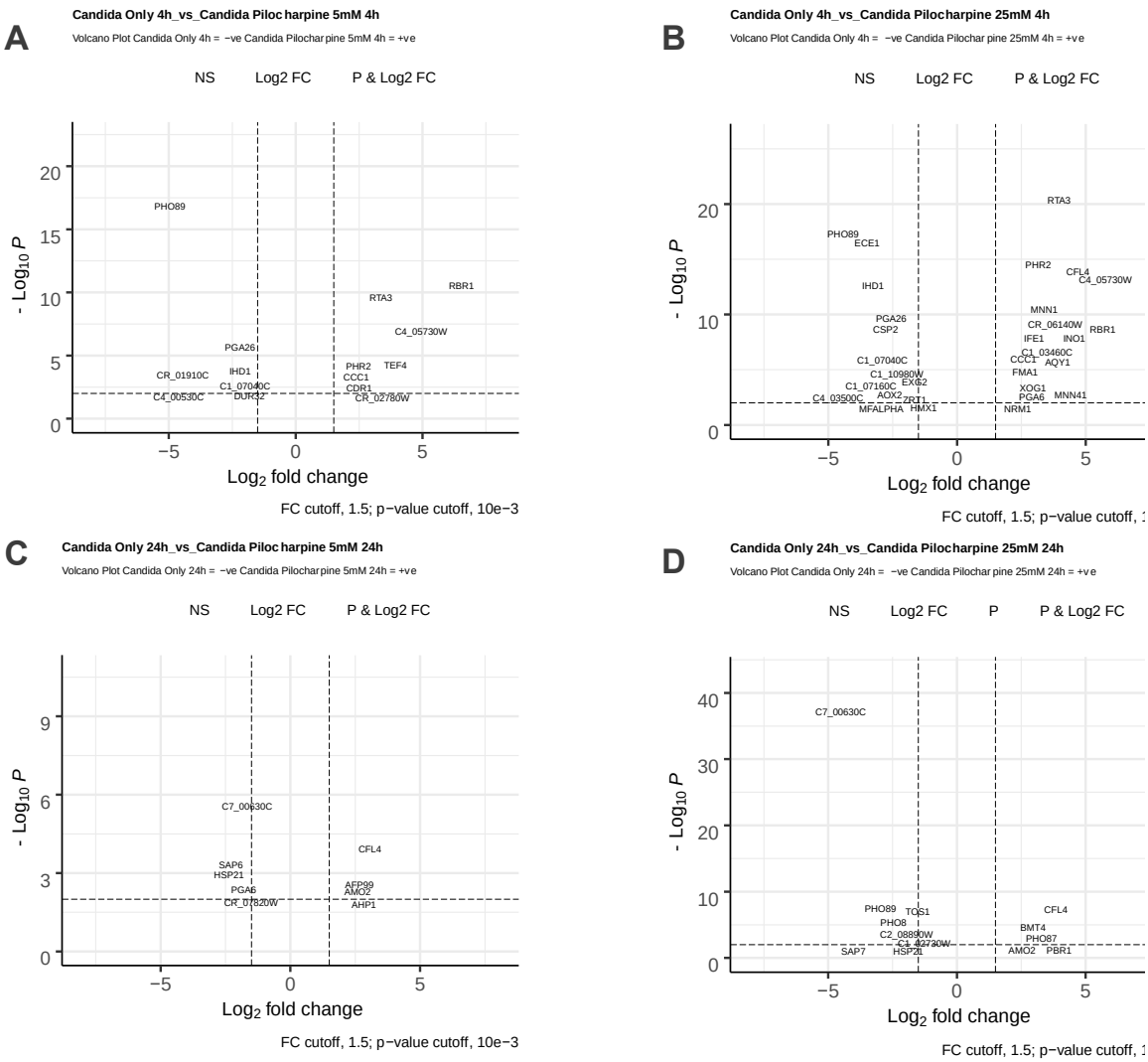

Figure 4.4 Volcano plots showing gene expression at different times in the presence of PHCl treatment. (A) transcriptional changes at 4 hours with 5 mM. (B) transcriptional changes at 4 hours with 25 mM. (C) transcriptional changes at 24 hours with 5 mM. (D) transcriptional changes at 24 hours with 25 mM. Upregulated genes in the presence of PHCl are represented by a +ve Log_2 fold

change and those upregulated in the absence of PHCl are represented with -ve Log_2 fold change. The increase in negative or positive values indicate a larger upregulation. The horizontal dotted lines indicate the cut-off p value < 0.01, (colours in blue or red). The vertical dotted lines indicate the cut-off of Log_2 fold change 1.5 (colours in green). Genes of interest that are significantly upregulated are the genes where expression levels are above or below the Log_2 fold change cut-offs; -1.5 and 1.5 and that are highly significant; P < 0.01.

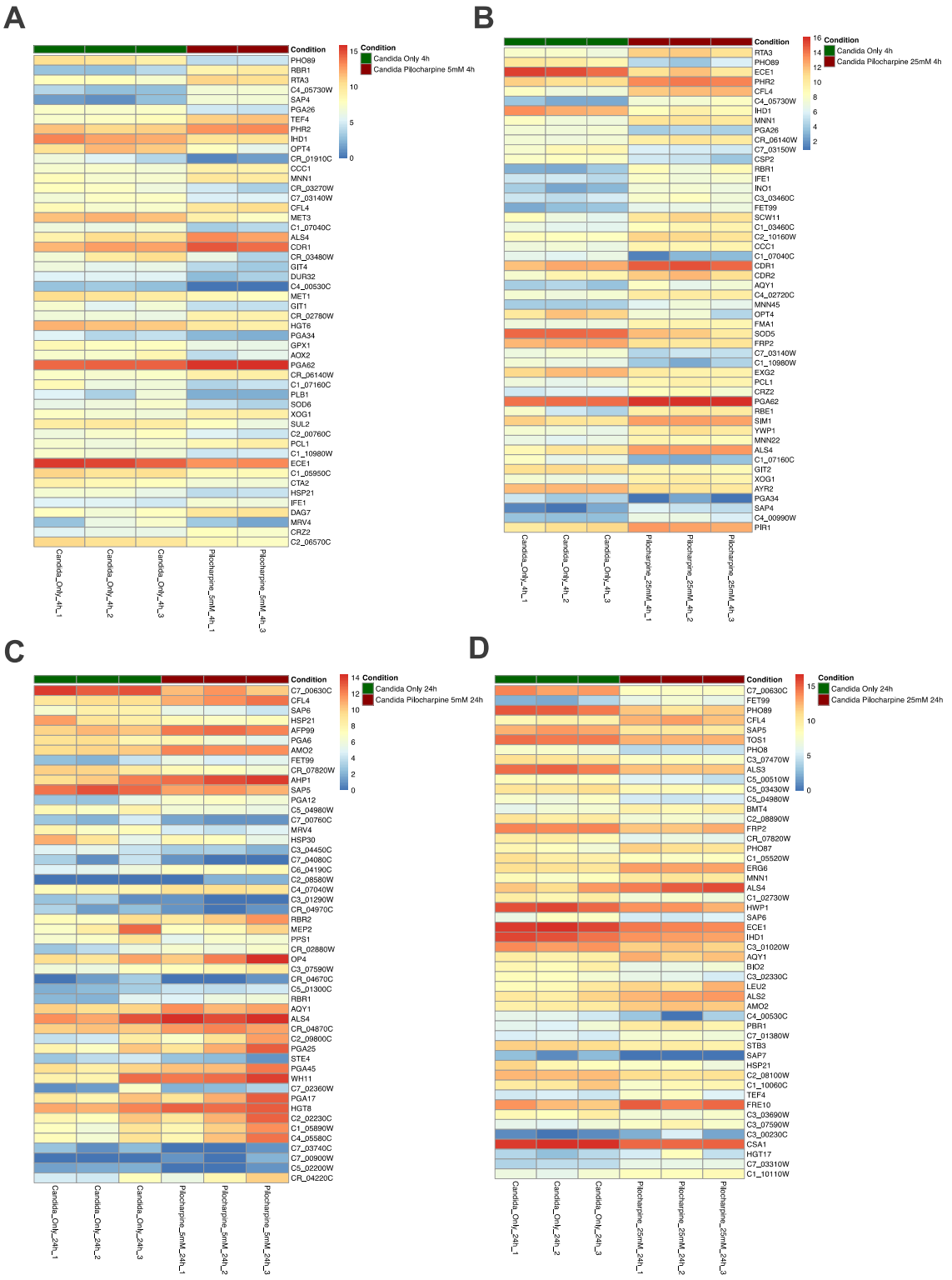

Figure 4.5 Heatmaps showing levels of relative gene expression at different times during treatment of *C. albicans* with different concentrations of PHCl. (A) transcriptional changes at 4 hours with 5 mM. (B) transcriptional changes at 4 hours with 25 mM. (C) transcriptional changes at 24 hours with 5 mM. (D) transcriptional changes at 24 hours with 25 mM. The colour key indicates level of relative expression under any of the conditions; the presence of PHCl treatment (red) and the absence (green).

4.3.3 Differences in gene regulation and influenced pathways in presence and absence of 5 mM PHCl at 4 hours of biofilm formation

Differential expression analysis revealed that *C. albicans* cells treated with 5 mM PHCl resulted in the significant upregulation of 20 genes such as *RBR1, RTA3, TEF4, PHR2, CCC1,* and *CDR1.* In addition, 39 genes were significantly downregulated including: *PHO89, PGA26, IHD1,* and *DUR32* (Figure 4.4 A and 4.5 A). Each gene encodes a specific protein that is responsible for a biological process detailed in (Table 4.1) and in appendix IV materials (Table 1). Differences in gene regulation in the presence and absence of PHCl were further investigated by determining the pathways that are influenced by the treatment. GlueGO plugin in Cytoscape was used to calculate and visualize the networks of functionally enriched pathways. Gene interaction networks showed that 5 mM of PHCl at 4 hours resulted in a differential expression of genes that are involved in several biological processes and among the highly regulated were pathogenesis related terms ($P < 0.0005$), sulfur compound biosynthetic processes ($P < 0.005 - 0.05$), response to temperature ($P < 0.005 - 0.05$), transmembrane transporter activities ($P < 0.005 - 0.1$) and interaction with host and cellular metal ion homeostasis ($P < 0.05 - 0.1$). The transcription profile of *C. albicans* when treated with 5 mM PHCl at 4 hours revealed that cellular metal ion homeostasis and cell substrate adhesion processes were upregulated. Furthermore, biological functions such as, transmembrane transporter activities, interaction with host, sulfur biosynthetic and metabolic, and pathogenesis were downregulated (Figure 4.6). Some genes were found to be implicated in regulating different biological functions in both directions. Upregulating *CCC1* resulted in upregulating cellular transition metal ion homeostasis and downregulating inorganic ion and cation transmembrane transporter activity. Downregulation of *HSP21* led to downregulation of pathogenesis and upregulation of response to temperature stimulus. Although *XOG1* upregulation resulted in cell substrate adhesion upregulation, it led to pathogenesis related terms downregulation. Upregulation of *ALS4* resulted in pathogenesis downregulation and upregulation of cell substrate adhesion and response to temperature.

Table 4.1 Top 10 up and top 10 down regulated genes by 5 mM PHCl treatment at 4 hours incubation. Table includes the common gene name, protein encoded description, the log_2 fold change (Log_2FC), and the P value.

Upregulated				Downregulated			
Gene Name	**Description**	**log_2FoldChange**	**Pvalue**	**Gene Name**	**Description**	**log_2FoldChange**	**Pvalue**
RBR1	Cell wall Glycosylphosphatidylinositol (GPI)-anchored protein.	6.03582729	7.72E-12	***C4_00530C_A***	Has domain(s) with predicted hydrolase activity.	-5.6112984	0.00516969
SAP4	Secreted aspartyl proteinase.	5.28245456	1.29E-07	***PHO89***	Putative phosphate permease.	-5.5683292	4.13E-18
C4_05730W	Adhesin-like protein.	3.90808373	3.74E-08	***CR_01910C_A***	Putative dethiobiotin synthetase.	-5.4786513	9.18E-05

TEF4	Putative translation elongation factor.	3.47486637	1.68E-05	***C1_10810W_A***	Pry family pathogenesis-related protein.	-4.2040378	0.0476169
RTA3	7-transmembrane receptor protein.	2.9101507	7.26E-11	***CR_03480W_A***	Ortholog of C. dubliniensis CD36 : Cd36_28730, *Candida tropicalis* MYA-3404 : CTRG_00749 and WO-1 : CAWG_01683.	-4.1607032	0.00344461
ALS4	GPI-anchored adhesin.	2.8472063	0.0008538484	***OPT4***	Oligopeptide transporter	-4.0602241	7.89E-05
CFL4	C-terminus similar to ferric reductases.	2.60099245	0.0004769697	***PLB1***	Phospholipase B.	-3.9128041	0.01164346

DAG7	Secretory protein.	2.40198804	0.0229246	***MRV4***	Protein of unknown function.	-3.8581611	0.02642543
CR_02780W	Protein with similarity to carbonic anhydrases.	2.35071858	0.00694301	***CR_01920W_A***	Ortholog(s) have adenosylmethionine-8-amino-7-oxononanoate transaminase activity and role in biotin biosynthetic process	-3.3596944	0.03267073
MNN1	Putative alpha-1,3-mannosyltransferase	2.11858294	0.00021111	***C1_07160C_A***	Protein conserved among the CTG-clade.	-3.3182581	0.01145171

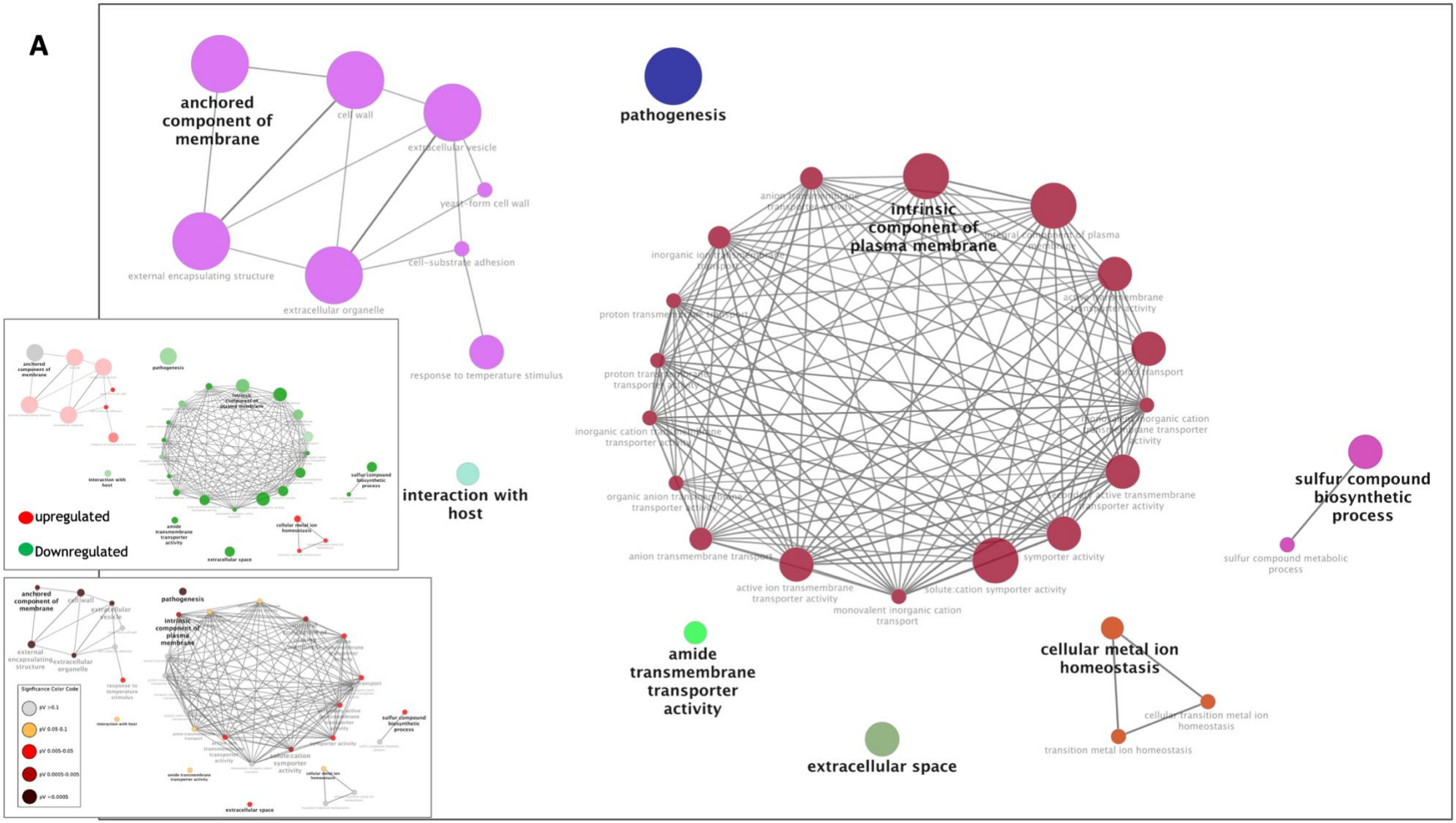
A
anchored component of membrane
cell wall
extracellular vesicle
yeast-form cell wall
cell-substrate adhesion
external encapsulating structure
extracellular organelle
response to temperature stimulus
pathogenesis
intrinsic component of plasma membrane
interaction with host
sulfur compound biosynthetic process
sulfur compound metabolic process
amide transmembrane transporter activity
cellular metal ion homeostasis
cellular transition metal ion homeostasis
transition metal ion homeostasis
extracellular space
anion transmembrane transporter activity
inorganic ion transmembrane transporter activity
proton transmembrane transporter activity
inorganic cation transmembrane transporter activity
organic anion transmembrane transporter activity
active transmembrane transporter activity
symporter activity
solute:cation symporter activity
active ion transmembrane transporter activity
monovalent inorganic cation transport
upregulated
Downregulated
Significance Color Code
pV >0.1
pV 0.05-0.1
pV 0.005-0.05
pV 0.0005-0.005
pV <0.0005

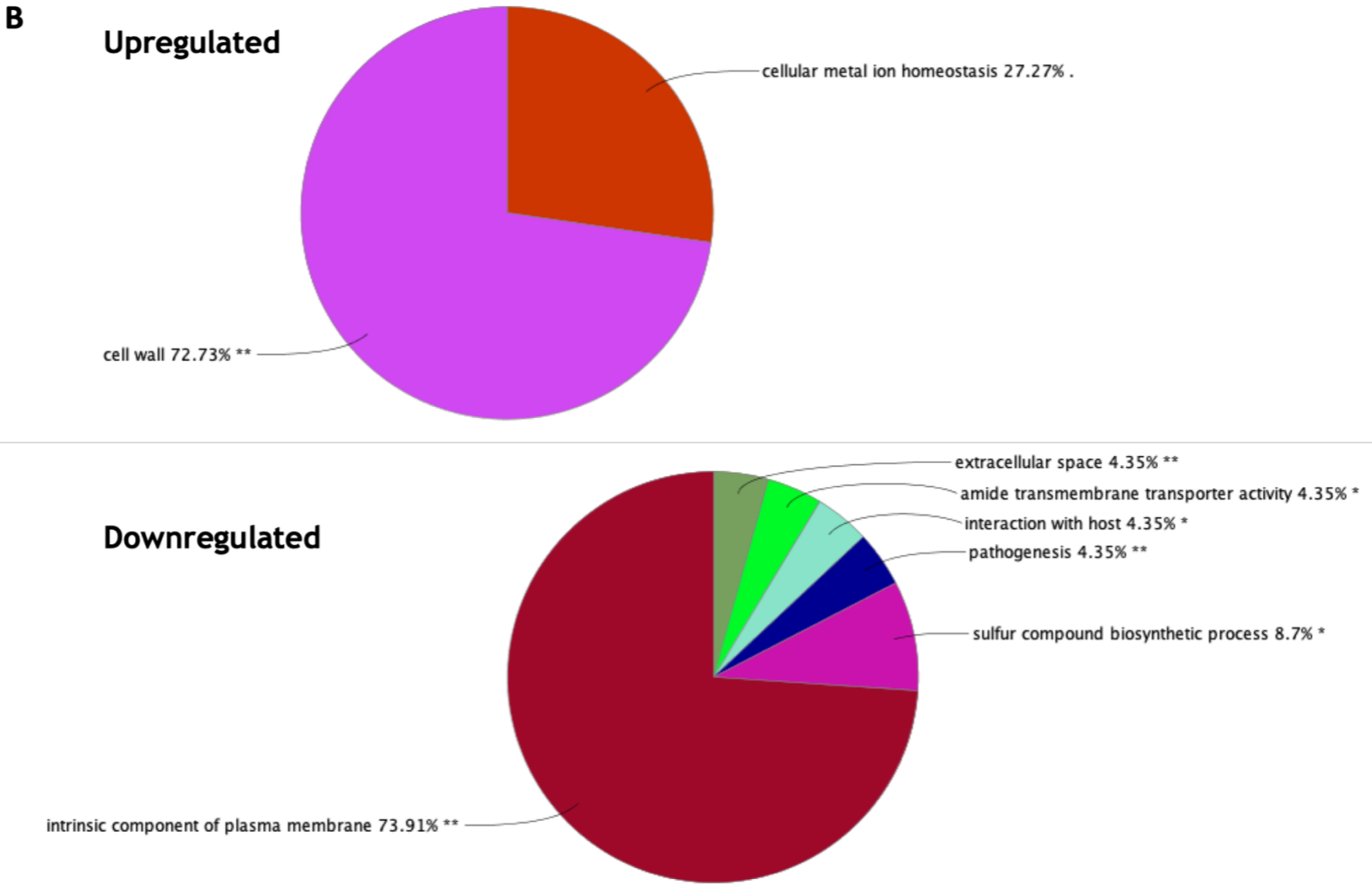
B
Upregulated
cellular metal ion homeostasis 27.27% .
cell wall 72.73% **
Downregulated
extracellular space 4.35% **
amide transmembrane transporter activity 4.35% *
interaction with host 4.35% *
pathogenesis 4.35% **
sulfur compound biosynthetic process 8.7% *
intrinsic component of plasma membrane 73.91% **

Figure 4.6 . ClueGO analysis of differential expressed genes and influenced pathways at 4 hours by 5 mM PHCl. Gene networks show the stimulated biological functions interactions and their pathways. Genes of similar function are grouped together to form nodes (circles). Nodes with similar functions are linked together by edges (lines) based upon their kappa score. (A) regulated genes composing groups of several biological functions and subnetworks related to different pathways. (B) Pie charts summarise the percentage of terms related to a specific subnetwork or biological function of pathways; colourised to illustrate the related subnetwork. Interaction Networks were created using ClueGO.

4.3.4 Differences in gene regulation and influenced pathways in presence and absence of 25 mM PHCl at 4 hours of biofilm formation

Increasing the concentration of PHCl to 25 mM at 4 hours resulted in a higher number of genes regulated; 68 genes were upregulated and 65 genes were downregulated. Similarly, heatmap and volcano plots showed that the genes *RTA3, PHR2, CFL4*, and other genes were significantly upregulated at 25 mM concentration, while *PHO89, PGA26, and IHD1* were amongst the most significant downregulated genes along with *ECE1* (Figure 4.4 B and 4.5 B). Each gene encodes a specific protein that is responsible for a biological process detailed in (Table 4.2) and in appendix IV materials (Table 2). ClueGO interaction networks analysis showed that 25 mM PHCl treatment revealed significant regulation of genes that are implicated in the following biological functions; pathogenesis, cell wall and external encapsulating structure organization, and cellular transition metal ion transport and homeostasis with the highest significance ($P < 0.0005$). Other biological functions are fungal type cell wall biogenesis, polysaccharide metabolic processes, response to temperature stimulus, lipid translocation, host defence evasion, biofilm formation, response to toxic substances, symbiotic processes, transmembrane transporter activity, and oxidoreductase activity (Figure 4.7). Genes involved in the following functions: Cell wall organization, response to temperature stimulus, polysaccharide metabolic process, lipid translocation, and iron ion transport were found to be upregulated by 25 mM PHCl at 4 hours. While other functions such as response to toxic substance and oxidative stress, oxidoreductase activity, pathogenesis, defenses evasion, symbiotic process, and transmembrane transporter activity were downregulated (Figure 4.7).

Table 4.2 Top 10 up and top 10 down regulated genes by 25 mM PHCl treatment at 4 hours incubation. Table includes the common gene name, protein encoded description, the log_2 fold change (Log_2FC), and the P value.

Upregulated				Downregulated			
Gene Name	**Description**	**log_2FoldChange**	**Pvalue**	**Gene Name**	**Description**	**log_2FoldChange**	**Pvalue**
RBR1	Cell wall Glycosylphosphatidylinositol (GPI)-anchored protein.	5.16110835	5.06E-10	***C4_03500C_A***	Protein of unknown function.	-5.601814	0.00077758
C4_05730W	Adhesin-like protein.	4.73815539	1.48E-14	***PHO89***	Putative phosphate permease.	-5.0379451	1.29E-18
CFL4	C-terminus similar to ferric reductases.	4.23719509	2.99E-15	***C4_00530C_A***	Has domain(s) with predicted hydrolase activity.	-4.5519024	0.01030596

INO1	Inositol-1-phosphate synthase.	4.12561257	3.60E-09	***CR_03480W_A***	Ortholog of C. dubliniensis CD36 : Cd36_28730, *Candida tropicalis* MYA-3404 : CTRG_00749 and WO-1 : CAWG_01683	-4.4695009	0.00033496
C2_06450C_A	Pseudogene.	3.9915129	0.04332982	***C1_07160C_A***	Protein conserved among the CTG-clade.	-4.3272547	7.26E-05
SAP4	Secreted aspartyl proteinase.	3.8138196	0.00021057	***OPT4***	Oligopeptide transporter.	-4.2596232	2.60E-06
MNN41	Ortholog(s) have enzyme activator activity and role in	3.78004819	0.00041898	***PLB1***	Phospholipase B.	-4.0805713	0.00288893

	protein N-linked glycosylation.						
RTA3	7-transmembrane receptor protein.	3.51680825	1.10E-21	***ECE1***	Candidalysin, cytolytic peptide.	-3.9800593	7.85E-18
FET99	Multicopper oxidase family protein.	3.49243986	2.11E-08	***PTR2***	Oligopeptide transporter involved in uptake of di-/tripeptides.	-3.9099938	0.001709
AQY1	Aquaporin water channel.	3.421532	5.07E-07	***FGR2***	Protein similar to phosphate transporters.	-3.9022027	0.00070297

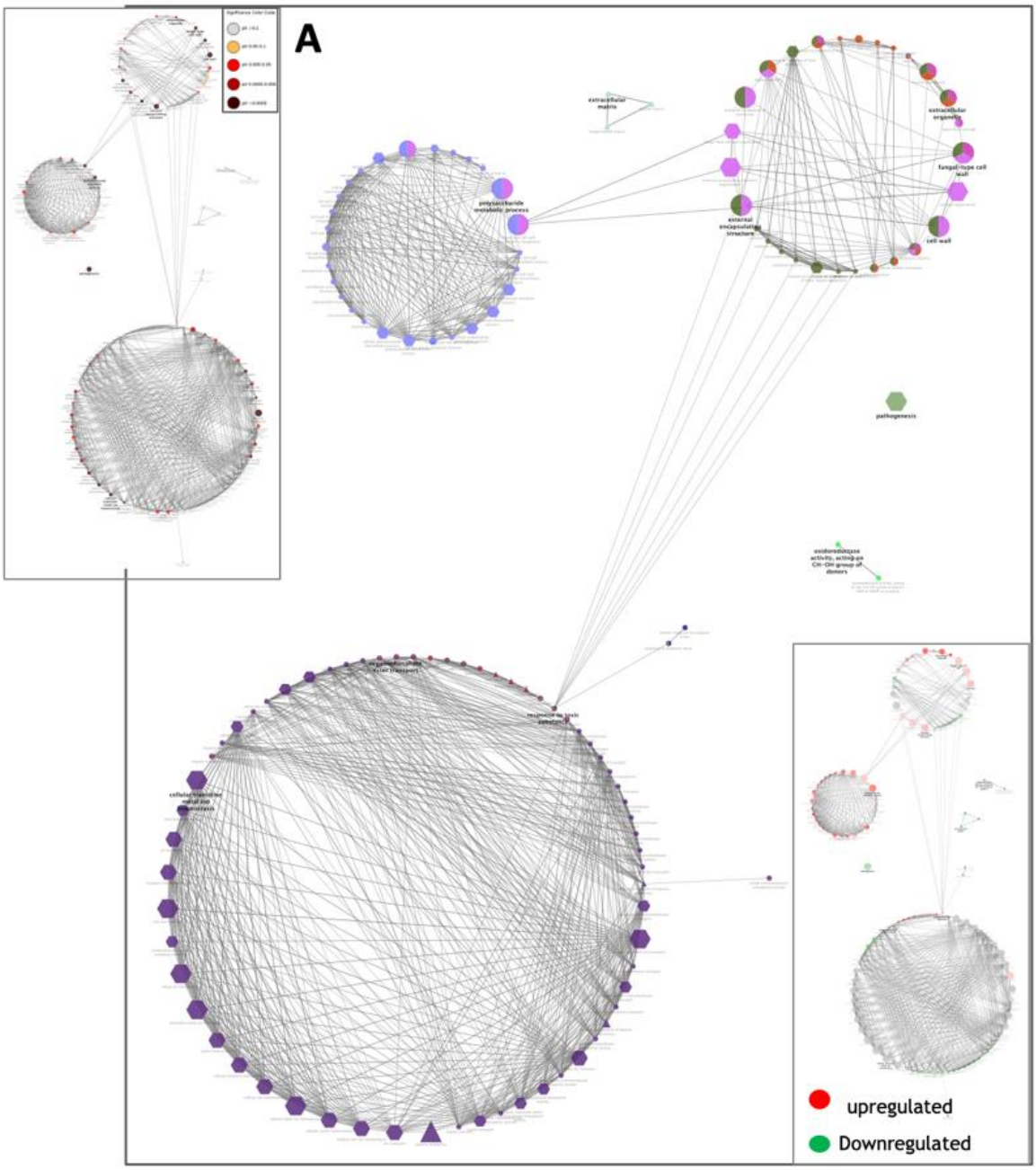
A
upregulated
Downregulated

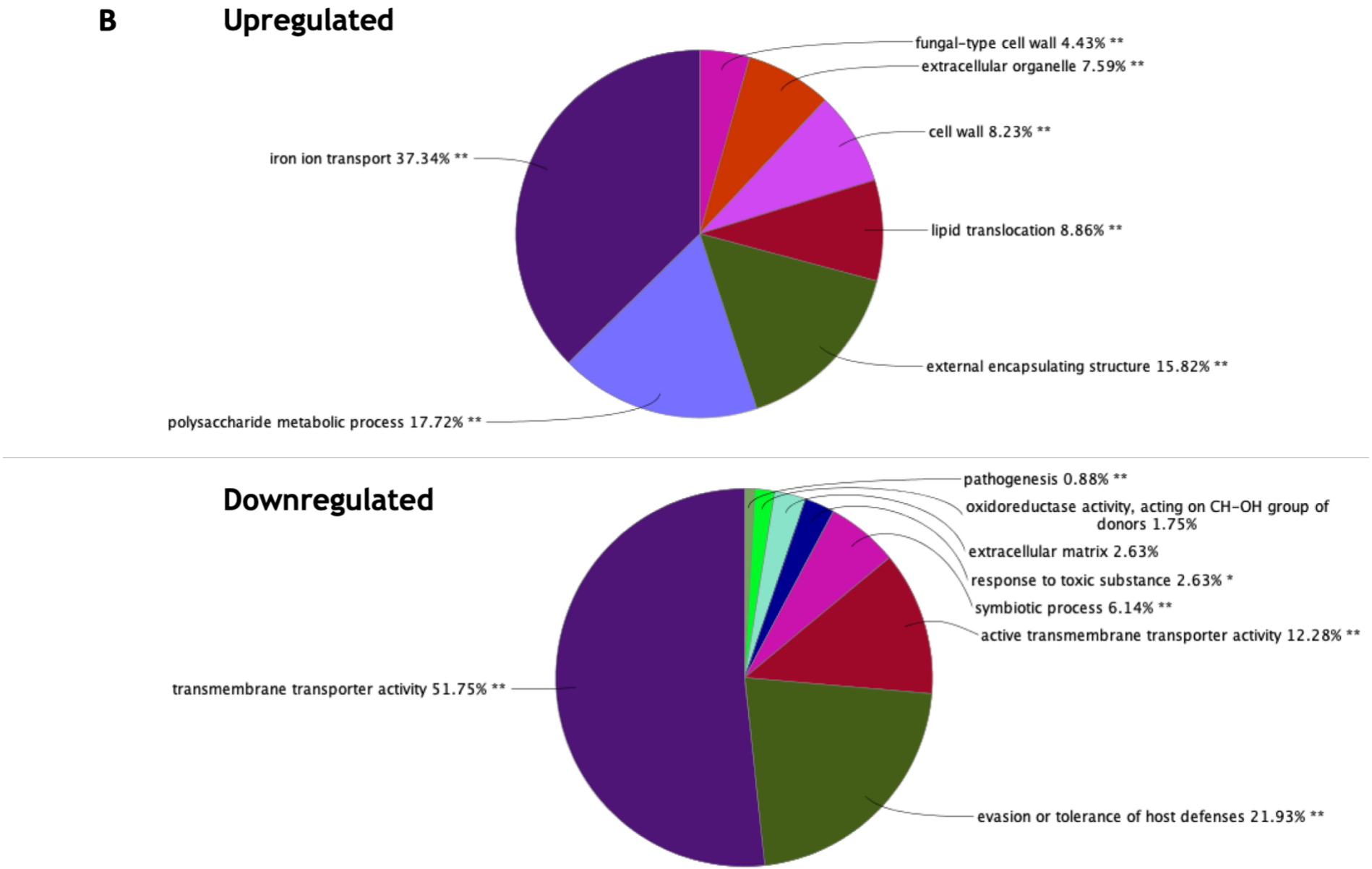
B
Upregulated
fungal-type cell wall 4.43% **
extracellular organelle 7.59% **
cell wall 8.23% **
iron ion transport 37.34% **
lipid translocation 8.86% **
external encapsulating structure 15.82% **
polysaccharide metabolic process 17.72% **
Downregulated
pathogenesis 0.88% **
oxidoreductase activity, acting on CH-OH group of donors 1.75%
extracellular matrix 2.63%
response to toxic substance 2.63% *
symbiotic process 6.14% **
active transmembrane transporter activity 12.28% **
transmembrane transporter activity 51.75% **
evasion or tolerance of host defenses 21.93% **

Figure 4.7 ClueGO analysis of differential expressed genes and influenced pathways at 4 hours by 25 mM PHCl. Gene networks show the stimulated biological functions interactions and their pathways. Genes of similar function are grouped together to form nodes (circles). Nodes with similar functions are linked together by edges (lines) based upon their kappa score. (A) regulated genes composing groups of several biological functions and subnetworks related to different pathways. (B) Pie charts summarise the percentage of terms related to a specific subnetwork or biological function of pathways; colourised to illustrate the related subnetwork. Interaction Networks were created using ClueGO.

4.3.5 Differences in gene regulation and influenced pathways in presence and absence of 5 mM PHCl at 24 hours of biofilm formation

At later stages of biofilm formation, analysis showed that 5 mM of PHCl treatment resulted in only 13 genes being significantly differentially expressed and regulated. Amongst the 6 upregulated genes are *CFL4, AFP99, AMO2*, and *AHP1* and the 7 downregulated genes are *C7_00630C, SAP6, HSP21, PGA6*, and *CR_07820W* (Figure 4.4 C and 4.5 C). Each gene encodes a specific protein that is responsible for a biological process detailed in Table 4.3. Gene interaction networks revealed that 5 mM of PHCl treatment resulted in the following biological processes to be differentially regulated; amine metabolic process, metal ion transition and homeostasis, copper ion binding were significantly upregulated ($P = 0.005 - 0.05$). In addition, aspartic type endopeptidase activity was downregulated with significance ($P = 0.0005 - 0.005$) (Figure 4.8).

Table 4.3 Top 10 up and top 10 down regulated genes by 5 mM PHCl treatment at 24 hours incubation. Table includes the common gene name, protein encoded description, the log_2 fold change (Log_2FC), and the P value.

Upregulated				Downregulated			
Gene Name	**Description**	**log_2FoldChange**	**Pvalue**	**Gene Name**	**Description**	**log_2FoldChange**	**Pvalue**
CFL4	C-terminus similar to ferric reductases.	2.62349212	6.82E-05	***HSP21***	Small heat shock protein; role in stress response and virulence.	-2.939976	0.00063296
PGA12	Putative GPI-anchored protein.	2.45511984	0.0324648	***SAP6***	Biofilm-specific aspartyl protease.	-2.7481664	0.00027105
AHP1	Alkyl hydroperoxide reductase.	2.35908698	0.00846874	***C7_00630C_A***	Putative protein of unknown function.	-2.6395121	1.57E-06

FET99	Multicopper oxidase family protein.	2.28856214	0.00680158	***CR_07820W_A***	Protein with monooxygenase domains.	-2.5536413	0.00726124
AFP99	Protein related to arginases.	2.11101229	0.00155799	***PGA6***	GPI-anchored cell wall adhesin-like protein.	-2.2867979	0.00244486
AMO2	Protein similar to A. niger predicted peroxisomal copper amino oxidase.	2.07365216	0.0028547	***SAP5***	Biofilm-specific aspartyl protease.	-1.6669787	0.03021878
				C5_04980W_A	Putative adhesin-like protein.	-1.6096709	0.03767064

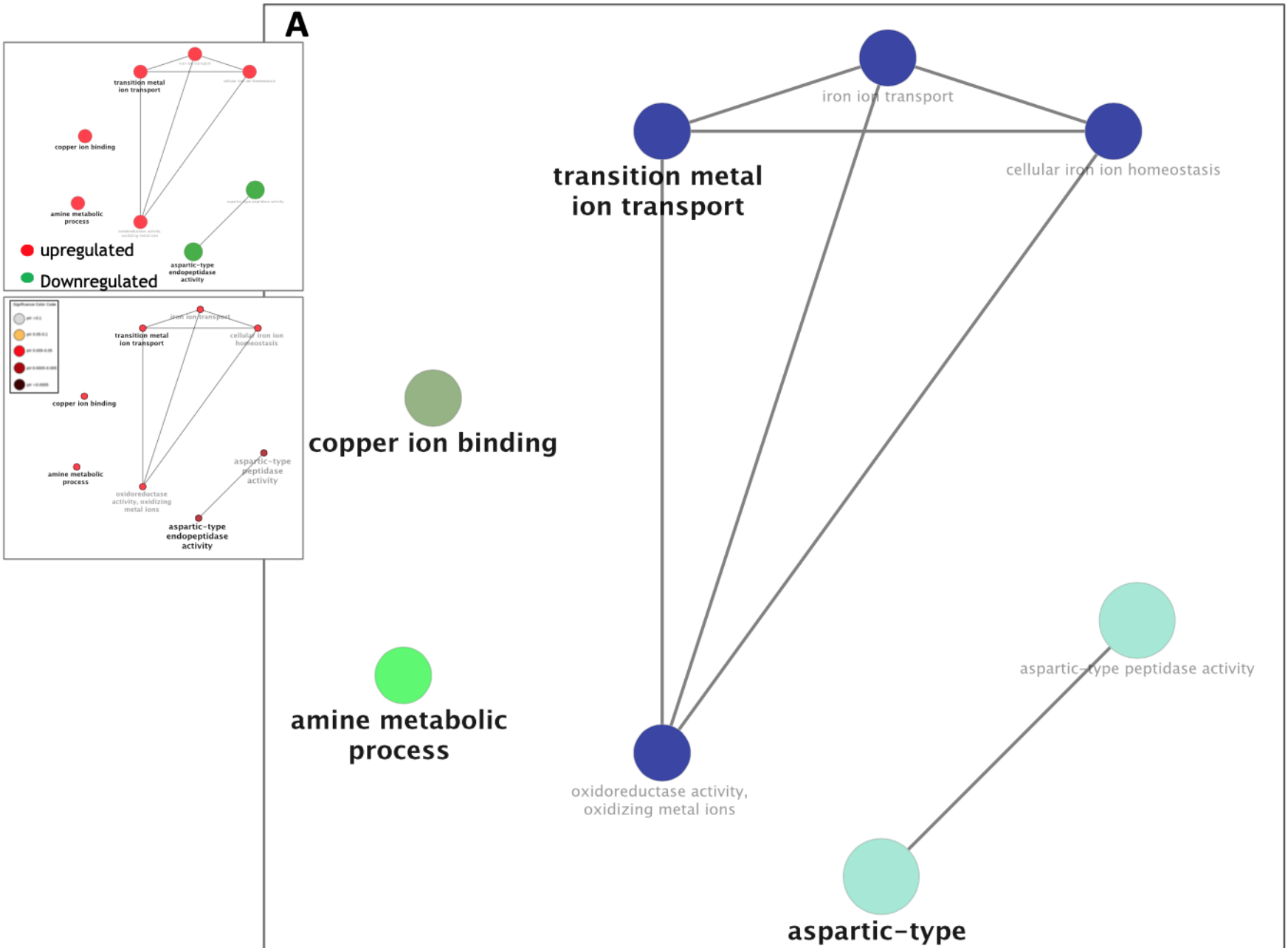
A
iron ion transport
transition metal ion transport
cellular iron ion homeostasis
copper ion binding
amine metabolic process
aspartic-type peptidase activity
oxidoreductase activity, oxidizing metal ions
aspartic-type
upregulated
Downregulated

B

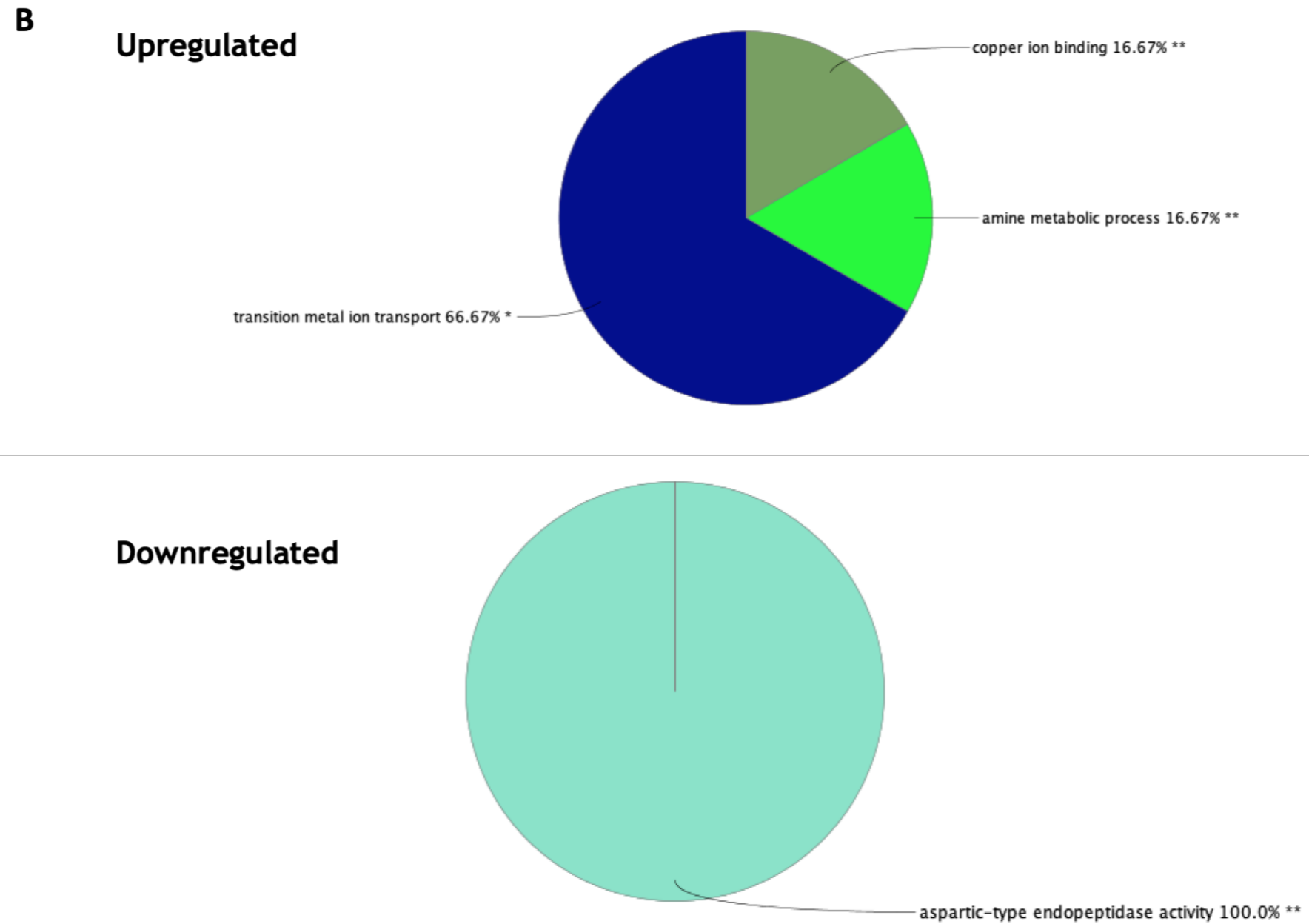
Upregulated
copper ion binding 16.67% **
amine metabolic process 16.67% **
transition metal ion transport 66.67% *
Downregulated
aspartic-type endopeptidase activity 100.0% **

Figure 4.8 ClueGO analysis of differential expressed genes and influenced pathways at 24 hours by 5 mM PHCl. Gene networks show the stimulated biological functions interactions and their pathways. Genes of similar function are grouped together to form nodes (circles). Nodes with similar functions are linked together by edges (lines) based upon their kappa score. (A) regulated genes composing groups of several biological functions and subnetworks related to different pathways. (B) Pie charts summarise the percentage of terms related to a specific subnetwork or biological function of pathways; colourised to illustrate the related subnetwork. Interaction Networks were created using ClueGO.

4.3.6 Differences in gene regulation and influenced pathways in presence and absence of 25 mM PHCl at 24 hours of biofilm formation

At a concentration of 25 mM PHCl, the volcano plot showed more genes to be differentially expressed. The upregulated genes totalled 30 and included *CFL4, BMT4, PHO87, PBR1,* and *AMO2* and the downregulated genes totalled 43 and included *PHO89, TOS1, PHO8, SAP7*, and *HSP21* (Figure 4.4 D and 4.5 D). Each gene encodes a specific protein that is responsible for a biological process detailed in (Table 4.4) and in Appendix IV (Table 3). Gene interaction network analysis revealed a different transcription profile and regulation of the following biological processes; oxidoreductase activity ($P < 0.0005$), cell wall organization ($P < 0.0005$), branched chain amino acid biosynthetic processes ($P = 0.005 - 0.05$) and ergosterol biosynthetic processes ($P = 0.05 - 0.1$) (Figure 4.8). Clustering interaction network analysis revealed that during the maturation stage, 25 mM PHCl resulted in downregulated cell wall organization and upregulated branched chain amino acid biosynthetic processes, oxidoreductase activity and ergosterol biosynthetic processes (Figure 4.8).

Table 4.4 Top 10 up and top 10 down regulated genes in response to 25 mM PHCl treatment at 24 hours. Table includes the common gene name, protein encoded description, the log_2 fold change (Log_2FC), and the P value.

Upregulated				**Downregulated**			
Gene Name	**Description**	**log_2FoldChange**	**Pvalue**	**Gene Name**	**Description**	**log_2FoldChange**	**Pvalue**
C3_00230C_A	Putative protein of unknown function.	4.73995336	0.0184308	***C7_00630C_A***	Putative protein of unknown function.	-5.5022731	5.47E-39
C4_05870C_A	Has domain(s) with predicted DNA binding, zinc ion binding activity, role in transcription, DNA-templated and nucleus localization.	4.11693802	0.04285637	***SAP7***	Pepstatin A-insensitive secreted aspartyl protease.	-4.494215	0.008349

FET99	Multicopper oxidase family protein.	3.86253466	5.82E-10	***C7_02360W_A***	Protein of unknown function.	-4.2488347	0.0229701
PBR1	Protein of unknown function; required for cohesion, adhesion, and RPMI biofilm formation.	3.48126324	0.00640103	***PHO89***	Putative phosphate permease.	-3.5819585	3.43E-09
CFL4	C-terminus similar to ferric reductases.	3.38817704	4.63E-09	***CR_07820W_A***	Protein with monooxygenase domains.	-3.3228602	6.55E-05
HGT17	Putative MFS family glucose transporter.	3.38196284	0.02034968	***MRV4***	Protein of unknown function.	-3.2926567	0.0404172

ALS4	GPI-anchored adhesin; role in adhesion, germ tube induction.	2.74902568	0.00041022	***HSP30***	Putative heat shock protein.	-3.2302353	0.03352864
LEU1	3-isopropylmalate dehydratase.	2.70965565	0.03566308	***C4_00530C_A***	Has domain(s) with predicted hydrolase activity.	-3.0531165	0.0055549
PHO87	Putative phosphate permease.	2.67819846	8.91E-05	***C5_00510W_A***	Ortholog of C. dubliniensis CD36 : Cd36_50520, C. parapsilosis CDC317 : CPAR2_304000, *Candida* tenuis NRRL Y-1498 : cten_CGOB_00233 and Debaryomyces	-3.0490938	7.04E-07

					hansenii CBS767 : DEHA2E12408g.		
BMT4	Beta-mannosyltransferase; for elongation of beta-mannose chains on the acid-labile fraction of cell wall phosphopeptidomannan.	2.46210761	2.48E-06	***C2_08890W_A***	Ortholog(s) have DNA binding activity.	-2.9813839	2.07E-05

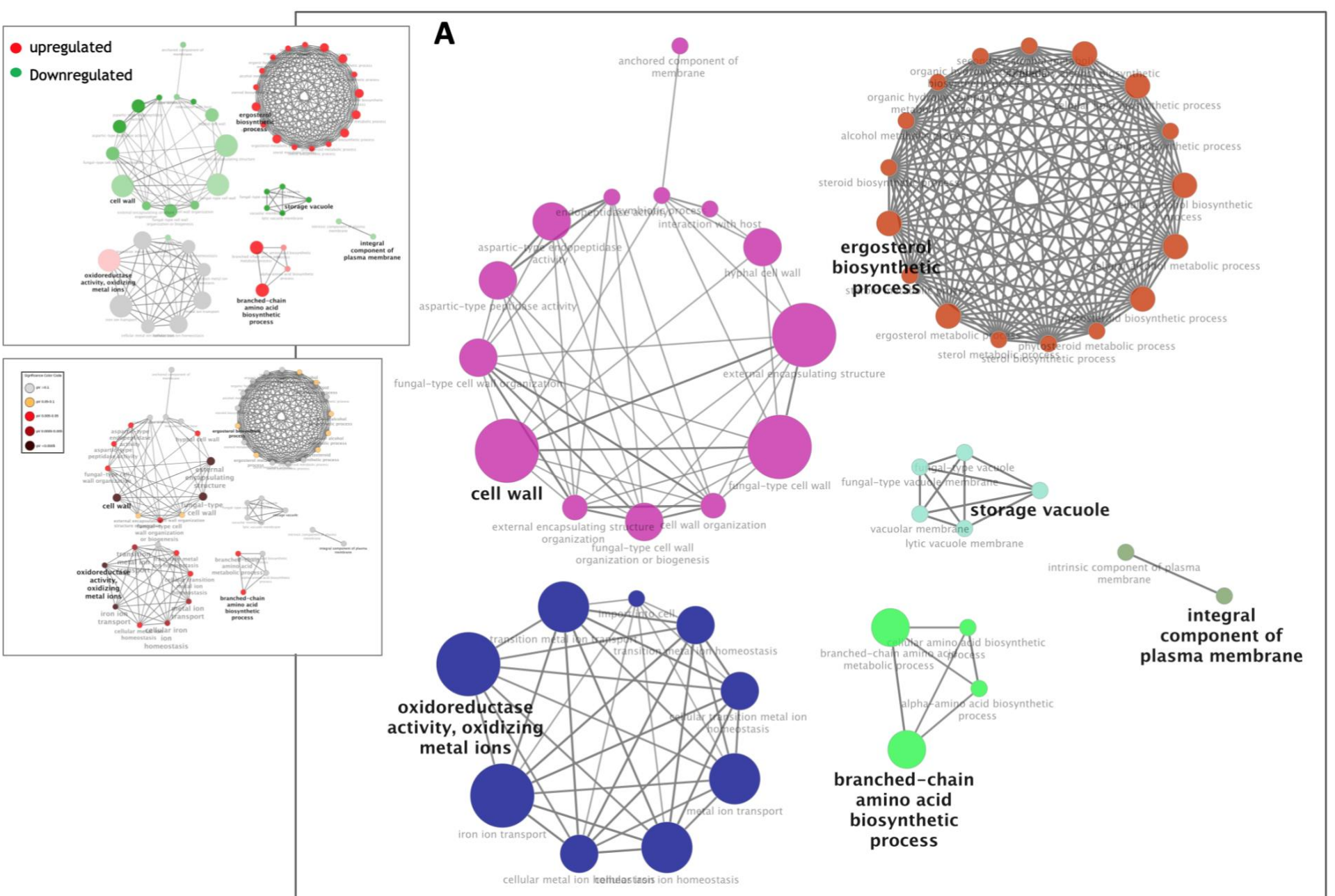
upregulated
Downregulated
A
anchored component of membrane
ergosterol biosynthetic process
cell wall
storage vacuole
integral component of plasma membrane
oxidoreductase activity, oxidizing metal ions
branched-chain amino acid biosynthetic process
aspartic-type endopeptidase activity
hyphal cell wall
aspartic-type peptidase activity
external encapsulating structure
fungal-type cell wall organization
fungal-type cell wall
external encapsulating structure organization
cell wall organization
fungal-type cell wall organization or biogenesis
fungal-type vacuole
fungal-type vacuole membrane
vacuolar membrane
lytic vacuole membrane
intrinsic component of plasma membrane
transition metal ion transport
transition metal ion homeostasis
cellular transition metal ion homeostasis
metal ion transport
iron ion transport
cellular metal ion homeostasis
cellular amino acid biosynthetic process
branched-chain amino acid metabolic process
alpha-amino acid biosynthetic process
ergosterol metabolic process
sterol metabolic process
sterol biosynthetic process
phytosteroid metabolic process

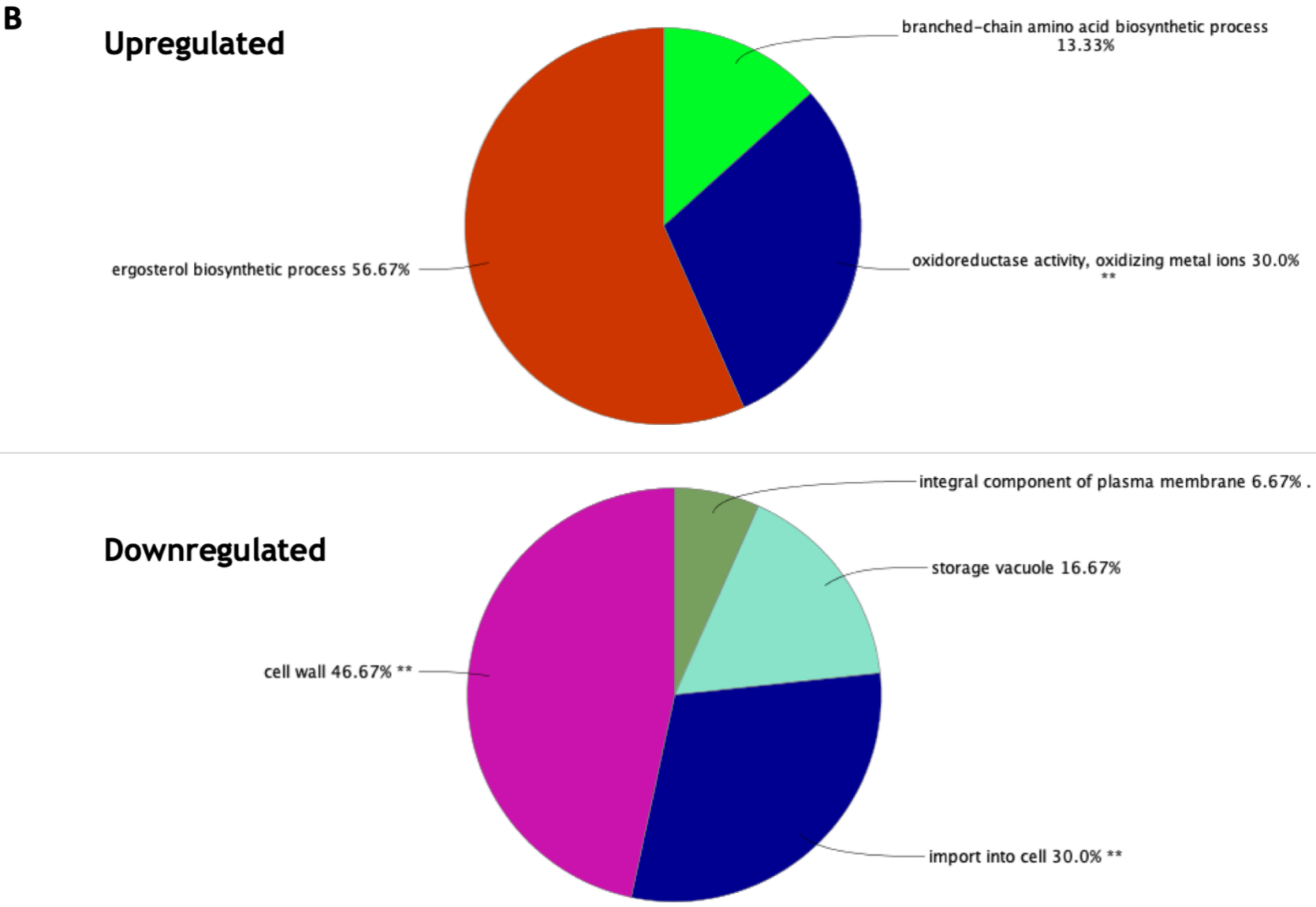
B
Upregulated
branched-chain amino acid biosynthetic process 13.33%
ergosterol biosynthetic process 56.67%
oxidoreductase activity, oxidizing metal ions 30.0% **
Downregulated
integral component of plasma membrane 6.67% .
storage vacuole 16.67%
cell wall 46.67% **
import into cell 30.0% **

Figure 4.9 ClueGO analysis of differential expressed genes and influenced pathways in response to 25 mM PHCl after 24 hours. Gene networks show the stimulated biological functions interactions and their pathways. Genes of similar function are grouped together to form nodes (circles). Nodes with similar functions are linked together by edges (lines) based upon their kappa score. (A) regulated genes composing groups of several biological functions and subnetworks related to different pathways. (B) Pie charts summarise the percentage of terms related to a specific subnetwork or biological function of pathways; colourised to illustrate the related subnetwork. Interaction Networks were created using ClueGO.

4.3.7Differential expression in response to ACh treatment

Volcano plots revealed the variation in *C. albicans* transcriptomic profile in the presence and absence of ACh. In general, the number of differentially expressed genes at 25 mM were fewer than 5 mM (Figure 4.9). Heatmaps show the top 50 differentially expressed genes with their relative expression at both timepoints, in the presence and absence of the treatment. Many differentially expressed genes are uncharacterized and referred to by their gene ID (Figure 4.10).

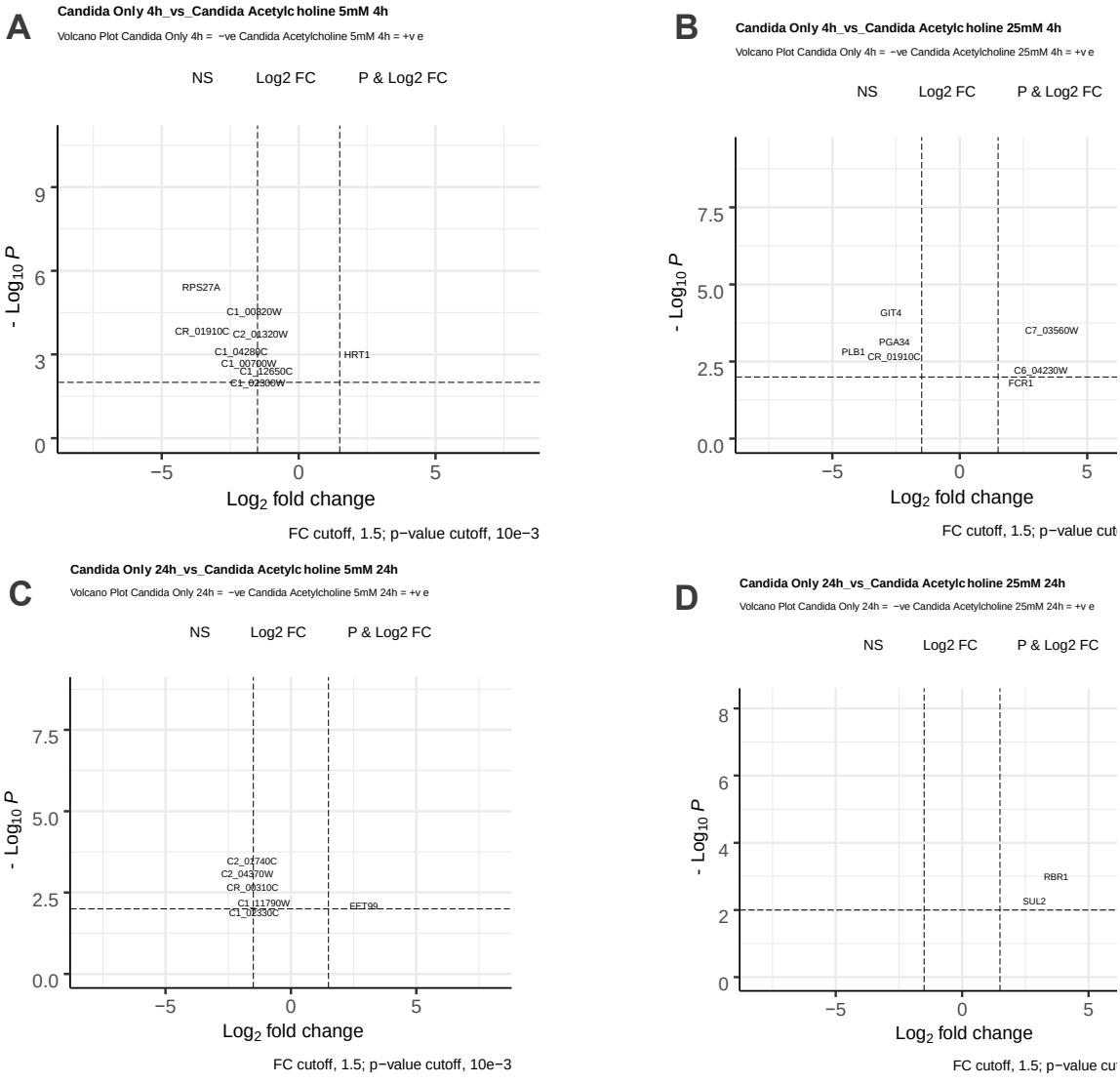

Figure 4.10 Volcano plots showing changes of genes expression at different time points after incubation with different concentrations of ACh. (A) transcriptional changes at 4 hours in response to 5 mM ACh. (B) transcriptional changes at 4 hours in response to 25 mM ACh. (C) transcriptional changes at 24 hours in response to 5 mM ACh. (D) transcriptional changes at 24 hours in response to 25 mM ACh. Upregulated genes in the presence of ACh are represented by a +ve Log_2 fold change and those upregulated in the absence of ACh are represented with -ve Log_2 fold change. The increase in negative or positive values indicate a larger upregulation. The horizontal dotted lines indicate the cut-off of the p value < 0.01, (colours in red). The vertical

dotted lines indicate the cut-off of Log_2 fold change 1.5 (colours in green). Genes of interest that are significantly upregulated are the genes where expression levels are above or below the Log_2 fold change cut-offs; -1.5 and 1.5 and that are highly significant; $P < 0.01$.

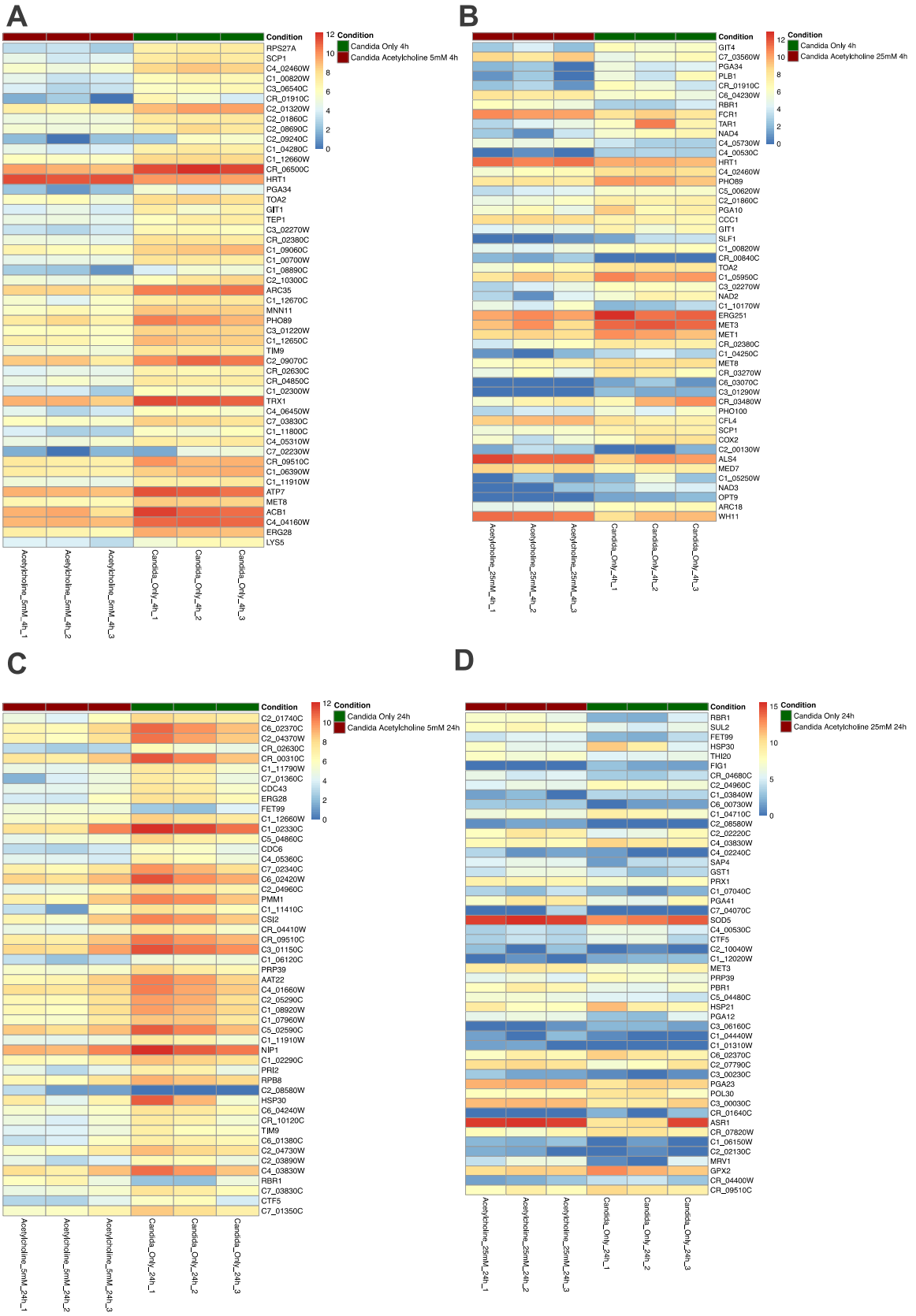

Figure 4.11 Heatmaps showing levels of relative genes expression at different times during treatment of *C. albicans* with different concentrations of ACh. (A) transcriptional changes at 4 hours with 5 mM. (B) transcriptional changes at 4 hours with 25 mM. (C) transcriptional changes at

24 hours with 5 mM. (D) transcriptional changes at 24 hours with 25 mM. The colour key indicates level of relative expression under any of the conditions; the presence of ACh treatment (red) and the absence (green).

4.3.8 Differences in gene regulation and influenced pathways in presence and absence of 5 mM ACh at 4 hours of biofilm formation

Differential expression analysis revealed that *C. albicans* cells treated with 5 mM ACh resulted in the upregulation of 4 genes significantly including *HRT1, CFL4, and RBR1.* In addition, 90 genes were significantly downregulated including: *RPS27A*, *C1_00820W, CR_01910C, C2_01320W, C1_04280C, C1_ 00700W, C1_12650C* and *C1_02300W* (Figure 4.9 A and 4.10 A). Each gene encodes specific protein that is responsible for a biological process detailed in (Table 4.5) and in Appendix V materials (Table 4). Differences in gene regulation in the presence and absence of ACh were further investigated by determining the pathways that are influenced by the treatment. GlueGO plugin in Cytoscape was used to calculate and visualize the networks of functionally enriched pathways. Gene interaction networks showed that 5 mM of ACh at 4 hours resulted in a differential expression of genes that are involved in several biological processes; among them are oxidoreductase activity, SCF-dependent proteasomal ubiquitin-dependent protein catabolic process and protein neddylation ($P > 0.1$) were upregulated. Furthermore, biological functions such as, organophosphate ester transmembrane transporter activity ($P = 0.005 — 0.05$), cellular amino acid biosynthetic process, monovalent inorganic cation transport, glycerolipid metabolic process, asparate family amino acid biosynthetic process were all downregulated ($P > 0.1$) (Figure 4.11).

Table 4.5 Top 10 up and top 10 down regulated genes by 5 mM ACh treatment at 4 hours incubation. Table includes the common gene name, protein encoded description, the log_2 fold change (Log_2FC), and the P value.

Upregulated				Downregulated			
Gene Name	**Description**	**log_2FoldChange**	**Pvalue**	**Gene Name**	**Description**	**log_2FoldChange**	**Pvalue**
RBR1	Glycosylphosphatidylinositol (GPI)-anchored cell wall protein; required for filamentous growth at acidic pH.	2.60827408	0.00055232	***C5_01790C_A***	Ortholog of WO-1 : CAWG_04564.	-5.0416787	0.01939982
C4_05730W_A	Adhesin-like protein.	2.22422942	0.01748582	***CR_01910C_A***	Putative dethiobiotin synthetase.	-4.5177031	8.21E-05
CFL4	C-terminus similar to ferric reductases.	1.83285357	0.01448421	***RPS27A***	Ribosomal protein S27.	-4.2519504	2.06E-06

HRT1	Ortholog of S. cerevisiae Hrt1; component of a nuclear ubiquitin-protein ligase complex involved in cell cycle control.	1.66378873	0.04279562	***C1_04250C_A***	Ortholog of WO-1: CAWG_00968.	-4.1146828	0.02795712
				C2_09240C_A	Protein of unknown function.	-4.05883	0.00038407
				NAD2	Subunit 2 of NADH:ubiquinone oxidoreductase (NADH:ubiquinone dehydrogenase), a multisubunit enzyme complex (complex I) of	-3.8685071	0.0364101

		the mitochondrial inner membrane that catalyzes the first step in mitochondrial respiration.		
	TNA1	Putative nicotinic acid transporter.	-3.769854	0.02869407
	C1_12940C_A	Ortholog of C. parapsilosis CDC317: CPAR2_801655, *Candida tropicalis* MYA-3404 : CTRG_06172 and	-3.7682406	0.048291

		WO-1 : CAWG_02233.		
	C7_02230W_A	Ortholog of WO-1 : CAWG_05572.	-3.7208712	0.0069718
	C5_03910C_A	Ortholog of C. parapsilosis CDC317 : CPAR2_302980, C. dubliniensis CD36 : Cd36_53630, Pichia stipitis Pignal : PICST_32155 and *Candida orthopsilosis* Co 90-125 : CORT_0E05120.	-3.7172003	0.01485963

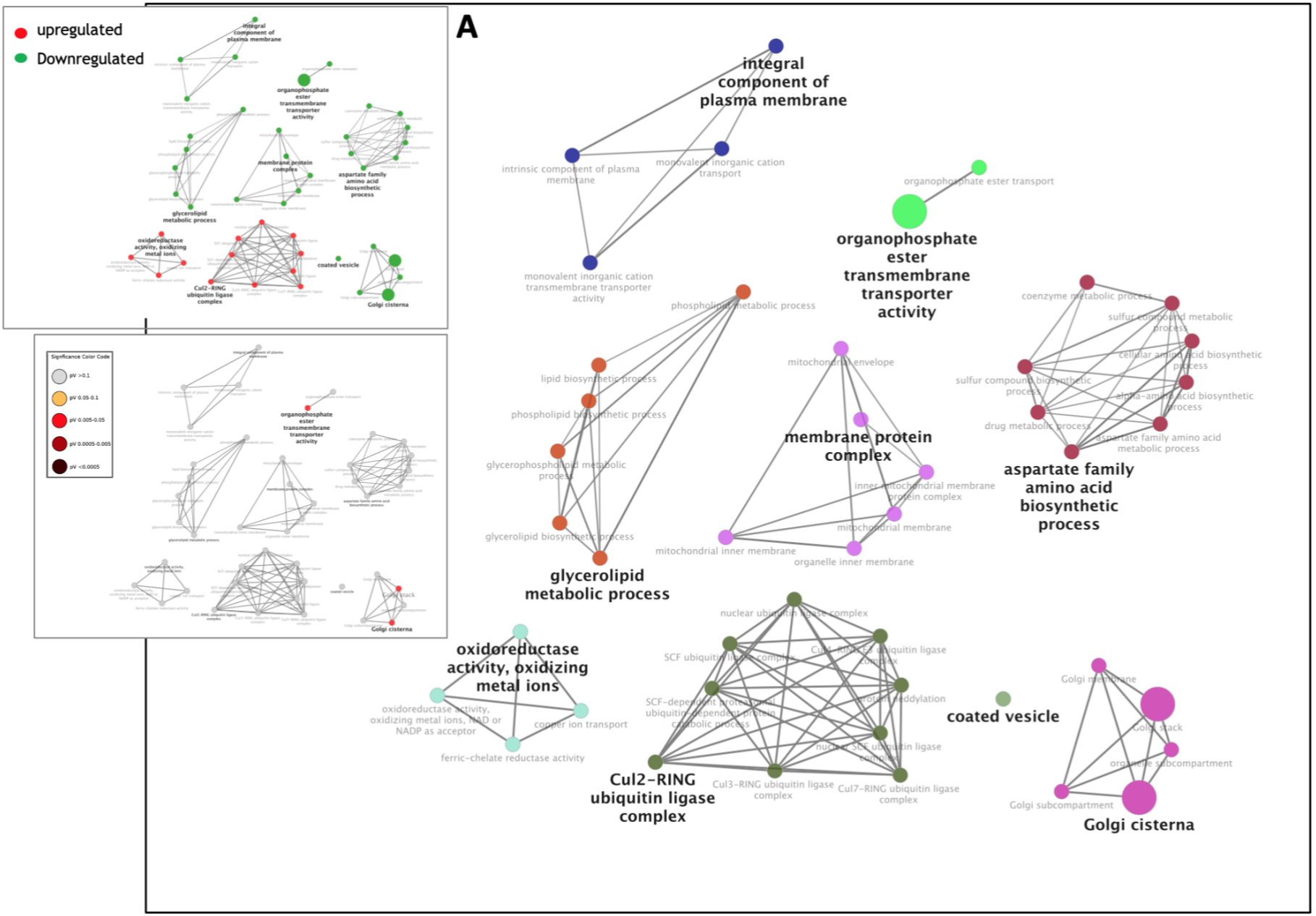
upregulated
Downregulated
A
integral component of plasma membrane
intrinsic component of plasma membrane
monovalent inorganic cation transport
monovalent inorganic cation transmembrane transporter activity
organophosphate ester transport
organophosphate ester transmembrane transporter activity
phospholipid metabolic process
lipid biosynthetic process
phospholipid biosynthetic process
glycerophospholipid metabolic process
glycerolipid biosynthetic process
glycerolipid metabolic process
mitochondrial envelope
membrane protein complex
inner mitochondrial membrane protein complex
mitochondrial membrane
mitochondrial inner membrane
organelle inner membrane
coenzyme metabolic process
sulfur compound metabolic process
cellular amino acid biosynthetic process
sulfur compound biosynthetic process
alpha-amino acid biosynthetic process
drug metabolic process
aspartate family amino acid metabolic process
aspartate family amino acid biosynthetic process
oxidoreductase activity, oxidizing metal ions
oxidoreductase activity, oxidizing metal ions, NAD or NADP as acceptor
copper ion transport
ferric-chelate reductase activity
nuclear ubiquitin ligase complex
SCF ubiquitin ligase complex
Cul4-RING ubiquitin ligase complex
SCF-dependent protein ubiquitin-dependent protein catabolic process
protein neddylation
nuclear SCF ubiquitin ligase complex
Cul2-RING ubiquitin ligase complex
Cul3-RING ubiquitin ligase complex
Cul7-RING ubiquitin ligase complex
coated vesicle
Golgi membrane
Golgi stack
organelle subcompartment
Golgi subcompartment
Golgi cisterna

B

Downregulated

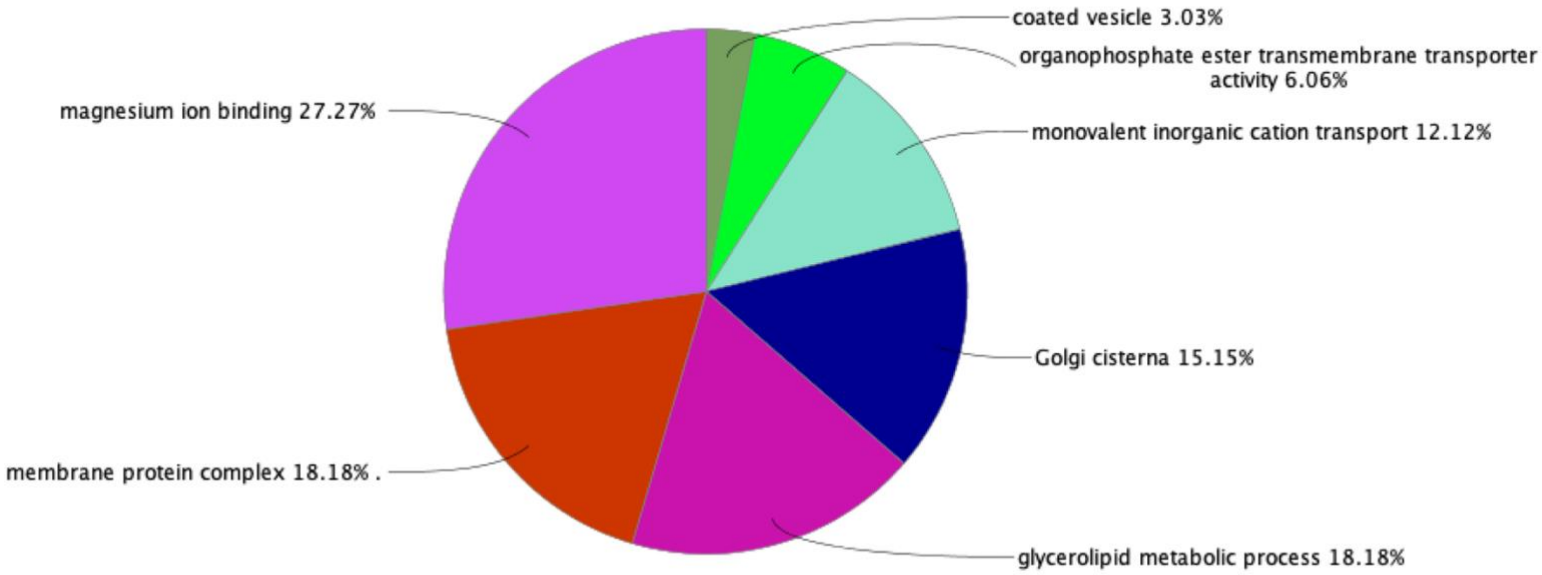

Figure 4.12 ClueGO analysis of differential expressed genes and influenced pathways at 4 hours by 5 mM ACh. Gene networks show the stimulated biological functions interactions and their pathways. Genes of similar function are grouped together to form nodes (circles). Nodes with similar functions are linked together by edges (lines) based upon their kappa score. (A) regulated genes composing groups of several biological functions and subnetworks related to different pathways. (B) Pie charts summarise the percentage of terms related to a specific subnetwork or biological function of pathways; colourised to illustrate the related subnetwork. Interaction Networks were created using ClueGO.

4.3.9 Differences in gene regulation and influenced pathways in presence and absence of 25 mM ACh at 4 hours of biofilm formation

Increasing the concentration of ACh to 25 mM resulted in smaller number of genes regulated; 6 genes were upregulated and 16 genes were downregulated. Similarly, heatmap and volcano plots showed that the genes *C7_03560W, C6_04230W,* and *FCR1* were significantly upregulated at 25 mM concentration, while *GIT4, PGA34, PLB1,* and *CR_01910C* were amongst the significant downregulated genes (Figure 4.9 B and 4.10 B). Each gene encodes a specific protein that is responsible for a biological process detailed in (Table 4.6) and in Appendix V materials (Table 5). ClueGo interaction networks analysis showed that at 25 mM ACh treatment revealed significant regulation of genes that are implicated in the following biological functions; glyceorphpsphodiester transmembrane transporter activity ($P < 0.0005$), symporter activity, and sulfur compound biosynthetic process ($P = 0.005 - 0.05$), which were all downregulated (Figure 4.12).

Table 4.6 Top 10 up and top 10 down regulated genes by 25 mM ACh treatment at 4 hours incubation. Table includes the common gene name, protein encoded description, the log_2 fold change (Log_2FC), and the Pvalue.

Upregulated				Downregulate			
Gene Name	**Description**	**log_2FoldChange**	**Pvalue**	**Gene Name**	**Description**	**log_2FoldChange**	**Pvalue**
CR_00840C_A	Ortholog of WO-1 : CAWG_01442.	4.31944599	0.04500712	***TAR1***	Ortholog of S. cerevisiae Tar1p; Transcript Antisense to Ribosomal RNA; encoded within the 25S rRNA gene on the opposite strand; induced by Tbf1.	-5.1833879	0.01000505
CR_04440C_A	Glycosylphosphatidylinositol (GPI)-anchored cell wall protein; required for	2.75915893	0.00922775	***PLB1***	Phospholipase B; host cell penetration and virulence in	-4.6279081	0.00088492

	filamentous growth at acidic pH.				mouse systemic infection.		
C7_03560W_A	Protein of unknown function.	2.56025984	0.00018171	***SLF1***	Putative polysome-associated RNA binding protein.	-4.5493929	0.04200602
C4_05730W_A	Adhesin-like protein.	2.26356571	0.01146103	***C4_00530C_A***	Has domain(s) with predicted hydrolase activity.	-4.3730336	0.01484241
C6_04230W_A	Ortholog of C. dubliniensis CD36 : Cd36_64900, C. parapsilosis CDC317 : CPAR2_600390, Pichia stipitis Pignal : PICST_30726 and *Candida guilliermondii*	2.13276008	0.00345523	***NAD4***	Subunit 4 of NADH:ubiquinone oxidoreductase (NADH:ubiquinone dehydrogenase), a multisubunit enzyme complex	-3.9380864	0.01065085

	ATCC 6260 : PGUG_04023.				(complex I) of the mitochondrial inner membrane that catalyzes the first step in mitochondrial respiration.		
C3_06850W_A	Transcription factor.	1.91366506	0.00957347	***CR_01910C_A***	Putative dethiobiotin synthetase.	-3.6140891	0.00126052
				PGA34	Putative GPI-anchored protein.	-3.1676507	0.00043437
				GIT4	Glycerophosphocholine	-3.1127035	4.86E-05

		transporter; fungal-specific.		
	PGA10	GPI anchored membrane protein; utilization of hemin and hemoglobin for Fe in host.	-2.1165442	0.03704329
	C4_02460W_A	Ortholog(s) have HDEL sequence binding activity, role in ER to Golgi vesicle-mediated transport, protein retention in ER lumen and integral	-2.0451841	0.01799031

	component of endoplasmic reticulum membrane localization.

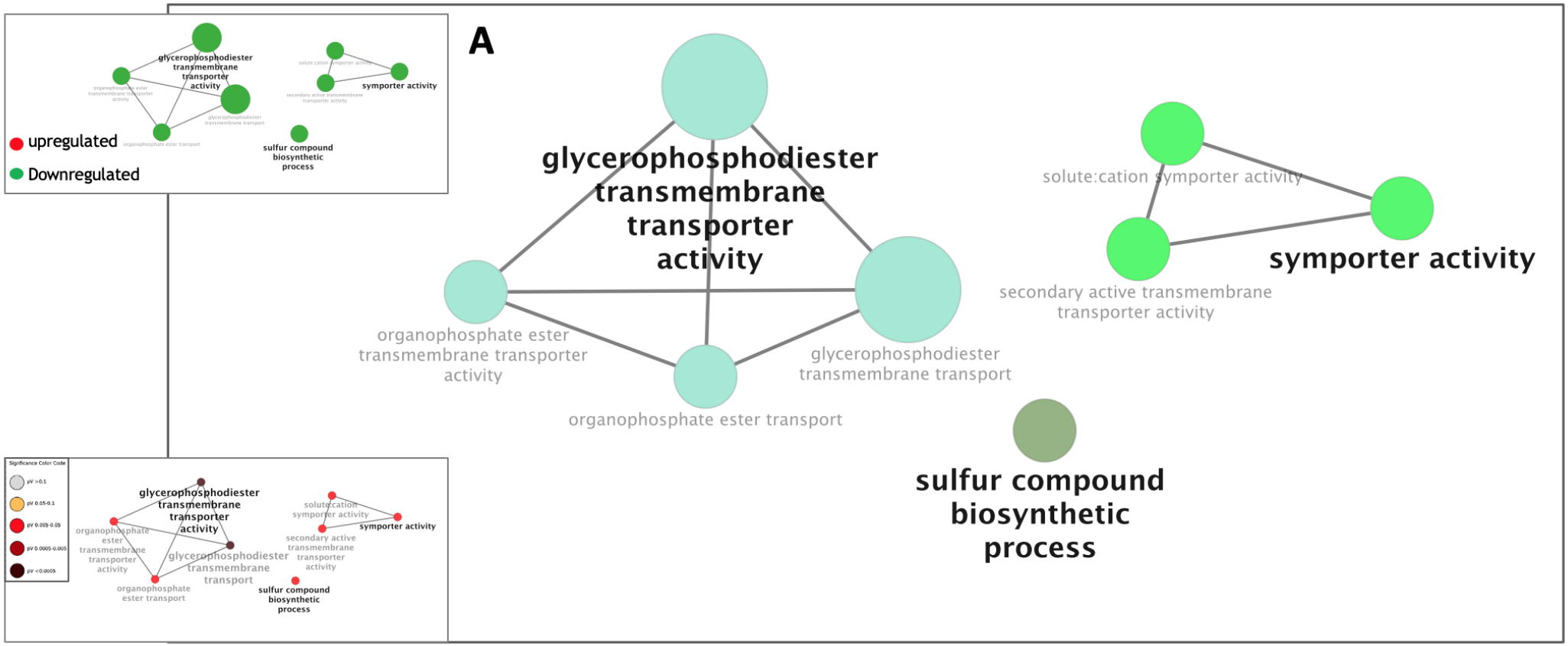
A
glycerophosphodiester transmembrane transporter activity
organophosphate ester transmembrane transporter activity
glycerophosphodiester transmembrane transport
organophosphate ester transport
solute:cation symporter activity
secondary active transmembrane transporter activity
symporter activity
sulfur compound biosynthetic process
upregulated
Downregulated
Significance Color Code
pV >0.1
pV 0.05-0.1
pV 0.005-0.05
pV 0.0005-0.005
pV <0.0005

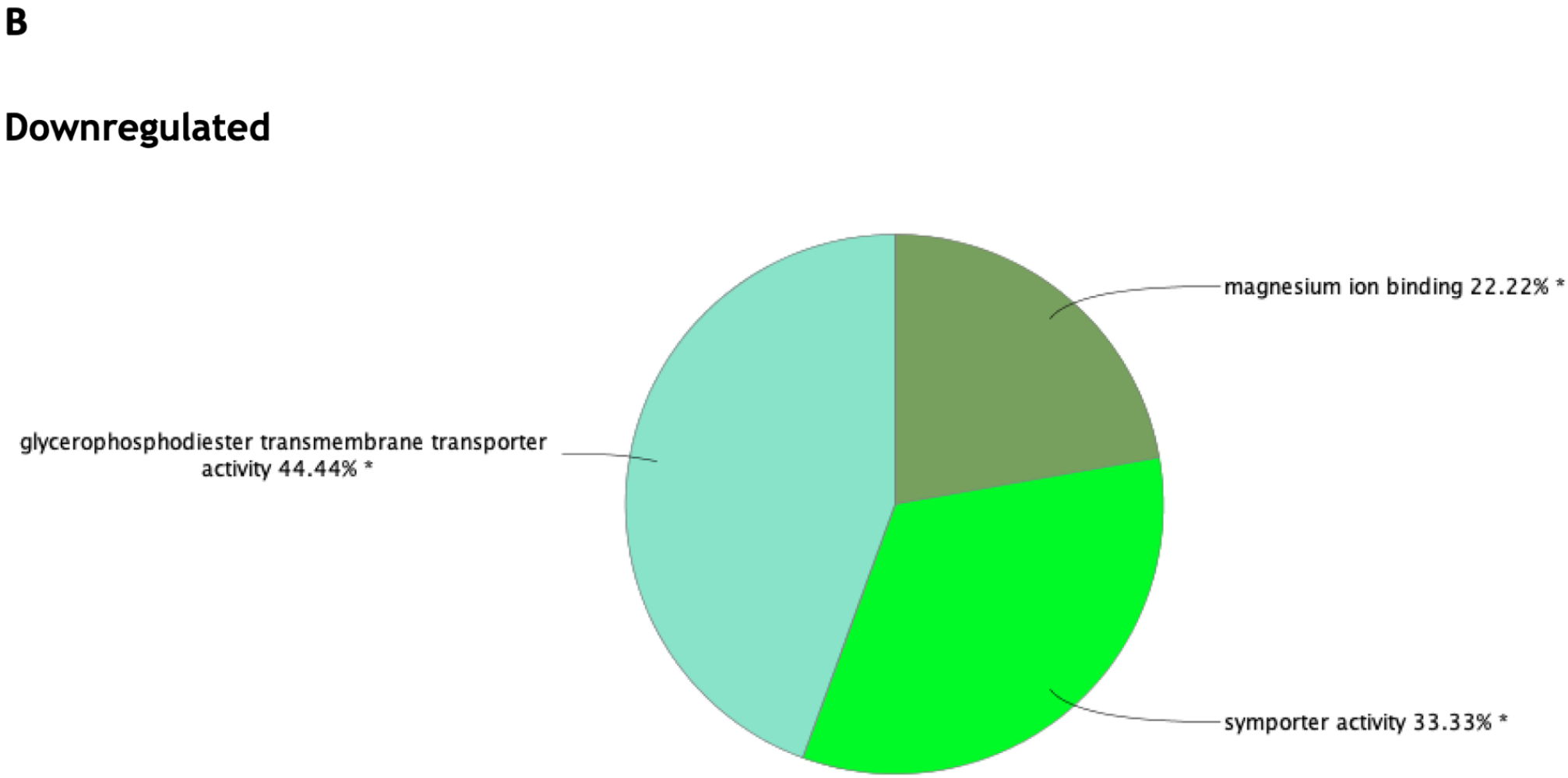

Figure 4.13 ClueGO analysis of differential expressed genes and influenced pathways at 4 hours by 25 mM ACh. Gene networks show the stimulated biological functions interactions and their pathways. Genes of similar function are grouped together to form nodes (circles). Nodes with similar functions are linked together by edges (lines) based upon their kappa score. (A) regulated genes composing groups of several biological functions and subnetworks related to different pathways. (B)

Pie charts summarise the percentage of terms related to a specific subnetwork or biological function of pathways; colourised to illustrate the related subnetwork. Interaction Networks were created using ClueGo.

4.3.10 Differences in gene regulation and influenced pathways in presence and absence of 5 mM ACh at 24 hours of biofilm formation

At later stages of biofilm maturation, analysis showed that 5 mM of ACh treatment resulted in upregulating fewer number of genes (3 genes) which are *C2_08580W, FET99,* and *RBR1*. In addition, 48 genes were downregulated such as: *C2_01740C, C2_04370W, CR_00310C, C1_11790W, and C1_02330C* (Figure 4.9 C and 4.10 C). Each gene encodes specific protein that is responsible for a biological process detailed in (Table 4.7) and in appendix V materials (Table 6). Gene interaction networks showed that 5 mM of ACh treatment resulted in downregulation of the following biological processes ribonucleoprotein complex subunit organization, protein localization to endoplasmic reticulum (P = 0.005 — 0.05), cytoplasmic translocation, and nuclear transport (P = 0.05 — 0.1) (Figure 4.13).

Table 4.7 Top 10 up and top 10 down regulated genes by 5 mM ACh treatment at 24 hours incubation. Table includes the common gene name, protein encoded description, the log_2 fold change (Log_2FC), and the Pvalue.

Upregulated				Downregulated			
Gene Name	**Description**	**log_2FoldChange**	**Pvalue**	**Gene Name**	**Description**	**log_2FoldChange**	**Pvalue**
C2_08580W_A	Possible pseudogene.	4.47098108	0.03311512	***HSP30***	Putative heat shock protein.	-3.2309265	0.0336154
FET99	Multicopper oxidase family protein.	2.34544489	0.00500563	***CR_02630C_A***	Essential component of the conserved oligomeric Golgi complex; role in fusion of transport vesicles to Golgi compartments.	-2.8469815	0.00099027

RBR1	Glycosylphosphatidylinositol (GPI)-anchored cell wall protein; required for filamentous growth at acidic pH.	2.3300989	0.04439682	***C7_01360C_A***	Putative heat shock protein with a zinc finger motif; required for protein import into mitochondria in S. cerevisiae.	-2.8200764	0.00418246
				C2_04370W_A	Protein of unknown function.	-2.7865403	0.00050543
				C6_02370C_A	Ortholog(s) have structural constituent of ribosome activity and mitochondrial small ribosomal	-2.7358926	0.00038689

		subunit localization.		
	C1_11410C_A	Predicted ORF from original SGTC Assembly 19 annotation.	-2.6977484	0.01421729
	CR_00310C_A	Protein of unknown function.	-2.5583551	0.00129855
	C2_01740C_A	Mitochondrial ribosomal protein of the large subunit.	-2.5449787	0.00020406
	ERG28	Ortholog(s) have protein binding, bridging activity, role in	-2.5042694	0.00478145

		demethylation, ergosterol biosynthetic process and endoplasmic reticulum membrane localization.		
	C1_02330C_A	Ribosomal 60S subunit protein.	-2.4696572	0.00813745

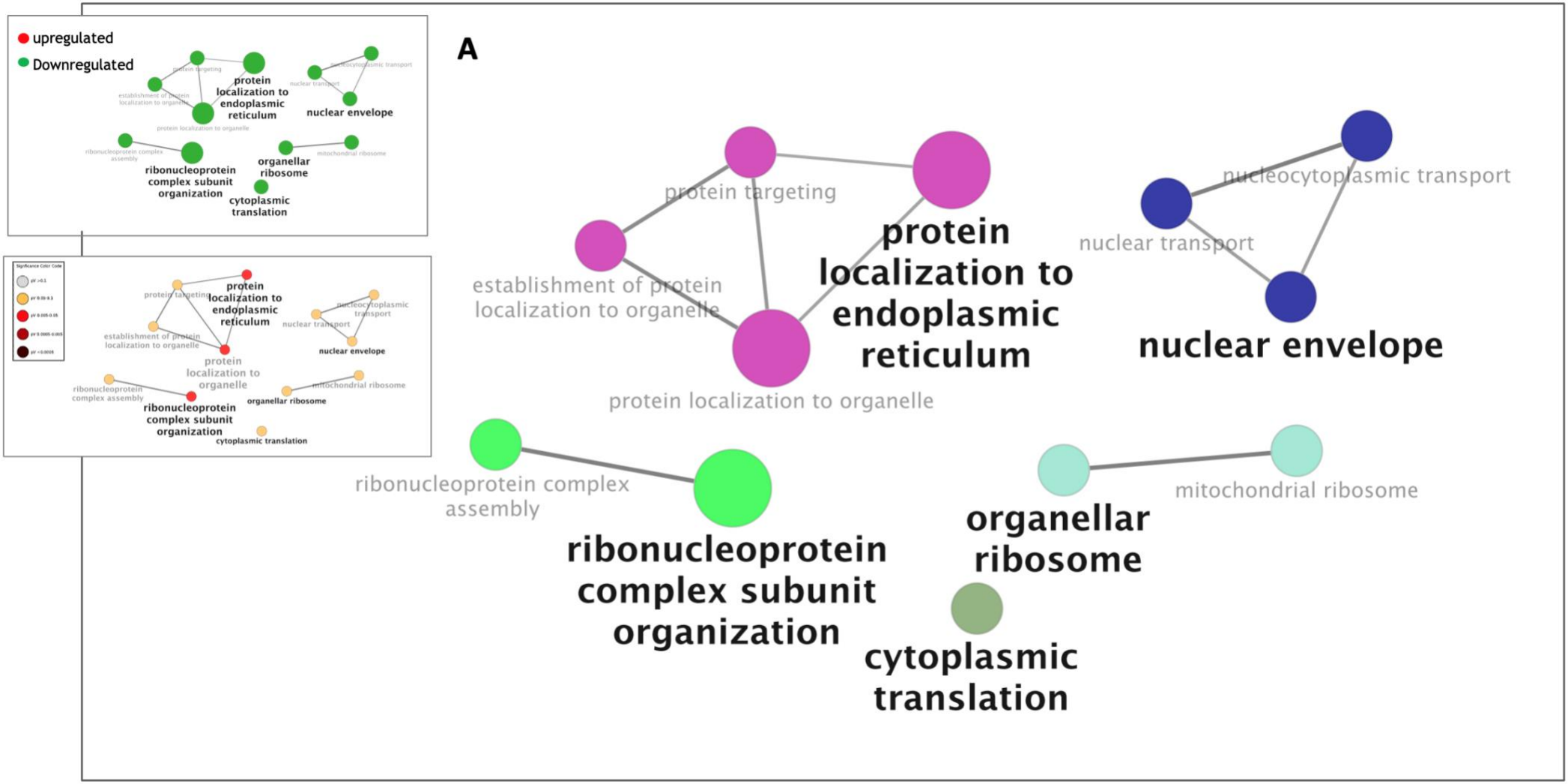
upregulated
Downregulated
protein localization to endoplasmic reticulum
nuclear envelope
ribonucleoprotein complex subunit organization
organellar ribosome
cytoplasmic translation
A
protein targeting
establishment of protein localization to organelle
protein localization to organelle
nucleocytoplasmic transport
nuclear transport
ribonucleoprotein complex assembly
mitochondrial ribosome

B

Downregulated

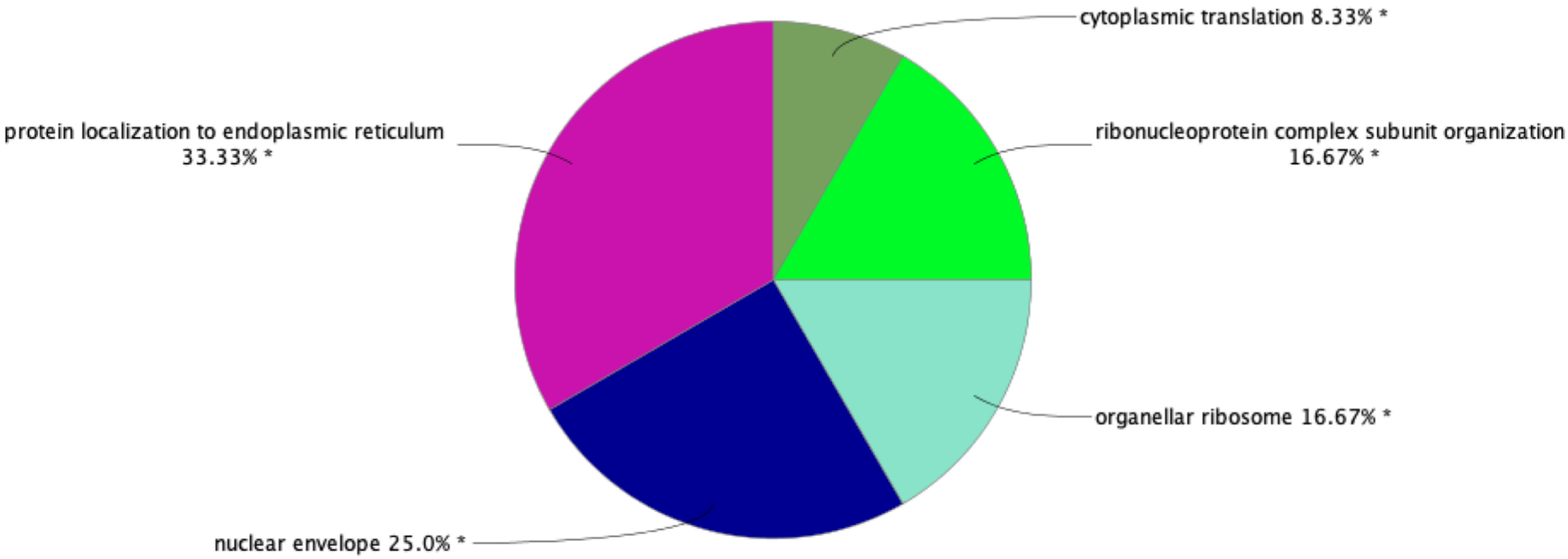

Figure 4.14 ClueGO analysis of differential expressed genes and influenced pathways at 4 hours by 25 mM ACh. Gene networks show the stimulated biological functions interactions and their pathways. Genes of similar function are grouped together to form nodes (circles). Nodes with similar functions are linked together by edges (lines) based upon their kappa score. (A) regulated genes composing groups of several biological functions and subnetworks related to different pathways. (B) Pie charts summarise the percentage of terms related to a specific subnetwork or biological function of pathways; colourised to illustrate the related subnetwork. Interaction Networks were created using ClueGo.

4.3.11 Differences in gene regulation and influenced pathways in presence and absence of 25 mM ACh at 24 hours of biofilm formation

At a concentration of 25 mM ACh, the volcano plot showed the upregulation of 5 genes such as; *RBR* and *SUL2* while the genes, *FIG1* and *HSP3*0 were downregulated (Figure 4.9 C and 4.10 D). Each gene encodes specific protein that is responsible for a biological process detailed in (Table 4.8). Gene interaction network revealed a different transcription profile and regulation of the following biological processes; hydroxymethylpyrimidine kinase activity (*P* = 0.05 − 0.5), divalent inorganic cation transport (*P* = 0.05 − 0.1), secondary active sulfate transmembrane transporter activity (P = 0.05 − 0.1), channel activity (P = 0.05 − 0.1), and ferroxidase activity (P > 0.1). Clustering interaction network revealed that during the maturation, 25 mM of ACh resulted in downregulating channel activity and divalent inorganic cation transport while upregulating hydroxymethylpyrimidine kinase activity, secondary active sulfate transmembrane transporter activity, and ferroxidase activity (Figure 4.14).

Table 4.8 Top 10 up and top 10 down regulated genes by 25 mM ACh treatment at 24 hours incubation. Table includes the common gene name, protein encoded description, the log_2 fold change (Log_2FC), and the Pvalue.

Upregulated				Downregulated			
Gene Name	Description	log_2FoldChange	Pvalue	Gene Name	Description	log_2FoldChange	Pvalue
RBR1	Glycosylphosphatidylinositol (GPI)-anchored cell wall protein; required for filamentous growth at acidic pH.	3.23831136	0.00064975	***FIG1***	S. cerevisiae Fig1 ortholog; an integral membrane protein required for mating; role in thigmotropism.	-4.0438883	0.04349722
SUL2	Putative sulfate transporter.	2.40680387	0.00350572	***HSP30***	Putative heat shock protein.	-3.3013015	0.02838493
FET99	Multicopper oxidase family protein.	2.15712499	0.01608833				

CR_04680C_A	Protein of unknown function.	1.87513312	0.04454048	
THI20	Putative trifunctional enzyme of thiamine biosynthesis, degradation and salvage.	1.66026159	0.03385169	

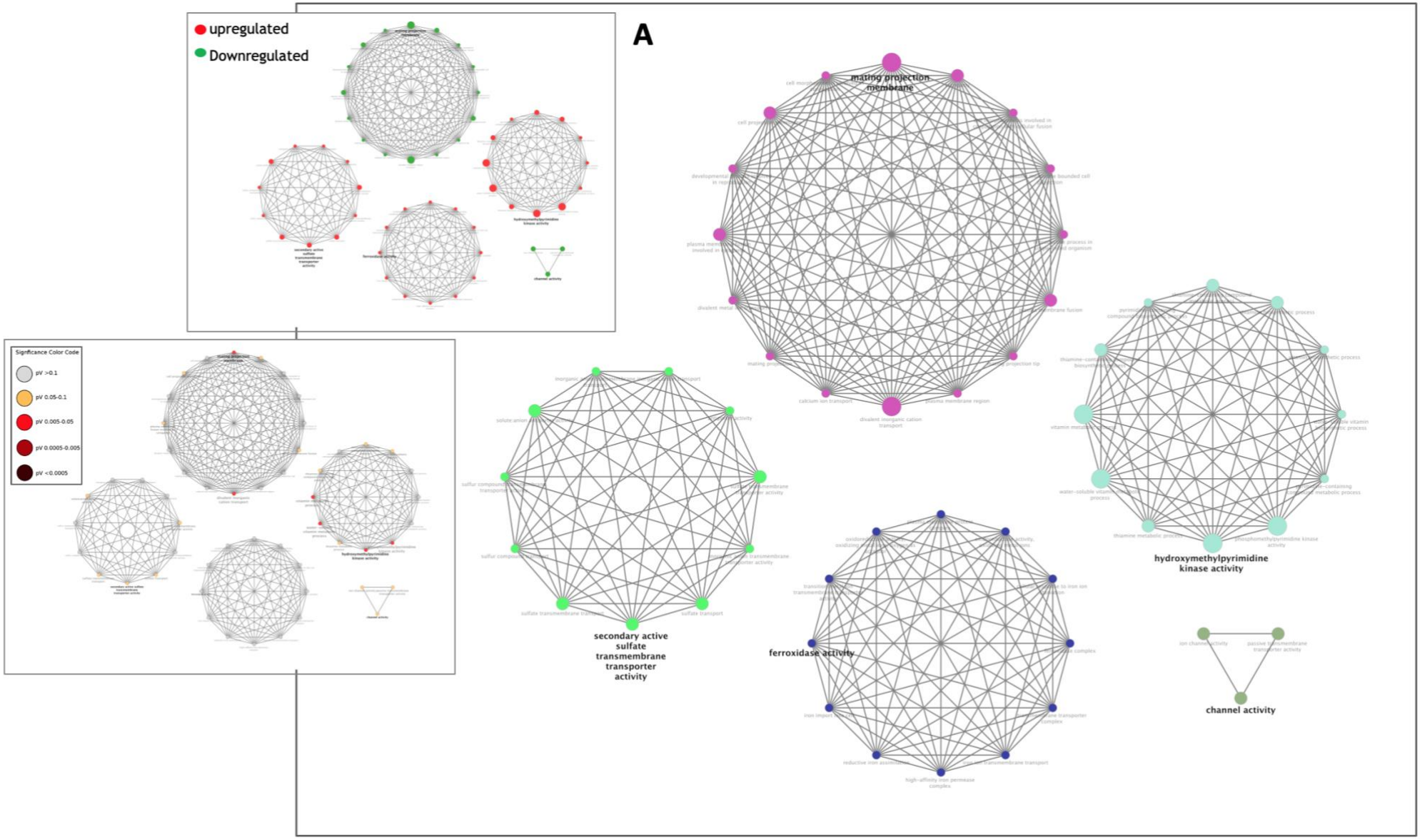
upregulated
Downregulated
A
mating projection membrane
hydroxymethylpyrimidine kinase activity
secondary active sulfate transmembrane transporter activity
ferroxidase activity
channel activity
Significance Color Code
pV >0.1
pV 0.05-0.1
pV 0.005-0.05
pV 0.0005-0.005
pV <0.0005

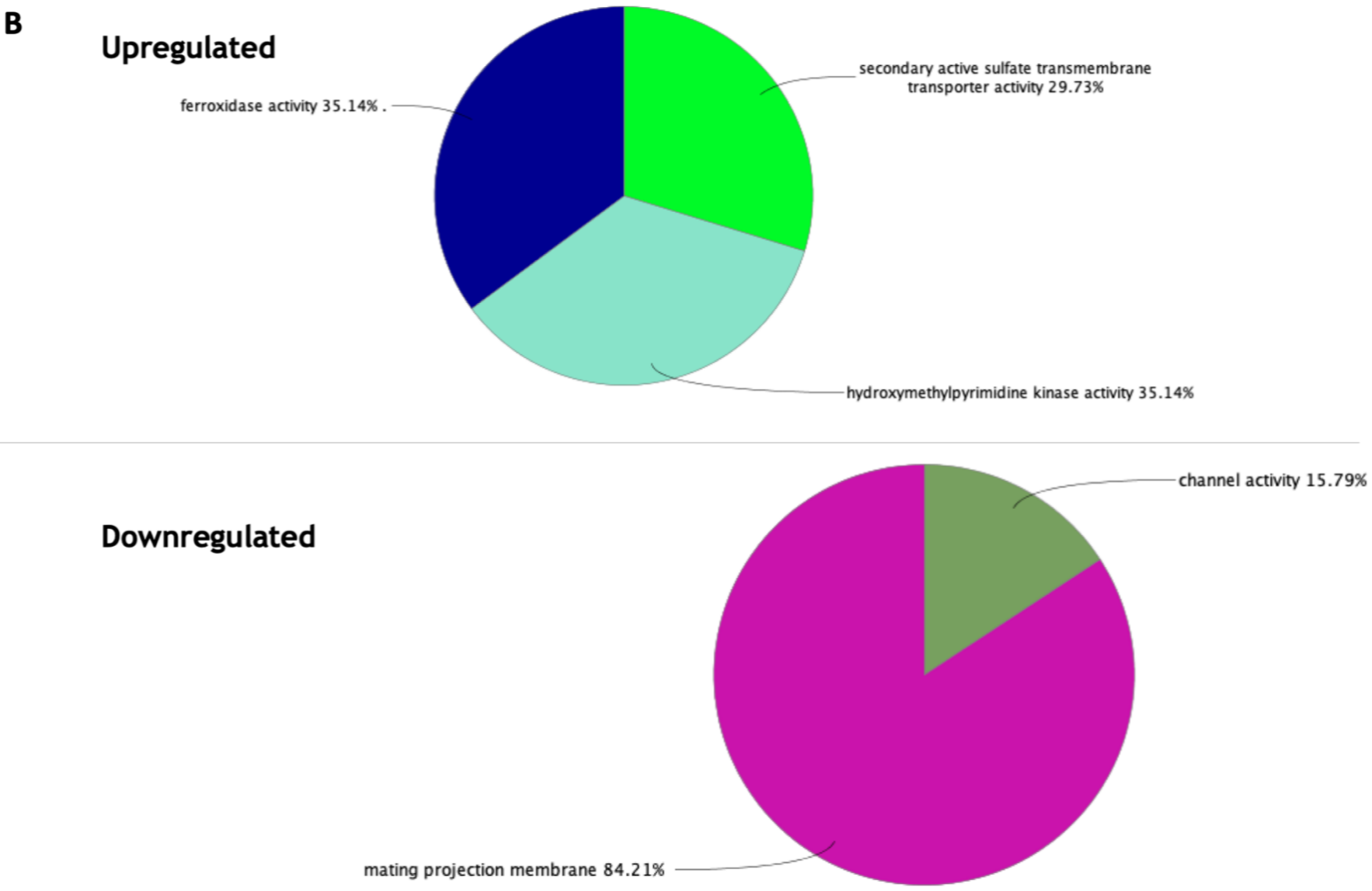
B
Upregulated
ferroxidase activity 35.14% .
secondary active sulfate transmembrane transporter activity 29.73%
hydroxymethylpyrimidine kinase activity 35.14%
Downregulated
channel activity 15.79%
mating projection membrane 84.21%

Figure 4.15 ClueGO analysis of differential expressed genes and influenced pathways at 24 hours by 25 mM ACh. Gene networks show the stimulated biological functions interactions and their pathways. Genes of similar function are grouped together to form nodes (circles). Nodes with similar functions are linked together by edges (lines) based upon their kappa score. (A) regulated genes composing groups of several biological functions and subnetworks related to different pathways. (B) Pie charts summarise the percentage of terms related to a specific subnetwork or biological function of pathways; colourised to illustrate the related subnetwork. Interaction Networks were created using ClueGo.

4.3.12 Overlap in genes regulation between *Candida albicans* exposure to ACh and PHCl

Analysis of co-expression levels using a Venn diagram showed that 192 genes were differentially expressed when cells treated with PHCl (5 and 25 mM) at 4 hours. Among them, 11 genes were uniquely differentially expressed at 5 mM and 85 genes were uniquely differentially expressed at 25 mM. Furthermore, 48 genes were overlapping from both concentrations of PHCl (Figure 4.15 A). At 24 hours, 86 genes were differentially expressed when cells treated with PHCl (5 and 25 mM). Among them, 3 genes were uniquely differentially expressed at 5 mM and 63 genes were uniquely differentially expressed at 25 mM Furthermore, 10 genes were overlapping from both concentrations of PHCl (Figure 4.15 B). This analysis was also applied to ACh treatment which revealed that at 4 hours, 116 genes were differentially expressed when cells treated with ACh (5 and 25 mM). Among them, 81 genes were uniquely differentially expressed at 5 mM and 9 genes were uniquely differentially expressed at 25 mM (Figure 4.16 A). Furthermore, 13 genes were overlapping from both concentrations of ACh. At 24 hours, 58 genes were differentially expressed when cells treated with ACh (5 and 25 mM). Among them 48 genes were uniquely differentially expressed at 5 mM, and 4 genes were uniquely differentially expressed at 25 mM (Figure 4.16 B). Furthermore, 3 genes were overlapping from both concentrations of ACh. Comparing treated *C. albicans* cells to untreated cells revealed that none of the genes regulated by both treatments, PHCl and ACh, were overlapping at any concentration or incubation time points (Figure 4.17 and Figure 4.18). Furthermore, comparing both treatments at matching time points of incubation and concentrations showed that at 4 hours incubation there was overlap between the 5 mM and 25 mM concentrations of both treatment in 13 genes and 10 genes, respectively. In addition, at 24 hours incubation there was overlapping between the 5 mM and 25 mM concentrations of both treatment in 1 gene and 2 genes, respectively (Figure 4.19). Genes overlapping between both treatments are listed in (Table 4.9).

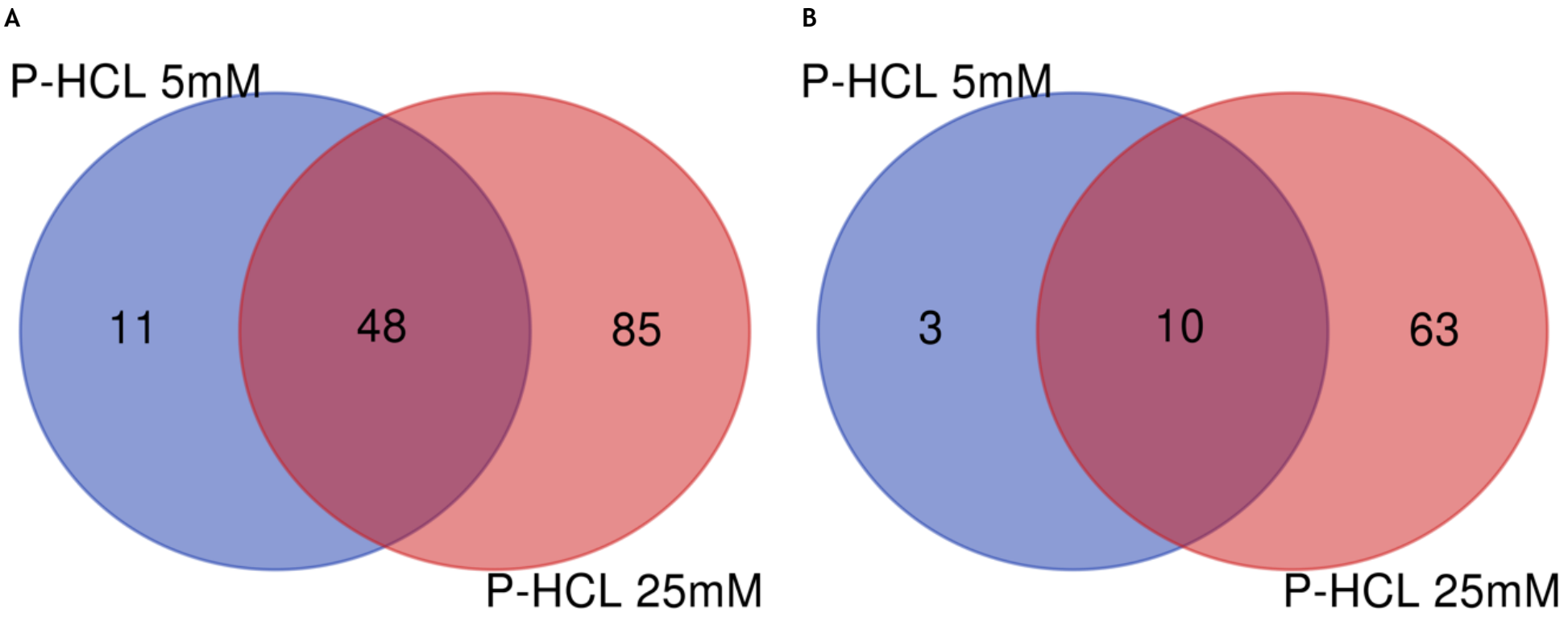

Figure 4.16 Venn diagram indicating number of genes differentially expressed by PHCl treatment. (A) Time of incubation 4 hours and (B) 24 hours. Red circle represents genes regulated by concentration 25 mM. Blue circle represents genes regulated by concentration 5 mM.

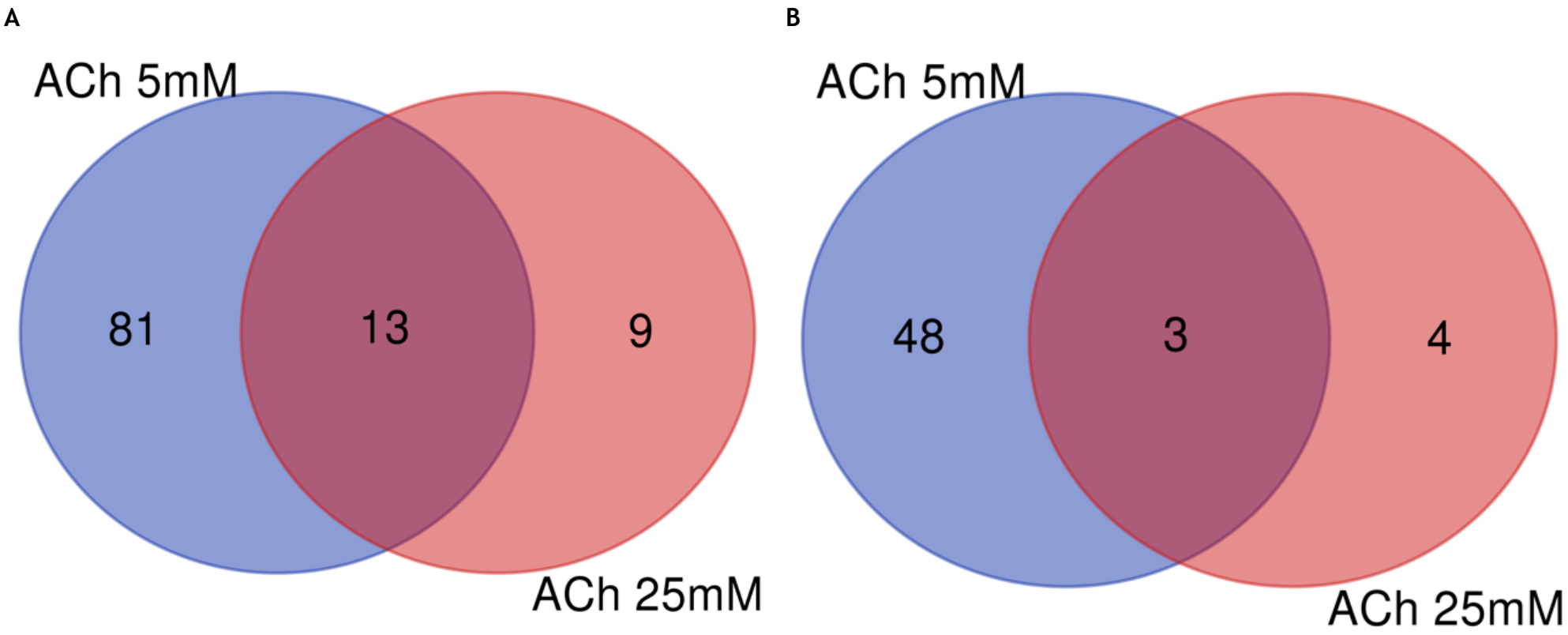

Figure 4.17 Venn diagram indicating number of genes differentially expressed by ACh treatment. (A) Time of incubation 4 hours and (B) 24 hours. Red circle represents genes regulated by concentration 25 mM. Blue circle represents genes regulated by concentration 5 mM

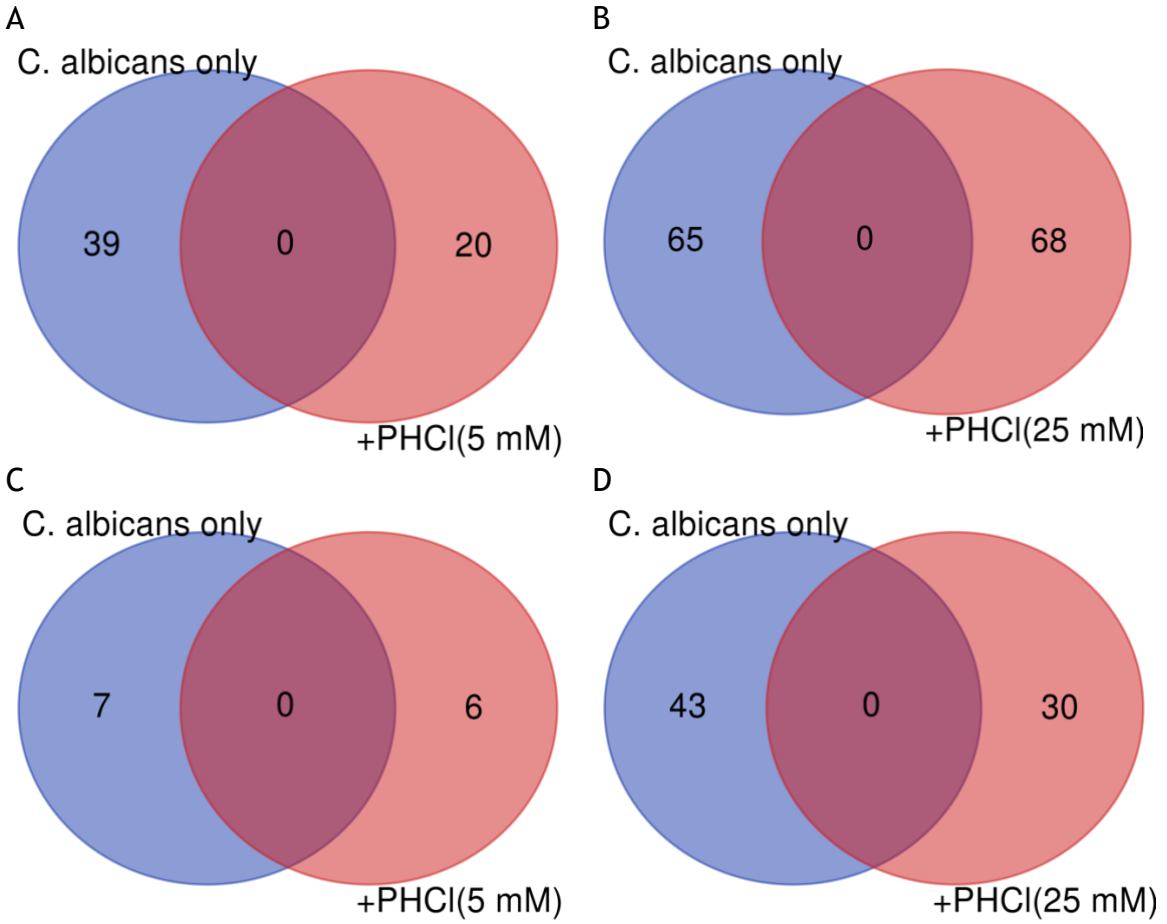

Figure 4.18 Venn diagram indicating number of genes differentially expressed by PHCl treatment. (A) and (B) Time of incubation 4 hours. (C) and (D) 24 hours. Red circle represents genes regulated by treatment. Blue circle represents genes regulated in *C. albicans* only.

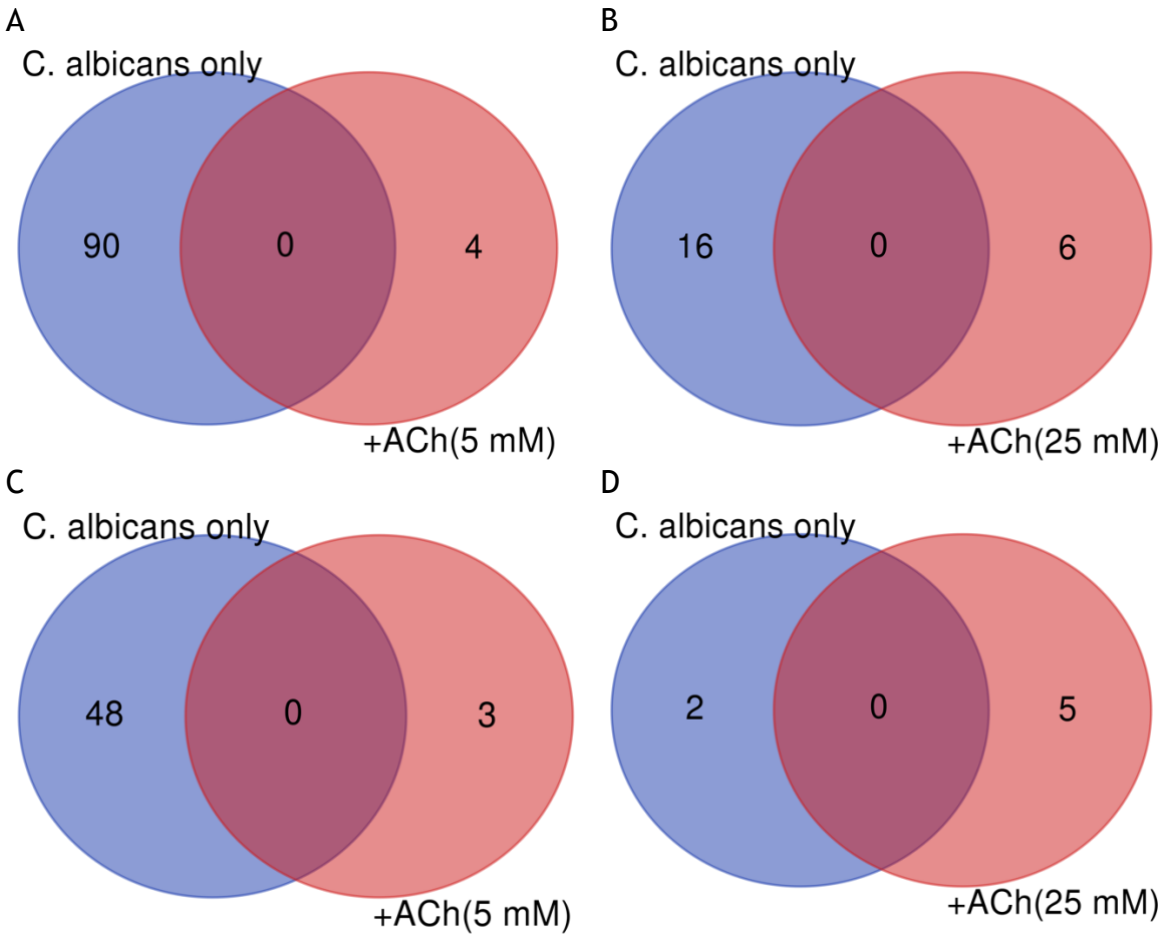

Figure 4.19 Venn diagram indicating number of genes differentially expressed by ACh treatment. (A) and (B) Time of incubation 4 hours. (C) and (D) 24 hours. Red circle represents genes regulated by treatment. Blue circles represent genes regulated in *C. albicans* only.

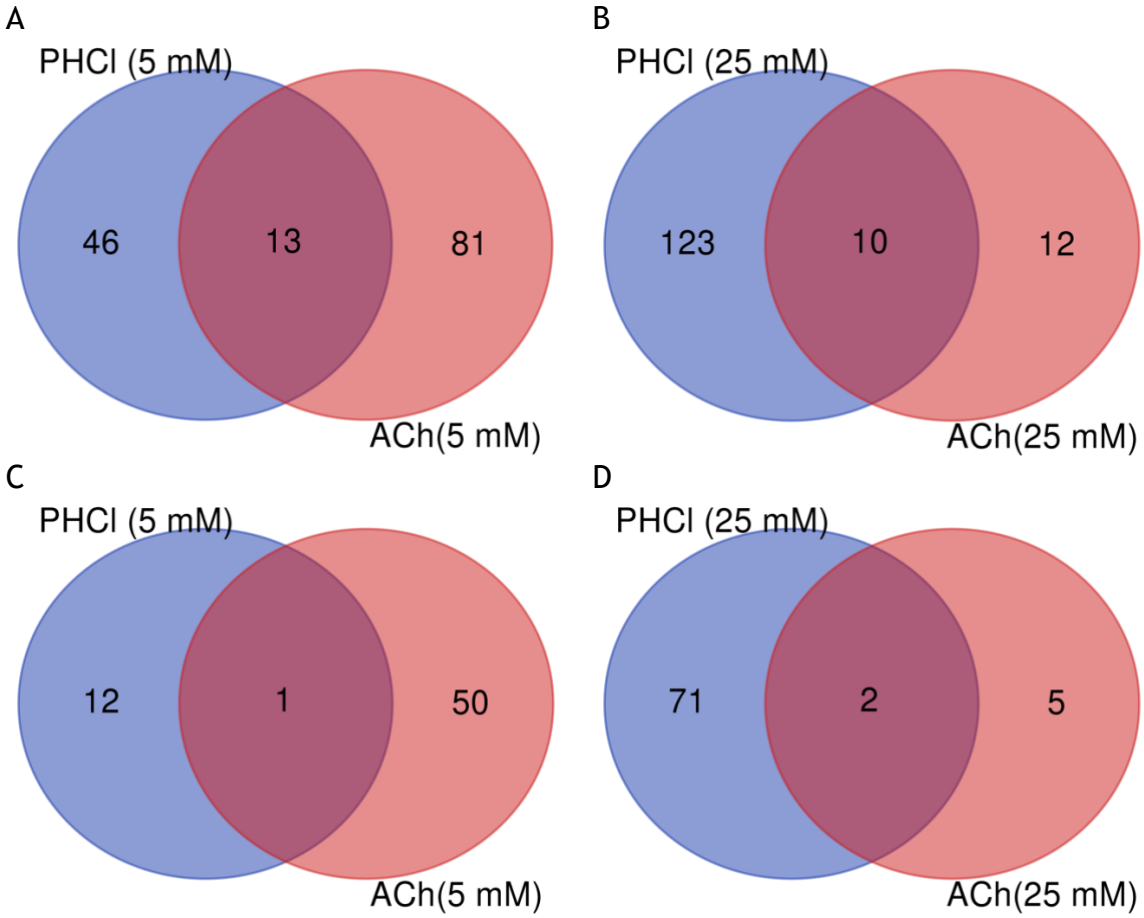

Figure 4.20 Venn diagram indicating number of genes differentially expressed by PHCl and ACh treatment. (A) and (B) Time of incubation 4 hours. (C) and (D) 24 hours. Red circle represents genes regulated by ACh treatment. Blue circles represent genes regulated by PHCl treatment.

Table 4.9 List of regulated genes overlapping between both treatments at different biofilm formation stages and concentrations.

Regulation	4 hours		24 hours	
Upregulated	5	25	5	25
	C4_05730W_A		*FET99*	
	RBR1			HSP30
	CFL4	*C7_03560W_A*		
Downregulated	*GIT4*			
	CR_01910C_A			
	PHO89			
	PGA34			
	GIT1			
	PLB1			
	C1_05950C_A	*C4_00530C_A*		
	MET3			
	C3_02330C_A			
	OPT4			

4.4 Discussion

C. albicans, the opportunistic fungal pathogen is a leading cause of bloodstream and life-threatening infections, with up to 50% mortality rate (Kuloyo et al., 2020). The characteristic of morphogenesis and biofilm formation possessed by *C. albicans* confer the fungus advantages of adaptation and surviving stressors posed by the environment; such as host immune response evasion and antifungal treatment resistance (Ciurea et al., 2020). In recent studies, it was reported that the general cholinergic receptor agonist ACh and the general muscarinic receptor agonist PHCl successfully inhibited the yeast to hyphae transition and biofilm formation (Nile et al., 2019, Rajendran et al., 2015). Yet, the molecular regulatory mechanisms behind these inhibitory effects remain unclear. Therefore, RNA sequencing was utilized to explore these possible molecular mechanisms. *Candida albicans* cells were exposed to different concentrations of ACh or PHCl for 4 and 24 hours before processing for RNA sequencing.

4.4.1 Genes upregulated by PHCl at 4 hours of biofilm formation

C. albicans treatment with PHCl and ACh, revealed that time of incubation has the largest impact on variables, followed by the treatments themselves. Data outlined in this chapter unravelled the molecular regulation behind the inhibitory effect of PHCl treatment during the early and maturation stages of biofilm formation. During the early stages of biofilm formation, PHCl upregulated cell wall related genes such as those involved in cell substrate adhesion and cell wall organization. For instance, genes such as *Mnn1* and *Mnn41*, which are involved in glycosylation, an important process for cell wall integrity, adhesion, virulence, and host-pathogen interactions (Bates et al., 2013, Wagener et al., 2012, Dutton et al., 2014). In addition, genes involved in cell wall integrity and remodeling and cell separation were also upregulated. These included the glycosidases, such as *KRE6, CHT3, SIM1, SCW11,* and *XOG1* and genes expressing cell wall proteins such *as RBR1, SCW11, PHR2, ALS4,* and *YWP1* (Sorgo et al., 2013).

In response to environmental conditions, *C. albicans* changes the protein secretome composition considerably which can be an indicative of the growth

morphology. For example, some of the cell wall proteins were found to be more enriched in yeast culture media representing the yeast secretome such as *PIR1, RBE1, SIM1, SCW11,* and *XOG1* (Sorgo et al., 2010). The gene *RBR1* encodes Glycosylphosphatidylinositol (GPI)-anchored cell wall protein, and *PHR2*, encodes beta glucan crosslinking glycosidase and are both regulated by Rim 101. Both genes are expressed at acidic pH levels and repressed by Rim101 at alkaline pH levels. Deletion of *rbr1Δ* led to filamentation defects when grown on M-199 soft agar media at pH 4.5 for 3 days. However, at pH 7.4 after 5 days incubation hyphae formation was observed (Lotz et al., 2004, Mühlschlegel and Fonzi, 1997, Chen et al., 2020). Thus, the upregulation of those genes by PHCl may indicate a reduction in pH levels and yeast form of growth which is the favourable growth form at lower pH levels.

The gene *PHR2* is a homolog of *PHR1*, and both encode proteins which play key roles in pH balance required for *C. albicans* growth at different ambient pH ranges. Higher pH levels promote hyphal growth of *C. albicans* whilst lower pH levels promote yeast cell growth. The *PHR1* gene is more expressed under alkaline conditions (pH 5.5 or higher) whilst *PHR2* is expressed under acidic conditions (pH 5.5 or lower). Research undertaken by Mühlschlegel and Fonzi (1997), revealed that cells that lack the *phr2Δ* gene ceased growth entirely after few hours of incubation at pH 4 which indicates a direct necessity and association of the expression of this gene for growth at such low pH levels. In addition, the lack of *phr2Δ* gene activity led to changes in cell wall structure by exposing the cell wall recognition sites to be more detectable to the host immune cells (Calderon et al., 2010, Bensen et al., 2004, Mühlschlegel and Fonzi, 1997).

The yeast cell wall protein, Ywp1, is known to promote yeast cell dispersion and it's expression is increased during the exponential growth phase and when phosphate concentration is low. In contrast, it's expression decreases upon filamentation and in the stationary growth phase. Cells that lack the *ywp1Δ* gene have demonstrated increased adhesion and biofilm formation capabilities; thus *YWP1* is considered to encode a yeast specific cell wall protein (Granger et al., 2005) and has been shown to play a partial role in regulating adhesion during the later stage of biofilm formation and dispersion during the early stages (McCall et

al., 2019). In this study, *YWP1* was upregulated in the presence of PHCl which reflects the growth phase and morphology of *C. albicans* driven by the treatment. This is also consistent with conclusion drawn from the upregulation of the genes mentioned above.

The cell wall proteins, Als4 and Als2 encode agglutinin like sequence proteins and upregulated expression is more associated with acidic pH levels (Klis et al., 2009, Sosinska et al., 2011). The Als surface protein family are known to be implicated in *C. albicans* pathogenicity and biofilm formation, mainly via facilitating adhesion to surfaces. Yet, various studies have shown that the genes of this family are expressed differently depending on the growth conditions and growth phase, which may indicate a compensatory role of these proteins. For example, while the loss of *als4Δ* had no effect on adhesion to an oral reconstituted human epithelium (RHE), epithelial cells, or biofilm formation in a catheter model, it reduced germ tube formation in RPMI-1640, and adhesion to vascular endothelial cells. On the other hand, although *als2Δ* loss reduced germ tube formation, it had no effect on adhesion to buccal epithelial cells (BEC) (Zhao et al., 2005, Nobile et al., 2008, Hoyer et al., 1998). In this study, although *ALS2* and *ALS4* were upregulated in the presence of PHCl, it did not aid the filamentation of *C. albicans*. This might be due to the significant downregulation of *ALS3* in the presence of PHCl, which is known to be hyphae associate gene. The compensatory role of Als surface proteins family members may explain the opposing regulations of those members by PHCl treatment. In this study the upregulation of *ALS2* and *ALS4* might be more related to yeast form adherence and aggregation than filamentation. For example, anti Als4 monoclonal antibodies immunolabeling studies showed that *Als4* expression was more associated with the yeast form. It was found that copious amount of Als4 cover the yeast cells surface with more abundance in cells grown at 30°C, which is the temperature preferred by yeast form. In contrast, Als3 was found to coat hyphae intensively but was not detectable on yeast cells (Song et al., 2011, Coleman et al., 2012).

In this study, PHCl treatment reduced *C. albicans* filamentation significantly, however it had no cytotoxic effects and *C. albicans* maintained the growth in the yeast form. The ability of *C. albicans* to circumvent the stress of PHCl in the

media might be attributed to the upregulation of ATP-binding cassette (*ABC*) superfamily member genes, *Candida* drug resistance-1 (*CDR1*) and -2 (*CDR2*). Cdr1 and Cdr2 are multidrug transporters that play a role in *C. albicans* virulence and resistance by acting as drug efflux pumps. Their upregulation is one of the most observed in azole resistance mechanisms in *C. albicans* clinical isolates (de Micheli et al., 2002). Interestingly, a recent study by Maras (2021), has revealed unexpected behaviour conferred by clinical isolate 1 (CI1) of *C. albicans* where hyperexpression of *CDR1* and *CDR2* resulted in a less virulent phenotype and a decrease in lethality in a *Galleria mellonella* infection model. Furthermore, the gene encoding the secretory protein Dag7 was upregulated by PHCl treatment. This has been shown to be involved in *C. albicans* protection against toxicity and cell wall remodeling and integrity. The upregulation of this gene was found to lower the sensitivity of yeast cells to toxic sterol analogues (Bandara et al., 2020, Sorgo et al., 2011). Similarly, *DAG7* has been shown to be one of the core pH responsive genes, which was significantly upregulated at pH 4 and was involved in cell wall remodeling (Cottier et al., 2019). Concomitant to the upregulation of *CDR1* and *CDR2*, the 7-transmembrane receptor protein gene, *RTA3* was also significantly upregulated. Rta3 is a protein similar to the G-protein-coupled receptors (GPCR) and is unique to the fungal kingdom. It is known to be involved in *C. albicans* azole resistance and the regulation of optimal asymmetric lipid distribution in the plasma membrane. Although *RTA3* was suggested to play a regulatory role in governing biofilm formation, the upregulation of this gene by PHCl did not enhance filamentation (Whaley et al., 2016, Rizzo et al., 2019, Srivastava et al., 2017). Taken together, the upregulation of those genes observed in this study equipped *C. albicans* with the required response to survive growing under the potential stress posed by PHCl treatment.

One of the most significant family of extracellular hydrolytic enzymes of *C. albicans* are the secreted aspartyl proteinases (Sap). The Sap family is encoded by 10 *SAP* genes, that are differentially expressed during *C. albicans* infection and implicated in it's virulence, mainly through nutrition acquisition, invasion, host immune response evasion, and tissue damage. Given the versatility of SAP proteins, their expression varies according to factors such as pH, progress of infection, type of infection, and site of infection. Although of the 10 genes, *SAP4*

- *SAP6* were found to be more associated with hyphal formation, *SAP4* - SAP6 are not required in oral mucosal infections which were suggested to be reliant on expression of *SAP1 - SAP3* (Naglik et al., 2003, Jackson et al., 2007, Staib et al., 2000). The data herein showed contradicting results, whilst PHCl treatment reduced filamentation *SAP4* and *SAP7* were upregulated and *SAP5* was downregulated. This observation might be due to the compensatory function amongst the Sap protein family where the downregulation of one is compensated by the upregulation of the other (Naglik et al., 2003).

Other biological processes that were upregulated during the early stages of biofilm formation during PHCl treatment is cellular metal ion homeostasis processes, such as transition metal ion homeostasis. Metals such as iron, copper, and zinc are essential factors for *C. albicans* virulence, especially iron as it is considered to be the most abundant micronutrient implicated with diverse cellular processes in *C. albicans*. Yet, high levels of iron can be toxic, and thus maintaining intracellular iron in equilibrium is vital for *C. albicans* survival (Gerwien et al., 2018). Of the upregulated genes by PHCl, a number of genes were involved in iron regulation such as, *CFL4*, C-terminus like ferric reductases, *FET99*, Multicopper oxidase, and *FRE10*, a major cell surface ferric reductase. *FRE10* plays a role in the reductive iron uptake system in *C. albicans* by reducing free iron at the cell surface to the soluble ferrous form. Research conducted by Jeeves et al. (2011), revealed that the expression of *FRE10* in iron restricted conditions was lower in the hyphae form than the yeast form. The ferric reductase *FRE10* expression is regulated by the transcription factor Tup1, a regulator known to be also involved in regulating filamentation repression in non-hyphae inducing conditions (Jeeves et al., 2011). It is interesting to speculate that the upregulation of this gene by PHCl in our data may be an indicative of the dominant form of growth resulted by the treatment. As suggested by Jeeves et al. (2011), the decrease in *FRE10* expression in the hyphae form might be due to the importance of the reductive iron uptake mechanism for yeast cells and the availability of other mechanisms for iron acquisition in hyphae as a primary source; such as the expression of the ferritin receptor *ALS3*. Als3 was less abundant in iron depleted conditions, and in the data presented here this gene was significantly downregulated after treatment with PHCl, which might be a clue of iron deficiency (Duval et al., 2020). It also

may indicate the abundance or the accessibility of free iron in the surrounding environment, which is utilized by the reductive iron uptake system.

Iron in the environment mainly presents in it's ferrous form which is more soluble at low pH and the ferric form is less soluble at neutral pH (Gerwien et al., 2018, Fourie et al., 2018). This observation agrees with the previous genes' regulation by PHCl treatment, which indicated an acidic pH environment and conditions more favourable for yeast cell growth. Further investigations are required to elucidate whether PHCl treatment results in iron repletion or depletion, especially knowing that FRE10 has been reported to be induced under both iron depleted or repleted conditions (Baek et al., 2008, Duval et al., 2020). One possibility is that PHCl treatment might be challenging *C. albicans* filamentation by imposing excess of free iron which stresses the fungus through reactive oxygen species (ROS) formation. Another possibility is that PHCl results in iron depletion which imposed the increase of ferric reductases genes expression. Furthermore, the vacuolar transporter *CCC1*, was upregulated which has been shown to play a role in maintaining intracellular iron balance via promoting vacuolar storage of iron. In this context, PHCl might also have played a role as a chelator molecule resulting in iron deprivation and thus restricting the availability of iron for *C. albicans*. The mechanism of micronutrients sequestration such as iron and metal ions was presented in the literature as an antifungal mechanism exerted by the host innate immune system (Fourie et al., 2018, Puri et al., 2019). In general, PHCl treatment might have resulted in iron homeostasis perturbation which imposed a challenging growth condition to *C. albicans* that is more adaptable for the yeast form compared to hyphal form. This has been observed in previous research, where *C. albicans* yeast were found to cope more with a wider range of changes in iron conditions. It was also noted that higher rates of iron were imported in the filamentous form, and it was suggested that hyphae require continual importation of iron (Duval et al., 2020).

4.4.2 Genes downregulated by PHCl at 4 hours of biofilm formation

During the early stages of biofilm formation, 5 and 25 mM PHCl resulted in the downregulation of crucial genes related to *C. albicans* morphogenesis and pathogenesis. For example, disturbing phosphate uptake and causing a

perturbation in phosphate homeostasis by downregulating genes involved in the phosphate-responsive signaling pathway (PHO) pathway; which plays a role in phosphate sensing, acquisition, and homeostasis (Lev and Djordjevic, 2018). Yet, further investigations are required to test if PHCl has a direct downregulation effect on PHO pathway genes or that the observed downregulation is due to the extensive biofilm formation by untreated *C. albicans* which may result in phosphate starvation. Phosphorous is an essential element that participates in many important biological cellular processes such as growth, organelle development, cell wall and membrane biosynthesis, ribosomal translation and biogenesis, DNA replication, chromosome development and energy storage. In addition, phosphate metabolism is important for metal homeostasis and stress resistance to pH, nitrosative and oxidative conditions and cationic stress, all of which can mediate *C. albicans* virulence (Liu et al., 2017, Urrialde et al., 2016, Köhler et al., 2020). The genes involved in phosphate homeostasis include: *PHO89, PHO84, PHO100*, and genes encoding phosphate permeases and transporters such as *FGR2*, filamentous growth regulator and a putative phosphate transmembrane transporter (Uhl et al., 2003). Deletion of the gene *fgr2Δ* resulted in reduced filamentation (Wang et al., 2021). For instance, *PHO100* was found to be downregulated by PHCl treatment and it has been reported that the *pho100Δ* deletion resulted in fungus virulence attenuation (Köhler et al., 2020). In addition, *PHO84,* plays a role in the Target of Rapamycin Complex1 (TORC1) pathway. This pathway coregulates nitrogen acquisition during nitrogen starvation and thus regulates morphogenesis in *C. albicans*. It is also essential for *C. albicans* growth in phosphate reduced media. *C. albicans* cells that lack *pho84Δ* were defective in virulence, hyphal growth, cell wall biosynthetic enzymes, and were hypersensitive to oxidative stress and cell wall stress (Köhler et al., 2020, Ikeh et al., 2017).

In this study, PHCl treatment resulted in downregulation of genes involved in host defence evasion such as *CR_01920W_A* and *CR_01910C_A*, which are involved in biotin biosynthesis. Biotin is a necessary nutrient for *C. albicans* hyphal growth and it's homeostasis is important for phagocytosis evasion (Sprenger et al., 2020). In addition, downregulation of GPI- anchored proteins, such as: Pga26, Csp2, and Exg2, can reduce cell wall regeneration and integrity. The *C. albicans* cell wall is an important virulence factor as it is the contact with

the ambient environment mediating adhesion, invasion, and host pathogen interactions (Laforet et al., 2011). For example, Laforet et al. (2011), revealed that *pga26Δ* deletion resulted in cell wall defects that led to yeast to hyphae switching imbalance and rendered the fungus weaker in terms of dissemination and infection. Although a *pga26Δ* mutant increased azole and amphotericin B sensitivity, it decreased caspofungin sensitivity. A rapid increase in filamentation and biofilm mass was observed, however this mutant displayed attenuated virulence and dissemination in a mouse model of candidiasis, which is a stage of biofilm formation more linked to the yeast form. Furthermore, no major structural changes in the cell wall were observed (Laforet et al., 2011).

Pilocarpine hydrochloride treatment also downregulated hyphal specific genes during the early stages of biofilm formation; such as *ECE1*, *HWP1*, and *IHD1* genes which are all involved in the filamentation process. These genes belong to the core filamentation response genes that are stimulus-independent filamentation associated genes. The GPI anchored protein induced during hypha formation, IHD1, is considered the centre of the core filamentation response genes. The hyphal cell wall protein (Hwp1) is required for filamentation and adherence to epithelial cells, and cells lacking this gene are defective in adherence (Martin et al., 2013, Wächtler et al., 2011). Candidalysin (*ECE1*), the cytolytic toxin peptide, plays a critical role in *C. albicans* pathogenicity, virulence, and promotes host tissue damage (Moyes et al., 2016, Swidergall et al., 2019). In agreement with data presented here, the genes *ECE1* and *IHD1* were also downregulated by *N*-[3-(allyloxy)-phenyl]-4- methoxybenzamide (compound 9029936), which is a small molecule inhibitor of filamentation (Martin et al., 2013, Romo et al., 2019). Downregulation of hyphal specific genes such as *ECE1* and *IHD1* might be an indication of low ambient pH. Previous studies showed that neutral and alkaline pH levels trigger yeast to hyphae transition and induced expression of hyphal regulator genes (Desai, 2018, Kadosh and Johnson, 2005, Bensen et al., 2004). Similarly, a study by Naseem et al. (2015) revealed that although a triple mutant lacking genes involved in *N*-acetylglucosamine (GlcNAc) metabolism displayed hyphal formation at low pH, the hyphal specific genes were not induced until the media was buffered to pH 7. The evidence from the literature supports the findings in this study which

highlights a proposed increase of the acidity level upon PHCl treatment and the downregulation of filamentation and biofilm formation associated genes.

Among the genes that were downregulated by PHCl treatment, genes involved in filamentation process such as *SAP5* and *PLB1* were also of interest. The phospholipase B gene, *PLB1,* is an important virulence factor in *C. albicans* pathogenesis and aid in host tissue invasion. It has been shown that *PLB1* activity is associated with increased virulence of *C. albicans* in a disseminated candidiasis murine model and mutations in this gene result in significant attenuation of virulence in a haematogenously disseminated candidiasis murine model (Mukherjee et al., 2003). The aspartyl protease, *SAP5,* is a member of the Sap family proteins and considered as a biofilm specific marker (Winter Michael et al., 2016). It is known to play a role in *C. albicans* hyphal formation, adherence, and host penetration. Although triple null mutants in *C. albicans* lacking *sap4, sap5,* and *sap6* were capable of filamentation, they exhibit strongly reduced invasiveness which indicates the importance of hypha formation along with those enzymes for full invasiveness characteristics. In addition, mutants lacking those genes are rendered more susceptible to phagocytosis, and this may indicate a role of *SAP* in host immune evasion (Naglik et al., 2003).

Treatment with PHCl was found to downregulate transmembrane transporter activities that facilitate nutrient transportation in *C. albicans*. This included genes such as *OPT4, ZRT1*, and *GIT4*. The glycerphosphocholine transporter *GIT4, is* required for glycerphosphocholine transportation which can be utilized as sole nutrient source of phosphate, and loss of glycerphosphocholine transportation can reduce virulence (Bishop et al., 2013). Another transporter, *OPT4*, the oligopeptide transporter is involved in peptide transportation to be utilized as a sole nitrogen source (Braun et al., 2005). In addition, the zinc transporter, *ZRT1*, which functions at pH 7 levels and above is important for *C. albicans* viability and virulence (Volkova et al., 2021).

Additionally, PHCL was shown in this study to downregulate other genes known to be linked to *C. albicans* pathogenicity and stress responses such as: *HSP21, PRA1, SOD5, SOD6. PRA1* is pH- regulated antigen 1 which is considered as a secreted zinc-binding protein and also plays a role in immune evasion (Wilson et

al., 2016). Superoxide dismutases are known to be critical to reduce the effect of oxidative stress. A *SOD5* mutant strain of *C. albicans* resulted in more susceptibility to eradication by reactive oxygen species released by neutrophils and macrophages (Gleason et al., 2014). Another study by Martchenko et al. (2004), has revealed that *SOD5* was upregulated during the yeast to hyphae transition and highly expressed in the hyphal form. Thus, *SOD5* is a hyphal induced gene, while *SOD4*, which was upregulated by PHCl, is expressed in yeast cells (Martchenko et al., 2004, Dantas et al., 2015). Genes involved in transmembrane transporter activities were also downregulated by PHCl treatment such as *RTA4*, fatty acids transporter, *SUL2*, sulfate transporter, and *PHO84*, phosphate transporter, thus limiting the availability of essential nutrients sources alternative to sugars (Lan et al., 2002, Miramón and Lorenz, 2017).

In relation to iron acquisition, some genes downregulated by treatment with PHCl have previously been shown to be related to the hyphal form of growth such as *FRP2, HMX1, and CSA2*. *FRP2* is a putative ferric reductase and has been shown to be induced during the invasion phase (Chen et al., 2013). *HMX1* is a heme oxygenase that plays an important role in candidemia pathogenesis in a mouse model and expression is induced under iron deprivation conditions (Navarathna and Roberts, 2010). Csa2 is an extracellular heme binding protein which is involved in iron acquisition from hemoglobin by *C. albicans* during hyphal growth (Okamoto-Shibayama et al., 2014). Transcriptomic profiling revealed that many cell wall genes were found to be involved in upregulating these pathways, such as Glycosylphosphatidylinositol (GPI)-anchored adhesins, enzymes, proteins encoding receptors, proteins with unknown functions, multidrug transporters, and ion transporters (Tables 4.1 and 4.2).

4.4.3 Genes upregulated by PHCl at 24 hours of biofilm formation

During the maturation stages of biofilm formation (24 hours), PHCl upregulated amine metabolic processes, branched chain amino acid biosynthetic processes, metal ion transition transport and homeostasis, copper ion binding, oxidoreductase activity, and ergosterol biosynthetic processes. At 24 hours of incubation, a number of genes involved in ergosterol biosynthesis were

upregulated such as *ERG6*, the Delta(24)-sterol C-methyltransferase, and *ERG 24*, a C-14 sterol reductase. Ergosterol is an essential component of the *C. albicans* cell membrane that provides integrity, rigidity, and fluidity to the fungus. Interestingly, previous studies have shown that ergosterol levels are significantly reduced at 12-30 hours of biofilm formation compared to the early stages (0-11 hours). This was correlated with reduced expression of ergosterol biosynthetic genes such as *ERG6* which is upregulated by the treatment herein (Lv et al., 2016). Furthermore, amino acids biosynthesis genes were also upregulated by the treatment such as the Ketol-acid reductoisomerase, *ILV5*, and the Isopropyl malate dehydrogenase. Amino acids can serve as an abundant source for nitrogen and carbon for *C. albicans* (Garbe and Vylkova, 2019).

4.4.4 Genes downregulated by PHCl at 24 hours of biofilm formation

The following biological functions, aspartic type endopeptidase activity and cell wall organization were down regulated by the treatment with PHCl for 24 hours. Additionally, the agglutinin like sequence protein (Als3) was downregulated by PHCl treatment. This protein is hyphae associated and forms one of the core filamentation response genes involved in *C. albicans* virulence and biofilm formation in multiple ways. *ALS3* mediates adherence, which is an essential step of colonization and biofilm formation. It is also an invasin expressed on the hyphal surface to bind host cell receptors upon endocytosis which facilitate the invasion of the fungus into the host tissue. *ALS3* can also mediate iron acquisition from the host by acting as a ferritin receptor. Finally, *ALS3* contributes to biofilm architecture and antifungal resistance. Moreover, *ALS3* is highly expressed by hyphae in a mouse model of disseminated candidiasis and oropharyngeal candidiasis. A mutant that lacks this gene has been shown to exhibit reduced adherence to epithelial and endothelial cells, reduced ability to cause host cell damage and rendered the fungus more susceptible to fluconazole, miconazole, and amphotericin B, (Martin et al., 2013, Liu and Filler, 2011, Mayer et al., 2013, Liu et al., 2021).

4.4.5 Genes upregulated by ACh treatment

Acetylcholine treatment during the early stages of biofilm formation caused upregulated expression of genes involved in the following biological functions: oxidoreductase activity, ubiquitin, and protein neddylation which is the process of post translational protein modification (Rabut and Peter, 2008). At the maturation stage of biofilm formation ACh caused upregulated expression of genes involved in hydroxymethylpyrimidine kinase activity, secondary active sulfate transmembrane transporter activity and ferroxidase activity. Although fewer signaling pathways were upregulated by ACh compared to PHCl treatment, some of the important genes that were upregulated were involved in sulfate transportation, filamentation, adhesion, and metal ion transportation and homeostasis such as *SUL2, RBR1, C4_05730W_A, FET99, PGA10, and CFL4*. ACh treatment also upregulated *HRT1*, which is a component of a nuclear ubiquitin-protein ligase complex. Ubiquitin is a protein that is implicated in cell cycle and proteostasis. These processes are known to play a role in modulating *C. albicans* nutrient adaptation and morphogenesis signaling pathways through mediating target protein degradation. Previous research showed that farnesol inhibited hyphal growth in *C. albicans* via blocking the ubiquitin ligase (*Ubr1*) mediated degradation of the transcriptional repressor Cup9. The Skp1-Cullin-F-box (SCF) ubiquitin ligase complex is one of the ubiquitin system of ligases that are involved in cell cycle and filamentation. In *S. cerevisiae*, this complex can target *TEC1*, a hyphae gene regulator, for degradation and thus preventing pseudohyphal growth. In *C. albicans*, the depletion of the polyubiquitin gene (*UBI4*) induced hyphal formation with abnormal nuclear segregation patterns. Targeting this gene for deletion on the other hand attenuated *C. albicans* virulence in a mouse model (Yang et al., 2020, Hossain et al., 2021, Hossain et al., 2020). Ubiquitination pathways in *S. cerevisiae* mediate assimilation of alternative carbon sources that can be used when glucose has been exhausted. On the contrary, in the presence of glucose, *C. albicans* can assimilate alternative carbon and glucose sources simultaneously. Interestingly, the addition of a ubiquitination site to *C. albicans* isocitrate lyase (*ICL1*) reduced it's metabolic flexibility by reducing it's ability to assimilate lactate and glucose simultaneously, which attenuated *C. albicans* colonization and virulence (Childers et al., 2016, Sandai et al., 2012).

4.4.6 Genes downregulated by ACh treatment

Downregulated biological processes induced by the treatment with ACh included organophosphate ester transmembrane transporter activity, cellular amino acid biosynthetic process, monovalent inorganic cation transport, glycerolipid metabolic process, asparate family amino acid biosynthetic process, glycerophsphodiester transmembrane transporter activity, magnesium ion binding, sulphur compound biosynthetic process and symporter activity. ACh treatment downregulated the NADH ubiquinone oxidoreductase (complex I) by targeting genes such as *NAD2* and *NAD5* which are involved in mitochondrial respiration. Recently, it has been shown that dysfunctionality of complex I can promote fungal cell death via mitochondrial ROS accumulation. In addition, deletion of proteins that regulate complex I can result in respiration and virulence deficiencies (Duvenage et al., 2019). In relation to NAD biosynthesis in *C. albicans*, nicotinic acid transporters were also one of the top 10 significantly downregulated genes by ACh, which indicates the involvement of this metabolite in the filamentation process. Research by Gunasegar et al. (2019), revealed that although exposure to high concentrations of nicotinic acid could inhibit fungus metabolism and decrease growth rate, at lower concentrations, it enhanced the attachment, biofilm formation, and the expression of adherence associated genes such as *HWP1* and *ALS3* (Gunasegar and Himratul-Aznita, 2019).

In opposition to the finding above, which demonstrated upregulation of a number of ubiquitination ligase complex genes with ACh treatment, the study also revealed that a significant number of downregulated genes were related to protein homeostasis and ubiquitination;such as *C1_02300W_A*, cytoskeleton organization protein, *C7_01360C_A*, putative heat shock protein required for protein import into mitochondria, and *C2_01320W_A*, protein with structural molecule activity and role in proteasome assembly, ubiquitin-dependent protein catabolic process. In addition, genes involved in ubiquinol-cytochrome-c reductase, ubiquitin conjugating enzyme activity, and ubiquitin C-terminal hydrolase such as *QCR7, C1_12650C_A, and C1_06390W_A*, respectively. Other genes downregulated by the treatment were involved in respiration and mitochondrial processes such as *TIM9*, that encodes a protein of the mitochondrial intermembrane space, and *C1_12640W_A*, which plays role in

mitochondrial respiratory chain complex assembly and proteolysis and mitochondrial inner membrane peptidase complex localization.

ACh also downregulated biological functions of importance to fungal pathogenicity such as glycerolipid and phospholipid metabolic processes, amino acids and sulfur biosynthetic processes. Compared to PHCl treatment, ACh negatively regulated pathways implicated in cell cycle, proteostasis, protein import, or protein transmembrane transporter activities. Although perturbation of proteostasis can induce filamentation, intriguingly the downregulation of genes linked to this process by ACh resulted in hyphal growth inhibition. It has been shown in previous research that pharmacological inhibition of the proteasome resulted in filamentation, yet the formed hyphae exhibit aberrant cellular morphology, defective septum formation, and nuclear segregation (Hossain et al., 2021). Downregulated proteins with similarity to acyl-coenzyme-A-binding (*ACB1*), and N-acetylglucosaminylphosphatidylinositol deacetylase activity (*C1_10320W_A*) are of importance in *C. albicans*, growth, viability, and virulence. For instance, the latter has been shown to be implicated in Glycosylphosphatidylinositol (GPI) biosynthesis, which include a diverse set of proteins that are involved in cell wall maintenance and biogenesis, immune response evasion, and hypha specific proteins. Furthermore, the reduction in it's activity was correlated with cell wall defects, filamentation defects, loss of host recognition molecules, virulence factors loss and increased susceptibility to cell wall targeting drugs (Yadav et al., 2018, Yadav et al., 2014).

Numerous downregulated genes after exposure to ACh were implicated in mitochondrial function and respiration. Mitochondria play a critical role in cellular metabolism, it is essential for *C. albicans* virulence to maintain mitochondrial integrity and functionality. Perturbations in those functions can reduce virulence, growth rates, and carbon source utilization. It can also negatively affect the cell wall and membrane structure and composition, morphogenesis, biofilm formation, and interaction with host. For instance, loss of electron transport chain components resulted in reduced virulence in the *G. mellonella* infection model, where loss of any one component of the electron transport chain attenuated virulence. *C. albicans* with respiration-deficient mitochondria were unable to grow on non-fermentable carbon sources and it

formed smaller colonies compared to normal cells due to the lower cell division rates. In addition, disruption in mitochondrial function increased tolerance to the antifungal amphotericin B (Sun et al., 2019, Mamouei et al., 2021, Geraghty and Kavanagh, 2003).

4.4.7Gene regulation overlapping between PHCl and ACh

In this study the transcriptome of *C. albicans* was investigated in the presence and absence of ACh and PHCl, to attempt to characterize the type of receptors and signaling pathways that mediate their action. Both compounds are characterized as cholinergic agonists. However, ACh can bind to both muscarinic and nicotinic receptors and PHCl is a general muscarinic receptor agonist (Carlson and Kraus, 2020, Nile et al., 2019, Rajendran et al., 2015). The data presented in this chapter revealed various similarities and differences in the transcriptomic profile of *C. albicans* under the different treatments discussed below.

C. albicans is equipped with complex signaling pathways that mediate the fungus flexibility to adapt to various environmental cues (Lotz et al., 2004). Those signaling pathways may converge, integrate, or intersect to regulate *C. albicans* growth and morphogenesis through expression of different regulators such as *NRG1*, *RIM101*, and *HAP43*. At 4 hours of biofilm formation, both treatments upregulated the adhesin like protein, (*C4_05730W_A*), and the Glycosylphosphatidylinositol (GPI)-anchored cell wall protein (*RBR1*) when used at concentrations of 5 and 25 mM, while *CFL4* was upregulated at 4 hours by 5 mM of both treatments. *CFL4* is repressed by *HAP43* and involved in iron transport and uptake has been shown to be one of the predominant upregulated genes in dispersed cells. The cell wall protein gene, *RBR1* as discussed previously is of importance in filamentous growth and it's expression is required under acidic conditions. Yet, it's upregulation did not cease or hinder the inhibitory effect of hyphal growth by any of the treatments. The previous observation might be due to what Lotz et al. (2004), proposed in his work which revealed that the transcriptional repressor of hyphal growth NRG1 was required for *RBR1* expression. Nrg1 protein targets the transcriptional factor Tup1 for repression of

genes involved in *C. albicans* virulence including hypha specific genes and yeast to hyphae transition process (Murad et al., 2001).

RBR1 and *C4_05730W_A* are *HAP43* induced, which is a repressor induced under low iron conditions. Although *HAP43* is not required for iron acquisition, it is essential for *C. albicans* growth under iron depleted conditions. It is responsible for repressing iron- dependent proteins involved in mitochondrial respiration and iron-sulphur cluster assembly. At 24 hours of biofilm formation, both treatments upregulated *FET99* at concentration of 5 and 25 mM, which is expressed in low iron conditions and involved in regulation of iron homeostasis. *FET99* mutation has been shown to result in significant growth and metabolic reduction in *C. albicans* (Uppuluri et al., 2018, Hsu et al., 2011, Mamouei et al., 2017, Mochochoko et al., 2021).

Both treatments using both concentrations at 4 hours of biofilm formation downregulated several biological processes such as the putative dethiobiotin synthetase (*CR_01910C_A*) and the putative GPI-anchored protein (*PGA34*), glycerophosphocholine transporter (*GIT4*), Glycerophosphoinositol permease, (*GIT1*) which is involved in the utilization of glycerophosphoinositol as a phosphate source, putative phosphate permease (*PHO89*), and phospholipase B (*PLB1*). As mentioned above, *PLB1* plays an important role in *C. albicans* virulence and host cell penetration. *GIT4*, *GIT1*, and *PHO89* are involved in phosphate utilization, transportation, and homeostasis, which is an important compound for anabolic processes in the fungus (Köhler et al., 2020). Phosphate is implicated in *C. albicans* virulence under various aspects such as stress resistance, cell cycle, and metal availability and homeostasis. Thus, the perturbation of phosphate homeostasis can attenuate *C. albicans* virulence. Plb1 can mediate deacylation of glycerophospholipids to produce glycerophosphodiesters such as glycerophosphocholine and glycerophosphoinositol, which can be utilized by the fungus as phosphate sources (Bishop et al., 2011, Liu et al., 2017, Ikeh et al., 2017).

The transcriptomic profile of *C. albicans* in this study revealed various aspects of similarities between both treatments, which might be due to the fact that both treatments are cholinergic agonists. In conclusion, taken all together the

similarities in terms of gene regulations, the evidence in the literature of GPCRs presence in fungi, and the presence of *ChAT* and *CrAT* enzymes in *C. albicans* genome support our hypothesis of the cholinergic regulations of *C. albicans* pathogenesis by PHCl through a cholinergic receptor or receptors of homology to muscarinic receptors subtype M1,3, or 5 (El-Defrawy and Hesham, 2020, Borghi et al., 2015).

Key summary points:

- The data herein highlighted a wide spectrum of signaling networks differentially regulated by both ACh and PHCl.

- Numerous numbers of unannotated genes were differentially regulated by both treatments that might expand our understanding of the signaling pathways they mediate and aid in receptor characterisation.

- The cholinergic agonists ACh and PHCl exhibited some similarities in the differential regulation of the transcriptomic profile especially at 4 hours.

- While PHCl triggered metal ion acquisition signaling pathways and pH dependent modulatory pathways, ACh was more involved in respiratory and mitochondrial function pathways.

- Further investigation and follow up experiments are required to elucidate the complete picture of the molecular mechanisms of the inhibitory effect carried out by ACh and PHCl.

5 General discussion

5.1 Summary

The work presented in this thesis investigated cholinergic modulation of biofilm formation in *C. albicans* infections. A number of different techniques were exploited to attempt to characterise the receptor in *C. albicans* which responds to cholinergic compounds and further elucidate the signaling pathways implicated in modulation of the yeast-hyphae transition and biofilm formation. The data herein revealed that, the general muscarinic agonist PHCl significantly inhibited biofilm formation in high and low biofilm forming *C. albicans* clinical isolates as well as a wild type laboratory strain. Furthermore, both PHCl and ACh modulate the expression of numerous vital genes and related signaling pathways which are involved in *C. albicans* biofilm formation and virulence. Different vital virulence genes and important signaling pathways related to *C. albicans* pathogenesis were downregulated by PHCl. In addition, PHCl also inhibits the innate immune response to *C. albicans* infection *in vitro* and protects epithelial tissues against *C. albicans* induced damage.

5.2 Challenges in combating *Candida albicans* infections

C. albicans as a leading cause of candidemia has a detrimental impact on human health and as it is a eukaryote it is more recalcitrant to therapeutic interventions than it's bacterial counterparts. As a eukaryotic pathogen, it shares similarities with the human host and this limits the number of unique molecules that can be utilised as antifungal treatments without causing adverse side effects. In addition, other attributes of *C. albicans* enable the fungus to evade the host immune response and resist antifungals such as morphogenesis, biofilm formation, metabolic flexibility and environmental adaptation. A rising challenge in microbial infection treatment is the increase in conventional antimicrobial resistance. *C. albicans* exhibits a number of intrinsic or acquired mechanisms of antifungal resistance. Worryingly, few new classes of antifungals have been developed and approved for treatment in recent years. This, combined with increased resistance to conventional antifungals, means that the availability of effective antifungal treatments is running low. Therefore, understanding the mechanisms employed by the fungus to resist and evade the

eradication by antifungals can make a crucial contribution for the development of more sophisticated and novel therapeutic interventions moving forwards (Lee et al., 2021, Mayers et al., 2009).

5.3 Cholinergic receptors characterization

Acetylcholine (ACh) is a general cholinergic agonist that can target both muscarinic and nicotinic receptors. Evidence in the literature has shown that ACh can modulate host-fungal interactions. It plays an inhibitory role against *C. albicans* filamentation and biofilm formation *in vitro* and *in vivo* using a *G. mellonella* larvae infection model. Furthermore, ACh provided protection to the *G. mellonella* from mortality caused by *C. albicans* infection. This role was by enhancing the function of hemocytes and inhibiting tissue damage induced by inflammation (Rajendran et al., 2015). In addition, previous *in silico* modelling by Ali et al. (2018) proposed that *C. albicans* expresses a protein with homology to the M1 receptor to which the muscarinic receptor antagonist dicyclomine can bind (Albuquerque et al., 2009, Rajendran et al., 2015, Ali et al., 2017). These findings led to the hypothesis that *C. albicans* possess a functional cholinergic receptor that may exhibit homology to human muscarinic receptors.

In the first chapter, different cholinergic compounds were used for the purpose of exploring our hypothesis for several reasons. Firstly, due to the nature of the proposed ligands which are not proteins, it was not feasible to study the interaction with the potential receptor using techniques such as pull-down assays, western blots, and gel electrophoresis. Secondly, we had no access to radiolabelled compounds and the facilities to use such compounds. Thirdly, protein localization and expression in *C. albicans* was challenging due to the lack of antibodies that are specific for the as yet uncharacterised receptor(s).

Therefore, to begin to try and characterise the potential receptor in *C. albicans* which may be modulating the effect of ACh on morphogenesis and biofilm formation we explored a number of pharmacological agonists, allosteric modulator, and antagonists. The data showed that treating *C. albicans* with PHCl caused a significant inhibition in biofilm formation but had no cytotoxic effect on the cells. In previous research investigating the antimicrobial activity of PHCl,

results revealed that PHCl increased the sensitivity of *Staphylococcus aureus* to antibacterial agents such as aminoglycosides gentamicin and neomycin, however had no antifungal activity on *C. albicans* even in combination with AMB (Araruna et al., 2012). The study by Araruna et al. (2012) aimed to evaluate the antifungal and antibacterial activity of pilocarpine alone, in combination with aminoglycoside and the antifungal amphotericin B, and determine the minimal inhibitory concentration. Our work herein examined more in depth the effect of PHCl on *C. albicans* virulence and biofilm formation and evaluated the toxicity of PHCl, which was not tested in the Araruna et al. study. In contrast to the previous work by Araruna et al. (2012), the inhibitory effect by PHCl showed in this study suggests that PHCl, which is known to be used for treatment of other diseases such as glaucoma and xerostomia, possess novel antifungal activity (Gil-Montoya et al., 2016, Nile et al., 2019, Sun and Dai, 2019, Randáková and Jakubík, 2021). The fact that PHCl does not exhibit a cytotoxic effect against *C. albicans* but can inhibit biofilm formation suggests that the organism may possess a specific receptor for ACh/PHCl which can inhibit morphogenesis. However, identification of this receptor and precise mechanism by which PHCl mediates inhibition of biofilm formation remained to be elucidated.

In the investigations reported in this thesis experiments were performed using a nonspecific muscarinic antagonist SCP and small molecule G protein and signaling pathways inhibitors such as U73122 and YM 254890 in order to block the inhibitory effect of PHCl on *C. albicans* morphogenesis. These experiments added weight to the evidence that *C. albicans* possess a functional muscarinic like receptor. In addition, the experiments using the small molecule inhibitors showed that YM, a Gq protein inhibitor, and U73122, a PLC inhibitor, had an inhibitory effect on the PHCl induced biofilm formation reduction. This suggested that *C. albicans* may possess a muscarinic receptor or receptors of M1, M3, M5 subtype. However, using pharmacological compounds has limitations in characterising a specific muscarinic receptor subtype. For example, there is a lack of commercially available selective agonists for some muscarinic receptor subtypes. So, whenever no agonist was available, either an allosteric modulator or antagonist was employed in this study. If the receptor of interest is to be a potential therapeutic target, then it is vital it has specificity for the receptor. Furthermore, there are different factors that can be challenging when using

cholinergic compounds such as host toxicity, affinity, efficacy, selectivity, binding site and time to bind (Strange, 2008).

5.4 Limitation in muscarinic receptors characterization

Muscarinic receptors possess two binding sites: an orthosteric and an allosteric binding site. The orthosteric site, which is the site to which conventional muscarinic ligands bind, are identical in structure in the different muscarinic receptor subtypes. Therefore, the affinity of a muscarinic agonist for a receptor is mainly influenced by the allosteric binding site. This can make the development of subtype selective compounds challenging. The allosteric site has a more distinctive structure in each receptor subtype to which an allosteric modulator can bind and promote conformational changes in the receptor. Although orthosteric sites can be targets for high affinity compounds they are less selective for different subtypes of mAChRs, and the allosteric modulator can target a less conserved site on the receptor or cooperate with the orthosteric ligand. Yet, few allosteric modulators have been reported (Kruse et al., 2014, Randáková and Jakubík, 2021). Another factor that can influence agonists/antagonists' efficacy is the time taken for a ligand to bind to a receptor. For example, the antagonist tiotropium is relatively slow in binding which makes it less effective in blocking M3AChRs (Svoboda et al., 2017).

Compound concentration is another limitation of using cholinergic agonists, antagonists, or modulators to identify and characterise different muscarinic receptors subtypes. High concentrations of cholinergic compounds might be associated with activating more than one receptor and instigating adverse effects that can be detrimental or lead to some of the side effects which are due to on-target overstimulation. In addition, higher concentrations of different positive allosteric modulators can have different effects than lower concentrations. For instance, *in vitro* testing of cholinergic toxicity in animals (rats, dogs, and cynomologous monkeys) was investigated using the following positive allosteric modulators: compound A, (3-((1S,2S)-2-hydrocyclohexyl)-6-((6-(1-methyl-1H-pyrazol-4-yl)pyridin-3-yl)methyl)benzo[h] quinazolin-4(3H)-one; compound B, 1-((4-cyano-4-(pyridin-2-yl)piperidin-1-yl)methyl)-4-oxo-4H-quinolizine-3 carboxylic acid; and compound C, (R)-ethyl 3-(2-

methylbenzamido)-[1,49- bipiperidine]-19-carboxylate. The results revealed that lower concentrations of these compounds potentiated the cellular Ca^{2+} response to ACh on M1AChRs, and at higher concentrations they had direct agonist activity on the receptor (50- to 100-fold higher than concentrations required for positive allosteric modulator activity) (Alt et al., 2016, van der Westhuizen et al., 2021). Furthermore, the concentrations of agonists or antagonists may affect their affinity to the receptors. For example, 4-DAMP, the M3AChR antagonist has been shown to have twice the affinity for M5AChRs as M3AChRs, so when used at M3AChR saturating concentrations it will also inhibit M5AChR signals (Radu et al., 2017).

5.5 Molecular basis behind PHCl inhibitory effect

To further delineate the mechanisms by which PHCl could inhibit *C. albicans* morphogenesis transcriptomic profiling of *C. albicans* was performed during the early and late stages of biofilm formation in the presence and absence of the compound.

Whole transcriptomic sequencing of *C. albicans* in the presence and absence of PHCl and ACh revealed a number of genes that regulate critical virulence signaling pathways. Results obtained from this technique provide a high throughput input that may pave the way toward characterizing the receptor mediating the cholinergic inhibitory effect and uncovering the possible responsible pathways. Thus, facilitating advanced development of novel drugs and antifungal combinations with high specificity for known pathogen specific virulence factors or biofilm specific tolerance mechanisms. Nevertheless, repurposing licensed drugs such as PHCl would be more advantageous and cheaper compared to designing a completely new drug (Tits et al., 2020).

PCA plot data from the transcriptomic profiling revealed that time of incubation has the most significant difference. This agrees with the findings in literature where the age of biofilm formed was linked to the development of antifungal resistance, which highlights the critical role of the biofilm stage and structure in *C. albicans* virulence and pathogenesis. For instance, 48 hours biofilms exhibited 5-8-fold higher resistance to antifungals compared to planktonic, and resistance

to amphotericin B, fluconazole, nystatin, and chlorhexidine was increased in 72 hours biofilms compared to early stage biofilms. Mature biofilms are therefore more resistant to antifungals and can also evade host immune responses (Cavalheiro and Teixeira, 2018, Sandai et al., 2016).

5.6 PHCl as an adjunctive therapy

Recent research also indicated a cholinergic negative regulation of *C. albicans* hyphal formation using the muscarinic receptor antagonist dicycloamine. Yet, further studies are required to investigate dicycloamine's toxicity and discriminate between on target inhibitory effects and fungicidal activity. We have used PHCl in combination with antifungals attempting to understand their effect on *C. albicans* virulence. Using a combination of drugs for *C. albicans* infection treatment may propose an effective therapeutic strategy in light of the increase in drug resistance and the limited development in novel active drug discovery (Araruna et al., 2012). Combining PHCl with antifungals may weaken *C. albicans* biofilm formation and thus render the biofilm more susceptible to conventional antifungals, which make the effect from combination therapy an effective strategy for *C. albicans* infections (Nobile and Johnson, 2015, Ali et al., 2018, Nile et al., 2019)

Several combinations of conventional antifungals with novel molecules have been reported in the literature. For example, using the calcium channel blocker, verapamil, in combination with fluconazole against *C. albicans* biofilms. In addition, unravelling the miconazole antifungal tolerance mechanisms has led to the finding of the synergistic interaction between miconazole and simvastatin. Simvastatin is an inhibitor of HMG-CoA reductase, which is an enzyme that plays a role in ergosterol biosynthesis. Ergosterol biosynthesis in turn was found to be involved in miconazole tolerance in *C. albicans*. The RNAseq data reported in this work showed that PHCl significantly differentially regulated crucial genes that are involved in several important virulence pathways and may be targets for therapies; such as components of the cell wall and cell membrane, nucleic acid metabolic pathways, filamentation, and the cell cycle (Tits et al., 2020, Ahmad Khan et al., 2020). In future, follow up experiments and further investigations are required to gain a comprehensive understanding of the mechanisms by which

PHCl mediates it's function. Unfortunately, due to the COVID-19 pandemic and prohibited access to laboratories this could not be done and therefore had a significant impact on the completion of this chapter.

5.7 PHCl in *Candida albicans* host pathogen interactions

It has previously been reported that ACh, in addition to modulating *C. albicans* virulence can also modulate the immune response to *C. albicans* infections (Rajendran et al., 2015). In this thesis it is reported that PHCl can also modulate the innate immune response induced by *C. albicans* infection using oral epithelial cell monolayers and a three-dimensional tissue model of the human oral epithelium. The notion that *C. albicans* morphogenesis is a key factor for host innate immune response induction and tissue damage has been proven in the literature and discussed in chapter 3 extensively (Mukaremera et al., 2017, Matuschak and Lechner, 1997). The role of PHCl in host immune response regulation has been discussed in the literature. For instance, it was suggested that tumour growth in a mouse model was inhibited due to modulation of the immune response upon PHCl treatment. However, this study did not investigate the type of immune response initiated by PHCl treatment. In addition, PHCl treatment also resulted in increased antibody production in a rabbit model of *Typhus bacillus* infection (Schneyer, 1957). In the context of PHCl's role in immune response to pathogens, up to date investigations and evidence in the literature are scarce. The data reported here showed the effect on the innate immune response by the host upon PHCl treatment in correlation with it's role as a potential antifungal. PHCl was found to downregulate the innate immune responses but the adaptive immune response was not investigated.

Although *in vitro* research has many advantages such as reduction in the use of animals, large scale throughput, control of chemical and physical environments, and affordability, they fail to mimic and replicate conditions in an organism (Graudejus O et al., 2018). Previous studies have reported differences between *in vitro* and *in vivo C. albicans* biofilm formation using a rat central venous catheter model. For example, the duration of the early stage of biofilm formation *in vivo* was reduced compared to *in vitro*. In addition, several layers

of yeast and hyphae was observed *in vivo* earlier (Cavalheiro and Teixeira, 2018, Andes et al., 2004).The findings from previous *in vitro* studies of PHCl role in regulating the host innate immune response was further confirmed by the *in vivo* work conducted by Nile et al. (2019) using a *Galleria mellonella* infection model. This work revealed that PHCl treatment, similarly to ACh, resulted in effective clearance of *C. albicans* and reducing critical tissue damage (Rajendran et al., 2015, Nile et al., 2019). For future studies to build on these findings, using a mouse model may be advantageous to investigate all aspects of host pathogen interactions which may confer more relevant conclusions due to the similarities with the human genetically, physically, and anatomically.

5.8 Future work and conclusion

The work reported in this thesis constitutes a starting point for future work to better understand the role of cholinergic regulation of *C. albicans* in commensalism and virulence. Moving forwards, a number of further techniques can be exploited to identify and characterise the potential receptors possessed by *C. albicans* which mediate the PHCl induced inhibition of morphogenesis. For example, building on the transcriptomic data and identifying key target genes for knockout using techniques such as CRISPR/Cas9 could be useful to further elucidate their role in PHCl signaling (Morio et al., 2020). In addition, *C. albicans* mutant libraries can be exploited to investigate the intracellular signaling pathways involved in *C. albicans* response to PHCl application (Noble et al., 2010). Furthermore, investigations into the potential role of PHCl as an adjunctive drug in combination with known conventional antifungals would be of critical importance using checkerboard assays, cell viability assays and XTT or CFU assays (Tits et al., 2020).

In conclusion, the data collected in this research suggest that *C. albicans* may possess one or more cholinergic receptors with homology to human muscarinic receptors which modulate *C. albicans* virulence, filamentation, and biofilm formation. The work presented here could contribute considerably to the development of novel therapeutic antifungal agents or treatments. In addition, it expands our knowledge of *C. albicans* pathogenicity, and proposes unique candidate molecules that can be exploited for treatment of *C. albicans*

infections. Furthermore, the cholinergic modulation of fungal virulence factors may provide an insight toward understanding and treating other fungal infections.

Appendices

Appendix I: Clinical isolates growth curve profile in presence and absence of 50 mM PHCl.

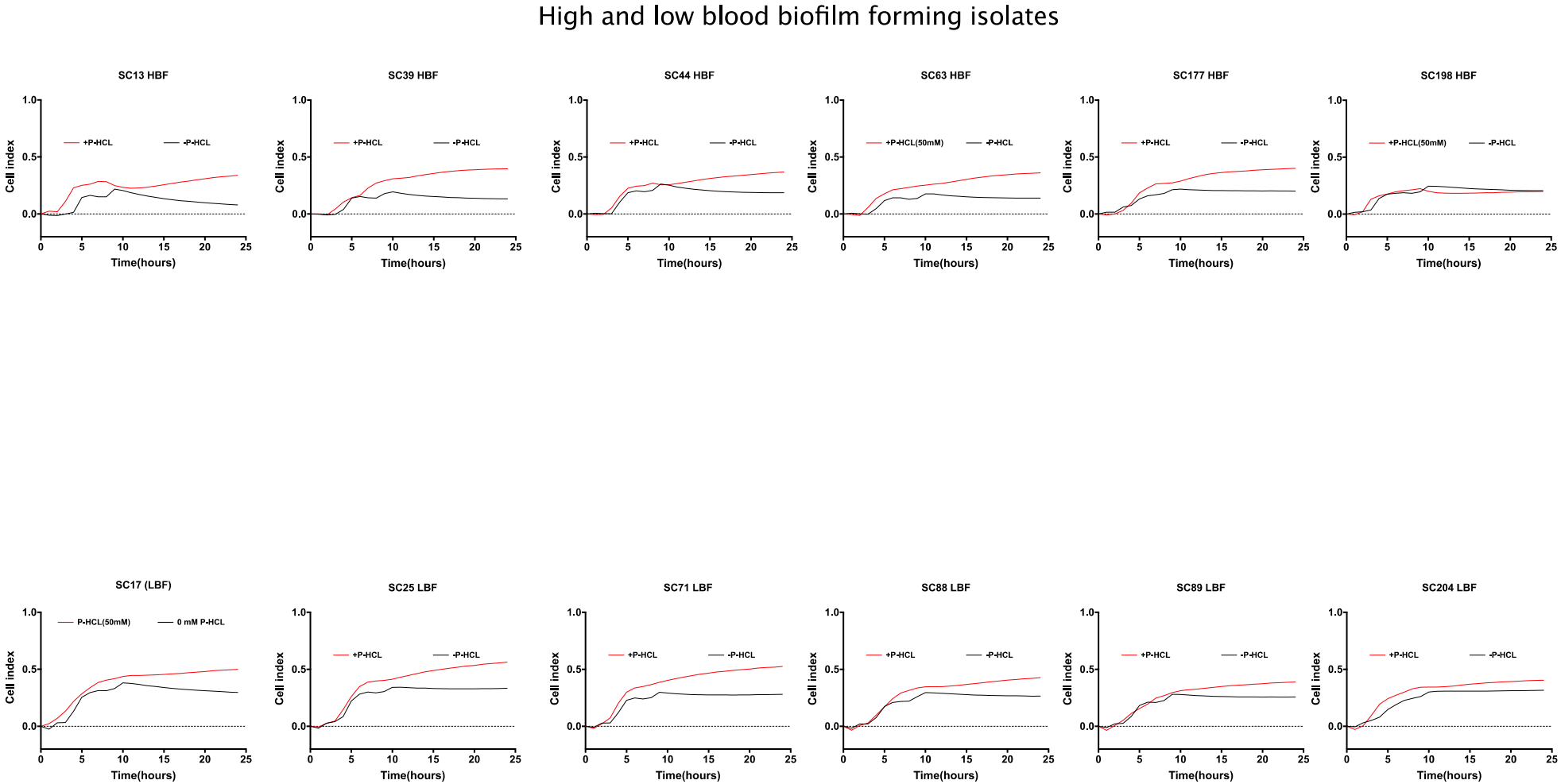

Figure 1 Electrical impedance profile of *C. albicans* blood biofilm forming isolates cultured in the presence and absence of pilocarpine Hydrochloride. Cells were cultured on E- plate in RPMI biofilm forming media in the presence and absence of 50 mM PHCl and growth was monitored over 24h in a real time manner by measuring the electrical impedance profile (EIP).

High and low oral biofilm forming isolates

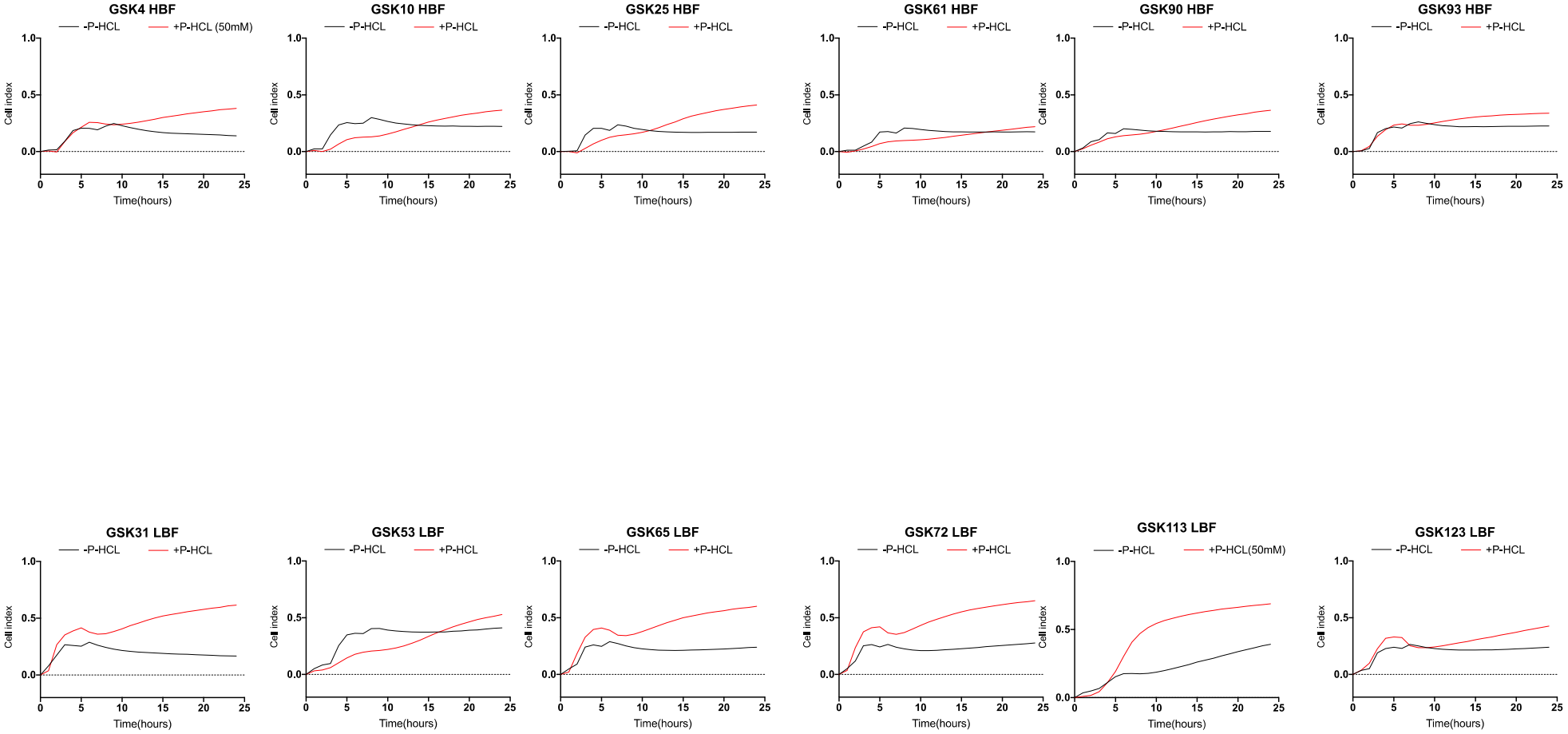

Figure 2 Electrical impedance profile of *C. albicans* oral biofilm forming isolates cultured in the presence and absence of pilocarpine Hydrochloride. Cells were cultured on E- plate in RPMI biofilm forming media in the presence and absence of 50 mM PHCl and growth was monitored over 24h in a real time manner by measuring the electrical impedance profile (EIP).

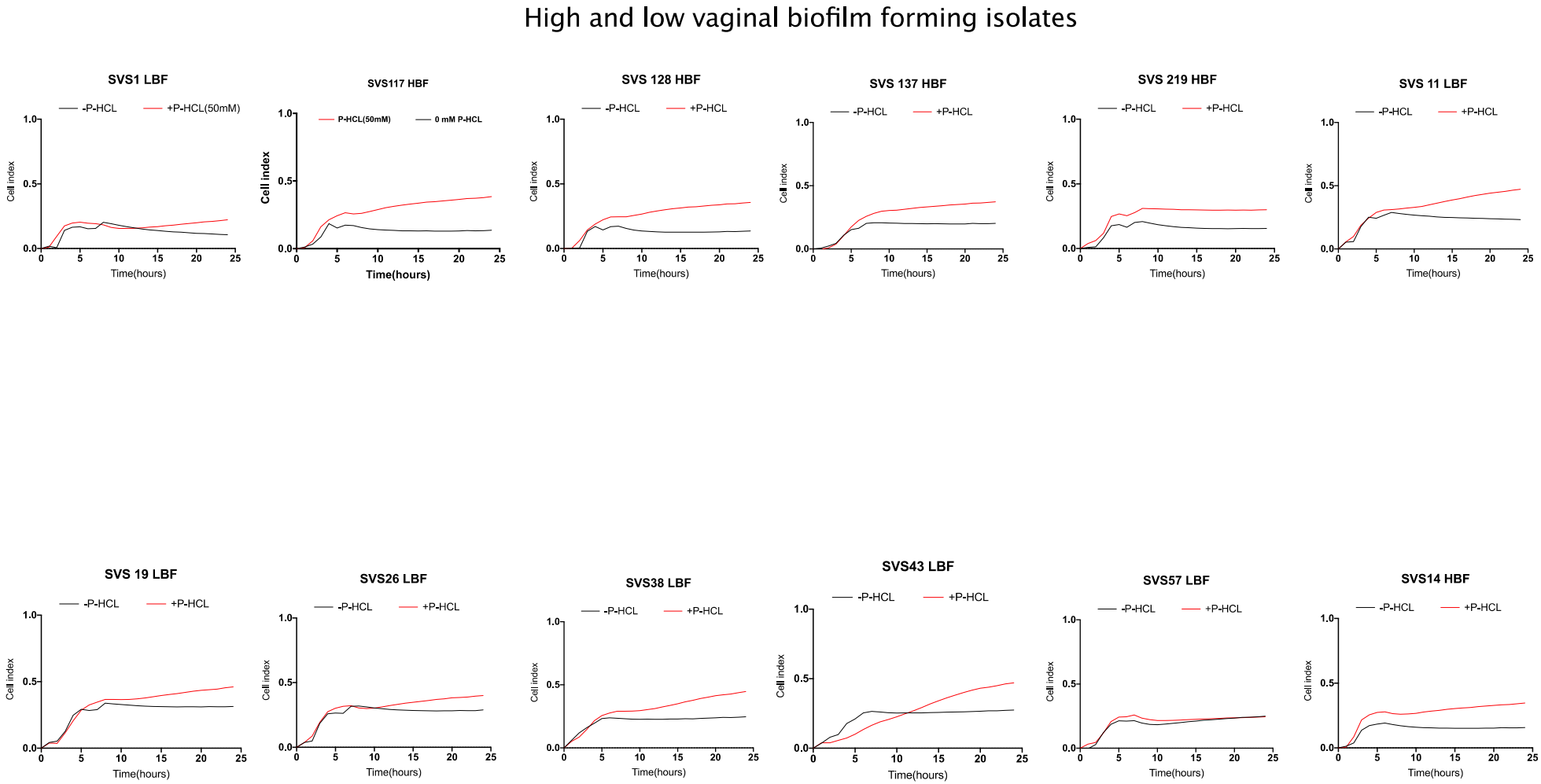

Figure 3 Electrical impedance profile of *C. albicans* vaginal biofilm forming isolates cultured in the presence and absence of pilocarpine Hydrochloride. Cells were cultured on E- plate in RPMI biofilm forming media in the presence and absence of 50 mM PHCl and growth was monitored over 24h in a real time manner by measuring the electrical impedance profile (EIP).

Appendix II: Clinical isolates growth curve profile treated with caspofungin antifungal in presence and absence of PHCl.

SC 31

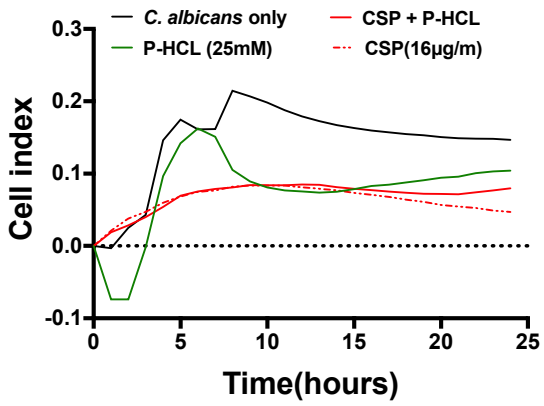

SC 44

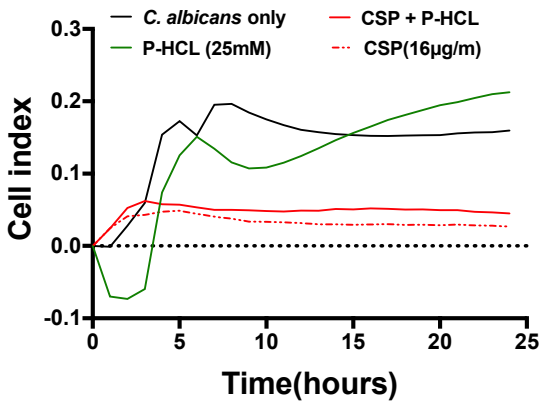

SC 63

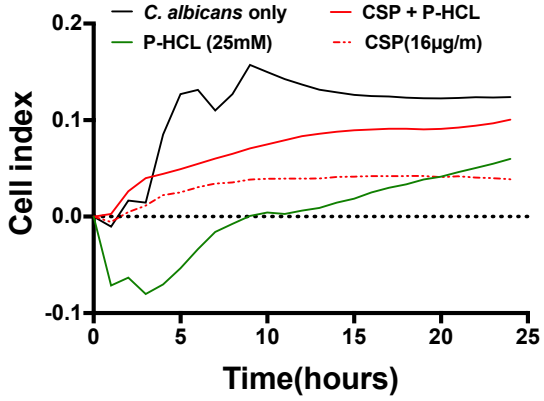

SC177

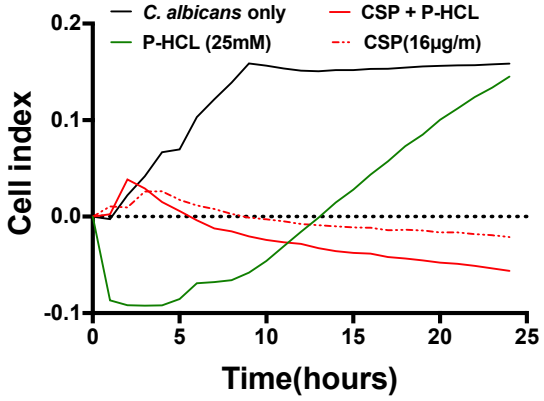

Figure 4 Electrical impedance profile of *C. albicans* cultured with Caspfungin antifungal in the presence and absence of pilocarpine Hydrochloride. Cells were cultured on E- plate in presence and absence of 50 mM PHCl. Growth curve was monitored on real time manner by measuring the electrical impedance profile (EIP).

Appendix III: Clinical isolates growth curve profile treated with Amphoetricin B in presence and absence of PHCl.

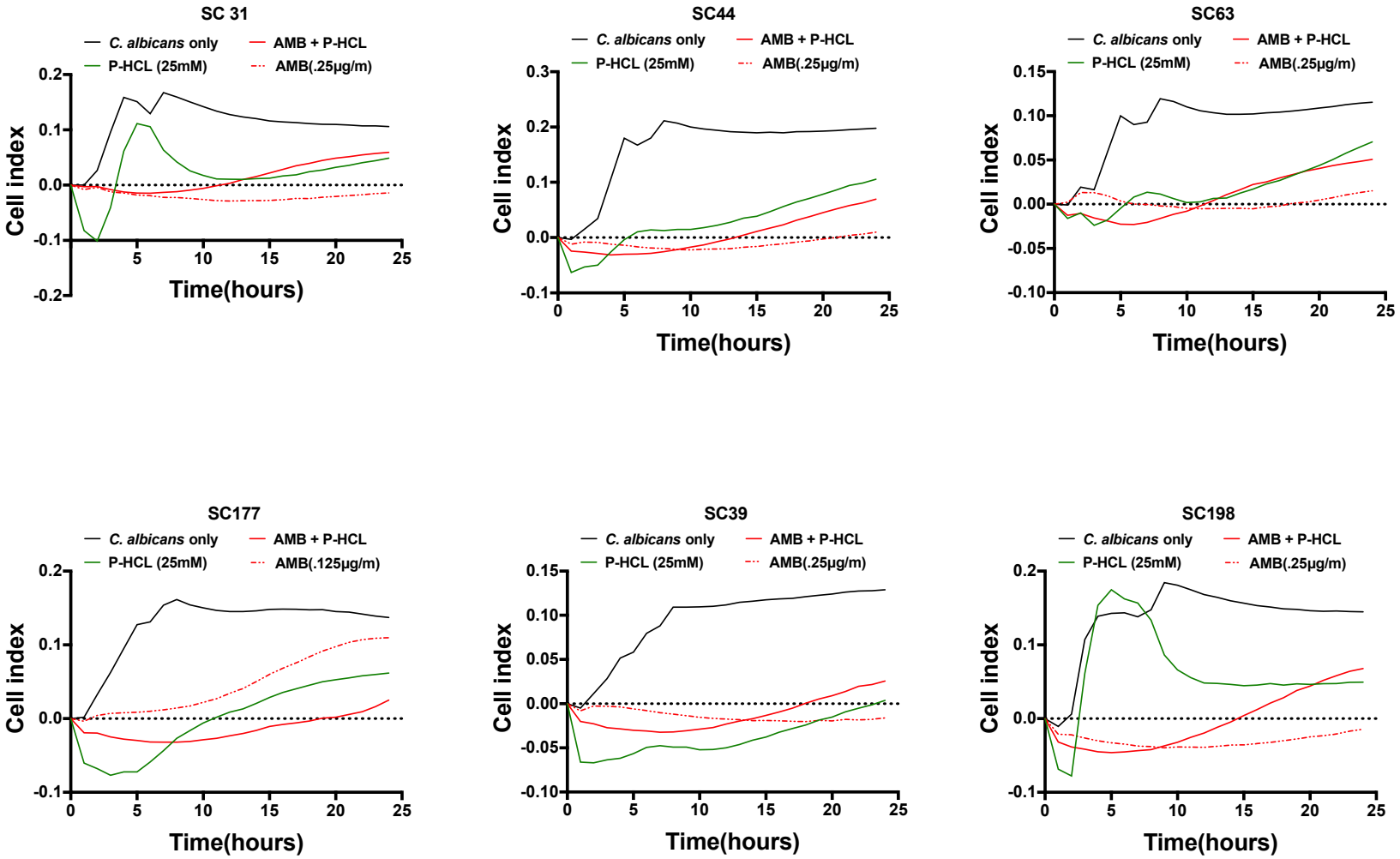

Figure 5 Electrical impedance profile of *C. albicans* cultured with Amphoetricin B antifungal in the presence and absence of pilocarpine Hydrochloride. Cells were cultured on E- plate in presence and absence of 50 mM PHCl. Growth curve was monitored on real time manner by measuring the electrical impedance profile (EIP).

Appendix IV: Gene regulation in presence and absence of PHCl.

Table 1 Upregulated and downregulated genes by 5 mM PHCl treatment at 4 hours incubation. Table includes the common gene name, protein encoded description, the log_2 fold change (Log_2FC), and the Pvalue.

Upregulated				Downregulated			
Gene Name	**Description**	**log_2FoldChange**	**Pvalue**	**Gene Name**	**Description**	**log_2FoldChange**	**Pvalue**
CRD2	Metallothionein; for adaptation to growth in high coppe.	2.11372695	0.03125436	**CR_03270W_A**	Predicted membrane transporter.	-3.1848598	0.00024956
ALS2	ALS family protein; role in adhesion.	2.09582562	0.03756346	**MET3**	ATP sulfurlyase; sulfate assimilation.	-3.0324918	0.00049435
XOG1	Exo-1,3-beta-glucanase.	2.01979094	0.01351014	**C1_07040C_A**	Pry family pathogenesis-related protein.	-2.98907	0.0007647
CDR1	Multidrug transporter of ABC superfamily.	1.98998574	0.0011366	**PGA26**	GPI-anchored adhesin-like protein of the cell wall.	-2.7865594	6.53E-07
PHR2	Glycosidase	1.98022915	1.89E-05	**AOX2**	Alternative oxidase.	-2.7080479	0.01054076
CRZ2	C2H2 transcription factor	1.90999737	0.0268402	**SOD6**	Copper-containing superoxide dismutase.	-2.6449317	0.01350893

PCL1	Cyclin homolog; transcript	1.89715394	0.01504504	**IHD1**	GPI-anchored protein.	-2.6146036	5.10E-05
CCC1	Manganese transporter; required for normal filamentous growth.	1.88111271	0.00013432	**GIT4**	Glycerophosphocholine transporter.	-2.5820185	0.00425156
CR_06140W_A	Protein of unknown function.	1.78322049	0.01076888	**PGA34**	Putative GPI-anchored protein.	-2.5796088	0.00923819
IFE1	Putative medium-chain alcohol dehydrogenase.	1.68748514	0.02253319	**HSP21**	Small heat shock protein.	-2.5203946	0.02236355
				GIT1	Glycerophosphoinositol permease.	-2.4716524	0.00654317
				DUR32	Putative urea transporter.	-2.4313013	0.00457458
				C1_10980W_A	Protein of unknown function.	-2.3367185	0.01746887
				C2_00760C_A	Protein of unknown function.	-2.331308	0.01414109
				SUL2	Putative sulfate transporter.	-2.2910922	0.01400165
				C7_03140W_A	Ortholog of Candida albicans WO-1 : CAWG_05647	-2.2598	0.00030565
				C2_06570C_A	Predicted ORF from Assembly	-2.1740373	0.03030284

		19; removed from Assembly 20; restored based on transcription data; similar to orf19.7550		
	C1_05950C_A	Protein of unknown function.	-2.1471365	0.01961333
	HGT6	Putative high-affinity MFS glucose transporter.	-2.0986297	0.00709648
	ECE1	Candidalysin, cytolytic peptide toxin.	-1.9103253	0.01866402
	MET1	Putative uroporphyrin-3 C-methyltransferase.	-1.8853545	0.00553641
	C3_02330C_A	Protein of unknown function.	-1.8849016	0.0328968
	C3_00190W_A	Ortholog of Candida guilliermondii ATCC 6260 : PGUG_05321, Candida	-1.8805667	0.03640554

		lusitaniae ATCC 42720 : CLUG_00887 and Candida albicans WO-1 : CAWG_02354		
	GPX1	Putative thiol peroxidase.	-1.8665637	0.01024012
	TLO8	Member of a family of telomere-proximal genes of unknown function.	-1.7632749	0.0312178
	TLO13	Member of a family of telomere-proximal genes of unknown function.	-1.7467762	0.04004343
	TLO5	Member of a family of telomere-proximal genes of unknown function.	-1.7164484	0.03687152
	CTA2	Putative transcription factor.	-1.7009267	0.02034154

	GIT2	Putative glycerophosphoinositol permease.	-1.5317645	0.03159682

Table 2 Upregulated and downregulated genes by 25 mM PHCl treatment at 4 hours incubation. Table includes the common gene name, protein encoded description, the log_2 fold change (Log_2FC), and the Pvalue.

Upregulated				Downregulated			
Gene Name	**Description**	**log_2FoldChange**	**Pvalue**	**Gene Name**	**Description**	**log_2FoldChange**	**Pvalue**
RBE1	Pry family cell wall protein.	3.2439397	4.35E-05	**C1_07040C_A**	Pry family pathogenesis-related protein.	-3.880906	2.90E-07
SCW11	Cell wall protein.	3.21011322	3.50E-08	**MFALPHA**	Alpha factor mating pheromone precursor.	-3.8066644	0.00836454
C4_00990W_A	NRAMP metal ion transporter.	3.12209325	0.00021218	**MRV4**	Protein of unknown.	-3.711331	0.01765844
ALS4	GPI-anchored adhesin.	2.97569957	6.70E-05	**IHD1**	GPI-anchored protein.	-3.6884919	5.22E-14
YWP1	Secreted yeast wall protein.	2.97003418	4.91E-05	**PGA34**	Putative GPI-anchored protein.	-3.375767	0.00012469
DAG7	Secretory protein.	2.95952283	0.00038217	**C1_10980W_A**	Protein of unknown.	-3.3639979	6.22E-06
MNN1	Putative alpha-1,3-mannosyltransferase.	2.85178607	7.74E-12	**C3_02750W_A**	Protein with a ribonuclease III domain.	-3.3085924	0.01052993

TEF4	Putative translation elongation factor.	2.81114329	0.00043653	**CSP2**	Putative cell wall associated protein.	-3.2608455	4.71E-10
CR_06140W_A	Protein of unknown function.	2.75567491	1.73E-10	**PGA26**	GPI-anchored adhesin-like protein of the cell wall.	-3.1503816	5.57E-11
C2_10020C_A	Has domain(s) with predicted catalytic activity.	2.68601087	0.00849249	**AOX2**	Alternative oxidase.	-3.0929737	0.0004864
MNN45	Mannosyltransferase.	2.67358545	1.37E-06	**C7_03150W_A**	Protein of unknown.	-3.0713958	3.91E-10
PHR2	Glycosidase.	2.6560794	6.61E-16	**SOD5**	Cu-containing superoxide dismutase.	-2.9723244	4.00E-06
FRE10	Major cell-surface ferric reductase.	2.63901992	0.00041907	**C2_00670C_A**	Ortholog of Candida albicans WO-1 : CAWG_03846	-2.9357431	0.00255756
CDR2	Multidrug transporter.	2.62619167	4.60E-07	**CR_01910C_A**	Putative dethiobiotin synthetase.	-2.8540613	0.01532461
C3_03460C_A	Protein of unknown function.	2.6199803	1.58E-08	**CIP1**	Possible oxidoreductase	-2.7335736	0.00031012
IFE1	Putative medium-chain alcohol dehydrogenase.	2.60305687	3.25E-09	**CR_03270W_A**	Predicted membrane transporter	-2.6906713	0.00122639
CRZ2	C2H2 transcription factor.	2.51681509	3.95E-05	**HSP21**	Small heat shock protein	-2.6604136	0.00532389

C1_03460C_A	Protein of unknown function.	2.51127925	6.43E-08	**CSA2**	Extracellular heme-binding protein involved in heme-iron acquisition	-2.5601769	0.00102525
C2_10160W_A	Secreted protein.	2.49400073	2.00E-07	**C5_03730W_A**	Protein of unknown.	-2.5318373	0.02255144
C4_02720C_A	Putative plasma membrane protein.	2.46965974	1.23E-06	**CFL11**	Superoxide-generating NADPH oxidase.	-2.5186868	0.00146844
SAP7	Pepstatin A-insensitive secreted aspartyl protease.	2.46770039	0.0056266	**GIT1**	Glycerophosphoinositol permease.	-2.4761476	0.0021771
XOG1	Exo-1,3-beta-glucanase; 5 glycosyl hydrolase family member.	2.4349431	0.00010527	**PHO84**	High-affinity phosphate transporter.	-2.4519522	0.00145843
CR_05210W_A	Protein of unknown function.	2.42797178	0.00113572	**C7_03140W_A**	Ortholog of Candida albicans WO-1 : CAWG_05647	-2.41545	6.15E-06
PGA6	GPI-anchored cell wall adhesin-like protein.	2.41205447	0.00071531	**FDH1**	Formate dehydrogenase.	-2.4134951	0.00722749
C4_04190C_A	Ortholog of C. parapsilosis CDC317 : CPAR2_402120, C. dubliniensis CD36 : Cd36_43870, Lodderomyces elongisporus NRLL YB-4239 : LELG_04437 and	2.40391126	0.00359736	**C3_00190W_A**	Ortholog of Candida guilliermondii ATCC 6260 : PGUG_05321, Candida lusitaniae ATCC 42720 : CLUG_00887 and	-2.3870265	0.00042939

	Candida orthopsilosis Co 90-125 : CORT_0E02170				Candida albicans WO-1 : CAWG_02354		
CDR1	Multidrug transporter of ABC superfamily.	2.37528083	4.33E-07	**CEK2**	MAP kinase	-2.2805622	0.01238608
C1_12800W_A	Ortholog of C. dubliniensis CD36 : Cd36_11980, C. parapsilosis CDC317 : CPAR2_201330, Candida tenuis NRRL Y-1498 : CANTEDRAFT_114815 and Debaryomyces hansenii CBS767 : DEHA2G10032g	2.37498169	0.00780355	**GIT4**	Glycerophosphocholine transporter.	-2.1955451	0.01269423
PCL1	Cyclin homolog.	2.37309567	3.32E-05	**PHO100**	Putative inducible acid phosphatase	-2.1771628	0.035
C1_11990W_A	Putative cell wall adhesin-like protein.	2.30632759	0.00069142	**C2_06570C_A**	Predicted ORF from Assembly 19; removed from Assembly 20; restored based on transcription data; similar to orf19.7550	-2.1571561	0.01694841
ALS2	ALS family protein.	2.25484404	0.00778532	**EXG2**	GPI-anchored cell wall protein.	-2.1419831	3.27E-05

HCM1	Protein with forkhead domain; similar to S. cerevisiae Hcm1p.	2.22681957	0.00550471	**C2_00760C_A**	Proten of unknown.	-2.1240373	0.0195588
CR_02780W_A	Protein with similarity to carbonic anhydrases.	2.22638169	0.00630488	**ZRT1**	Putative zinc transporte.	-2.1065466	0.00129635
MNN22	Alpha-1,2-mannosyltransferase.	2.20817845	6.14E-05	**IFE2**	Putative alcohol dehydrogenase.	-2.0757985	0.02067591
FMA1	Putative oxidoreductase.	2.15452735	3.59E-06	**C1_10060C_A**	Protein of unknown function.	-2.0375676	0.04885197
CR_06550C_A	Protein of unknown function.	2.13690533	0.00657714	**RTA4**	Protein similar to S. cerevisiae Rsb1p, involved in fatty acid transport.	-2.0341641	0.00861829
C5_01300C_A	Ortholog(s) have mRNA 3'-UTR binding activity.	2.12784493	0.00194705	**HGT6**	Putative high-affinity MFS glucose transporter.	-2.0159312	0.0053603
PIR1	1,3-beta-glucan-linked cell wall protein.	2.08648737	0.00021429	**PRA1**	Cell surface protein that sequesters zinc from host tissue.	-2.0052554	0.00539571
CCC1	Manganese transporter.	2.06829264	2.79E-07	**SAP5**	Biofilm-specific aspartyl protease.	-1.9534984	0.00238469
SIM1	Adhesin-like protein.	2.0356703	4.60E-05	**HWP1**	Hyphal cell wall protein.	-1.9492258	0.00778212
HGT8	High-affinity glucose transporter.	1.99210105	0.00206917	**FRP2**	Putative ferric reductase.	-1.9462406	5.84E-06

CDC6	Putative ATP-binding protein.	1.98249689	0.02435368	**C6_03240W_A**	Predicted 3-methylbutanol:NAD(P) oxidoreductase and methylglyoxal reductase (NADPH-dependent).	-1.9354061	0.02131564
CRD2	Metallothionein.	1.98064683	0.03528162	**C3_02330C_A**	Protein of unknown function.	-1.9200192	0.01296101
CHT3	Major chitinase..	1.97443603	0.00104501	**GIT2**	Putative glycerophosphoinositol permease.	-1.8692105	8.83E-05
C2_02910W_A	Protein of unknown function.	1.97312381	0.02860897	**CR_07220C_A**	Homolog of nuclear distribution factor NudE, NUDEL.	-1.847692	0.00174519
PGA38	Putative adhesin-like GPI-anchored protein.	1.91309356	0.00722708	**ATO1**	Putative fungal-specific transmembrane protein	-1.8378982	0.03873022
C1_02370C_A	Ortholog of C. dubliniensis CD36 : Cd36_02210, C. parapsilosis CDC317 : CPAR2_106350, Candida tenuis NRRL Y-1498 : CANTEDRAFT_116785	1.89469401	0.00795108	**HMX1**	Heme oxygenase	-1.809084	0.00667969

	and Debaryomyces hansenii CBS767 : DEHA2C01980g						
ESC4	Protein similar to S. cerevisiae Esc4; a protein that represses transposition.	1.84661451	0.04579945	**C3_02790W_A**	Ortholog of C. parapsilosis CDC317 : CPAR2_102150, C. dubliniensis CD36 : Cd36_82780, Pichia stipitis Pignal : psti_CGOB_00155 and Candida orthopsilosis Co 90-125 : CORT_0B03450	-1.7937354	0.00967323
C7_03560W_A	Protein of unknown function.	1.82955994	0.04707581	**GPX1**	Putative thiol peroxidase.	-1.7453552	0.01300228
NRM1	Transcriptional regulator of cell cycle gene expression.	1.82557173	0.00847368	**C2_07180W_A**	Ortholog of C. dubliniensis CD36 : Cd36_21450, Candida tropicalis MYA-3404 : CTRG_01739 and Candida albicans WO-1 : CAWG_05814	-1.6675336	0.04605874

STP4	C2H2 transcription factor.	1.75048109	0.0188662	**THI13**	Thiamin pyrimidine synthase	-1.6652944	0.00550965
RTA2	Flippase involved in sphingolipid long chain base release.	1.72935796	0.0105333 2	**TLO5**	Member of a family of telomere-proximal genes of unknown function.	-1.6431654	0.03498707
C1_04470C_A	Protein of unknown function.	1.72221714	0.0060790 7	**AYR2**	Putative NADPH-dependent 1-acyl dihydroxyaceton e phosphate reductase.	-1.6070342	0.00011971
C5_02780W_A	Ortholog(s) have role in chromatin silencing at rDNA.	1.69366077	0.0382979 9	**C5_03430W_A**	Protein of unknown function.	-1.5703133	0.01943321
PGA62	Adhesin-like cell wall protein.	1.68967833	4.12E-05	**DCK1**	Putative guanine nucleotide exchange factor.	-1.5663499	0.00188322
SWE1	Putative protein kinase with a role in control of growth and morphogenesis.	1.61244244	0.0423990 5	**C4_03370C_A**	Ortholog of C. parapsilosis CDC317 : CPAR2_403360, Debaryomyces hansenii CBS767 : DEHA2D00814g, Pichia stipitis Pignal : PICST_32156 and Candida	-1.5132534	0.01174954

				guilliermondii ATCC 6260 : PGUG_04611
C5_04030W_A	Protein of unknown function.	1.60866745	0.04011682	
KRE6	Essential beta-1,6-glucan synthase subunit.	1.60364189	0.00899908	
C6_02940C_A	Protein of unknown function.	1.50835616	0.03884282	

Table 3 Upregulated and downregulated genes by 25 mM PHCl treatment at 24 hours incubation. Table includes the common gene name, protein encoded description, the log_2 fold change (Log_2FC), and the Pvalue.

Upregulated				Downregulated			
Gene Name	**Description**	**log_2FoldChange**	**Pvalue**	**Gene Name**	**Description**	**log_2FoldChange**	**Pvalue**
ERG6	Delta(24)-sterol C-methyltransferase.	2.41754936	0.0002095	**PHO8**	Putative repressible vacuolar alkaline phosphatase.	-2.9727093	3.71E-07
AQY1	Aquaporin water channel.	2.39725196	0.00145719	**C6_03090W_A**	Ortholog of C. dubliniensis CD36 : Cd36_63980, Candida tenuis NRRL Y-1498 : CANTEDRAFT_115187, Candida tropicalis MYA-3404 : CTRG_02719 and Candida albicans WO-1 : CAWG_05060	-2.8972216	0.04779346
ALS2	ALS family protein.	2.38783146	0.00317396	**SAP5**	Biofilm-specific aspartyl protease.	-2.7956164	5.73E-09
TEF4	Putative translation elongation factor.	2.33671423	0.01213443	**ALS3**	Cell wall adhesin.	-2.7451626	6.43E-07

LEU2	Isopropyl malate dehydrogenase.	2.30657679	0.00245893	**ARG1**	Argininosuccinate synthase.	-2.6071501	0.0229555
C7_03310W_A	Protein of unknown function.	2.20748255	0.02070762	**SAP6**	Biofilm-specific aspartyl protease.	-2.575171	0.00095924
OAC1	Putative mitochondrial inner membrane transporter.	2.1704761	0.03646595	**HSP21**	Small heat shock protein.	-2.473654	0.00928937
FRE10	Major cell-surface ferric reductase.	2.15595963	0.01276069	**C5_04980W_A**	Putative adhesin-like protein.	-2.4564089	2.21E-06
C5_04480C_A	Has domain(s) with predicted nucleic acid binding, nucleotide binding activity.	2.14445049	0.04939466	**C3_07470W_A**	Putative plasma membrane protein.	-2.4493867	5.11E-07
AHP1	Alkyl hydroperoxide reductase.	2.06794042	0.03857085	**BIO2**	Putative biotin synthase.	-2.4035088	0.00154927
AMO2	Protein similar to A. niger predicted peroxisomal copper amino oxidase.	2.00304576	0.00532412	**C1_10060C_A**	Protein of unknown function.	-2.3400032	0.01021186
MNN1	Putative alpha-1,3-mannosyltransferase.	1.98025088	0.00025714	**C1_02730W_A**	Protein of unknown function.	-2.2996937	0.00061967
C3_07590W_A	Protein of unknown function.	1.92381988	0.01786504	**HWP1**	Hyphal cell wall protein.	-2.1977014	0.00078422
C4_02190C_A	CoA-transferase family protein.	1.8457926	0.04728545	**C5_03430W_A**	Protein of unknown function.	-2.1570616	1.26E-06

C7_01380W_A	Ortholog of C. dubliniensis CD36 : Cd36_71210, C. parapsilosis CDC317 : CPAR2_702710, Candida tenuis NRRL Y-1498 : CANTEDRAFT_116256 and Debaryomyces hansenii CBS767 : DEHA2E17732g	1.82756042	0.00687848	**IHD1**	GPI-anchored protein.	-2.1514622	0.00120696
C1_10110W_A	Protein of unknown function.	1.71809514	0.02122069	**ECE1**	Candidalysin, cytolytic peptide toxin.	-2.1328832	0.00106304
ERG24	C-14 sterol reductase.	1.65824737	0.02169703	**C3_02330C_A**	Protein of unknown function.	-2.1260047	0.00178137
ILV5	Ketol-acid reductoisomerase.	1.63062731	0.04232992	**C1_05520W_A**	Protein of unknown function.	-2.0410005	9.44E-05
ERG4	Protein similar to sterol C-24 reductase.	1.57370202	0.03179516	**TOS1**	Protein similar to alpha agglutinin anchor subunit.	-1.9970249	9.75E-09
SIM1	Adhesin-like protein.	1.56851048	0.02496216	**CFL11**	Superoxide-generating NADPH oxidase.	-1.9807984	0.02450146
				C5_03440W_A	Protein of unknown function.	-1.9542281	0.0265683
				FRP2	Putative ferric reductase.	-1.8734758	2.68E-05

	C3_01020W_A	Protein of unknown function.	-1.8708595	0.00124553
	C3_03440C_A	Putative spermidine export pump; fungal-specific (no human or murine homolog)	-1.8182418	0.03741999
	HGT6	Putative high-affinity MFS glucose transporter.	-1.7656052	0.03573881
	C3_03690W_A	Putative vacuolar membrane transporter for cationic amino acids.	-1.7598751	0.01280243
	PGA34	Putative GPI-anchored protein.	-1.7555683	0.03298727
	CSP2	Putative cell wall associated protein.	-1.7542533	0.02650876
	C1_11320C_A	Protein of unknown function.	-1.6998233	0.02770854
	STB3	Putative SIN3-binding protein 3 homolog.	-1.6343768	0.00783491

	CR_07220C_A	Homolog of nuclear distribution factor NudE, NUDEL.	-1.5401967	0.04876058
	ARH2	Putative adrenodoxin-NADPH oxidoreductase.	-1.5343026	0.04476947
	CLB2	B-type mitotic cyclin (cyclin-dependent protein kinase regulatory subunit).	-1.5119852	0.02372383

Appendix V: Gene regulation in presence and absence of ACh.

Table 4 Downregulated genes by 5 mM ACh treatment at 4 hours incubation. Table includes the common gene name, protein encoded description, the log_2 fold change (Log_2FC), and the Pvalue.

Downregulated			
Gene Name	**Description**	**log_2FoldChange**	**Pvalue**
C2_10020C_A	Has domain(s) with predicted catalytic activity.	-3.4102508	0.0213197
SCP1	Putative cortical actin cytoskeleton protein.	-3.3109277	2.23E-06
PLB1	Phospholipase B.	-3.3087694	0.02156831
C1_08890C_A	Putative U2B" component of the U2 snRNP.	-3.2397229	0.00110324
PGA34	Putative GPI-anchored protein.	-3.11611	0.00058141
C3_02270W_A	Ortholog of C. dubliniensis CD36 : Cd36_82240, C. parapsilosis CDC317 : CPAR2_405130, Candida tenuis NRRL Y-1498 : CANTEDRAFT_127317 and Debaryomyces hansenii CBS767 : DEHA2G02244g	-3.0652264	0.00090113
C1_04280C_A	Ortholog(s) have dolichyl-phosphate-mannose-glycolipid alpha-mannosyltransferase activity.	-3.0627517	0.00044003

C4_02460W_A	Ortholog(s) have HDEL sequence binding activity.	-2.9837108	1.06E-05
C3_06540C_A	Ortholog of C. dubliniensis CD36 : Cd36_86510, C. parapsilosis CDC317 : CPAR2_206110, Candida tenuis NRRL Y-1498 : CANTEDRAFT_112184 and Debaryomyces hansenii CBS767 : DEHA2F17292g	-2.8759752	7.28E-05
CR_02380C_A	Protein similar to S. cerevisiae Kre27p, which has a role in resistance to killer toxin.	-2.8464041	0.00097999
C1_00700W_A	Protein of unknown function; repressed by nitric oxide	-2.8239913	0.00108868
MFALPHA	Alpha factor mating pheromone precursor.	-2.8067249	0.04889017
C1_11800C_A	Ortholog(s) have AP-2 adaptor complex localization.	-2.6609138	0.00668995
GIT1	Glycerophosphoinositol permease.	-2.6300241	0.00089524
C1_00820W_A	Ortholog of C. dubliniensis CD36 : Cd36_00770, Candida tenuis NRRL Y-1498 : CANTEDRAFT_112621, Debaryomyces hansenii CBS767 : DEHA2D09812g and Pichia stipitis Pignal : PICST_61958	-2.6299678	1.55E-05
C2_10300C_A	Protein of unknown function.	-2.5278502	0.00112443
CR_06500C_A	Protein of unknown function.	-2.5176771	0.00053403
C1_02300W_A	Ortholog(s) have unfolded protein binding activity.	-2.4983013	0.00577187
FGR2	Protein similar to phosphate transporters.	-2.4811058	0.03492409
LYS5	Phosphopantetheinyl transferase.	-2.4527416	0.01172614
ARC35	Putative ARP2/3 complex subunit.	-2.4434105	0.00126014
MNN11	Ortholog(s) have alpha-1,6-mannosyltransferase activity.	-2.4336134	0.001424

C1_02700C_A	Gene induced by hypoxia and ketoconazole.	-2.4095702	0.0473221
C7_01360C_A	Putative heat shock protein with a zinc finger motif.	-2.4021894	0.02969799
C2_01320W_A	Ortholog(s) have structural molecule activity, role in proteasome assembly, ubiquitin-dependent protein catabolic process.	-2.399554	9.87E-05
PHO89	Putative phosphate permease.	-2.3974819	0.00154396
C2_08690C_A	Ortholog of C. dubliniensis CD36 : Cd36_22860, C. parapsilosis CDC317 : CPAR2_806540, Candida tenuis NRRL Y-1498 : CANTEDRAFT_108823 and Debaryomyces hansenii CBS767 : DEHA2B13596g	-2.3974115	0.00032512
C7_03830C_A	Ortholog(s) have role in posttranslational protein targeting to endoplasmic reticulum membrane and TRC complex localization	-2.3849422	0.00637396
OPT4	Oligopeptide transporter.	-2.3844263	0.04519626
CCE1	Putative Holliday junction resolving enzyme.	-2.3829204	0.03598881
TIM9	Predicted protein of the mitochondrial intermembrane space.	-2.3756938	0.00368573
C2_01860C_A	Ortholog(s) have role in L-methionine salvage from methylthioadenosine and cytosol localization.	-2.3525154	0.00030303
HRQ2	Protein of unknown function.	-2.3153259	0.01917984
C1_11910W_A	Putative nuclear pore-associated protein.	-2.3023243	0.00808278
ACB1	Protein similar to a region of acyl-coenzyme-A-binding protein.	-2.2880551	0.01043288
TOA2	Putative TFIIA small subunit.	-2.2876614	0.00088391
ERG28	Ortholog(s) have protein binding, bridging activity.	-2.2847363	0.01138244
CR_02630C_A	Essential component of the conserved oligomeric Golgi complex; role in fusion of transport vesicles to Golgi compartments.	-2.2846496	0.00479536

C3_01220W_A	Putative transcription factor with zinc finger DNA-binding motif.	-2.2809032	0.0019919
TRX1	Thioredoxin; involved in response to reactive oxygen species.	-2.2799698	0.00597667
MET3	ATP sulfurlyase; sulfate assimilation.	-2.2756408	0.01439453
C1_09060C_A	Protein of unknown function.	-2.2703323	0.00100238
C1_12660W_A	Ortholog(s) have protein-containing complex binding activity.	-2.2619543	0.00049837
TEP1	Putative protein phosphatase of the PTP family (tyrosine-specific), similar to S. cerevisiae Tep1p	-2.2487946	0.00089915
CR_06980W_A	Putative protein of unknown function.	-2.2484298	0.01270129
CR_02600W_A	Ortholog of C. dubliniensis CD36 : Cd36_27570, C. parapsilosis CDC317 : CPAR2_801010, Candida tenuis NRRL Y-1498 : cten_CGOB_00198 and Debaryomyces hansenii CBS767 : DEHA2E09306g	-2.2385318	0.03642282
CR_09510C_A	Putative mitochondrial protein.	-2.2048218	0.00746895
C4_06450W_A	Ortholog(s) have role in ATP-dependent chromatin remodeling and positive regulation of cellular response to phosphate starvation.	-2.2035572	0.00623984
C2_09070C_A	Putative glycerol-3-phosphate acyltransferase.	-2.201995	0.00385539
QCR7	Putative ubiquinol-cytochrome-c reductase.	-2.1963006	0.02269052
C6_01380C_A	Ortholog(s) have role in protein import into nucleus and nucleus localization.	-2.1913285	0.01974672
C2_06280C_A	Ortholog of C. dubliniensis CD36 : Cd36_20670, C. parapsilosis CDC317 : CPAR2_104720, Candida tenuis NRRL Y-1498 :	-2.1672877	0.03731841

	CANTEDRAFT_103989 and Debaryomyces hansenii CBS767 : DEHA2F02046g.		
CR_04850C_A	Ortholog of Candida albicans WO-1 : CAWG_01818.	-2.1668991	0.00482137
C1_12670C_A	Ortholog(s) have role in mRNA splicing, via spliceosome and U4/U6 snRNP, U4/U6 x U5 tri-snRNP complex localization.	-2.1665482	0.00130337
COX7	Putative cytochrome c oxidase.	-2.1542058	0.03703265
C4_05890W_A	Protein with a selenoprotein domain and a thioredoxin-like fold domain; similar to S. cerevisiae Vhs3p, which is a putative phosphopantothenoylcysteine decarboxylase.	-2.152379	0.01621476
C1_12650C_A	Ortholog(s) have ubiquitin conjugating enzyme activity, ubiquitin-protein transferase activity and role in free ubiquitin chain polymerization, postreplication repair, protein K63-linked ubiquitination.	-2.1494452	0.00216972
C1_12640W_A	Ortholog(s) have role in mitochondrial respiratory chain complex assembly, proteolysis and mitochondrial inner membrane peptidase complex localization.	-2.1001676	0.0451675
C4_05310W_A	Ortholog of S. cerevisiae : MRX12, C. glabrata CBS138 : CAGL0J11110g, C. dubliniensis CD36 : Cd36_44970, C. parapsilosis CDC317 : CPAR2_500860 and Candida tenuis NRRL Y-1498 : CANTEDRAFT_113509	-2.0987776	0.00675283
C2_04370W_A	Protein of unknown function.	-2.0655092	0.03645587
C1_12480W_A	Ortholog of C. dubliniensis CD36 : Cd36_11670, C. parapsilosis CDC317 : CPAR2_201750, Candida tenuis NRRL Y-1498 : CANTEDRAFT_115679 and Debaryomyces hansenii CBS767 : DEHA2E16940g.	-2.0561966	0.04637035
C5_01260W_A	Ortholog of C. parapsilosis CDC317 : CPAR2_302610, C. dubliniensis CD36 : Cd36_51070, Candida orthopsilosis Co 90-125	-2.0447559	0.01796786

	: CORT_0E04770 and Spathaspora passalidarum NRRL Y-27907 : SPAPADRAFT_50634.		
C5_00620W_A	Ortholog(s) have role in positive regulation of transcription by RNA polymerase II, regulation of cell aging, telomere maintenance via recombination and EKC/KEOPS complex localization.	-2.0192546	0.01231252
C6_03420W_A	Ortholog(s) have role in DNA replication initiation, establishment of mitotic sister chromatid cohesion, mitotic spindle assembly checkpoint and condensed nuclear chromosome kinetochore localization.	-2.0183948	0.03209369
C5_04860C_A	Ortholog(s) have role in ER to Golgi vesicle-mediated transport, retrograde transport, endosome to Golgi and COPII-coated ER to Golgi transport vesicle, Golgi cis cisterna, Golgi membrane, endoplasmic reticulum localization.	-2.0111921	0.03736394
ATP7	Putative subunit of the F1F0-ATPase complex; colony morphology-related gene regulation by Ssn6; farnesol, macrophage-downregulated protein abundance; protein present in exponential and stationary yeast growth phases.	-2.005155	0.00979384
MET8	Putative bifunctional dehydrogenase and ferrochelatase with a predicted role in siroheme biosynthesis.	-1.9993117	0.01001049
C1_05950C_A	Protein of unknown function.	-1.9753287	0.02650159
GIT4	Glycerophosphocholine transporter.	-1.9521687	0.04685535
C7_01740C_A	Ortholog(s) have SNAP receptor activity, role in Golgi vesicle transport, vesicle fusion and Golgi medial cisterna, SNARE complex localization.	-1.9435614	0.04695456
C1_06390W_A	Putative ubiquitin C-terminal hydrolase.	-1.9313276	0.00761932
BET4	Ortholog(s) have Rab geranylgeranyltransferase activity, role in ER to Golgi vesicle-mediated transport, protein	-1.9181508	0.02498801

	geranylgeranylation, protein targeting to membrane and Rab-protein geranylgeranyltransferase complex, peroxisome localization.		
CR_05310W_A	Ortholog(s) have role in Golgi to vacuole transport, endosomal transport and AP-1 adaptor complex, endosome localization.	-1.8643418	0.0197086
C4_04160W_A	Ortholog of C. dubliniensis CD36 : Cd36_43710, C. parapsilosis CDC317 : CPAR2_402940, Candida tenuis NRRL Y-1498 : CANTEDRAFT_114940 and Debaryomyces hansenii CBS767 : DEHA2C09196g	-1.8513662	0.01128264
C1_09110W_A	Protein of unknown function.	-1.7968021	0.02215654
C3_02330C_A	Protein of unknown function.	-1.7829942	0.03504151
C7_01500W_A	Ortholog of C. dubliniensis CD36 : Cd36_71340, C. parapsilosis CDC317 : CPAR2_301350, Candida tenuis NRRL Y-1498 : CANTEDRAFT_114098 and Debaryomyces hansenii CBS767 : DEHA2D03432g	-1.7180841	0.02206224
C3_02420C_A	Ortholog of S. cerevisiae Pet111; a mitochondrial translational activator specific for the COX2 mRNA.	-1.7163945	0.03006747
C1_10320W_A	Ortholog(s) have N-acetylglucosaminylphosphatidylinositol deacetylase activity.	-1.7163498	0.02405979
C6_03330C_A	Putative protein of unknown function.	-1.5732766	0.02007939

Table 5 Downregulated genes by 25 mM ACh treatment at 4 hours incubation. Table includes the common gene name, protein encoded description, the log_2 fold change (Log_2FC), and the Pvalue.

Downregulated			
Gene Name	**Description**	**log_2FoldChange**	**Pvalue**
PHO89	Putative phosphate permease.	-2.0363673	0.01860629
GIT1	Glycerophosphoinositol permease.	-1.982478	0.03874188
C5_00620W_A	Ortholog(s) have role in positive regulation of transcription by RNA polymerase II, regulation of cell aging, telomere maintenance via recombination and EKC/KEOPS complex localization.	-1.8929242	0.02604617
C2_01860C_A	Ortholog(s) have role in L-methionine salvage from methylthioadenosine and cytosol localization.	-1.7810726	0.03230678
TOA2	Putative TFIIA small subunit.	-1.7514893	0.0492698
C1_00820W_A	Ortholog of C. dubliniensis CD36 : Cd36_00770, Candida tenuis NRRL Y-1498 : CANTEDRAFT_112621, Debaryomyces hansenii CBS767 : DEHA2D09812g and Pichia stipitis Pignal : PICST_61958	-1.7024413	0.04275326

Table 6. Downregulated genes by 5 mM ACh treatment at 24 hours incubation. Table includes the common gene name, protein encoded description, the log_2 fold change (Log_2FC), and the Pvalue.

Downregulated			
Gene Name	Description	log_2FoldChange	Pvalue
CDC6	Putative ATP-binding protein with a predicted role in DNA replication.	-2.3715734	0.01035348
CSI2	Putative 66S pre-ribosomal particle component.	-2.2993471	0.01498626
C5_04860C_A	Ortholog(s) have role in ER to Golgi vesicle-mediated transport, retrograde transport, endosome to Golgi and COPII-coated ER to Golgi transport vesicle, Golgi cis cisterna, Golgi membrane, endoplasmic reticulum localization.	-2.2938355	0.00867058
CDC43	Beta subunit of heterodimeric protein geranylgeranyltransferase type I; GGTase I enzyme binds zinc, is Mg-dependent; Cdc42p is GGTase I substrate.	-2.2868197	0.00420481

PRI2	Putative DNA primase.	-2.2699716	0.0319792
C1_06120C_A	Has domain(s) with predicted flap-structured DNA binding activity and role in double-strand break repair via single-strand annealing, removal of nonhomologous ends.	-2.2613131	0.02075785
PMM1	Phosphomannomutase; enzyme of O- and N-linked mannosylation; interconverts mannose-6-phosphate and mannose-l-phosphate.	-2.2565082	0.01339288
AAT22	Aspartate aminotransferase.	-2.2310564	0.02134709
CTF5	Predicted component of the kinetochore sub-complex COMA.	-2.1593474	0.04532681
C1_11790W_A	Thymidylate kinase of unknown role.	-2.1215762	0.00414801
C1_11910W_A	Putative nuclear pore-associated protein.	-2.1214303	0.026424

C2_05290C_A	Has domain(s) with predicted role in transport and integral component of membrane localization.	-2.1065626	0.02302341
C2_04960C_A	Protein of unknown function.	-2.0980568	0.01284016
C6_01380C_A	Ortholog(s) have role in protein import into nucleus and nucleus localization.	-2.0860896	0.04178825
CR_09510C_A	Putative mitochondrial protein.	-2.0767414	0.01661267
C7_02340C_A	Ortholog(s) have tRNA (guanine-N7-)-methyltransferase activity, role in tRNA (guanine-N7)-methylation and cytosol, nucleus, tRNA (m7G46) methyltransferase complex localization.	-2.0737445	0.0119503
C6_02420W_A	Putative phosphatidyl glycerol phospholipase C.	-2.0597331	0.01249918

C3_01150C_A	Ortholog of S. cerevisiae Apd1; required for normal localization of actin patches and normal tolerance of sodium ions and hydrogen peroxide.	-2.0586978	0.01739154
C7_03830C_A	Ortholog(s) have role in posttranslational protein targeting to endoplasmic reticulum membrane and TRC complex localization.	-2.0482746	0.04508623
TIM9	Predicted protein of the mitochondrial intermembrane space.	-2.0349092	0.03881033
C4_05360C_A	Ortholog(s) have mRNA 5'-UTR binding, pre-mRNA intronic binding, translation regulator activity and role in Group I intron splicing, mitochondrial mRNA processing, positive regulation of mitochondrial translation.	-2.0216353	0.01186844
CR_04410W_A	Protein with a UV radiation resistance protein/autophagy-related protein 14 domain.	-2.0165637	0.01601098
C2_03890W_A	Protein likely to be essential for growth.	-2.0077791	0.04402846

C1_12660W_A	Ortholog(s) have protein-containing complex binding activity.	-1.9822622	0.0076821
C1_07960W_A	Predicted nuclear exosome-associated nucleic acid binding protein.	-1.9564878	0.02445889
C1_08920W_A	Ortholog(s) have structural constituent of ribosome activity and mitochondrial small ribosomal subunit localization.	-1.9526491	0.02362271
PRP39	Putative component of the U1 snRNP; involved in splicing.	-1.9424028	0.02092874
CR_10120C_A	Ortholog of S. cerevisiae : RRG7, C. glabrata CBS138 : CAGL0I09680g, C. dubliniensis CD36 : Cd36_35140, C. parapsilosis CDC317 : CPAR2_200670 and Candida tenuis NRRL Y-1498 : CANTEDRAFT_117734.	-1.919732	0.03804394
C4_03830W_A	Predicted tRNA (guanine) methyltransferase activity.	-1.8948064	0.04427604

C5_02590C_A	Putative mitochondrial membrane protein; ortholog of S. cerevisiae Sls1; coordinates expression of mitochondrially-encoded genes.	-1.8793737	0.02465796
RPB8	Putative subunit of RNA polymerases I, II, and III; regulated by Gcn4p; repressed in response to amino acid starvation (3-aminotriazole treatment).	-1.820566	0.03200681
C6_04240W_A	Protein with an Alba DNA/RNA-binding protein domain.	-1.811567	0.03647002
TOM70	Ortholog(s) have mitochondrion targeting sequence binding, protein transmembrane transporter activity and role in protein import into mitochondrial inner membrane, protein import into mitochondrial matrix.	-1.7874484	0.04857914
C7_01350C_A	Ortholog(s) have unfolded protein binding activity, role in mitochondrial proton-transporting ATP synthase complex assembly and mitochondrion localization.	-1.7734823	0.0473646

NIP1	Putative translation initiation factor.	-1.7722934	0.02815409
C2_04730W_A	Ortholog of C. dubliniensis CD36 : Cd36_19300, C. parapsilosis CDC317 : CPAR2_209720, Candida tenuis NRRL Y-1498 : CANTEDRAFT_114035 and Debaryomyces hansenii CBS767 : DEHA2E10494g.	-1.7606413	0.04353848
C1_02290C_A	Ortholog(s) have protein domain specific binding activity, role in mitochondrial proton-transporting ATP synthase complex assembly and mitochondrion localization.	-1.6983945	0.03151169
C4_01660W_A	Ortholog(s) have structural constituent of nuclear pore activity.	-1.6869315	0.02184883

List of References

[CDC], C. F. D. C. A. P. 2021. *Invasive Candidiasis* [Online]. Available: https://www.cdc.gov/fungal/diseases/candidiasis/invasive/index.html [Accessed 4/08/2021 2021].

ADLER-MOORE, J. & PROFFITT, R. T. 2002. AmBisome: liposomal formulation, structure, mechanism of action and pre-clinical experience. *Journal of Antimicrobial Chemotherapy,* 49**,** 21-30.

AGUSTINHO, D. P., DE OLIVEIRA, M. A., TAVARES, A. H., DERENGOWSKI, L., STOLZ, V., GUILHELMELLI, F., MORTARI, M. R., KUCHLER, K. & SILVA-PEREIRA, I. 2017. Dectin-1 is required for miR155 upregulation in murine macrophages in response to Candida albicans. *Virulence,* 8**,** 41-52.

AHMAD KHAN, M. S., ALSHEHREI, F., AL-GHAMDI, S. B., BAMAGA, M. A., AL-THUBIANI, A. S. & ALAM, M. Z. 2020. Virulence and biofilms as promising targets in developing antipathogenic drugs against candidiasis. *Future science OA,* 6**,** FSO440.

AKINS, R. A. & SOBEL, J. D. 2009. Antifungal targets, mechanisms of action, and resistance in Candida albicans. *Antimicrobial drug resistance*. Springer.

ALBUQUERQUE, E. X., PEREIRA, E. F., ALKONDON, M. & ROGERS, S. W. 2009. Mammalian nicotinic acetylcholine receptors: from structure to function. *Physiol Rev,* 89**,** 73-120.

ALI, A., JADHAV, A., JANGID, P., PATIL, R., SHELAR, A. & KARUPPAYIL, S. M. 2018. The human muscarinic acetylcholine receptor antagonist, Dicyclomine targets signal transduction genes and inhibits the virulence factors in the human pathogen, Candida albicans. *J Antibiot (Tokyo),* 71**,** 456-466.

ALI, A., WAKHARDE, A. & KARUPPAYIL, S. 2017. Rrp9 as a Potential Novel Antifungal Target in Candida albicans: Evidences from. Silico.

ALSHANTA, O. A., SHABAN, S., NILE, C. J., MCLEAN, W. & RAMAGE, G. 2019. Candida albicans biofilm heterogeneity and tolerance of clinical isolates: implications for secondary endodontic infections. *Antibiotics,* 8**,** 204.

ALT, A., PENDRI, A., BERTEKAP, R. L., JR., LI, G., BENITEX, Y., NOPHSKER, M., ROCKWELL, K. L., BURFORD, N. T., SUM, C. S., CHEN, J., HERBST, J. J., FERRANTE, M., HENDRICSON, A., CVIJIC, M. E., WESTPHAL, R. S., O'CONNELL, J., BANKS, M., ZHANG, L., GENTLES, R. G., JENKINS, S., LOY, J. & MACOR, J. E. 2016. Evidence for Classical Cholinergic Toxicity Associated with Selective Activation of M1 Muscarinic Receptors. *J Pharmacol Exp Ther,* 356**,** 293-304.

ANDES, D., NETT, J., OSCHEL, P., ALBRECHT, R., MARCHILLO, K. & PITULA, A. 2004. Development and characterization of an in vivo central venous catheter Candida albicans biofilm model. *Infection and immunity,* 72**,** 6023-6031.

ANTINORI, S., MILAZZO, L., SOLLIMA, S., GALLI, M. & CORBELLINO, M. 2016. Candidemia and invasive candidiasis in adults: A narrative review. *Eur J Intern Med,* 34**,** 21-28.

ANTONINI, S. & SUDBERY, P. 2004. Filamentous growth in Saccharomyces cerevisiae. *Brazilian Journal of Microbiology - BRAZ J MICROBIOL,* 35.

ANWAR, M., MUHAMMAD, F., AWAIS, M. & AKHTAR, M. 2017. A review of β-glucans as a growth promoter and antibiotic alternative against enteric pathogens in poultry. *World's Poultry Science Journal,* 73**,** 651-661.

ARARUNA, M. K. A., BRITO, S. A., MORAIS-BRAGA, M. F. B., SANTOS, K. K. A., SOUZA, T. M., LEITE, T. R., COSTA, J. G. M. & COUTINHO, H. D. M. 2012. Evaluation of antibiotic & antibiotic modifying activity of pilocarpine & rutin. *The Indian journal of medical research,* 135**,** 252-254.

ARNAUD, M. B., COSTANZO, M. C., SKRZYPEK, M. S., BINKLEY, G., LANE, C., MIYASATO, S. R. & SHERLOCK, G. 2005. The Candida Genome Database (CGD), a community resource for Candida albicans gene and protein information. *Nucleic acids research,* 33**,** D358-D363.

ARREDONDO, J., HALL, L. L., NDOYE, A., CHERNYAVSKY, A. I., JOLKOVSKY, D. L. & GRANDO, S. A. 2003. Muscarinic acetylcholine receptors regulating cell cycle progression are expressed in human gingival keratinocytes. *J Periodontal Res,* 38**,** 79-89.

BAEK, Y.-U., LI, M. & DAVIS, D. A. 2008. Candida albicans ferric reductases are differentially regulated in response to distinct forms of iron limitation by the Rim101 and CBF transcription factors. *Eukaryotic cell,* 7**,** 1168-1179.

BANDARA, H., WOOD, D. L. A., VANWONTERGHEM, I., HUGENHOLTZ, P., CHEUNG, B. P. K. & SAMARANAYAKE, L. P. 2020. Fluconazole resistance in Candida albicans is induced by Pseudomonas aeruginosa quorum sensing. *Sci Rep,* 10**,** 7769.

BARATHI, V. A., WEON, S. R. & BEUERMAN, R. W. 2009. Expression of muscarinic receptors in human and mouse sclera and their role in the regulation of scleral fibroblasts proliferation. *Mol Vis,* 15**,** 1277-93.

BARLOW, R. & WESTON-SMITH, P. 1985. The relative potencies of some agonists at M2 muscarinic receptors in guinea-pig ileum, atria and bronchi. *British journal of pharmacology,* 85**,** 437.

BASSO, V., D'ENFERT, C., ZNAIDI, S. & BACHELLIER-BASSI, S. 2018. From genes to networks: the regulatory circuitry controlling Candida albicans morphogenesis. *Fungal Physiology and Immunopathogenesis***,** 61-99.

BASU, S., QUILICI, C., ZHANG, H. H., GRAIL, D. & DUNN, A. R. 2008. Mice lacking both G-CSF and IL-6 are more susceptible to Candida albicans infection: critical role of neutrophils in defense against Candida albicans. *Growth Factors,* 26**,** 23-34.

BATES, S., HALL, R. A., CHEETHAM, J., NETEA, M. G., MACCALLUM, D. M., BROWN, A. J. P., ODDS, F. C. & GOW, N. A. R. 2013. Role of the Candida albicans MNN1 gene family in cell wall structure and virulence. *BMC Research Notes,* 6**,** 294.

BEN-AMI, R. 2018. Treatment of Invasive Candidiasis: A Narrative Review. *Journal of fungi (Basel, Switzerland),* 4**,** 97.

BENSEN, E. S., MARTIN, S. J., LI, M., BERMAN, J. & DAVIS, D. A. 2004. Transcriptional profiling in Candida albicans reveals new adaptive responses to extracellular pH and functions for Rim101p. *Mol Microbiol,* 54**,** 1335-51.

BHATTACHARYA, S., SAE-TIA, S. & FRIES, B. C. 2020. Candidiasis and Mechanisms of Antifungal Resistance. *Antibiotics (Basel, Switzerland),* 9**,** 312.

BINDEA, G., MLECNIK, B., HACKL, H., CHAROENTONG, P., TOSOLINI, M., KIRILOVSKY, A., FRIDMAN, W.-H., PAGÈS, F., TRAJANOSKI, Z. & GALON, J. 2009. ClueGO: a Cytoscape plug-in to decipher functionally grouped gene ontology and pathway annotation networks. *Bioinformatics (Oxford, England),* 25**,** 1091-1093.

BISHOP, A. C., GANGULY, S., SOLIS, N. V., COOLEY, B. M., JENSEN-SEAMAN, M. I., FILLER, S. G., MITCHELL, A. P. & PATTON-VOGT, J. 2013.

Glycerophosphocholine utilization by Candida albicans: role of the Git3 transporter in virulence. *The Journal of biological chemistry,* 288**,** 33939-33952.

BISHOP, A. C., SUN, T., JOHNSON, M. E., BRUNO, V. M. & PATTON-VOGT, J. 2011. Robust utilization of phospholipase-generated metabolites, glycerophosphodiesters, by Candida albicans: role of the CaGit1 permease. *Eukaryotic cell,* 10**,** 1618-1627.

BISWAS, S., VAN DIJCK, P. & DATTA, A. 2007. Environmental sensing and signal transduction pathways regulating morphopathogenic determinants of Candida albicans. *Microbiology and molecular biology reviews : MMBR,* 71**,** 348-376.

BLANKENSHIP, J. R. & HEITMAN, J. 2005. Calcineurin is required for Candida albicans to survive calcium stress in serum. *Infect Immun,* 73**,** 5767-74.

BOBER, L. A., GRACE, M. J., PUGLIESE-SIVO, C., ROJAS-TRIANA, A., WATERS, T., SULLIVAN, L. M. & NARULA, S. K. 1995. The effect of GM-CSF and G-CSF on human neutrophil function. *Immunopharmacology,* 29**,** 111-119.

BODGE, M. & CUMPSTON, A. 2019. Chapter 2 - Pharmacology of Drugs Used in Hematopoietic Cell Transplantation. *In:* BASHIR, Q. & HAMADANI, M. (eds.) *Hematopoietic Cell Transplantation for Malignant Conditions.* Elsevier.

BOGACHEV, M. I., VOLKOV, V. Y., MARKELOV, O. A., TRIZNA, E. Y., BAYDAMSHINA, D. R., MELNIKOV, V., MURTAZINA, R. R., ZELENIKHIN, P. V., SHARAFUTDINOV, I. S. & KAYUMOV, A. R. 2018. Fast and simple tool for the quantification of biofilm-embedded cells sub-populations from fluorescent microscopic images. *PLOS ONE,* 13**,** e0193267.

BORGHI, E., MORACE, G., BORGO, F., RAJENDRAN, R., SHERRY, L., NILE, C. & RAMAGE, G. 2015. New strategic insights into managing fungal biofilms. *Front Microbiol,* 6**,** 1077.

BOSCH, R. R., PATEL, A. M. P., VAN EMST-DE VRIES, S. E., SMEETS, R. L. L., DE PONT, J. J. H. H. M. & WILLEMS, P. H. G. M. 1998. U73122 and U73343 inhibit receptor-mediated phospholipase D activation downstream of phospholipase C in CHO cells. *European Journal of Pharmacology,* 346**,** 345-351.

BOURGEOIS, C. & KUCHLER, K. 2012. Fungal pathogens—a sweet and sour treat for toll-like receptors. *Frontiers in cellular and infection microbiology,* 2**,** 142.

BRAJTBURG, J., POWDERLY, W., KOBAYASHI, G. S. & MEDOFF, G. 1990. Amphotericin B: current understanding of mechanisms of action. *Antimicrobial agents and chemotherapy,* 34**,** 183.

BRAUN, B. R., VAN HET HOOG, M., D'ENFERT, C., MARTCHENKO, M., DUNGAN, J., KUO, A., INGLIS, D. O., UHL, M. A., HOGUES, H., BERRIMAN, M., LORENZ, M., LEVITIN, A., OBERHOLZER, U., BACHEWICH, C., HARCUS, D., MARCIL, A., DIGNARD, D., IOUK, T., ZITO, R., FRANGEUL, L., TEKAIA, F., RUTHERFORD, K., WANG, E., MUNRO, C. A., BATES, S., GOW, N. A., HOYER, L. L., KÖHLER, G., MORSCHHÄUSER, J., NEWPORT, G., ZNAIDI, S., RAYMOND, M., TURCOTTE, B., SHERLOCK, G., COSTANZO, M., IHMELS, J., BERMAN, J., SANGLARD, D., AGABIAN, N., MITCHELL, A. P., JOHNSON, A. D., WHITEWAY, M. & NANTEL, A. 2005. A human-curated annotation of the Candida albicans genome. *PLoS genetics,* 1**,** 36-57.

BRIDGES, T. M., LEBOIS, E. P., HOPKINS, C. R., WOOD, M. R., JONES, C. K., CONN, P. J. & LINDSLEY, C. W. 2010. The antipsychotic potential of muscarinic allosteric modulation. *Drug news & perspectives,* 23**,** 229.

BROCKLEBANK, A. & MARAJ, H. 2013. Vulvovaginal candidiasis. *InnovAiT,* 6**,** 643-651.

BROWN, A. J., BUDGE, S., KALORITI, D., TILLMANN, A., JACOBSEN, M. D., YIN, Z., ENE, I. V., BOHOVYCH, I., SANDAI, D. & KASTORA, S. 2014a. Stress adaptation in a pathogenic fungus. *Journal of Experimental Biology,* 217**,** 144-155.

BROWN, A. J. P., BROWN, G. D., NETEA, M. G. & GOW, N. A. R. 2014b. Metabolism impacts upon Candida immunogenicity and pathogenicity at multiple levels. *Trends in microbiology,* 22**,** 614-622.

BROWN, G. D., DENNING, D. W., GOW, N. A., LEVITZ, S. M., NETEA, M. G. & WHITE, T. C. 2012. Hidden killers: human fungal infections. *Sci Transl Med,* 4**,** 165rv13.

BROWN, N. A., SCHREVENS, S., VAN DIJCK, P. & GOLDMAN, G. H. 2018. Fungal G-protein-coupled receptors: mediators of pathogenesis and targets for disease control. *Nature Microbiology,* 3**,** 402-414.

BURLAGE, F. R., FABER, H., KAMPINGA, H. H., LANGENDIJK, J. A., VISSINK, A. & COPPES, R. P. 2009. Enhanced proliferation of acinar and progenitor cells by prophylactic pilocarpine treatment underlies the observed amelioration of radiation injury to parotid glands. *Radiotherapy and Oncology,* 90**,** 253-256.

BURR, J., AZUARA-BLANCO, A., AVENELL, A. & TUULONEN, A. 2012. Medical versus surgical interventions for open angle glaucoma. *Cochrane Database of Systematic Reviews*.

CALDERON, J., ZAVREL, M., RAGNI, E., FONZI, W. A., RUPP, S. & POPOLO, L. 2010. PHR1, a pH-regulated gene of Candida albicans encoding a glucan-remodelling enzyme, is required for adhesion and invasion. *Microbiology,* 156**,** 2484-2494.

CALDERONE, R. A. & BRAUN, P. C. 1991. Adherence and receptor relationships of Candida albicans. *Microbiological reviews,* 55**,** 1-20.

CAMPOY, S. & ADRIO, J. L. 2017. Antifungals. *Biochemical pharmacology,* 133**,** 86-96.

CARLSON, A. B. & KRAUS, G. P. 2020. *Physiology, Cholinergic Receptors*, StatPearls Publishing, Treasure Island (FL).

CAROLUS, H., PIERSON, S., LAGROU, K. & VAN DIJCK, P. 2020. Amphotericin B and Other Polyenes-Discovery, Clinical Use, Mode of Action and Drug Resistance. *J Fungi (Basel),* 6.

CARPINO, N., NASEEM, S., FRANK, D. M. & KONOPKA, J. B. 2017. Modulating host signaling pathways to promote resistance to infection by Candida albicans. *Frontiers in cellular and infection microbiology,* 7**,** 481.

CASADEVALL, A. & PIROFSKI, L. A. 1999. Host-pathogen interactions: redefining the basic concepts of virulence and pathogenicity. *Infect Immun,* 67**,** 3703-13.

CAVALHEIRO, M. & TEIXEIRA, M. C. 2018. Candida Biofilms: Threats, Challenges, and Promising Strategies. *Frontiers in medicine,* 5**,** 28-28.

CHAFFIN, W. L. 2008. Candida albicans Cell Wall Proteins. *Microbiology and Molecular Biology Reviews,* 72**,** 495.

CHAFFIN, W. L., LÓPEZ-RIBOT, J. L., CASANOVA, M., GOZALBO, D. & MARTÍNEZ, J. P. 1998. Cell wall and secreted proteins of Candida albicans: identification, function, and expression. *Microbiology and molecular biology reviews : MMBR,* 62**,** 130-180.

CHANDRASEKAR, P. 2008. Amphotericin B lipid complex: treatment of invasive fungal infections in patients refractory to or intolerant of amphotericin B deoxycholate. *Therapeutics and clinical risk management,* 4**,** 1285-1294.

CHANG, Y.-L., YU, S.-J., HEITMAN, J., WELLINGTON, M. & CHEN, Y.-L. 2017. New facets of antifungal therapy. *Virulence,* 8**,** 222-236.

CHAUHAN, N. M. & MOHAN KARUPPAYIL, S. 2021. Dual identities for various alcohols in two different yeasts. *Mycology,* 12**,** 25-38.

CHEN, C. & HUANG, X. 2018. Candida albicans Commensalism and Human Diseases. *In:* SUN, J. & DUDEJA, P. K. (eds.) *Mechanisms Underlying Host-Microbiome Interactions in Pathophysiology of Human Diseases.* Boston, MA: Springer US.

CHEN, H., ZHOU, X., REN, B. & CHENG, L. 2020. The regulation of hyphae growth in Candida albicans. *Virulence,* 11**,** 337-348.

CHEN, Y.-Q., LI, Q., ZHANG, T.-Y. & LIU, N.-N. 2021. Candidalysin: From Mechanism of Action to Biomarker Development and Therapeutic Response. *Innovations in Digital Health, Diagnostics, and Biomarkers,* 1**,** 41-44.

CHEN, Y. Y., CHAO, C.-C., LIU, F.-C., HSU, P.-C., CHEN, H.-F., PENG, S.-C., CHUANG, Y.-J., LAN, C.-Y., HSIEH, W.-P. & WONG, D. S. H. 2013. Dynamic transcript profiling of Candida albicans infection in zebrafish: a pathogen-host interaction study. *PloS one,* 8**,** e72483-e72483.

CHENG, M.-F., YANG, Y.-L., YAO, T.-J., LIN, C.-Y., LIU, J.-S., TANG, R.-B., YU, K.-W., FAN, Y.-H., HSIEH, K.-S., HO, M. & LO, H.-J. 2005. Risk factors for fatal candidemia caused by Candida albicans and non-albicans Candida species. *BMC Infectious Diseases,* 5**,** 22.

CHENG, S. C., JOOSTEN, L. A., KULLBERG, B. J. & NETEA, M. G. 2012. Interplay between Candida albicans and the mammalian innate host defense. *Infect Immun,* 80**,** 1304-13.

CHILDERS, D. S., RAZIUNAITE, I., MOL AVELAR, G., MACKIE, J., BUDGE, S., STEAD, D., GOW, N. A., LENARDON, M. D., BALLOU, E. R. & MACCALLUM, D. M. 2016. The rewiring of ubiquitination targets in a pathogenic yeast promotes metabolic flexibility, host colonization and virulence. *PLoS pathogens,* 12**,** e1005566.

CHIN, V. K., FOONG, K. J., MAHA, A., RUSLIZA, B., NORHAFIZAH, M. & CHONG, P. P. 2014. Early expression of local cytokines during systemic Candida albicans infection in a murine intravenous challenge model. *Biomed Rep,* 2**,** 869-874.

CHONG, P. P., CHIN, V. K., WONG, W. F., MADHAVAN, P., YONG, V. C. & LOOI, C. Y. 2018. Transcriptomic and Genomic Approaches for Unravelling Candida albicans Biofilm Formation and Drug Resistance-An Update. *Genes,* 9**,** 540.

CHOW, E. W. L., PANG, L. M. & WANG, Y. From Jekyll to Hyde: The Yeast-Hyphal Transition of Candida albicans. 2021.

CHROMEK, M., SLAMOVÁ, Z., BERGMAN, P., KOVÁCS, L., PODRACKÁ, L. U., EHRÉN, I., HÖKFELT, T., GUDMUNDSSON, G. H., GALLO, R. L. & AGERBERTH, B. 2006. The antimicrobial peptide cathelicidin protects the urinary tract against invasive bacterial infection. *Nature medicine,* 12**,** 636-641.

CIUREA, C. N., KOSOVSKI, I.-B., MARE, A. D., TOMA, F., PINTEA-SIMON, I. A. & MAN, A. 2020. Candida and Candidiasis—Opportunism Versus Pathogenicity: A Review of the Virulence Traits. *Microorganisms,* 8**,** 857.

COLEMAN, D. A., OH, S.-H., MANFRA-MARETTA, S. L. & HOYER, L. L. 2012. A monoclonal antibody specific for Candida albicans Als4 demonstrates overlapping localization of Als family proteins on the fungal cell surface and

highlights differences between Als localization in vitro and in vivo. *FEMS immunology and medical microbiology,* 64**,** 321-333.

CORTÉS, J. A. & CORRALES, I. F. 2018. Invasive candidiasis: epidemiology and risk factors. *Fungal Infection*.

COSFORD, N. D., BLEICHER, L., HERBAUT, A., MCCALLUM, J. S., VERNIER, J.-M., DAWSON, H., WHITTEN, J. P., ADAMS, P., CHAVEZ-NORIEGA, L. & CORREA, L. D. 1996. (S)-(−)-5-Ethynyl-3-(1-methyl-2-pyrroli-dinyl) pyridine Maleate (SIB-1508Y): A Novel Anti-Parkinsonian Agent with Selectivity for Neuronal Nicotinic Acetylcholine Receptors. *Journal of medicinal chemistry,* 39**,** 3235-3237.

COSTA-SILVA, J., DOMINGUES, D. & LOPES, F. M. 2017. RNA-Seq differential expression analysis: An extended review and a software tool. *PLoS One,* 12**,** e0190152.

COTA, E. & HOYER, L. L. 2015. The Candida albicans agglutinin-like sequence family of adhesins: functional insights gained from structural analysis. *Future microbiology,* 10**,** 1635-1548.

COTTIER, F., SHERRINGTON, S., COCKERILL, S., DEL OLMO TOLEDO, V., KISSANE, S., TOURNU, H., ORSINI, L., PALMER, G. E., PÉREZ, J. C. & HALL, R. A. 2019. Remasking of Candida albicans ß-Glucan in Response to Environmental pH Is Regulated by Quorum Sensing. *mBio,* 10.

COTTIER, F., TAN, A. S. M., CHEN, J., LUM, J., ZOLEZZI, F., POIDINGER, M. & PAVELKA, N. 2015. The Transcriptional Stress Response of Candida albicans to Weak Organic Acids. *G3 Genes|Genomes|Genetics,* 5**,** 497-505.

CZURA, C. J., ROSAS-BALLINA, M. & TRACEY, K. J. 2007. CHAPTER 3 - Cholinergic Regulation of Inflammation. *In:* ADER, R. (ed.) *Psychoneuroimmunology (Fourth Edition)*. Burlington: Academic Press.

D'SOUZA, G. X. & WALDVOGEL, H. J. 2016. Targeting the Cholinergic System to Develop a Novel Therapy for Huntington's Disease. *J Huntingtons Dis,* 5**,** 333-342.

DA SILVA DANTAS, A., LEE, K. K., RAZIUNAITE, I., SCHAEFER, K., WAGENER, J., YADAV, B. & GOW, N. A. 2016. Cell biology of Candida albicans-host interactions. *Curr Opin Microbiol,* 34**,** 111-118.

DADAR, M., TIWARI, R., KARTHIK, K., CHAKRABORTY, S., SHAHALI, Y. & DHAMA, K. 2018. Candida albicans - Biology, molecular characterization, pathogenicity, and advances in diagnosis and control - An update. *Microb Pathog,* 117**,** 128-138.

DANHOF, H. A., VYLKOVA, S., VESELY, E. M., FORD, A. E., GONZALEZ-GARAY, M. & LORENZ, M. C. 2016. Robust extracellular pH modulation by Candida albicans during growth in carboxylic acids. *MBio,* 7**,** e01646-16.

DANTAS, A. D. S., DAY, A., IKEH, M., KOS, I., ACHAN, B. & QUINN, J. 2015. Oxidative stress responses in the human fungal pathogen, Candida albicans. *Biomolecules,* 5**,** 142-165.

DARBY, M., SCHNOELLER, C., VIRA, A., CULLEY, F. J., BOBAT, S., LOGAN, E., KIRSTEIN, F., WESS, J., CUNNINGHAM, A. F., BROMBACHER, F., SELKIRK, M. E. & HORSNELL, W. G. 2015. The M3 muscarinic receptor is required for optimal adaptive immunity to helminth and bacterial infection. *PLoS Pathog,* 11**,** e1004636.

DATABASE, C. G. 2004-2021. *Candida genome database* [Online]. Available: http://www.candidagenome.org/ [Accessed January 11, 2021].

DE MICHELI, M., BILLE, J., SCHUELLER, C. & SANGLARD, D. 2002. A common drug-responsive element mediates the upregulation of the Candida albicans ABC

transporters CDR1 and CDR2, two genes involved in antifungal drug resistance. *Mol Microbiol,* 43**,** 1197-214.

DE REPENTIGNY, L., LEWANDOWSKI, D. & JOLICOEUR, P. 2004. Immunopathogenesis of oropharyngeal candidiasis in human immunodeficiency virus infection. *Clin Microbiol Rev,* 17**,** 729-59, table of contents.

DESAI, J. V. 2018. Candida albicans hyphae: from growth initiation to invasion. *Journal of Fungi,* 4**,** 10.

DEWASTHALE, S., MANI, I. & VASDEV, K. 2018. Microbial biofilm: current challenges in health care industry. *J Appl Biotechnol Bioeng,* 5**,** 160-164.

DIJCK, P. V. 2009. Nutrient sensing G protein-coupled receptors: interesting targets for antifungals? *Medical Mycology,* 47**,** 671-680.

DONGARI-BAGTZOGLOU, A. & KASHLEVA, H. 2003. Candida albicans triggers interleukin-8 secretion by oral epithelial cells. *Microbial pathogenesis,* 34**,** 169-177.

DRESCHERS, S., SAUPP, P., HORNEF, M., PREHN, A., PLATEN, C., MORSCHHÄUSER, J. & ORLIKOWSKY, T. W. 2016. Reduced PICD in monocytes mounts altered neonate immune response to Candida albicans. *PLoS One,* 11**,** e0166648.

DU, H. & HUANG, G. 2016. Environmental pH adaption and morphological transitions in Candida albicans. *Current genetics,* 62**,** 283-286.

DUTTON, L. C., NOBBS, A. H., JEPSON, K., JEPSON, M. A., VICKERMAN, M. M., ALAWFI, S. A., MUNRO, C. A., LAMONT, R. J., JENKINSON, H. F. & CASSONE, A. 2014. Mannosylation in Candida albicans Enables Development of Interkingdom Biofilm Communities. *mBio,* 5**,** e00911-14.

DUVAL, C., MACABIOU, C., GARCIA, C., LESUISSE, E., CAMADRO, J.-M. & AUCHÈRE, F. 2020. The adaptive response to iron involves changes in energetic strategies in the pathogen Candida albicans. *MicrobiologyOpen,* 9**,** e970-e970.

DUVENAGE, L., MUNRO, C. A. & GOURLAY, C. W. 2019. The potential of respiration inhibition as a new approach to combat human fungal pathogens. *Current Genetics,* 65**,** 1347-1353.

EL-DEFRAWY, M. M. H. & HESHAM, A. E.-L. 2020. G-protein-coupled Receptors in Fungi. *Fungal Biotechnology and Bioengineering***,** 37-126.

ELIOPOULOS, G. M., PEREA, S. & PATTERSON, T. F. 2002. Antifungal Resistance in Pathogenic Fungi. *Clinical Infectious Diseases,* 35**,** 1073-1080.

ELLIS, D. 2002. Amphotericin B: spectrum and resistance. *Journal of Antimicrobial Chemotherapy,* 49**,** 7-10.

ELSING, C., HÜBNER, C., FITSCHER, B. A., KASSNER, A. & STREMMEL, W. 1997. Muscarinic acetylcholine receptor stimulation of biliary epithelial cells and its effect on bile secretion in the isolated perfused liver [corrected]. *Hepatology,* 25**,** 804-13.

ENE, I. V., ADYA, A. K., WEHMEIER, S., BRAND, A. C., MACCALLUM, D. M., GOW, N. A. & BROWN, A. J. 2012. Host carbon sources modulate cell wall architecture, drug resistance and virulence in a fungal pathogen. *Cell Microbiol,* 14**,** 1319-35.

EVANS, R., ZDEBIK, A., CIURTIN, C. & WALSH, S. B. 2015. Renal involvement in primary Sjögren's syndrome. *Rheumatology,* 54**,** 1541-1548.

FELLER, L., KHAMMISSA, R. A., CHANDRAN, R., ALTINI, M. & LEMMER, J. 2014. Oral candidosis in relation to oral immunity. *J Oral Pathol Med,* 43**,** 563-9.

FIGUEROA, K. W., GRIFFIN, M. T. & EHLERT, F. J. 2009. Selectivity of agonists for the active state of M1 to M4 muscarinic receptor subtypes. *J Pharmacol Exp Ther,* 328**,** 331-42.

FISHER, A., PITTEL, Z., HARING, R., BAR-NER, N., KLIGER-SPATZ, M., NATAN, N., EGOZI, I., SONEGO, H., MARCOVITCH, I. & BRANDEIS, R. 2003. M 1 muscarinic agonists can modulate some of the hallmarks in Alzheimer's disease. *Journal of Molecular Neuroscience,* 20**,** 349-356.

FLAHERTY, D. K. 2012. Chapter 23 - Cytokines and Biologic Modifiers. *In:* FLAHERTY, D. K. (ed.) *Immunology for Pharmacy*. Saint Louis: Mosby.

FOURIE, R., KULOYO, O. O., MOCHOCHOKO, B. M., ALBERTYN, J. & POHL, C. H. 2018. Iron at the Centre of Candida albicans Interactions. *Frontiers in Cellular and Infection Microbiology,* 8.

FRYER, A. D., CHRISTOPOULOS, A. & NATHANSON, N. M. 2012. *Muscarinic receptors*, Springer Science & Business Media.

FU, J., DING, Y., WEI, B., WANG, L., XU, S., QIN, P., WEI, L. & JIANG, L. 2017. Epidemiology of Candida albicans and non-C.albicans of neonatal candidemia at a tertiary care hospital in western China. *BMC Infect Dis,* 17**,** 329.

FUJII, T., MASHIMO, M., MORIWAKI, Y., MISAWA, H., ONO, S., HORIGUCHI, K. & KAWASHIMA, K. 2017. Physiological functions of the cholinergic system in immune cells. *J Pharmacol Sci,* 134**,** 1-21.

GARBE, E. & VYLKOVA, S. 2019. Role of Amino Acid Metabolism in the Virulence of Human Pathogenic Fungi. *Current Clinical Microbiology Reports,* 6**,** 108-119.

GARCIA-RUBIO, R., DE OLIVEIRA, H. C., RIVERA, J. & TREVIJANO-CONTADOR, N. 2020. The Fungal Cell Wall: Candida, Cryptococcus, and Aspergillus Species. *Frontiers in Microbiology,* 10.

GAVIRIA, J. M., VAN BURIK, J. A., DALE, D. C., ROOT, R. K. & LILES, W. C. 1999. Modulation of neutrophil-mediated activity against the pseudohyphal form of Candida albicans by granulocyte colony-stimulating factor (G-CSF) administered in vivo. *J Infect Dis,* 179**,** 1301-4.

GAZI, U. & MARTINEZ-POMARES, L. 2009. Influence of the mannose receptor in host immune responses. *Immunobiology,* 214**,** 554-561.

GERAGHTY, P. & KAVANAGH, K. 2003. Disruption of mitochondrial function in Candida albicans leads to reduced cellular ergosterol levels and elevated growth in the presence of amphotericin B. *Archives of microbiology,* 179**,** 295-300.

GERWIEN, F., SKRAHINA, V., KASPER, L., HUBE, B. & BRUNKE, S. 2018. Metals in fungal virulence. *FEMS microbiology reviews,* 42**,** fux050.

GHANNOUM, M., ROILIDES, E., KATRAGKOU, A., PETRAITIS, V. & WALSH, T. J. 2015. The Role of Echinocandins in Candida Biofilm-Related Vascular Catheter Infections: In Vitro and In Vivo Model Systems. *Clin Infect Dis,* 61 Suppl 6**,** S618-21.

GHANNOUM, M. A. & RICE, L. B. 1999. Antifungal agents: mode of action, mechanisms of resistance, and correlation of these mechanisms with bacterial resistance. *Clinical microbiology reviews,* 12**,** 501-517.

GIL-MONTOYA, J.-A., SILVESTRE, F.-J., BARRIOS, R. & SILVESTRE-RANGIL, J. 2016. Treatment of xerostomia and hyposalivation in the elderly: A systematic review. *Medicina oral, patologia oral y cirugia bucal,* 21**,** e355.

GILDOR, T., SHEMER, R., ATIR-LANDE, A. & KORNITZER, D. 2005. Coevolution of cyclin Pcl5 and its substrate Gcn4. *Eukaryotic Cell,* 4**,** 310-318.

GINTJEE, T. J., DONNELLEY, M. A. & THOMPSON, G. R., 3RD 2020. Aspiring Antifungals: Review of Current Antifungal Pipeline Developments. *J Fungi (Basel),* 6.

GIOSA, D., FELICE, M. R., LAWRENCE, T. J., GULATI, M., SCORDINO, F., GIUFFRÈ, L., LO PASSO, C., D'ALESSANDRO, E., CRISEO, G., ARDELL, D. H., HERNDAY, A. D., NOBILE, C. J. & ROMEO, O. 2017. Whole RNA-Sequencing and Transcriptome Assembly of Candida albicans and Candida africana under Chlamydospore-Inducing Conditions. *Genome Biology and Evolution,* 9**,** 1971-1977.

GLEASON, J. E., GALALELDEEN, A., PETERSON, R. L., TAYLOR, A. B., HOLLOWAY, S. P., WANINGER-SARONI, J., CORMACK, B. P., CABELLI, D. E., HART, P. J. & CULOTTA, V. C. 2014. Candida albicans SOD5 represents the prototype of an unprecedented class of Cu-only superoxide dismutases required for pathogen defense. *Proceedings of the National Academy of Sciences,* 111**,** 5866-5871.

GOOGHERI, M. S., HOUSAINDOKHT, M. R. & SABZYAN, H. 2014. Reaction mechanism and free energy profile for acylation of Candida Antarctica lipase B with methylcaprylate and acetylcholine: density functional theory calculations. *J Mol Graph Model,* 54**,** 131-40.

GOW, N. A. R. & HUBE, B. 2012. Importance of the Candida albicans cell wall during commensalism and infection. *Current Opinion in Microbiology,* 15**,** 406-412.

GOW, N. A. R., LATGE, J. P. & MUNRO, C. A. 2017. The Fungal Cell Wall: Structure, Biosynthesis, and Function. *Microbiol Spectr,* 5.

GOW, N. A. R. & YADAV, B. 2017. Microbe Profile: Candida albicans: a shape-changing, opportunistic pathogenic fungus of humans. *Microbiology (Reading),* 163**,** 1145-1147.

GOYAL, S., CASTRILLÓN-BETANCUR, J. C., KLAILE, E. & SLEVOGT, H. 2018. The Interaction of Human Pathogenic Fungi With C-Type Lectin Receptors. *Frontiers in immunology,* 9**,** 1261-1261.

GRANGER, B. L., FLENNIKEN, M. L., DAVIS, D. A., MITCHELL, A. P. & CUTLER, J. E. 2005. Yeast wall protein 1 of Candida albicans. *Microbiology (Reading),* 151**,** 1631-1644.

GRAUDEJUS O, PONCE WONG RD & VARGHESE N, W. S. A. M. B. 2019. Bridging the gap between in vivo and in vitro research:

Reproducing in vitro the mechanical and electrical environment of cells in vivo. MEA Meeting 2018 | 11th International Meeting on Substrate Integrated Microelectrode Arrays., 2018 Germany.

GREER, N. D. 2003. Voriconazole: the newest triazole antifungal agent. *Proceedings (Baylor University. Medical Center),* 16**,** 241-248.

GREETHAM, D., LAPPIN, D. F., RAJENDRAN, R., O'DONNELL, L., SHERRY, L., RAMAGE, G. & NILE, C. 2017. The application of phenotypic microarray analysis to anti-fungal drug development. *J Microbiol Methods,* 134**,** 35-37.

GRESNIGT, M. S., JOOSTEN, L. A., VERSCHUEREN, I., VAN DER MEER, J. W., NETEA, M. G., DINARELLO, C. A. & VAN DE VEERDONK, F. L. 2012. Neutrophil-mediated inhibition of proinflammatory cytokine responses. *The Journal of Immunology,* 189**,** 4806-4815.

GRIFFITHS, J. S., CAMILLI, G., KOTOWICZ, N. K., HO, J., RICHARDSON, J. P. & NAGLIK, J. R. 2021. Role for IL-1 Family Cytokines in Fungal Infections. *Frontiers in Microbiology,* 12**,** 132.

GROCHULSKI, P., LI, Y., SCHRAG, J. D., BOUTHILLIER, F., SMITH, P., HARRISON, D., RUBIN, B. & CYGLER, M. 1993. Insights into interfacial activation from an open structure of Candida rugosa lipase. *J Biol Chem,* 268**,** 12843-7.

GRUBB, S. E., MURDOCH, C., SUDBERY, P. E., SAVILLE, S. P., LOPEZ-RIBOT, J. L. & THORNHILL, M. H. 2008. Candida albicans-endothelial cell interactions: a key step in the pathogenesis of systemic candidiasis. *Infection and immunity,* 76**,** 4370-4377.

GULATI, M. & NOBILE, C. J. 2016. Candida albicans biofilms: development, regulation, and molecular mechanisms. *Microbes and infection,* 18**,** 310-321.

GUNASEGAR, S. & HIMRATUL-AZNITA, W. H. 2019. Nicotine enhances the thickness of biofilm and adherence of Candida albicans ATCC 14053 and Candida parapsilosis ATCC 22019. *FEMS Yeast Research,* 19.

HALL, R. A., COTTIER, F. & MÜHLSCHLEGEL, F. A. 2009. Chapter 6 Molecular Networks in the Fungal Pathogen Candida albicans. *Advances in Applied Microbiology*. Academic Press.

HALL, R. A., DE SORDI, L., MACCALLUM, D. M., TOPAL, H., EATON, R., BLOOR, J. W., ROBINSON, G. K., LEVIN, L. R., BUCK, J. & WANG, Y. 2010. CO 2 acts as a signalling molecule in populations of the fungal pathogen Candida albicans. *PLoS Pathog,* 6**,** e1001193.

HAMPE, I. A., FRIEDMAN, J., EDGERTON, M. & MORSCHHÄUSER, J. 2017. An acquired mechanism of antifungal drug resistance simultaneously enables Candida albicans to escape from intrinsic host defenses. *PLoS pathogens,* 13**,** e1006655.

HAN, T.-L., CANNON, R. D., GALLO, S. M. & VILLAS-BÔAS, S. G. 2019. A metabolomic study of the effect of Candida albicans glutamate dehydrogenase deletion on growth and morphogenesis. *npj Biofilms and Microbiomes,* 5**,** 1-14.

HAN, Y., GAO, S., MUEGGE, K., ZHANG, W. & ZHOU, B. 2015. Advanced Applications of RNA Sequencing and Challenges. *Bioinformatics and biology insights,* 9**,** 29-46.

HESHAM, A. E.-L., UPADHYAY, R. S., SHARMA, G. D., MANOHARACHARY, C. & GUPTA, V. K. 2020. *Fungal Biotechnology and Bioengineering*, Springer.

HOLMES, A. R., CANNON, R. D. & SHEPHERD, M. G. 1991. Effect of calcium ion uptake on Candida albicans morphology. *FEMS microbiology letters,* 77**,** 187-193.

HORIUCHI, Y., KIMURA, R., KATO, N., FUJII, T., SEKI, M., ENDO, T., KATO, T. & KAWASHIMA, K. 2003. Evolutional study on acetylcholine expression. *Life Sci,* 72**,** 1745-56.

HORN, D. L., NEOFYTOS, D., ANAISSIE, E. J., FISHMAN, J. A., STEINBACH, W. J., OLYAEI, A. J., MARR, K. A., PFALLER, M. A., CHANG, C. H. & WEBSTER, K. M. 2009. Epidemiology and outcomes of candidemia in 2019 patients: data from the prospective antifungal therapy alliance registry. *Clin Infect Dis,* 48**,** 1695-703.

HOSSAIN, S., LASH, E., VERI, A. O. & COWEN, L. E. 2021. Functional connections between cell cycle and proteostasis in the regulation of Candida albicans morphogenesis. *Cell Reports,* 34**,** 108781.

HOSSAIN, S., VERI AMANDA, O., COWEN LEAH, E. & LORENZ, M. 2020. The Proteasome Governs Fungal Morphogenesis via Functional Connections with Hsp90 and cAMP-Protein Kinase A Signaling. *mBio,* 11**,** e00290-20.

HOVHANNISYAN, H. & GABALDÓN, T. 2018. Transcriptome sequencing approaches to elucidate host–microbe interactions in opportunistic human fungal pathogens. *Fungal Physiology and Immunopathogenesis*, 193-235.

HOYER, L. L., PAYNE, T. L. & HECHT, J. E. 1998. Identification of Candida albicans ALS2 and ALS4 and localization of als proteins to the fungal cell surface. *Journal of bacteriology,* 180, 5334-5343.

HSU, P.-C., YANG, C.-Y. & LAN, C.-Y. 2011. Candida albicans Hap43 is a repressor induced under low-iron conditions and is essential for iron-responsive transcriptional regulation and virulence. *Eukaryotic Cell,* 10, 207-225.

HUANG, G., HUANG, Q., WEI, Y., WANG, Y. & DU, H. 2019. Multiple roles and diverse regulation of the Ras/cAMP/protein kinase A pathway in Candida albicans. *Molecular Microbiology,* 111, 6-16.

IKEH, M., AHMED, Y. & QUINN, J. 2017. Phosphate acquisition and virulence in human fungal pathogens. *Microorganisms,* 5, 48.

IKEZAKI, S., CHO, T., NAGAO, J. I., TASAKI, S., YAMAGUCHI, M., ARITA-MORIOKA, K. I., YASUMATSU, K., CHIBANA, H., IKEBE, T. & TANAKA, Y. 2019. Mild Heat Stress Affects on the Cell Wall Structure in Candida albicans Biofilm. *Med Mycol J,* 60, 29-37.

JABRA-RIZK, M. A., KONG, E. F., TSUI, C., NGUYEN, M. H., CLANCY, C. J., FIDEL, P. L., JR. & NOVERR, M. 2016. Candida albicans Pathogenesis: Fitting within the Host-Microbe Damage Response Framework. *Infect Immun,* 84, 2724-39.

JACKSON, B. E., WILHELMUS, K. R. & HUBE, B. 2007. The Role of Secreted Aspartyl Proteinases in Candida albicans Keratitis. *Investigative Ophthalmology & Visual Science,* 48, 3559-3565.

JACOBSEN, J., VAN DEURS, B., PEDERSEN, M. & RASSING, M. R. 1995. TR146 cells grown on filters as a model for human buccal epithelium: I. Morphology, growth, barrier properties, and permeability. *International Journal of Pharmaceutics,* 125, 165-184.

JADHAV, A. & KARUPPAYIL, S. M. 2017. Candida Albicans Biofilm as a Clinical Challenge. *In:* SATYANARAYANA, T., DESHMUKH, S. K. & JOHRI, B. N. (eds.) *Developments in Fungal Biology and Applied Mycology*. Singapore: Springer Singapore.

JAVORKA, P., RAXWAL, V. K., NAJVAREK, J. & RIHA, K. 2019. artMAP: A user-friendly tool for mapping ethyl methanesulfonate-induced mutations in Arabidopsis. *Plant direct,* 3, e00146-e00146.

JEEVES, R. E., MASON, R. P., WOODACRE, A. & CASHMORE, A. M. 2011. Ferric reductase genes involved in high-affinity iron uptake are differentially regulated in yeast and hyphae of Candida albicans. *Yeast,* 28, 629-644.

JONES, C. K., BYUN, N. & BUBSER, M. 2012. Muscarinic and Nicotinic Acetylcholine Receptor Agonists and Allosteric Modulators for the Treatment of Schizophrenia. *Neuropsychopharmacology,* 37, 16-42.

JOSE, A., COCO, B. J., MILLIGAN, S., YOUNG, B., LAPPIN, D. F., BAGG, J., MURRAY, C. & RAMAGE, G. 2010. Reducing the incidence of denture stomatitis: are denture cleansers sufficient? *Journal of Prosthodontics: Implant, Esthetic and Reconstructive Dentistry,* 19, 252-257.

JUNKA, A. F., JANCZURA, A., SMUTNICKA, D., MACZYNSKA, B., SECEWICZ, A., NOWICKA, J., BARTOSZEWICZ, M. & GOSCINIAK, G. 2012. Use of the real time xCelligence system for purposes of medical microbiology. *Pol. J. Microbiol,* 61, 191-197.

KABIR, M. A., HUSSAIN, M. A. & AHMAD, Z. 2012. Candida albicans: A Model Organism for Studying Fungal Pathogens. *ISRN Microbiology,* 2012, 538694.

KADOSH, D. & JOHNSON, A. D. 2005. Induction of the Candida albicans filamentous growth program by relief of transcriptional repression: a genome-wide analysis. *Mol Biol Cell,* 16, 2903-12.

KADOSH, D. & LOPEZ-RIBOT, J. L. 2013. Candida albicans: adapting to succeed. *Cell host & microbe,* 14, 483-485.

KALANTAR, E., ASSADI, M., PORMAZAHERI, H., HATAMI, S., BARARI, M. A., ASGARI, E., MAHMOUDI, E., KABIR, K. & AMIN MARASHI, S. M. 2014. Candida non albicans with a High amphotericin B resistance pattern causing candidemia among cancer patients. *Asian Pac J Cancer Prev,* 15, 10933-5.

KAPAŁCZYŃSKA, M., KOLENDA, T., PRZYBYŁA, W., ZAJĄCZKOWSKA, M., TERESIAK, A., FILAS, V., IBBS, M., BLIŹNIAK, R., ŁUCZEWSKI, Ł. & LAMPERSKA, K. 2018. 2D and 3D cell cultures - a comparison of different types of cancer cell cultures. *Arch Med Sci,* 14, 910-919.

KARAKIULAKIS, G. & ROTH, M. 2012. Muscarinic receptors and their antagonists in COPD: anti-inflammatory and antiremodeling effects. *Mediators of inflammation,* 2012.

KASPER, L., KÖNIG, A., KOENIG, P.-A., GRESNIGT, M. S., WESTMAN, J., DRUMMOND, R. A., LIONAKIS, M. S., GROS, O., RULAND, J., NAGLIK, J. R. & HUBE, B. 2018. The fungal peptide toxin Candidalysin activates the NLRP3 inflammasome and causes cytolysis in mononuclear phagocytes. *Nature Communications,* 9, 4260.

KAUFMAN, D., LIKEN, H. & ODACKAL, N. J. 2019. Chapter 7 - Diagnosis, Risk Factors, Outcomes, and Evaluation of Invasive Candida Infections. *In:* BENITZ, W. E. & SMITH, P. B. (eds.) *Infectious Disease and Pharmacology*. Philadelphia: Elsevier.

KAWASHIMA, K., FUJII, T., MORIWAKI, Y. & MISAWA, H. 2012. Critical roles of acetylcholine and the muscarinic and nicotinic acetylcholine receptors in the regulation of immune function. *Life Sci,* 91, 1027-32.

KIM, D., PAGGI, J. M., PARK, C., BENNETT, C. & SALZBERG, S. L. 2019. Graph-based genome alignment and genotyping with HISAT2 and HISAT-genotype. *Nat Biotechnol,* 37, 907-915.

KITAICHI, K., DAY, J. C. & QUIRION, R. 1999. A novel muscarinic M4 receptor antagonist provides further evidence of an autoreceptor role for the muscarinic M2 receptor sub-type. *European journal of pharmacology,* 383, 53-56.

KIYOURA, Y. & TAMAI, R. 2015. Innate immunity to Candida albicans. *Japanese Dental Science Review,* 51, 59-64.

KLENGEL, T., LIANG, W.-J., CHALOUPKA, J., RUOFF, C., SCHRÖPPEL, K., NAGLIK, J. R., ECKERT, S. E., MOGENSEN, E. G., HAYNES, K. & TUITE, M. F. 2005. Fungal adenylyl cyclase integrates CO2 sensing with cAMP signaling and virulence. *Current Biology,* 15, 2021-2026.

KLIS, F. M., SOSINSKA, G. J., DE GROOT, P. W. J. & BRUL, S. 2009. Covalently linked cell wall proteins of Candida albicans and their role in fitness and virulence. *FEMS Yeast Research,* 9, 1013-1028.

KOARAI, A., TRAVES, S. L., FENWICK, P. S., BROWN, S. M., CHANA, K. K., RUSSELL, R. E., NICHOLSON, A. G., BARNES, P. J. & DONNELLY, L. E. 2012. Expression of muscarinic receptors by human macrophages. *Eur Respir J,* 39, 698-704.

KÖHLER, J. R., ACOSTA-ZALDÍVAR, M. & QI, W. 2020. Phosphate in Virulence of Candida albicans and Candida glabrata. *Journal of Fungi,* 6, 40.

KÖNIG, A., HUBE, B. & KASPER, L. 2020. The Dual Function of the Fungal Toxin Candidalysin during Candida albicans-Macrophage Interaction and Virulence. *Toxins,* 12**,** 469.

KORNITZER, D. 2019. Regulation of Candida albicans hyphal morphogenesis by endogenous signals. *Journal of Fungi,* 5**,** 21.

KOVÁCS, R. & MAJOROS, L. 2020. Fungal Quorum-Sensing Molecules: A Review of Their Antifungal Effect against Candida Biofilms. *J Fungi (Basel),* 6.

KRAIDLOVA, L., SCHREVENS, S., TOURNU, H., VAN ZEEBROECK, G., SYCHROVA, H. & VAN DIJCK, P. 2016. Characterization of the Candida albicans amino acid permease family: Gap2 is the only general amino acid permease and Gap4 is an S-adenosylmethionine (SAM) transporter required for SAM-induced morphogenesis. *Msphere,* 1**,** e00284-16.

KRUPPA, M. 2009. Quorum sensing and Candida albicans. *Mycoses,* 52**,** 1-10.

KRUSE, A. C., KOBILKA, B. K., GAUTAM, D., SEXTON, P. M., CHRISTOPOULOS, A. & WESS, J. 2014. Muscarinic acetylcholine receptors: novel opportunities for drug development. *Nature reviews. Drug discovery,* 13**,** 549-560.

KSIEZOPOLSKA, E. & GABALDÓN, T. 2018. Evolutionary Emergence of Drug Resistance in Candida Opportunistic Pathogens. *Genes (Basel),* 9.

KULLBERG, B. J. & ARENDRUP, M. C. 2015. Invasive Candidiasis. *N Engl J Med,* 373**,** 1445-56.

KULOYO, O., FOURIE, R., CASON, E., ALBERTYN, J. & POHL, C. H. 2020. Transcriptome Analyses of Candida albicans Biofilms, Exposed to Arachidonic Acid and Fluconazole, Indicates Potential Drug Targets. *G3 (Bethesda),* 10**,** 3099-3108.

KURZAI, O. 2013. *Human Fungal Pathogens*, Springer Science & Business Media.

LABED, S. A., WANI, K. A., JAGADEESAN, S., HAKKIM, A., NAJIBI, M. & IRAZOQUI, J. E. 2018. Intestinal Epithelial Wnt Signaling Mediates Acetylcholine-Triggered Host Defense against Infection. *Immunity,* 48**,** 963-978.e3.

LAFORET, L., MORENO, I., S·NCHEZ-FRESNEDA, R., MARTÌNEZ-ESPARZA, M., MARTÌNEZ, J. P., ARG¸ELLES, J., GROOT, P. D. D. & VALENTÌN-GOMEZ, E. 2011. Pga26 mediates filamentation and biofilm formation and is required for virulence in Candida albicans. *FEMS yeast research,* 11 5**,** 389-97.

LAN, C.-Y., NEWPORT, G., MURILLO, L. A., JONES, T., SCHERER, S., DAVIS, R. W. & AGABIAN, N. 2002. Metabolic specialization associated with phenotypic switching in Candidaalbicans. *Proceedings of the National Academy of Sciences of the United States of America,* 99**,** 14907-14912.

LAUDENBACH, J. M. & EPSTEIN, J. B. 2009. Treatment strategies for oropharyngeal candidiasis. *Expert Opin Pharmacother,* 10**,** 1413-21.

LEACH, M. D., BUDGE, S., WALKER, L., MUNRO, C., COWEN, L. E. & BROWN, A. J. 2012. Hsp90 orchestrates transcriptional regulation by Hsf1 and cell wall remodelling by MAPK signalling during thermal adaptation in a pathogenic yeast. *PLoS Pathog,* 8**,** e1003069.

LEBLANC, E. V., POLVI, E. J., VERI, A. O., PRIVÉ, G. G. & COWEN, L. E. 2020. Structure-guided approaches to targeting stress responses in human fungal pathogens. *Journal of Biological Chemistry,* 295**,** 14458-14472.

LEE, Y., PUUMALA, E., ROBBINS, N. & COWEN, L. E. 2021. Antifungal Drug Resistance: Molecular Mechanisms in Candida albicans and Beyond. *Chem Rev,* 121**,** 3390-3411.

LEV, S. & DJORDJEVIC, J. T. 2018. Why is a functional PHO pathway required by fungal pathogens to disseminate within a phosphate-rich host: a paradox

explained by alkaline pH-simulated nutrient deprivation and expanded PHO pathway function. *PLoS pathogens,* 14**,** e1007021.

LI, J., NING, Y., HEDLEY, W., SAUNDERS, B., CHEN, Y., TINDILL, N., HANNAY, T. & SUBRAMANIAM, S. 2002. The Molecule Pages database. *Nature,* 420**,** 716-7.

LIAO, Y., SMYTH, G. K. & SHI, W. 2014. featureCounts: an efficient general purpose program for assigning sequence reads to genomic features. *Bioinformatics,* 30**,** 923-30.

LIESCHKE, G. J., GRAIL, D., HODGSON, G., METCALF, D., STANLEY, E., CHEERS, C., FOWLER, K. J., BASU, S., ZHAN, Y. F. & DUNN, A. R. 1994. Mice lacking granulocyte colony-stimulating factor have chronic neutropenia, granulocyte and macrophage progenitor cell deficiency, and impaired neutrophil mobilization.

LIMA, S. L., COLOMBO, A. L. & DE ALMEIDA JUNIOR, J. N. 2019. Fungal Cell Wall: Emerging Antifungals and Drug Resistance. *Frontiers in Microbiology,* 10.

LIN, C.-J. & CHEN, Y.-L. 2018. Conserved and Divergent Functions of the cAMP/PKA Signaling Pathway in Candida albicans and Candida tropicalis. *Journal of fungi (Basel, Switzerland),* 4**,** 68.

LIU, C., XU, C., DU, Y., LIU, J. & NING, Y. 2021. Role of agglutinin-like sequence protein 3 (Als3) in the structure and antifungal resistance of Candida albicans biofilms. *FEMS Microbiology Letters,* 368.

LIU, N.-N., FLANAGAN, P. R., ZENG, J., JANI, N. M., CARDENAS, M. E., MORAN, G. P. & KÖHLER, J. R. 2017. Phosphate is the third nutrient monitored by TOR in Candida albicans and provides a target for fungal-specific indirect TOR inhibition. *Proceedings of the National Academy of Sciences,* 114**,** 6346-6351.

LIU, S., LI, J., TAN, D. T. & BEUERMAN, R. W. 2007. Expression and function of muscarinic receptor subtypes on human cornea and conjunctiva. *Investigative ophthalmology & visual science,* 48**,** 2987-2996.

LIU, Y. & FILLER, S. G. 2011. Candida albicans Als3, a multifunctional adhesin and invasin. *Eukaryotic cell,* 10**,** 168-173.

LÓPEZ-GARCÍA, B., LEE, P. H., YAMASAKI, K. & GALLO, R. L. 2005. Anti-fungal activity of cathelicidins and their potential role in Candida albicans skin infection. *Journal of Investigative Dermatology,* 125**,** 108-115.

LOTZ, H., SOHN, K., BRUNNER, H., MUHLSCHLEGEL, F. A. & RUPP, S. 2004. RBR1, a novel pH-regulated cell wall gene of Candida albicans, is repressed by RIM101 and activated by NRG1. *Eukaryotic cell,* 3**,** 776-784.

LOWE, R., SHIRLEY, N., BLEACKLEY, M., DOLAN, S. & SHAFEE, T. 2017. Transcriptomics technologies. *PLoS computational biology,* 13**,** e1005457.

LOWRY, M. B., GUO, C., BORREGAARD, N. & GOMBART, A. F. 2014. Regulation of the human cathelicidin antimicrobial peptide gene by 1α,25-dihydroxyvitamin D3 in primary immune cells. *The Journal of steroid biochemistry and molecular biology,* 143**,** 183-191.

LU, J. & WU, W. 2021. Cholinergic modulation of the immune system–A novel therapeutic target for myocardial inflammation. *International Immunopharmacology,* 93**,** 107391.

LU, Q., JAYATILAKE, J. A., SAMARANAYAKE, L. P. & JIN, L. 2006. Hyphal invasion of Candida albicans inhibits the expression of human β-defensins in experimental oral candidiasis. *Journal of Investigative Dermatology,* 126**,** 2049-2056.

LV, Q.-Z., YAN, L. & JIANG, Y.-Y. 2016. The synthesis, regulation, and functions of sterols in Candida albicans: Well-known but still lots to learn. *Virulence,* 7, 649-659.

M HARANDI, A. & MEDAGLINI, D. 2010. Mucosal adjuvants. *Current HIV research,* 8, 330-335.

MAIDAN, M. M., DE ROP, L., SERNEELS, J., EXLER, S., RUPP, S., TOURNU, H., THEVELEIN, J. M. & VAN DIJCK, P. 2005. The G protein-coupled receptor Gpr1 and the Galpha protein Gpa2 act through the cAMP-protein kinase A pathway to induce morphogenesis in Candida albicans. *Molecular biology of the cell,* 16, 1971-1986.

MAMOUEI, Z., SINGH, S., LEMIRE, B., GU, Y., ALQARIHI, A., NABEELA, S., LI, D., IBRAHIM, A. & UPPULURI, P. 2021. An evolutionarily diverged mitochondrial protein controls biofilm growth and virulence in Candida albicans. *PLOS Biology,* 19, e3000957.

MAMOUEI, Z., ZENG, G., WANG, Y.-M. & WANG, Y. 2017. Candida albicans possess a highly versatile and dynamic high-affinity iron transport system important for its commensal-pathogenic lifestyle. *Molecular Microbiology,* 106, 986-998.

MARAS, B., MAGGIORE, A., MIGNOGNA, G., D'ERME, M. & ANGIOLELLA, L. 2021. Hyperexpression of CDRs and HWP1 genes negatively impacts on Candida albicans virulence. *PLoS One,* 16, e0252555.

MARCHI, N., BATRA, A., TUXHORN, I., GRANATA, T., DE CURTIS, M. & JANIGRO, D. 2009. INFLAMMATION | Cerebrovascular Diseases, Seizures, and Epilepsy. *In:* SCHWARTZKROIN, P. A. (ed.) *Encyclopedia of Basic Epilepsy Research.* Oxford: Academic Press.

MARTCHENKO, M., ALARCO, A.-M., HARCUS, D. & WHITEWAY, M. 2004. Superoxide dismutases in Candida albicans: transcriptional regulation and functional characterization of the hyphal-induced SOD5 gene. *Molecular biology of the cell,* 15, 456-467.

MARTÍN, J. P. & DI PIETRO, A. 2012. *Morphogenesis and pathogenicity in fungi*, Springer Science & Business Media.

MARTIN, R., ALBRECHT-ECKARDT, D., BRUNKE, S., HUBE, B., HÜNNIGER, K. & KURZAI, O. 2013. A core filamentation response network in Candida albicans is restricted to eight genes. *PloS one,* 8, e58613-e58613.

MARTINEZ-POMARES, L. 2012. The mannose receptor. *J Leukoc Biol,* 92, 1177-86.

MATHÉ, L. & VAN DIJCK, P. 2013. Recent insights into Candida albicans biofilm resistance mechanisms. *Current Genetics,* 59, 251-264.

MATUSCHAK, G. M. & LECHNER, A. J. 1997. The yeast to hyphal transition following hematogenous candidiasis induces shock and organ injury independent of circulating tumor necrosis factor-alpha. *Critical care medicine,* 25, 111-120.

MAYER, F. L., WILSON, D. & HUBE, B. 2013. Candida albicans pathogenicity mechanisms. *Virulence,* 4, 119-128.

MAYERS, D. L., SOBEL, J. D., OUELLETTE, M., KAYE, K. S. & MARCHAIM, D. 2009. *Antimicrobial drug resistance*, Springer.

MBA, I. E. & NWEZE, E. I. 2020. Mechanism of Candida pathogenesis: revisiting the vital drivers. *Eur J Clin Microbiol Infect Dis,* 39, 1797-1819.

MCCALL, A. D., PATHIRANA, R. U., PRABHAKAR, A., CULLEN, P. J. & EDGERTON, M. 2019. Candida albicans biofilm development is governed by cooperative attachment and adhesion maintenance proteins. *npj Biofilms and Microbiomes,* 5, 21.

MEHTA, H. M., MALANDRA, M. & COREY, S. J. 2015. G-csf and gm-csf in neutropenia. *The Journal of Immunology,* 195**,** 1341-1349.

MILLHOUSE, E., JOSE, A., SHERRY, L., LAPPIN, D. F., PATEL, N., MIDDLETON, A. M., PRATTEN, J., CULSHAW, S. & RAMAGE, G. 2014. Development of an in vitro periodontal biofilm model for assessing antimicrobial and host modulatory effects of bioactive molecules. *BMC oral health,* 14**,** 1-11.

MIRAMÓN, P. & LORENZ, M. C. 2017. A feast for Candida: metabolic plasticity confers an edge for virulence. *PLoS pathogens,* 13**,** e1006144.

MIWA, T., TAKAGI, Y., SHINOZAKI, M., YUN, C.-W., SCHELL, W. A., PERFECT, J. R., KUMAGAI, H. & TAMAKI, H. 2004. Gpr1, a putative G-protein-coupled receptor, regulates morphogenesis and hypha formation in the pathogenic fungus Candida albicans. *Eukaryotic cell,* 3**,** 919-931.

MOCHOCHOKO, B. M., EZEOKOLI, O. T., SEBOLAI, O., ALBERTYN, J. & POHL, C. H. 2021. Role of the high-affinity reductive iron acquisition pathway of Candida albicans in prostaglandin E2 production, virulence, and interaction with Pseudomonas aeruginosa. *Medical Mycology,* 59**,** 869-881.

MOOSA, M.-Y. S., SOBEL, J. D., ELHALIS, H., DU, W. & AKINS, R. A. 2004. Fungicidal activity of fluconazole against Candida albicans in a synthetic vagina-simulative medium. *Antimicrobial agents and chemotherapy,* 48**,** 161-167.

MØRCK NIELSEN, H. & RØMER RASSING, M. 2000. TR146 cells grown on filters as a model of human buccal epithelium: V. Enzyme activity of the TR146 cell culture model, human buccal epithelium and porcine buccal epithelium, and permeability of leu-enkephalin. *Int J Pharm,* 200**,** 261-70.

MORGAN, J., MELTZER, M. I., PLIKAYTIS, B. D., SOFAIR, A. N., HUIE-WHITE, S., WILCOX, S., HARRISON, L. H., SEABERG, E. C., HAJJEH, R. A. & TEUTSCH, S. M. 2005. Excess mortality, hospital stay, and cost due to candidemia: a case-control study using data from population-based candidemia surveillance. *Infect Control Hosp Epidemiol,* 26**,** 540-7.

MORIO, F., JENSEN, R. H., LE PAPE, P. & ARENDRUP, M. C. 2017. Molecular basis of antifungal drug resistance in yeasts. *International Journal of Antimicrobial Agents,* 50**,** 599-606.

MORIO, F., LOMBARDI, L. & BUTLER, G. 2020. The CRISPR toolbox in medical mycology: State of the art and perspectives. *PLoS pathogens,* 16**,** e1008201-e1008201.

MORIOKA, S., SHIGEMORI, T., HARA, K., MORISAKA, H., KURODA, K. & UEDA, M. 2013. Effect of sterol composition on the activity of the yeast G-protein-coupled receptor Ste2. *Applied microbiology and biotechnology,* 97**,** 4013-4020.

MOYES, D. L., RICHARDSON, J. P. & NAGLIK, J. R. 2015. Candida albicans-epithelial interactions and pathogenicity mechanisms: scratching the surface. *Virulence,* 6**,** 338-46.

MOYES, D. L., SHEN, C., MURCIANO, C., RUNGLALL, M., RICHARDSON, J. P., ARNO, M., ALDECOA-OTALORA, E. & NAGLIK, J. R. 2014. Protection against epithelial damage during Candida albicans infection is mediated by PI3K/Akt and mammalian target of rapamycin signaling. *J Infect Dis,* 209**,** 1816-26.

MOYES, D. L., WILSON, D., RICHARDSON, J. P., MOGAVERO, S., TANG, S. X., WERNECKE, J., HÖFS, S., GRATACAP, R. L., ROBBINS, J. & RUNGLALL, M. 2016. Candidalysin is a fungal peptide toxin critical for mucosal infection. *Nature,* 532**,** 64-68.

MROCZYŃSKA, M. & BRILLOWSKA-DĄBROWSKA, A. 2020. Review on Current Status of Echinocandins Use. *Antibiotics,* 9**,** 227.

MÜHLSCHLEGEL, F. A. & FONZI, W. A. 1997. PHR2 of Candida albicans encodes a functional homolog of the pH-regulated gene PHR1 with an inverted pattern of pH-dependent expression. *Mol Cell Biol,* 17**,** 5960-7.

MUKAREMERA, L., LEE, K. K., MORA-MONTES, H. M. & GOW, N. A. 2017. Candida albicans yeast, pseudohyphal, and hyphal morphogenesis differentially affects immune recognition. *Frontiers in immunology,* 8**,** 629.

MUKHERJEE, P. K., CHANDRA, J., KUHN, D. M. & GHANNOUM, M. A. 2003. Differential expression of Candida albicans phospholipase B (PLB1) under various environmental and physiological conditions. *Microbiology (Reading),* 149**,** 261-7.

MURAD, A. M. A., LENG, P., STRAFFON, M., WISHART, J., MACASKILL, S., MACCALLUM, D., SCHNELL, N., TALIBI, D., MARECHAL, D. & TEKAIA, F. 2001. NRG1 represses yeast–hypha morphogenesis and hypha-specific gene expression in Candida albicans. *The EMBO journal,* 20**,** 4742-4752.

NAGLIK, J. R. 2014. Candida Immunity. *New Journal of Science,* 2014**,** 390241.

NAGLIK, J. R., CHALLACOMBE, S. J. & HUBE, B. 2003. Candida albicans secreted aspartyl proteinases in virulence and pathogenesis. *Microbiology and molecular biology reviews : MMBR,* 67**,** 400-428.

NAGLIK, J. R., GAFFEN, S. L. & HUBE, B. 2019. Candidalysin: discovery and function in Candida albicans infections. *Current opinion in microbiology,* 52**,** 100-109.

NASEEM, S., ARAYA, E. & KONOPKA, J. B. 2015. Hyphal growth in Candida albicans does not require induction of hyphal-specific gene expression. *Molecular biology of the cell,* 26**,** 1174-1187.

NAVARATHNA, D. H. M. L. P. & ROBERTS, D. D. 2010. Candida albicans heme oxygenase and its product CO contribute to pathogenesis of candidemia and alter systemic chemokine and cytokine expression. *Free radical biology & medicine,* 49**,** 1561-1573.

NETEA, M. G., JOOSTEN, L. A. B., VAN DER MEER, J. W. M., KULLBERG, B.-J. & VAN DE VEERDONK, F. L. 2015. Immune defence against Candida fungal infections. *Nature Reviews Immunology,* 15**,** 630-642.

NETT, J., LINCOLN, L., MARCHILLO, K., MASSEY, R., HOLOYDA, K., HOFF, B., VANHANDEL, M. & ANDES, D. 2007. Putative role of beta-1,3 glucans in Candida albicans biofilm resistance. *Antimicrob Agents Chemother,* 51**,** 510-20.

NEVILLE, B. A., D'ENFERT, C. & BOUGNOUX, M.-E. 2015. Candida albicans commensalism in the gastrointestinal tract. *FEMS Yeast Research,* 15.

NIKOU, S. A., KICHIK, N., BROWN, R., PONDE, N. O., HO, J., NAGLIK, J. R. & RICHARDSON, J. P. 2019. Candida albicans Interactions with Mucosal Surfaces during Health and Disease. *Pathogens,* 8.

NILE, C., FALLENI, M., CIRASOLA, D., ALGHAMDI, A., ANDERSON, O. F., DELANEY, C., RAMAGE, G., OTTAVIANO, E., TOSI, D. & BULFAMANTE, G. 2019. Repurposing pilocarpine hydrochloride for treatment of Candida albicans infections. *Msphere,* 4.

NISHIMURA, A., OKAMOTO, M., SUGAWARA, Y., MIZUNO, N., YAMAUCHI, J. & ITOH, H. 2006. Ric-8A potentiates Gq-mediated signal transduction by acting downstream of G protein-coupled receptor in intact cells. *Genes Cells,* 11**,** 487-98.

NOBILE, C. J., FOX, E. P., NETT, J. E., SORRELLS, T. R., MITROVICH, Q. M., HERNDAY, A. D., TUCH, B. B., ANDES, D. R. & JOHNSON, A. D. 2012. A recently evolved transcriptional network controls biofilm development in Candida albicans. *Cell,* 148**,** 126-138.

NOBILE, C. J. & JOHNSON, A. D. 2015. Candida albicans Biofilms and Human Disease. *Annu Rev Microbiol,* 69**,** 71-92.

NOBILE, C. J., SCHNEIDER, H. A., NETT, J. E., SHEPPARD, D. C., FILLER, S. G., ANDES, D. R. & MITCHELL, A. P. 2008. Complementary adhesin function in C. albicans biofilm formation. *Current biology : CB,* 18**,** 1017-1024.

NOBLE, S. M., FRENCH, S., KOHN, L. A., CHEN, V. & JOHNSON, A. D. 2010. Systematic screens of a Candida albicans homozygous deletion library decouple morphogenetic switching and pathogenicity. *Nature Genetics,* 42**,** 590-598.

O'DONNELL, L. E., ALALWAN, H. K., KEAN, R., CALVERT, G., NILE, C. J., LAPPIN, D. F., ROBERTSON, D., WILLIAMS, C., RAMAGE, G. & SHERRY, L. 2017. Candida albicans biofilm heterogeneity does not influence denture stomatitis but strongly influences denture cleansing capacity. *Journal of medical microbiology,* 66**,** 54-60.

OCKENGA, W., KÜHNE, S., BOCKSBERGER, S., BANNING, A. & TIKKANEN, R. 2013. Non-neuronal functions of the m2 muscarinic acetylcholine receptor. *Genes (Basel),* 4**,** 171-97.

ODDS, F. C., BROWN, A. J. & GOW, N. A. 2004. Candida albicans genome sequence: a platform for genomics in the absence of genetics. *Genome Biol,* 5**,** 230.

OKAMOTO-SHIBAYAMA, K., KIKUCHI, Y., KOKUBU, E., SATO, Y. & ISHIHARA, K. 2014. Csa2, a member of the Rbt5 protein family, is involved in the utilization of iron from human hemoglobin during Candida albicans hyphal growth. *FEMS Yeast Res,* 14**,** 674-7.

OKUMA, Y. & NOMURA, Y. 2001. The Non-neuronal Cholinergic System: Roles of Muscarinic Acetylcholine Receptors in Interleukin-2 Synthesis in Lymphocytes. *Japanese Journal of Pharmacology,* 85**,** 16-19.

OWOTADE, F., GULUBE, Z., RAMLA, S. & PATEL, M. 2016. Antifungal susceptibility of Candida albicans isolated from the oral cavities of patients with HIV infection and cancer. *South African Dental Journal,* 71**,** 8-11.

PANDEY, N., GUPTA, M. K. & TILAK, R. 2018. Extracellular hydrolytic enzyme activities of the different Candida spp. isolated from the blood of the Intensive Care Unit-admitted patients. *Journal of laboratory physicians,* 10**,** 392-396.

PATIL, S., MAJUMDAR, B., SARODE, S. C., SARODE, G. S. & AWAN, K. H. 2018. Oropharyngeal Candidosis in HIV-Infected Patients-An Update. *Frontiers in microbiology,* 9**,** 980-980.

PAVLOV, V. A. & TRACEY, K. J. 2005. The cholinergic anti-inflammatory pathway. *Brain Behav Immun,* 19**,** 493-9.

PELLON, A., SADEGHI NASAB, S. D. & MOYES, D. L. 2020. New Insights in Candida albicans Innate Immunity at the Mucosa: Toxins, Epithelium, Metabolism, and Beyond. *Front Cell Infect Microbiol,* 10**,** 81.

PENTLAND, D. R., MUHLSCHLEGEL, F. A. & GOURLAY, C. W. 2020. CO2 enhances the ability of Candida albicans to form biofilms, overcome nutritional immunity and resist antifungal treatment. *BioRxiv*.

PEREIRA, R., DOS SANTOS FONTENELLE, R. O., DE BRITO, E. H. S. & DE MORAIS, S. M. 2020. Biofilm of Candida albicans: formation, regulation and resistance. *Journal of Applied Microbiology*.

PERUMAL, P., MEKALA, S. & CHAFFIN, W. L. 2007. Role for cell density in antifungal drug resistance in Candida albicans biofilms. *Antimicrobial agents and chemotherapy,* 51, 2454-2463.

PFALLER, M. A. & DIEKEMA, D. J. 2007. Epidemiology of invasive candidiasis: a persistent public health problem. *Clin Microbiol Rev,* 20, 133-63.

PHAN, Q. T., MYERS, C. L., FU, Y., SHEPPARD, D. C., YEAMAN, M. R., WELCH, W. H., IBRAHIM, A. S., EDWARDS, J. E., JR. & FILLER, S. G. 2007. Als3 is a Candida albicans invasin that binds to cadherins and induces endocytosis by host cells. *PLoS Biol,* 5, e64.

PIANALTO, K. M. & ALSPAUGH, J. A. 2016. New Horizons in Antifungal Therapy. *Journal of fungi (Basel, Switzerland),* 2, 26.

POHANKA, M. 2012. Alpha7 nicotinic acetylcholine receptor is a target in pharmacology and toxicology. *Int J Mol Sci,* 13, 2219-38.

POLAK, A. 2004. Antifungal Drugs. *Encyclopedic Reference of Molecular Pharmacology*. Berlin, Heidelberg: Springer Berlin Heidelberg.

POPP, C., RAMÍREZ-ZAVALA, B., SCHWANFELDER, S., KRÜGER, I. & MORSCHHÄUSER, J. 2019. Evolution of fluconazole-resistant Candida albicans strains by drug-induced mating competence and parasexual recombination. *MBio,* 10.

PRASAD, R. 2017. *Candida albicans: Cellular and Molecular Biology,* Cham, Springer International Publishing.

PURI, S., KUMAR, R., ROJAS, I. G., SALVATORI, O. & EDGERTON, M. 2019. Iron Chelator Deferasirox Reduces Candida albicans Invasion of Oral Epithelial Cells and Infection Levels in Murine Oropharyngeal Candidiasis. *Antimicrobial agents and chemotherapy,* 63, e02152-18.

QIN, Y., ZHANG, L., XU, Z., ZHANG, J., JIANG, Y. Y., CAO, Y. & YAN, T. 2016. Innate immune cell response upon Candida albicans infection. *Virulence,* 7, 512-26.

QUINDÓS, G., MARCOS-ARIAS, C., SAN-MILLÁN, R., MATEO, E. & ERASO, E. 2018. The continuous changes in the aetiology and epidemiology of invasive candidiasis: from familiar Candida albicans to multiresistant Candida auris. *Int Microbiol,* 21, 107-119.

RABUT, G. & PETER, M. 2008. Function and regulation of protein neddylation. 'Protein modifications: beyond the usual suspects' review series. *EMBO reports,* 9, 969-976.

RADU, B. M., OSCULATI, A. M. M., SUKU, E., BANCIU, A., TSENOV, G., MERIGO, F., DI CHIO, M., BANCIU, D. D., TOGNOLI, C., KACER, P., GIORGETTI, A., RADU, M., BERTINI, G. & FABENE, P. F. 2017. All muscarinic acetylcholine receptors (M1-M5) are expressed in murine brain microvascular endothelium. *Scientific Reports,* 7, 5083.

RAJENDRAN, R., BORGHI, E., FALLENI, M., PERDONI, F., TOSI, D., LAPPIN, D. F., O'DONNELL, L., GREETHAM, D., RAMAGE, G. & NILE, C. 2015. Acetylcholine Protects against Candida albicans Infection by Inhibiting Biofilm Formation and Promoting Hemocyte Function in a Galleria mellonella Infection Model. *Eukaryot Cell,* 14, 834-44.

RAJENDRAN, R., MAY, A., SHERRY, L., KEAN, R., WILLIAMS, C., JONES, B. L., BURGESS, K. V., HERINGA, J., ABELN, S., BRANDT, B. W., MUNRO, C. A. & RAMAGE, G. 2016a. Integrating Candida albicans metabolism with biofilm heterogeneity by transcriptome mapping. *Sci Rep,* 6, 35436.

RAJENDRAN, R., SHERRY, L., LAPPIN, D. F., NILE, C. J., SMITH, K., WILLIAMS, C., MUNRO, C. A. & RAMAGE, G. 2014. Extracellular DNA release confers

heterogeneity in Candida albicans biofilm formation. *BMC microbiology,* 14**,** 1-9.

RAJENDRAN, R., SHERRY, L., NILE, C. J., SHERRIFF, A., JOHNSON, E. M., HANSON, M. F., WILLIAMS, C., MUNRO, C. A., JONES, B. J. & RAMAGE, G. 2016b. Biofilm formation is a risk factor for mortality in patients with Candida albicans bloodstream infection-Scotland, 2012-2013. *Clin Microbiol Infect,* 22**,** 87-93.

RAKER, V. K., BECKER, C. & STEINBRINK, K. 2016. The cAMP Pathway as Therapeutic Target in Autoimmune and Inflammatory Diseases. *Frontiers in immunology,* 7**,** 123-123.

RAMAGE, G., SAVILLE, S. P., WICKES, B. L. & LÓPEZ-RIBOT, J. L. 2002. Inhibition of Candida albicans biofilm formation by farnesol, a quorum-sensing molecule. *Applied and environmental microbiology,* 68**,** 5459-5463.

RANDÁKOVÁ, A. & JAKUBÍK, J. 2021. Functionally selective and biased agonists of muscarinic receptors. *Pharmacological Research,* 169**,** 105641.

RAPALA-KOZIK, M., ZAWROTNIAK, M., GOGOL, M., BARTNICKA, D., SATALA, D., SMOLARZ, M., KARKOWSKA-KULETA, J. & KOZIK, A. 2018. Interactions of Candida albicans Cells with Aerobic and Anaerobic Bacteria during Formation of Mixed Biofilms in the Oral Cavity. *Candida Albicans.* IntechOpen.

RAUSEO, A. M., COLER-REILLY, A., LARSON, L. & SPEC, A. 2020. Hope on the Horizon: Novel Fungal Treatments in Development. *Open Forum Infectious Diseases,* 7.

RAZANI-BOROUJERDI, S., BEHL, M., HAHN, F. F., PENA-PHILIPPIDES, J. C., HUTT, J. & SOPORI, M. L. 2008. Role of muscarinic receptors in the regulation of immune and inflammatory responses. *Journal of neuroimmunology,* 194**,** 83-88.

REALE, M. & COSTANTINI, E. 2021. Cholinergic Modulation of the Immune System in Neuroinflammatory Diseases. *Diseases,* 9**,** 29.

REYNA-BELTRÁN, E., ISAAC BAZÁN MÉNDEZ, C., IRANZO, M., MORMENEO, S. & PEDRO LUNA-ARIAS, J. 2019. The cell wall of Candida albicans: A proteomics view. *Candida Albicans***,** 71-92.

RICCOMBENI, A. & BUTLER, G. 2012. Role of Genomics and RNA-seq in Studies of Fungal Virulence. *Current Fungal Infection Reports,* 6**,** 267-274.

RIVAS-SANTIAGO, B., HERNANDEZ-PANDO, R., CARRANZA, C., JUAREZ, E., CONTRERAS, J. L., AGUILAR-LEON, D., TORRES, M. & SADA, E. 2008. Expression of cathelicidin LL-37 during Mycobacterium tuberculosis infection in human alveolar macrophages, monocytes, neutrophils, and epithelial cells. *Infection and immunity,* 76**,** 935-941.

RIZZO, J., STANCHEV, L. D., DA SILVA, V. K. A., NIMRICHTER, L., POMORSKI, T. G. & RODRIGUES, M. L. 2019. Role of lipid transporters in fungal physiology and pathogenicity. *Computational and Structural Biotechnology Journal,* 17**,** 1278-1289.

ROBSON, A.-L., DASTOOR, P. C., FLYNN, J., PALMER, W., MARTIN, A., SMITH, D. W., WOLDU, A. & HUA, S. 2018. Advantages and Limitations of Current Imaging Techniques for Characterizing Liposome Morphology. *Frontiers in Pharmacology,* 9.

ROEMER, T. & KRYSAN, D. J. 2014. Antifungal drug development: challenges, unmet clinical needs, and new approaches. *Cold Spring Harbor perspectives in medicine,* 4**,** a019703.

ROMANI, L. 2011. Immunity to fungal infections. *Nat Rev Immunol,* 11**,** 275-88.

ROMO, J. A., ZHANG, H., CAI, H., KADOSH, D., KOEHLER, J. R., SAVILLE, S. P., WANG, Y. & LOPEZ-RIBOT, J. L. 2019. Global Transcriptomic Analysis of the Candida albicans Response to Treatment with a Novel Inhibitor of Filamentation. *mSphere,* 4.

ROSENBAUM, D. M., RASMUSSEN, S. G. F. & KOBILKA, B. K. 2009. The structure and function of G-protein-coupled receptors. *Nature,* 459**,** 356-363.

RUIZ-HERRERA, J., VICTORIA ELORZA, M., VALENTÍN, E. & SENTANDREU, R. 2006. Molecular organization of the cell wall of Candida albicans and its relation to pathogenicity. *FEMS yeast research,* 6**,** 14-29.

RUPNIAK, H. T., ROWLATT, C., LANE, E. B., STEELE, J. G., TREJDOSIEWICZ, L. K., LASKIEWICZ, B., POVEY, S. & HILL, B. T. 1985. Characteristics of four new human cell lines derived from squamous cell carcinomas of the head and neck. *J Natl Cancer Inst,* 75**,** 621-35.

SADEGHI GOOGHERI, M. S., HOUSAINDOKHT, M. R. & SABZYAN, H. 2015. Theoretical studies on the deacylation step of acylated Candida Antarctica lipase B: structural and reaction pathway analysis. *J Mol Graph Model,* 57**,** 9-19.

SAKAGUCHI, S., SHIBUYA, K., IIDA, H., ANRAKU, Y. & SUZUKI, T. 1997. Roles of Ca 2+ in hyphal and yeast-form growth inCandida albicans. Growth regulation by altered extracellular and intracellular free Ca 2+ concentrations. *Mycoscience,* 38**,** 215-225.

SAM, Q. H., YEW, W. S., SENEVIRATNE, C. J., CHANG, M. W. & CHAI, L. Y. A. 2018. Immunomodulation as Therapy for Fungal Infection: Are We Closer? *Frontiers in Microbiology,* 9.

SAMARANAYAKE, L. P., KEUNG LEUNG, W. & JIN, L. 2009. Oral mucosal fungal infections. *Periodontol 2000,* 49**,** 39-59.

SANDAI, D., TABANA, Y. M., EL OUWEINI, A. & AYODEJI, I. O. 2016. Resistance of Candida albicans biofilms to drugs and the host immune system. *Jundishapur journal of microbiology,* 9.

SANDAI, D., YIN, Z., SELWAY, L., STEAD, D., WALKER, J., LEACH, M. D., BOHOVYCH, I., ENE, I. V., KASTORA, S. & BUDGE, S. 2012. The evolutionary rewiring of ubiquitination targets has reprogrammed the regulation of carbon assimilation in the pathogenic yeast Candida albicans. *MBio,* 3**,** e00495-12.

SARAVOLATZ, L. D., DERESINSKI, S. C. & STEVENS, D. A. 2003. Caspofungin. *Clinical Infectious Diseases,* 36**,** 1445-1457.

SARDI, J. C. O., SCORZONI, L., BERNARDI, T., FUSCO-ALMEIDA, A. M. & MENDES GIANNINI, M. J. S. 2013. Candida species: current epidemiology, pathogenicity, biofilm formation, natural antifungal products and new therapeutic options. *J Med Microbiol,* 62**,** 10-24.

SCHALLER, M., BORELLI, C., KORTING, H. C. & HUBE, B. 2005. Hydrolytic enzymes as virulence factors of Candida albicans. *Mycoses,* 48**,** 365-77.

SCHALLER, M., MAILHAMMER, R., GRASSL, G., SANDER, C. A., HUBE, B. & KORTING, H. C. 2002. Infection of human oral epithelia with Candida species induces cytokine expression correlated to the degree of virulence. *J Invest Dermatol,* 118**,** 652-7.

SCHIJNS, V. & O'HAGAN, D. 2016. *Immunopotentiators in modern vaccines*, Academic Press.

SCHNEYER, C. A. 1957. The effect of pilocarpine on tumor growth. *Cancer research,* 17**,** 332-335.

SCHWARZ, S., LUCAS, S. D., SOMMERWERK, S. & CSUK, R. 2014. Amino derivatives of glycyrrhetinic acid as potential inhibitors of cholinesterases. *Bioorg Med Chem,* 22**,** 3370-8.

SHANNON, P., MARKIEL, A., OZIER, O., BALIGA, N. S., WANG, J. T., RAMAGE, D., AMIN, N., SCHWIKOWSKI, B. & IDEKER, T. 2003. Cytoscape: a software environment for integrated models of biomolecular interaction networks. *Genome Res,* 13**,** 2498-504.

SHAPIRO, R. S., ROBBINS, N. & COWEN, L. E. 2011. Regulatory circuitry governing fungal development, drug resistance, and disease. *Microbiology and molecular biology reviews : MMBR,* 75**,** 213-267.

SHERRINGTON, S. L., SORSBY, E., MAHTEY, N., KUMWENDA, P., LENARDON, M. D., BROWN, I., BALLOU, E. R., MACCALLUM, D. M. & HALL, R. A. 2017. Adaptation of Candida albicans to environmental pH induces cell wall remodelling and enhances innate immune recognition. *PLoS pathogens,* 13**,** e1006403.

SHERRY, L., JOSE, A., MURRAY, C., WILLIAMS, C., JONES, B., MILLINGTON, O., BAGG, J. & RAMAGE, G. 2012. Carbohydrate derived fulvic acid: an in vitro investigation of a novel membrane active antiseptic agent against Candida albicans biofilms. *Frontiers in microbiology,* 3**,** 116.

SHERRY, L., KEAN, R., MCKLOUD, E., O'DONNELL, L. E., METCALFE, R., JONES, B. L. & RAMAGE, G. 2017. Biofilms formed by isolates from recurrent vulvovaginal candidiasis patients are heterogeneous and insensitive to fluconazole. *Antimicrobial agents and chemotherapy,* 61.

SHERRY, L., RAJENDRAN, R., LAPPIN, D. F., BORGHI, E., PERDONI, F., FALLENI, M., TOSI, D., SMITH, K., WILLIAMS, C. & JONES, B. 2014. Biofilms formed by Candida albicans bloodstream isolates display phenotypic and transcriptional heterogeneity that are associated with resistance and pathogenicity. *BMC microbiology,* 14**,** 1-14.

SHIGEMURA, K., OSAWA, K., JIKIMOTO, T., YOSHIDA, H., HAYAMA, B., OHJI, G., IWATA, K., FUJISAWA, M. & ARAKAWA, S. 2014. Comparison of the clinical risk factors between Candida albicans and Candida non-albicans species for bloodstream infection. *The Journal of Antibiotics,* 67**,** 311-314.

SHOHAM, S. & LEVITZ, S. M. 2005. The immune response to fungal infections. *Br J Haematol,* 129**,** 569-82.

SINGH, A., VERMA, R., MURARI, A. & AGRAWAL, A. 2014. Oral candidiasis: An overview. *Journal of oral and maxillofacial pathology : JOMFP,* 18**,** S81-S85.

SMEEKENS, S. P., GRESNIGT, M. S., BECKER, K. L., CHENG, S.-C., NETEA, S. A., JACOBS, L., JANSEN, T., VAN DE VEERDONK, F. L., WILLIAMS, D. L. & JOOSTEN, L. A. 2015. An anti-inflammatory property of Candida albicans ß-glucan: induction of high levels of interleukin-1 receptor antagonist via a Dectin-1/CR3 independent mechanism. *Cytokine,* 71**,** 215-222.

SOBEL, J. D., FARO, S., FORCE, R. W., FOXMAN, B., LEDGER, W. J., NYIRJESY, P. R., REED, B. D. & SUMMERS, P. R. 1998. Vulvovaginal candidiasis: epidemiologic, diagnostic, and therapeutic considerations. *Am J Obstet Gynecol,* 178**,** 203-11.

SONG, W., WANG, H. & CHEN, J. 2011. Candida albicans Sfl2, a temperature-induced transcriptional regulator, is required for virulence in a murine gastrointestinal infection model. *FEMS Yeast Research,* 11**,** 209-222.

SORGO, A. G., HEILMANN, C. J., BRUL, S., DE KOSTER, C. G. & KLIS, F. M. 2013. Beyond the wall: Candida albicans secret(e)s to survive. *FEMS Microbiology Letters,* 338**,** 10-17.

SORGO, A. G., HEILMANN, C. J., DEKKER, H. L., BEKKER, M., BRUL, S., DE KOSTER, C. G., DE KONING, L. J. & KLIS, F. M. 2011. Effects of fluconazole on the secretome, the wall proteome, and wall integrity of the clinical fungus Candida albicans. *Eukaryot Cell,* 10**,** 1071-81.

SORGO, A. G., HEILMANN, C. J., DEKKER, H. L., BRUL, S., DE KOSTER, C. G. & KLIS, F. M. 2010. Mass spectrometric analysis of the secretome of Candida albicans. *Yeast,* 27**,** 661-672.

SOSINSKA, G. J., DE KONING, L. J., DE GROOT, P. W. J., MANDERS, E. M. M., DEKKER, H. L., HELLINGWERF, K. J., DE KOSTER, C. G. & KLIS, F. M. 2011. Mass spectrometric quantification of the adaptations in the wall proteome of Candida albicans in response to ambient pH. *Microbiology,* 157**,** 136-146.

SPAMPINATO, C. & LEONARDI, D. 2013. Candida Infections, Causes, Targets, and Resistance Mechanisms: Traditional and Alternative Antifungal Agents. *BioMed Research International,* 2013**,** 204237.

SPRENGER, M., HARTUNG, T. S., ALLERT, S., WISGOTT, S., NIEMIEC, M. J., GRAF, K., JACOBSEN, I. D., KASPER, L. & HUBE, B. 2020. Fungal biotin homeostasis is essential for immune evasion after macrophage phagocytosis and virulence. *Cellular microbiology,* 22**,** e13197.

SRIVASTAVA, A., SIRCAIK, S., HUSAIN, F., THOMAS, E., ROR, S., RASTOGI, S., ALIM, D., BAPAT, P., ANDES, D. R., NOBILE, C. J. & PANWAR, S. L. 2017. Distinct roles of the 7-transmembrane receptor protein Rta3 in regulating the asymmetric distribution of phosphatidylcholine across the plasma membrane and biofilm formation in Candida albicans. *Cell Microbiol,* 19.

STAIB, P., KRETSCHMAR, M., NICHTERLEIN, T., HOF, H. & MORSCHHÄUSER, J. 2000. Differential activation of a Candida albicans virulence gene family during infection. *Proceedings of the National Academy of Sciences,* 97**,** 6102-6107.

STERIN-BORDA, L., ORMAN, B., PITA, A. D. C. & BORDA, E. 2011. Inflammation Triggers Constitutive Activity and Agonist-induced Negative Responses at M3 Muscarinic Receptor in Dental Pulp. *Journal of endodontics,* 37**,** 185-190.

STERLING, T. R. & MERZ, W. G. 1998. Resistance to amphotericin B: emerging clinical and microbiological patterns. *Drug Resistance Updates,* 1**,** 161-165.

STEVENS, D. A., ESPIRITU, M. & PARMAR, R. 2004. Paradoxical effect of caspofungin: reduced activity against Candida albicans at high drug concentrations. *Antimicrobial agents and chemotherapy,* 48**,** 3407-3411.

STONE, N. R. H., BICANIC, T., SALIM, R. & HOPE, W. 2016. Liposomal Amphotericin B (AmBisome(®)): A Review of the Pharmacokinetics, Pharmacodynamics, Clinical Experience and Future Directions. *Drugs,* 76**,** 485-500.

STRANGE, P. G. 2008. Agonist binding, agonist affinity and agonist efficacy at G protein-coupled receptors. *British journal of pharmacology,* 153**,** 1353-1363.

SUDBERY, P., GOW, N. & BERMAN, J. 2004. The distinct morphogenic states of Candida albicans. *Trends Microbiol,* 12**,** 317-24.

SUGAR, A. M. 1995. Use of amphotericin B with azole antifungal drugs: what are we doing? *Antimicrob Agents Chemother,* 39**,** 1907-12.

SUN, J. N., SOLIS, N. V., PHAN, Q. T., BAJWA, J. S., KASHLEVA, H., THOMPSON, A., LIU, Y., DONGARI-BAGTZOGLOU, A., EDGERTON, M. & FILLER, S. G.

2010. Host Cell Invasion and Virulence Mediated by Candida albicans Ssa1. *PLOS Pathogens,* 6**,** e1001181.

SUN, N., PARRISH REBECCA, S., CALDERONE RICHARD, A., FONZI WILLIAM, A., LJUNGDAHL PER, O. & HUBE, B. 2019. Unique, Diverged, and Conserved Mitochondrial Functions Influencing Candida albicans Respiration. *mBio,* 10**,** e00300-19.

SUN, X. & DAI, Y. 2019. *Medical Treatment of Glaucoma*, Springer.

SVOBODA, J., POPELIKOVA, A. & STUCHLIK, A. 2017. Drugs Interfering with Muscarinic Acetylcholine Receptors and Their Effects on Place Navigation. *Frontiers in Psychiatry,* 8.

SWIDERGALL, M. & FILLER, S. G. 2017. Oropharyngeal Candidiasis: Fungal Invasion and Epithelial Cell Responses. *PLoS Pathog,* 13**,** e1006056.

SWIDERGALL, M., KHALAJI, M., SOLIS, N. V., MOYES, D. L., DRUMMOND, R. A., HUBE, B., LIONAKIS, M. S., MURDOCH, C., FILLER, S. G. & NAGLIK, J. R. 2019. Candidalysin is required for neutrophil recruitment and virulence during systemic Candida albicans infection. *The Journal of infectious diseases,* 220**,** 1477-1488.

TAFF, H. T., MITCHELL, K. F., EDWARD, J. A. & ANDES, D. R. 2013. Mechanisms of Candida biofilm drug resistance. *Future microbiology,* 8**,** 1325-1337.

TAKASAKI, J., SAITO, T., TANIGUCHI, M., KAWASAKI, T., MORITANI, Y., HAYASHI, K. & KOBORI, M. 2004. A novel Galphaq/11-selective inhibitor. *J Biol Chem,* 279**,** 47438-45.

TALAPKO, J., JUZBAŠIĆ, M., MATIJEVIĆ, T., PUSTIJANAC, E., BEKIĆ, S., KOTRIS, I. & ŠKRLEC, I. 2021. Candida albicans-The Virulence Factors and Clinical Manifestations of Infection. *J Fungi (Basel),* 7.

TANG, J., LIN, G., LANGDON, W. Y., TAO, L. & ZHANG, J. 2018. Regulation of C-Type Lectin Receptor-Mediated Antifungal Immunity. *Frontiers in immunology,* 9**,** 123-123.

THOMPSON, D. S., CARLISLE, P. L. & KADOSH, D. 2011. Coevolution of morphology and virulence in Candida species. *Eukaryotic cell,* 10**,** 1173-1182.

THOMPSON, G. R., 3RD, PATEL, P. K., KIRKPATRICK, W. R., WESTBROOK, S. D., BERG, D., ERLANDSEN, J., REDDING, S. W. & PATTERSON, T. F. 2010. Oropharyngeal candidiasis in the era of antiretroviral therapy. *Oral surgery, oral medicine, oral pathology, oral radiology, and endodontics,* 109**,** 488-495.

TITS, J., CAMMUE, B. & THEVISSEN, K. 2020. Combination therapy to treat fungal biofilm-based infections. *International Journal of Molecular Sciences,* 21**,** 8873.

TRAPNELL, B. C. & ABE, S. 2006. COLONY STIMULATING FACTORS. *In:* LAURENT, G. J. & SHAPIRO, S. D. (eds.) *Encyclopedia of Respiratory Medicine.* Oxford: Academic Press.

TRONCHIN, G., BOUCHARA, J. P., ANNAIX, V., ROBERT, R. & SENET, J. M. 1991. Fungal cell adhesion molecules in Candida albicans. *European Journal of Epidemiology,* 7**,** 23-33.

TSUI, C., KONG, E. F. & JABRA-RIZK, M. A. 2016. Pathogenesis of Candida albicans biofilm. *Pathog Dis,* 74**,** ftw018.

UHL, M. A., BIERY, M., CRAIG, N. & JOHNSON, A. D. 2003. Haploinsufficiency-based large-scale forward genetic analysis of filamentous growth in the diploid human fungal pathogen C. albicans. *The EMBO journal,* 22**,** 2668-2678.

UPPULURI, P., ACOSTA ZALDÍVAR, M., ANDERSON MATTHEW, Z., DUNN MATTHEW, J., BERMAN, J., LOPEZ RIBOT JOSE, L., KÖHLER JULIA, R. & DOERING TAMARA, L. 2018. Candida albicans Dispersed Cells Are Developmentally Distinct from Biofilm and Planktonic Cells. *mBio,* 9**,** e01338-18.

URRIALDE, V., PRIETO, D., PLA, J. & ALONSO-MONGE, R. 2016. The Candida albicans Pho4 transcription factor mediates susceptibility to stress and influences fitness in a mouse commensalism model. *Frontiers in microbiology,* 7**,** 1062.

VAN DER WESTHUIZEN, E. T., CHOY, K. H. C., VALANT, C., MCKENZIE-NICKSON, S., BRADLEY, S. J., TOBIN, A. B., SEXTON, P. M. & CHRISTOPOULOS, A. 2021. Fine Tuning Muscarinic Acetylcholine Receptor Signaling Through Allostery and Bias. *Frontiers in Pharmacology,* 11.

VAN DYCK, K., VIELA, F., MATHELIÉ-GUINLET, M., DEMUYSER, L., HAUBEN, E., JABRA-RIZK, M. A., VELDE, G. V., DUFRÊNE, Y. F., KROM, B. P. & VAN DIJCK, P. 2020. Adhesion of Staphylococcus aureus to Candida albicans during co-infection promotes bacterial dissemination through the host immune response. *Frontiers in cellular and infection microbiology,* 10.

VAN ENCKEVORT, F. H., NETEA, M. G., HERMUS, A. R., SWEEP, C. G., MEIS, J. F., VAN DER MEER, J. W. & KULLBERG, B. J. 1999. Increased susceptibility to systemic candidiasis in interleukin-6 deficient mice. *Med Mycol,* 37**,** 419-26.

VAN ENDE, M., WIJNANTS, S. & VAN DIJCK, P. 2019. Sugar Sensing and Signaling in Candida albicans and Candida glabrata. *Frontiers in Microbiology,* 10.

VARDANYAN, R. & HRUBY, V. 2016. Chapter 33 - Antifungal Drugs. *In:* VARDANYAN, R. & HRUBY, V. (eds.) *Synthesis of Best-Seller Drugs.* Boston: Academic Press.

VATANSHENASSAN, M., BOEKHOUT, T., LASS-FLÖRL, C., LACKNER, M., SCHUBERT, S., KOSTRZEWA, M. & SPARBIER, K. 2018. Proof of Concept for MBT ASTRA, a Rapid Matrix-Assisted Laser Desorption Ionization-Time of Flight Mass Spectrometry (MALDI-TOF MS)-Based Method To Detect Caspofungin Resistance in Candida albicans and Candida glabrata. *J Clin Microbiol,* 56.

VERBOUT, N. & JACOBY, D. 2012. Muscarinic Receptor Agonists and Antagonists: Effects on Inflammation and Immunity. *Handbook of experimental pharmacology,* 208**,** 403-27.

VERMA, A., GAFFEN, S. L. & SWIDERGALL, M. 2017. Innate immunity to mucosal Candida infections. *Journal of Fungi,* 3**,** 60.

VEZYS, V., MASOPUST, D., DESMARETS, M., WESS, J. & ZIMRING, J. C. 2007. Analysis of CD8+ T cell-mediated anti-viral responses in mice with targeted deletions of the M1 or M5 muscarinic cholinergic receptors. *Life sciences,* 80**,** 2330-2333.

VILLA, S., HAMIDEH, M., WEINSTOCK, A., QASIM, M. N., HAZBUN, T. R., SELLAM, A., HERNDAY, A. D. & THANGAMANI, S. 2020. Transcriptional control of hyphal morphogenesis in Candida albicans. *FEMS Yeast Research,* 20.

VOLKOVA, M., ATAMAS, A., TSARENKO, A., ROGACHEV, A. & GUSKOV, A. 2021. Cation Transporters of Candida albicans—New Targets to Fight Candidiasis? *Biomolecules,* 11**,** 584.

VONK, A. G., NETEA, M. G., VAN KRIEKEN, J. H., IWAKURA, Y., VAN DER MEER, J. W. & KULLBERG, B. J. 2006. Endogenous interleukin (IL)–1α and IL-1β are crucial for host defense against disseminated candidiasis. *The Journal of infectious diseases,* 193**,** 1419-1426.

WÄCHTLER, B., CITIULO, F., JABLONOWSKI, N., FÖRSTER, S., DALLE, F., SCHALLER, M., WILSON, D. & HUBE, B. 2012. Candida albicans-epithelial interactions: dissecting the roles of active penetration, induced endocytosis and host factors on the infection process. *PloS one,* 7**,** e36952.

WÄCHTLER, B., WILSON, D., HAEDICKE, K., DALLE, F. & HUBE, B. 2011. From Attachment to Damage: Defined Genes of Candida albicans Mediate Adhesion, Invasion and Damage during Interaction with Oral Epithelial Cells. *PLOS ONE,* 6**,** e17046.

WAGENER, J., WEINDL, G., DE GROOT, P. W. J., DE BOER, A. D., KAESLER, S., THAVARAJ, S., BADER, O., MAILÄNDER-SANCHEZ, D., BORELLI, C., WEIG, M., BIEDERMANN, T., NAGLIK, J. R., KORTING, H. C. & SCHALLER, M. 2012. Glycosylation of Candida albicans cell wall proteins is critical for induction of innate immune responses and apoptosis of epithelial cells. *PloS one*, 7**,** e50518-e50518.

WAKHARDE, A. & KARUPPAYIL, S. M. Muscarinic Acetylcholine Receptor Agonists and Antagonists Regulate Yeast to Hyphal form Transition in Candida albicans. 2018.

WALL, G., MONTELONGO-JAUREGUI, D., VIDAL BONIFACIO, B., LOPEZ-RIBOT, J. L. & UPPULURI, P. 2019. Candida albicans biofilm growth and dispersal: contributions to pathogenesis. *Curr Opin Microbiol,* 52**,** 1-6.

WAN, L., ZHANG, Y., LAI, Y., JIANG, M., SONG, Y., ZHOU, J., ZHANG, Z., DUAN, X., FU, Y., LIAO, L. & WANG, C. 2015. Effect of Granulocyte-Macrophage Colony-Stimulating Factor on Prevention and Treatment of Invasive Fungal Disease in Recipients of Allogeneic Stem-Cell Transplantation: A Prospective Multicenter Randomized Phase IV Trial. *Journal of Clinical Oncology,* 33**,** 3999-4006.

WANG, J. M., WOODRUFF, A. L., DUNN, M. J., FILLINGER, R. J., BENNETT, R. J., ANDERSON, M. Z. & LORENZ, M. 2021. Intraspecies Transcriptional Profiling Reveals Key Regulators of Candida albicans Pathogenic Traits. *mBio,* 12**,** e00586-21.

WANG, T., XIU, J., ZHANG, Y., WU, J., MA, X., WANG, Y., GUO, G. & SHANG, X. 2017. Transcriptional Responses of Candida albicans to Antimicrobial Peptide MAF-1A. *Frontiers in microbiology,* 8**,** 894-894.

WANG, Z., GERSTEIN, M. & SNYDER, M. 2009. RNA-Seq: a revolutionary tool for transcriptomics. *Nature reviews genetics,* 10**,** 57-63.

WEINDL, G., WAGENER, J. & SCHALLER, M. 2010. Epithelial cells and innate antifungal defense. *Journal of dental research,* 89**,** 666-675.

WESSLER, I. & KIRKPATRICK, C. J. 2008. Acetylcholine beyond neurons: the non-neuronal cholinergic system in humans. *British journal of pharmacology,* 154**,** 1558-1571.

WESSLER, I. K. & KIRKPATRICK, C. J. 2012. Activation of muscarinic receptors by non-neuronal acetylcholine. *Handb Exp Pharmacol***,** 469-91.

WHALEY, S. G., TSAO, S., WEBER, S., ZHANG, Q., BARKER, K. S., RAYMOND, M. & ROGERS, P. D. 2016. The RTA3 Gene, Encoding a Putative Lipid Translocase, Influences the Susceptibility of Candida albicans to Fluconazole. *Antimicrobial Agents and Chemotherapy,* 60**,** 6060-6066.

WHIBLEY, N. & GAFFEN, S. L. 2014. Brothers in arms: Th17 and Treg responses in Candida albicans immunity. *PLoS Pathog,* 10**,** e1004456.

WILLEMS, H. M. E., AHMED, S. S., LIU, J., XU, Z. & PETERS, B. M. 2020. Vulvovaginal Candidiasis: A Current Understanding and Burning Questions. *Journal of fungi (Basel, Switzerland),* 6**,** 27.

WILSON, D., NAGLIK, J. R. & HUBE, B. 2016. The missing link between Candida albicans hyphal morphogenesis and host cell damage. *PLoS pathogens,* 12**,** e1005867.

WINGETT, S. W. & ANDREWS, S. 2018. FastQ Screen: A tool for multi-genome mapping and quality control. *F1000Res,* 7**,** 1338.

WINTER MICHAEL, B., SALCEDO EUGENIA, C., LOHSE MATTHEW, B., HARTOONI, N., GULATI, M., SANCHEZ, H., TAKAGI, J., HUBE, B., ANDES DAVID, R., JOHNSON ALEXANDER, D., CRAIK CHARLES, S., NOBILE CLARISSA, J., TAYLOR JOHN, W., LOPEZ-RIBOT, J. & COENYE, T. 2016. Global Identification of Biofilm-Specific Proteolysis in Candida albicans. *mBio,* 7**,** e01514-16.

XUE, C., HSUEH, Y.-P. & HEITMAN, J. 2008. Magnificent seven: roles of G protein-coupled receptors in extracellular sensing in fungi. *FEMS microbiology reviews,* 32**,** 1010-1032.

YADAV, B., BHATNAGAR, S., AHMAD, M. F., JAIN, P., PRATYUSHA, V. A., KUMAR, P. & KOMATH, S. S. 2014. First step of glycosylphosphatidylinositol (GPI) biosynthesis cross-talks with ergosterol biosynthesis and Ras signaling in Candida albicans. *The Journal of biological chemistry,* 289**,** 3365-3382.

YADAV, B., MORA-MONTES, H. M., WAGENER, J., CUNNINGHAM, I., WEST, L., HAYNES, K., BROWN, A. J. P. & GOW, N. A. R. 2020. Differences in fungal immune recognition by monocytes and macrophages: N-mannan can be a shield or activator of immune recognition. *The Cell Surface,* 6**,** 100042.

YADAV, U., RAI, T. K., SETHI, S. C., CHANDRAKER, A., KHAN, M. A. & KOMATH, S. S. 2018. Characterising N-acetylglucosaminylphosphatidylinositol de-N-acetylase (CaGpi12), the enzyme that catalyses the second step of GPI biosynthesis in Candida albicans. *FEMS Yeast Research,* 18.

YANG, D., HU, Y., YIN, Z., GAO, Q., ZHANG, Y., CHAN, F. Y., ZENG, G., WENG, L., WANG, L. & WANG, Y. 2020. Candida albicans Ubiquitin and Heat Shock Factor-Type Transcriptional Factors Are Involved in 2-Dodecenoic Acid-Mediated Inhibition of Hyphal Growth. *Microorganisms,* 8.

YANG, Q., GAO, L., TAO, M., CHEN, Z., YANG, X. & CAO, Y. 2016. Transcriptomics Analysis of Candida albicans Treated with Huanglian Jiedu Decoction Using RNA-seq. *Evidence-Based Complementary and Alternative Medicine,* 2016**,** 3198249.

YANG, W., YAN, L., WU, C., ZHAO, X. & TANG, J. 2014. Fungal invasion of epithelial cells. *Microbiological Research,* 169**,** 803-810.

YAPAR, N. 2014. Epidemiology and risk factors for invasive candidiasis. *Therapeutics and clinical risk management,* 10**,** 95-105.

YU, L.-H., WEI, X., MA, M., CHEN, X.-J. & XU, S.-B. 2012. Possible inhibitory molecular mechanism of farnesol on the development of fluconazole resistance in Candida albicans biofilm. *Antimicrobial agents and chemotherapy,* 56**,** 770-775.

YU, S.-J., CHANG, Y.-L. & CHEN, Y.-L. 2015. Calcineurin signaling: lessons from Candida species. *FEMS yeast research,* 15.

ZAOUTIS, T. E., ARGON, J., CHU, J., BERLIN, J. A., WALSH, T. J. & FEUDTNER, C. 2005. The epidemiology and attributable outcomes of candidemia in adults and children hospitalized in the United States: a propensity analysis. *Clin Infect Dis,* 41**,** 1232-9.

ZARNOWSKI, R., WESTLER, W. M., LACMBOUH, G. A., MARITA, J. M., BOTHE, J. R., BERNHARDT, J., SAHRAOUI, A. L.-H., FONTAINE, J., SANCHEZ, H. &

HATFIELD, R. D. 2014. Novel entries in a fungal biofilm matrix encyclopedia. *MBio,* 5.

ZHANG, Z., ZHU, R., LUAN, Z. & MA, X. 2020. Risk of invasive candidiasis with prolonged duration of ICU stay: a systematic review and meta-analysis. *BMJ Open,* 10**,** e036452.

ZHAO, X., OH, S. H., YEATER, K. M. & HOYER, L. L. 2005. Analysis of the Candida albicans Als2p and Als4p adhesins suggests the potential for compensatory function within the Als family. *Microbiology (Reading, England),* 151**,** 1619-1630.

ZHENG, N.-X., WANG, Y., HU, D.-D., YAN, L. & JIANG, Y.-Y. 2015. The role of pattern recognition receptors in the innate recognition of Candida albicans. *Virulence,* 6**,** 347-361.